2021

Understanding the Potential of Plasma Activated Liquids for Biomedical Applications

Evanthia Tsoukou
Technological University Dublin, evanthia.tsoukou@tudublin.ie

UNDERSTANDING THE POTENTIAL OF PLASMA ACTIVATED LIQUIDS FOR BIOMEDICAL APPLICATIONS

Evanthia Tsoukou B.Sc. (Hons)

A thesis submitted to Technological University Dublin in fulfilment of the requirements for the degree of

Doctor of Philosophy

Supervisors:

Dr. Daniela Boehm

Prof. Paula Bourke

Technological University Dublin

School of Food Science and Environmental health

November 2021

Publications

Achievements

E. Tsoukou, P. Bourke, D. Boehm (2018). Understanding the differences between antimicrobial and cytotoxic properties of plasma activated liquids. Plasma Medicine 8(3), 299-320 DOI: 10.1615/PlasmaMed.2018028261E

S. Ng, E. Tsoukou, S. Chaple, D. Boehm, P. Bourke (2020). Plasma treatment of liquids. Innovative Food Processing Technologies: A Comprehensive review, 610-634 DOI: 10.1016/B978-0-12-815781-7.00003-2

E. Tsoukou, P. Bourke, D. Boehm (2020). Temperature Stability and Effectiveness of Plasma-Activated Liquids over an 18 Months Period. Water, 12(11), 302 DOI: 10.3390/w12113021

E. Tsoukou, M. Delit, L. Treint, P. Bourke, D. Boehm (2021). Distinct Chemistries Define the Diverse Biological Effects of Plasma Activated Water Generated with Spark and Glow Plasma Discharges. Applied Sciences, 11(3), 1178 DOI: 10.3390/app11031178

E. Tsoukou, P. Bourke, D. Boehm (2021). Efficacy and mechanisms of plasma activated saline in a co-culture infection control model. Scientific Reports (under review)

Oral Presentations

Tsoukou E., Bourke P., Boehm D. Investigation of the chemical composition, antimicrobial properties and cytotoxic effects of plasma activated water. Oral presentation at 6th Young Professionals Workshop on Plasma Medicine, 23-26 October 2017 (Rostock, Germany)

Tsoukou E., Bourke P., Boehm D. Stability of the biological activity of plasma activated liquids. Oral presentation at 7th Young Professionals Workshop on Plasma Medicine, 23-26 September 2018 (Rostock, Germany)

Tsoukou E., Bourke P., Boehm D. Harnessing the potential of plasma activated liquids for biomedical applications. Oral presentation at 'Biomedical Sciences Annual Meeting conference' organised by Royal Academy of Medicine in Ireland, 3rd February 2021 (online)

Poster Presentations

Tsoukou E., Bourke P., Boehm D. Investigation of the chemical composition, antimicrobial properties and cytotoxic effects of plasma activated liquids. Poster presented at 8th Annual Graduate Research Symposium at Technological University Dublin, 11 December 2017 (Dublin, Ireland)

Tsoukou E., Bourke P., Boehm D. Understanding the differences between antimicrobial and cytotoxic properties of plasma activated liquids. Poster presented at 9th Annual Graduate Research Symposium at Technological University Dublin, 1 November 2018 (Dublin, Ireland)

Tsoukou E., Bourke P., Boehm D. Understanding the differences between antimicrobial and cytotoxic properties of plasma activated liquids. Poster presented at 7th International Conference on Plasma Medicine at Drexel University, 17-22 June 2018 (Philadelphia, USA)

Tsoukou E., Lu P., Bourke P., Boehm D. Modulating the cytotoxic effects of plasma activated water against cancerous cell lines. Poster presented at 6th International Workshop on Plasma for Cancer Treatment, 1-3 April 2019 at University of Antwerp (Antwerp, Belgium)

Tsoukou E., Bourke P., Boehm D. Plasma activated liquids: New decontamination solutions. Poster presented at Microbes in medicine: A century of Microbiology at Trinity College Dublin, 25-26 October 2019 (Dublin, Ireland)

Abstract

Atmospheric cold plasma has evolved as a new technology for applications used in biomedicine, agriculture and food industry. Recently, treatment of liquids using various atmospheric pressure plasmas has attracted much attention owing to multiple practical applications such as water purification, surface cleaning and decontamination with impact in dentistry, wound healing and sterilisation, or cancer therapy. The over-arching aim of this study is to build a better understanding of the parameters which govern the liquid chemistry generated in a liquid exposed to cold plasma and how these translate into biological effects on pro- and eu-karyotic organisms. The objective was to investigate the effects of plasma activated liquids (PAL) generated by different custom-made plasma systems in Technological University Dublin.

Non-buffered and buffered liquids treated by a high voltage dielectric barrier discharge system were used to investigate the role of the liquid composition on resultant reactive species and their bactericidal and cytotoxic effects against prokaryotic and eukaryotic cells, respectively.

The impact of process and storage parameters such as temperature and storage time on chemical composition and bactericidal efficacy of plasma activated water and saline was also investigated, including the influence of supra and sub-ambient temperatures and long-term storage of up to 18 months. Bactericidal efficacy showed stability to mild heating and remained at lowest temperatures over prolonged storage, whereas changes in the physicochemical properties of solutions were observed after different storage times and temperatures.

A reactive species selective spark and glow discharge set-up was used to elucidate the role of ROS and RNS in bacterial inactivation and cytotoxic effects of plasma

activated water and saline. The effects of treatment time, mode of discharge and contact time of PAL on antimicrobial efficacy and cytotoxic effects in various cancerous and healthy cell lines were investigated to provide a primary understanding of how ROS and RNS affect different biological targets.

Finally, a co-culture model consisting of bacteria and keratinocytes was developed to mimic the environment of an infected wound and provide a more complex challenge for microbial inactivation. Results showed that plasma activated saline can reduce the bacterial load under these conditions but caused cytotoxic effects with earlier onset than the bactericidal efficacy. A mechanistic approach for the mammalian cell death showed that PAL with acidic pH can cause increase of intracellular ROS and mitochondria depolarisation, reduction of glutathione, cytokine alteration and finally lysis of mammalian cells.

Overall, these data demonstrate that plasma activated liquids show an efficient decontamination approach against bacteria and have anticancer effects, with the chemical composition playing a crucial role in the inactivation processes, highlighting the potential to make plasma solutions attractive for applications in biomedicine but also indicating limiting factors which require further elucidation.

Abbreviations

°C	degrees Celsius
ACP	atmospheric cold plasma
ANOVA	Analysis of Variance
APPJ	Atmospheric Pressure Plasma Jet
Ar	Argon
ATCC	American Type Culture Collection
ATP	adenosine triphosphate
Caspase	Cysteine aspartate-specific protease
CFU	colony forming unit
CHO	Chinese hamster ovarian
CRT	chaperone calreticulin
DAMP	Damage associated molecular patterns
DBD	dielectric barrier discharge
DMEM	Dulbecco's modified Eagle's medium
DNA	deoxyribonucleic acid
ERC	extracellular regulated kinase
FBS	Fetal Bovine Serum
g (centrifuge)	Gravitational Force
g (mass)	gram
HaCaT	Cultured Human Keratinocyte cells
h	hour
H_2DCFDA	2,7-dichlorodihydrofluorescein diacetate
He	Helium
Hmox1	heme oxygenase-1
Hz	Hertz
IL	Interleukin
KI	potassium iodide
min	min
MRD	maximum recovery diluent
MRSA	methicillin resistant *Staphylococcus aureus*

OPA	Ortho-phthalaldehyde
PAL	plasma activated liquids
PAM	plasma activated media
PAS	plasma activated saline
PAW	plasma activated water
PAPB	plasma activated phosphate buffer solution
PAPBS	plasma activated phosphate buffered saline
PB	phosphate buffer solution
PBS	phosphate buffered saline
RNS	Reactive Nitrogen species
RONS	Reactive Oxygen Nitrogen species
ROS	Reactive Oxygen species
RSS	Reactive species specificity
sec	second
TNF	Tumour necrosis factor
TSA	Tryptic Soy agar
TSB	Tryptic Soy Broth
V	Volt

Contents

Chapter 1: Introduction 1
1.1 Atmospheric Cold Plasma (ACP) technology 2
1.2 Sources of ACP 3
1.2.1 Corona discharge 3
1.2.2 Gliding arc (GA) 3
1.2.3 Atmospheric Pressure Plasma jets (APPJs) 3
1.2.4 Dielectric Barrier Discharge (DBD) 5
1.3 Plasma Medicine 7
1.3.1 Plasma Disinfection/Sterilisation 9
1.3.2 Plasma Cancer Treatment 11
1.3.3 Plasma-induced Blood Coagulation 12
1.3.4 Plasma Dentistry 13
1.3.5 Plasma Applications in Wound Healing 14
1.3.6 Plasma for Gene Therapy 16
1.4 Plasma Activated Liquids 16
1.4.1 Reactive species in PAL 18
1.4.2 Plasma activated Water (PAW) 22
1.4.3 Plasma activated Saline (PAS) 22
1.4.4 Plasma activated Buffered solutions (PAPB/PAPBS) 23
1.4.5 Plasma activated Cell culture media (PAM) 23
1.5 Potential of PAL for biomedical applications 25
1.5.1 PAL as disinfectant 25
1.5.2 Anticancer effects of PAL 29
1.5.3 Role of PAL in blood coagulation 30
1.5.4 PAL in Dentistry 31
1.5.5 PAL for wound healing 31
1.6 Mechanisms of interaction of PAL 32
1.6.1 Effects of PAL on bacterial cells 32
1.6.2 Effects of PAL on mammalian cells 40
1.7 Antimicrobial agents for disinfection and antisepsis 49
1.7.1 Disinfectants for surfaces/medical instruments 50
1.7.2 Topical antimicrobial agents in wound care 54
1.8 Advantages and limitations of PAL 59
1.8.1 Biosafety concerns 60
1.8.2 Environmental considerations 62

1.9 Objectives of the study **63**
Chapter 2: Materials and Methods **66**
2.1 Plasma Sources Evaluated and Sample treatment **66**
2.1.1 DBD-120 system **66**
2.1.2 RSS system **67**
2.2 Antimicrobial efficacy **68**
2.2.1 Bacterial strains and growth conditions **68**
2.2.2 Preparation of cell suspensions **69**
2.2.3 Microbiological analysis **69**
2.2.4 Adjusted pH experiments **69**
2.3 Effect of Temperature on PAL stability **70**
2.3.1 PAL heated to supra-ambient Temperatures **70**
2.3.2 PAL stored in sub-ambient temperatures **71**
2.4 Investigation of the chemical composition of PAL **71**
2.4.1 Quantification of Hydrogen Peroxide using Titanium Oxysulfate **71**
2.4.2 Quantification of Peroxides using potassium iodine **72**
2.4.3 Determination of Nitrite **72**
2.4.4 Determination of Nitrate **72**
2.5.5 pH and conductivity measurements **73**
2.4.6 Temperature measurements **73**
2.5 Mammalian Cell Culture **73**
2.5.1 Eukaryotic cell lines **73**
2.5.2 Analysis of cytotoxicity **74**
2.5.3 Protein expression analysis **77**
2.6 Co-culture model setup **78**
2.6.1 Microbial inactivation in co-culture model **78**
2.6.2 Antibiotic Invasion assay **78**
2.6.3 Disinfectants testing **79**
2.7 Statistical analysis **80**
Chapter 3: Bactericidal and Cytotoxic Effects of PAL by DBD-120 ..... **81**
3.1 Chemical properties of PAL **83**
3.1.1 pH measurements of PAL **83**
3.1.2 Chemical composition **84**
3.2 Antimicrobial Activity and Stability of PAL **86**
3.2.1 Bacterial inactivation of PAL **86**
3.2.2 Antibacterial stability of PAL **100**
3.2.3 Effects of pH on antimicrobial activity **103**

3.2.4 Effects of chemical composition on antimicrobial effects 109
3.3 Cytotoxic evaluation of PAL 110
3.4 Conclusion 111
Chapter 4: Effects of process and storage conditions on PAL efficacy and stability .. 113
4.1 Effect of supra-ambient temperatures on PAL by DBD-120 114
4.1.1 Antimicrobial effects 114
4.1.2 Chemical characterisation 118
4.2 Discussion 120
4.3 Sub-ambient Temperature Stability and Effectiveness of PAL over 18 Months 122
4.3.1 Antimicrobial effects 122
4.3.2 Chemical characterisation of PAL 126
4.3.3 Freezing behaviour 133
4.4 Discussion 135
4.5 Conclusion 138
Chapter 5: Biological effects of plasma activated water generated with spark and glow plasma discharges 140
5.1 Chemical Composition of PAW 142
5.2 Bactericidal efficacy of PAW 145
5.3 Heat stability of plasma activated water by spark and glow discharges 149
5. 4 Cytotoxic effects of PAW 152
5. 5 Discussion 153
5.6 Conclusion 157
Chapter 6: Effects of PAW on cancerous cell lines 159
6.1 Anticancer capacity of PAW 160
6.2 Discussion 164
6.3 Conclusion 168
Chapter 7: Efficacy and mechanisms of plasma activated saline in a co-culture infection control model 169
7.1 Hydrogen peroxide and nitrates are the main species detected in PAS 171
7.2 Bactericidal effects of PAS in co-culture model 173
7.3 Balancing cytotoxic and bactericidal effects 176
7.4 Internalisation of bacteria to host cells 178
7. 5 Comparison of PAS to disinfectants 179
7.6 Decrease of cell viability and cell death of HaCaT cells induced by PAS 181
7.7 Extracellular pH expected to be an important parameter influencing cell viability 183
7.8 Oxidative stress analysis 185

7. 9 Cytokine expression **188**
7.10 Discussion **189**
7.11 Conclusion **196**
Chapter 8: Conclusions and future recommendations **198**
Appendices **207**
Appendix I Supplementary Information for Chapter 4 ..... **207**
Appendix II Supplementary Information for Chapter 7 ..... **212**
Bibliography **214**

List of figures and tables

Figure 1.1 Schematic setup of the non-thermal atmospheric pressure plasma jet (top) and plasma jet in action (below) (Höntsch et al., 2012). 5
Figure 1.2 Figure Schematic (a) and a photograph (b) of an atmospheric pressure diffuse plasma generated by DBD (Laroussi, 2018). 6
Figure 1.3 Timeline showing some milestones of the new field of the medical applications of ACP (Laroussi, 2018). 8
Figure 1.4 Applications of Plasma Medicine 9
Table 1.1 Role of chemical species in bactericidal effects of PAL 39
Table 1.2 Effects of PAL on mammalian cells 44
Figure 2.1 Schematic of the experimental setup of the DBD-120 plasma generator. 67
Figure 2.2 Schematic of air discharge in contact with water, (a) spark discharge, (b) glow discharge (Lu et al., 2017a). 68
Figure 3.1 Dependence of pH on time of activation for PAL (n=3). 83
Figure 3.2 Chemical composition of PAL after 1, 5, 10 min DBD plasma activation time at 80kV. (A) Generation of hydrogen peroxide, (B) nitrite and (C) nitrate concentrations n=3). Graphs represent averages of 3 independent plasma treatments (circles + lines), with the individual data sets represented as symbols only. 85
Figure 3.3 Surviving bacterial cells in response to PAL after 1, 5, or 10 min plasma treatment. (A) PAW- E.coli, (B) PAW-S. aureus, (C) PAPBS-E. coli, (D) PAPBS- S. aureus, (E) PAS-E. coli, (F) PAS-S. aureus, (G) PAPB - E. coli , (H) PAPB-S. aureus (set 2). 88
Table 3.1 E. coli and S. aureus planktonic inactivation efficacy by PAW. Limit of detection: 2 log10 CFU/mL. 90
Table 3.2 E. coli and S. aureus planktonic inactivation efficacy by PAPBS. Limit of detection: 2 log10 CFU/mL. 93
Table 3.3 E. coli and S. aureus planktonic inactivation efficacy by PAS. Limit of detection: 2 log10 CFU/mL. 95
Table 3.4 E. coli and S. aureus planktonic inactivation efficacy by PAPB. Limit of detection: 2 log10 CFU/mL. 98
Figure 3.4 Antibacterial stability in response to PAL after 1, 5, or 10 min plasma treatment on day 2. (A) PAW- E. coli, (B) PAW-S. aureus, (C) PAPBS-E. coli, (D) PAPBS- S. aureus, (E) PAS-E. coli, (F) PAS-S. aureus, (G) PAPB - E. coli , (H) PAPB-S. aureus (set 2). 102
Figure 3.5 pH measurements of adjusted PAL. 104
Figure 3.6 Effects of adjusted pH PAL on microbial inactivation of E. coli. Bactericidal effects of plasma treated and non-plasma treated (controls) (A) water and buffered water, (B) PBS and acidified PBS, (C) saline and buffered saline (D) phosphate buffer solution and acidified phosphate buffer solution. 106
Figure 3.7 Effects of adjusted pH PAL on microbial inactivation of S. aureus. Bactericidal effects of plasma treated and non-plasma treated (controls) (A) water and buffered water, (B) PBS and acidified PBS, (C) saline and buffered saline (D) phosphate buffer solution and acidified phosphate buffer solution. 108
Figure 3.8 Growth inhibition of PAL on CHO-K1 cells. 111
Figure 4.1 Bactericidal activity in response to heated PAW after 10 min plasma treatment and different contact times. (A) PAW- E. coli 15 min contact time, (B) PAW-S. aureus 15 min, (C) PAW-E. coli 30 min, (D) PAW- S. aureus 30 min, (E) PAW-E. coli 60 min, (F) PAW-S. aureus 60 min. Graphs represent averages of 3 independent plasma treatments. 116
Figure 4.2 Bactericidal activity in response to heated PAS after 10 min plasma treatment and different contact times. (A) PAS- E. coli 15 min contact time, (B) PAS-S. aureus 15 min, (C)

PAS-E. coli 30 min, (D) PAS-S. aureus 30 min, (E) PAS-E. coli 60 min, (F) PAS-S. aureus 60 min. Graphs represent averages of 3 independent plasma treatments. 117
Figure 4.3 Chemical composition of PAW and PAS heated from 50-100°C for 5 min after 10 min DBD plasma activation time at 80kV. (A, B) pH measurements, (C, D) generation of peroxides measured by buffered KI, (E, F) nitrate concentrations) (n=3). Graphs represent averages of 3 independent plasma treatments. 119
Figure 4.4 Microbial inactivation of E. coli and S. aureus at 60 min contact time, treated with PAW stored at different temperatures for up to 18 months. Graphs represent averages of 2 independent plasma treatments (Set 1 and 2). 124
Figure 4.5 Microbial inactivation of E. coli and S. aureus at 60 min contact time, treated with PAS stored at different temperatures for up to 18 months. Graphs represent averages of 2 independent plasma treatments (Set 1 and 2). 125
Figure 4.6 Microbial inactivation of E. coli and S. aureus at different contact times, treated with PAW stored at different temperatures for up to 6 months. (Set 4). 125
Figure 4.7 Microbial inactivation of E. coli and S. aureus at 60 min time, treated with PAS stored at different temperatures for up to 6 months (Set 4). 126
Figure 4.8 pH measurements of PAW and PAS the first day of their generation. 127
Figure 4.9 Chemical properties of PAW stored at different temperatures for 6 - 18 months showing ROS concentrations in the column on the left and nitrate concentrations in the column on the right. Samples were analysed after 1, 3 and 6 months and 18 months (set 1 and 2). Set 4 was also analysed after 1, 2 and 3 weeks of storage. 130
Figure 4.10 Chemical properties of 4 different sets of PAS stored at different temperatures for 6 - 18 months showing ROS concentrations in the column on the left and nitrate concentrations in the column on the right. Samples were analysed after 1, 3 and 6 months and 18 months (set 1 and 2). Set 4 was also analysed after 1, 2 and 3 weeks of storage. 133
Figure 4.11 Hydrogen peroxide concentrations of PAW set 3 (A) and set 4 (B) stored at different temperatures for 6 months. 133
Figure 4.12 Schematic of typical freezing curve. 134
Figure 4.13 Freezing curve of PAW. 135
Figure 5.1 Chemical composition of PAW made by spark and glow discharges on the day of generation (Day 0) and after 1 week storage. (A) pH, (B) conductivity measurements, (C) hydrogen peroxide measured by $TiOSO_4$, (D) peroxides measured by KI buffered with PB, (E) peroxides measured by KI and water, (F) nitrite concentration, (G) nitrate concentration (n=3 experiments with measurements performed in triplicate). 144
Figure 5.2 Bactericidal effects of PAW after 5, 10 or 15 min plasma activation, made by spark and glow discharges, on E. coli and S. aureus with contact times of 15, 30, 60 and 24 h on the day of PAW generation. (A) E. coli-15 min, (B) S. aureus-15 min, (C) E. coli-30 min, (D) S. aureus-30 min (E) E. coli-60 min, (F) S. aureus-60 min, (G) E. coli-24 h, (H) S. aureus 24 h (average of 3 experiments). Limit of detection: 2 $\log_{10}$ CFU/mL. 148
Figure 5.3 Bactericidal stability of PAW after 5, 10 or 15 min plasma activation, made by spark and glow discharges on E. coli and S. aureus with 30 and 60 min contact time a week after PAW generation. (A) E. coli-30 min, (B) S. aureus-30 min, (C) E. coli-60 min, (D) S. aureus-60 min (average of 3 experiments). Limit of detection: 2 $\log_{10}$ CFU/mL. 148
Figure 5.4 Effect of heating at 100 °C and heating time duration on retention of antimicrobial efficacy of PAW (SD15, GD15). (A) Bactericidal effects after 60 min contact time. (B) Chemical composition of hydrogen peroxide measured by TiOSO4, peroxides measured by buffered KI and non-buffered KI. nd = no colonies detected. Limit of detection: 2 $\log_{10}$ CFU/mL. 149
Figure 5.5 Effect of autoclaving on retention of antimicrobial activity of SD15 and GD15 PAW over 15-60 minute contact time (CT). (A) E. coli-15 min, (B) S. aureus-15 min, (C) E.

coli-30 min, (D) S. aureus-30 min (E) E. coli-60 min, (F) S. aureus-60 min (n=3). Limit of detection: 2 $\log_{10}$ CFU/mL. 151
Table 5.1 Chemical composition of SD15 and GD15 PAW, before and after autoclaving. ND = not detected. Set 1 and 2 correspond to sets 1 and 2 in figure 6, set 4 is an additional set. 152
Figure 5.6 Cell growth of CHO-K1 (A) and HaCaT (B) cell lines exposed to PAW generated by SD and GD discharge at 20% (v/v) as plasma activation time of PAW increases (n=3). 153
Figure 6.1 Cell growth of A375 cancer cell line as plasma activation time of PAW increases. 161
Figure 6.3 Cell growth of SW480 cancer cell line as plasma activation time of PAW increases. 162
Figure 6.4 Cell growth of U373mg cancer cell lines as plasma activation time of PAW increases. 162
Figure 6.5 Cell growth of cancer cell lines relative to concentration of chemical species determined in SD PAW. 163
Figure 7.1 Chemical composition of PAS after exposure to spark plasma discharge for activation times of 0-30 min. The results are the mean ± S.D. of three determinations. 171
Figure 7.2 Bacterial inactivation in a co-culture model of HaCaT cells and E. coli or S. aureus under incubation with PAS 20 or PAS 30 as a function of contact time. (A) E. coli – PAS 20, (B) E. coli – PAS 30, (C) S. aureus ATCC 1803 – PAS 20, (D) S. aureus ATCC 1803- PAS 30, (E) S. aureus ATCC 25923 –PAS 20, (F) S. aureus ATCC 25923 - PAS 30. The results are the mean ± S.D. of three determinations. 174
Figure 7.3 The antimicrobial efficacy of PAS 20 and PAS 30 within the co-culture model between HaCaT cells and E. coli or S. aureus and incubation with diluted PAS 20 or PAS 30 after 60 min contact time. (A) E. coli – PAS 20, (B) E. coli – PAS 30, (C) S. aureus ATCC 1803 – PAS 20, (D) S. aureus ATCC 1803 – PAS 30, (E) S. aureus ATCC 25923 – PAS 20, (F) S. aureus ATCC 25923 - PAS 30. 177
Table 7.1 Antibiotic invasion assay against E. coli, S. aureus ATCC 1803 and S. aureus ATCC 25923. Results are the surviving bacterial concentration in log CFU/mL shown as mean ± S.D. of three determinations. ND = not detected, limit of detection 2log. 178
Table 7.2 List of the chemical disinfectants used and their antimicrobial activity and HaCaT cell viability after 15 min contact time (ND=not detected, limit of detection 2log). 179
Figure 7.4 Cell viability of diluted PAS 20 (A) and PAS 30 (B) at 15 min, 30 min, 40 min and 60 min contact time. 181
Figure 7.5 Apoptosis and lysis of HaCaT cells after incubation with 70% PAS at different contact times 182
Figure 7.6 pH values of diluted PAS 20 and PAS 30. 183
Figure 7.7 Cell viability of acidic solution at pH values similar to pH values observed for PAS 20, compared with different dilutions of PAS 20. 184
Figure 7.8 Cell viability of HaCaT cells at different concentrations of hydrogen peroxide after 60 min contact time. 184
Figure 7.9 Mitochondrial membrane potential after incubation with PAS 20 for different contact times: (A) after 15 min, (B) 30 min, (C) 40 min, (D) 60 min contact time. Graphs represent averages of three independent plasma treatments. 186
Figure 7.10 Detection of intracellular ROS after incubation of HaCaT with PAS 20 at different contact times. One representative experiment is represented. 187
Figure 7.11 Measurements of total GSH and GSSH after 60 min exposure of PAS and neutralized PAS. 188
Table 7.3 Cytokine analysis after treatment with 50% or 68% PAS. Results are shown as % of induced cytokine production compared to positive control. 188

Declaration

I certify that this thesis which I now submit for examination for the award of PhD, is entirely my own work and has not been taken from the work of others, save and to the extent that such work has been cited and acknowledged within the text of my work.

This thesis was prepared according to the regulations for graduate study by research of the Technological University Dublin and has not been submitted in whole or in part for another award in any other third level institution.

The work reported on in this thesis conforms to the principles and requirements of the TU Dublin's guidelines for ethics in research.

TU Dublin has permission to keep, lend or copy this thesis in whole or in part, on condition that any such use of the material of the thesis be duly acknowledged.

Signature:  Date: 28/11/2021

Acknowledgement

I would like to thank my supervisors Dr. Daniela Boehm and Prof. Paula Bourke for their valuable guidance and suggestions throughout this project. They provided me an opportunity to join ‘Plasma group’ and they were always there to guide me. Both have been a positive influence academically.

I also thank all academic and technical staff in Technological University Dublin for their assistance.

Finally, I express my profound gratitude to my family and my partner for their continuous support and encouragement throughout the years of study and research. I really appreciate them for being supportive and understanding during difficult periods.

I would also like to acknowledge the financial support from Science Foundation Ireland (Starting Investigator Research Grant 15/SIRG/3466).

Chapter 1: Introduction

Part of this introduction has been published (Book Chapter).

S. Ng, E. Tsoukou, S. Chaple, D. Boehm, P. Bourke (2020). Plasma treatment of liquids. Innovative Food Processing Technologies: A Comprehensive review, 610-634

DOI: 10.1016/B978-0-12-815781-7.00003-2

1.1 Atmospheric Cold Plasma (ACP) technology

Plasma was described first by Langmuir in 1930 as the fourth state of matter, which is a partially or fully-ionized gas, consisting of neutral molecules, free electrons, and positive and negative ions and constitutes ~99% of the universe (Niemira, 2012). Depending on the temperature and electron temperature, plasmas can be classified as thermal and non-thermal (cold) plasma. Thermal plasma is generated at high temperatures, reaching values of several thousands of degrees Kelvin (Scholtz *et al.*, 2015). In all plasmas that are generated in the presence of an electric field, electrons receive energy much faster than heavier particles. In cold plasmas, cooling of heavier particles, such as gas ions and uncharged atoms, is much faster than the energy transfer from heated electrons to their environment, which causes the gas to remain at low temperature.

There are numerous parameters that must be taken into consideration for the generation of cold atmospheric plasma sources depending on the application such as: temperature, chemical composition, air flow, frequency, voltage, pressure and sustainment of the electrical field (Conrads and Schmidt, 2000). Thus, each design is created specifically for its application.

ACP has been successfully used for inactivation of bacteria, fungi, viruses and also as an anticancer treatment (Weiss *et al.*, 2017; Laroussi, 2018). The antimicrobial effect of cold plasma against bacteria growing in a biofilm has been reported (Ziuzina *et al.*, 2015). Moreover, plasma has been reported to promote wound healing. Furthermore, ACP has offered advantages in the sterilization or cauterization and coagulation processes (López-Callejas *et al.*, 2018; Brun *et al.*, 2015).

1.2 Sources of ACP

In the last decade, atmospheric cold plasmas have been generated by many new technologies and the following are examples of those which have been developed for the biomedical sector; corona discharge, gliding arc, atmospheric pressure plasma jet, dielectric barrier discharge (DBD), plasma needle.

1.2.1 Corona discharge

Corona discharge was the first method used to generate cold atmospheric plasma. It can be defined as non-uniform discharges that develop near a sharp electrode spreading out towards a planar electrode (Tendero *et al.*, 2006). Corona discharge is produced by a strong electric field associated with a small diameter wire, needle, or sharp edge towards the electrode and it is powered by continuous or pulsed DC voltage.

1.2.2 Gliding arc (GA)

The Gliding arc is an electrical discharge which is generated between two or more electrodes connected to a high voltage power supply with high-velocity gas flow between the divergent electrodes. The arc moves from the ignition zone along the electrodes until the power system is not capable to compensate losses, which results from the increased plasma volume. Then the arc extinguishes and is rebuilt again in the ignition zone (Pawłat *et al.*, 2019).

1.2.3 Atmospheric Pressure Plasma jets (APPJs)

In the last years, atmospheric pressure plasma jets have received considerable attention due to their widespread applications in diverse fields. Different designs have been investigated for their use in medical applications like dentistry, wound healing, blood coagulation and surface sterilisation and they could be employed for large scale

application by moving the jet or by applying multiple nozzles. APPJs consist of a gas nozzle equipped with one or two electrodes (Figure 1.1). APPJs can differ in electrode configuration, size, gas, and electrical parameters (Winter, Brandenburg and Weltmann, 2015). Different working gases can be used such as helium (He), argon (Ar), mixtures of other gases or atmospheric air. The plasma is ignited inside the nozzle and transported to the outside as well as to the object to be treated by a flow of the working gas. In APPJs, the plasma is potential free (which is for some medical indications advantageous and necessary) and consists of reactive components generated such as excited atoms, free radicals, charged particles, reactive species etc.

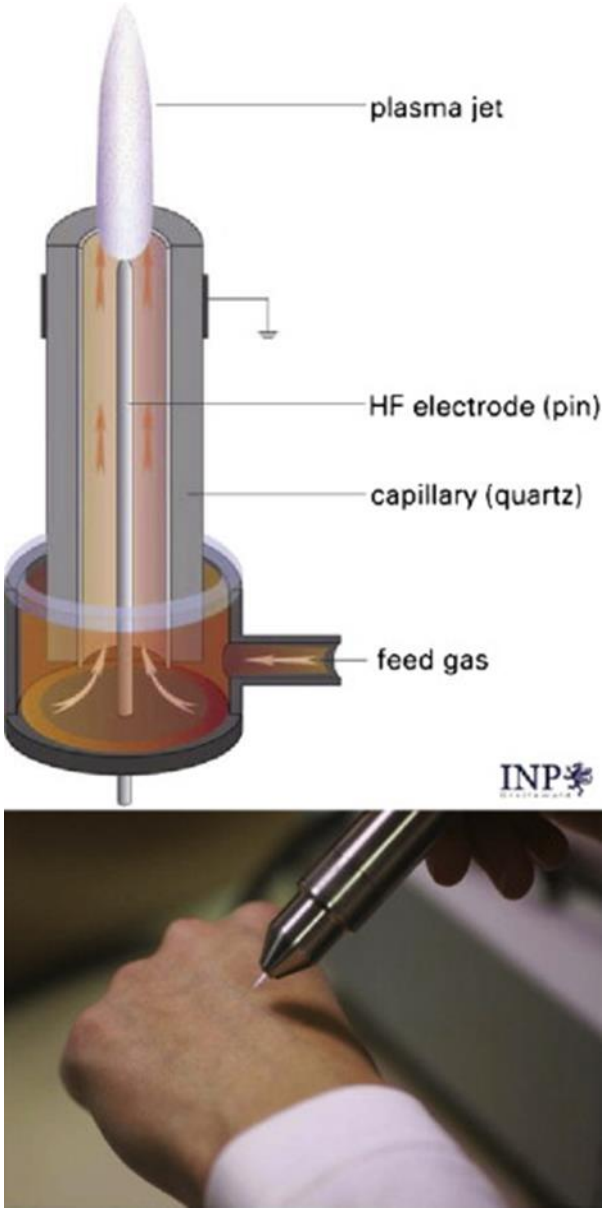

Figure 1.1: Schematic setup of the non-thermal atmospheric pressure plasma jet (top) and plasma jet in action (below) (Höntsch *et al.*, 2012).

1.2.4 Dielectric Barrier Discharge (DBD)

Dielectric barrier discharges have been known for more than a century - first experimental investigations were reported by Siemens in 1857 and focused on the generation of ozone (Kogelschatz, 2003). A DBD system was the device used in the first experiments on the inactivation of bacteria by Laroussi et al. (Laroussi, 1996). Dielectric barrier discharge is a specific type of AC discharge, which provides a strong thermodynamic plasma at moderate gas temperature (Figure 1.2). A DBD plasma

setup employs two electrodes, at least one of which is covered with a dielectric layer placed in the current path between the metal electrodes. Most widely used dielectric materials in DBD plasma setups are glass, quartz and some ceramic materials. One of the major differences between the classical and a DBD discharge is that in a classical discharge, the electrodes are directly in contact with the discharge gas and plasmas. On the contrary, in DBDs the electrode and discharge are separated by a dielectric barrier, which eliminates electrode etching and corrosion. The properties and amount of plasma generation depend on the working gas composition, distance between the electrodes, applied voltage and frequency (Kogelschatz, 2002). The DBD has motivated a wide range of applications and fundamental studies (Ehlbeck *et al.*, 2011).

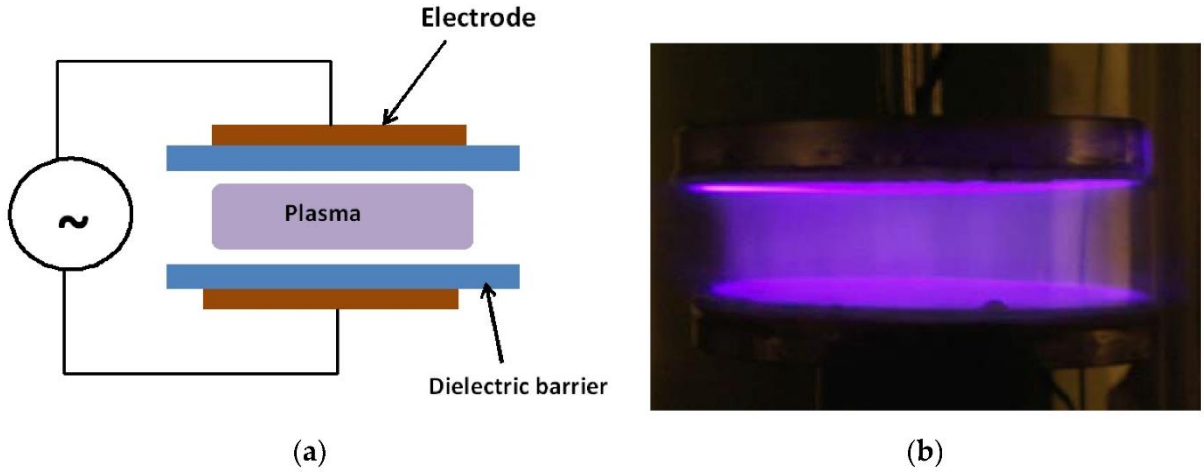

Figure 1.2 Figure Schematic (a) and a photograph (b) of an atmospheric pressure diffuse plasma generated by DBD (Laroussi, 2018).

1.2.5 Plasma Needle

The plasma needle is a small atmospheric, radio-frequency discharge, generated at the tip of a needle, which can be used for localized disinfection of biological tissues. The first plasma needle was designed by Stoffels et al., and used Helium as the feeder gas (Stoffels *et al.*, 2002). Plasma needles have been used for many applications such as

wound treatment and disinfection and dental applications (Stoffels *et al.*, 2002; Sladek *et al.*, 2004).

1.3 Plasma Medicine

Thermal (hot) plasmas were used in medicine for many decades in medical applications requiring heat, such as cauterization and blood coagulation. Argon (Ar) plasma coagulation method is used for bleeding control in surgeries and for vascular abnormalities treatment, such as hemangioma (Manner, 2008). Thermal pulsing nitrogen plasma developed by Rhytec Inc. is used in the cosmetics field for applications such as rejuvenation of skin and treatment of scars and wrinkles (Kilmer *et al.*, 2007). In the last years, there has been an increasing interest in applications of cold plasma in the medical field due to their potential for use on living tissues.

In the mid-1990s, experiments from the Plasma Science Laboratory of the University of Tennessee showed that glow discharge at atmospheric pressure could be used as a new sterilization technique (Laroussi, 1996). Therefore, plasma attracted the attention of the plasma physics community to new applications of ACP in biology and medicine (Figure 1.3). By the early 2000s, plasma research experiments were conducted in mammalian cells also. Short plasma treatment times were reported to enhance phagocytosis, accelerate the proliferation of fibroblasts, detach mammalian cells without causing necrosis, and eventually lead to apoptosis (Stoffels *et al.*, 2002). Today, the potential of plasma for biological and medical applications is known by the term plasma medicine. This field includes applications for: dentistry, dermatology, cancer treatment, wound healing, sterilization, disinfection, and decontamination. In the last decade, some ACP sources were approved for cosmetic and medical use. In 2008, a plasma jet named ‘the Rhytec Portrait®’ was approved by the US FDA for use in dermatology. Later, the Bovie J-Plasma® and the Canady Helios Cold Plasma and

Hybrid PlasmaTM Scalpel were approved for medical applications. In Europe, the first approval for a plasma jet was for kINPen® in Germany, in 2013, and later the PlasmaDerm® device (CINOGY GmbH) was also approved (Laroussi, 2018). Moreover, the CE certified MicroPlaSter β® (ADTEC Plasma Technology Co. Ltd., Fukuyama, Japan) associated with the Max Planck Institute for Extraterrestrial Physics, Garching, Germany, has been used as a plasma jet device for clinical trials using argon as a feeder gas (Heinlin *et al.*, 2013).

The Following pages explain different applications of non-thermal plasma in the medical field (Figure 1.4).

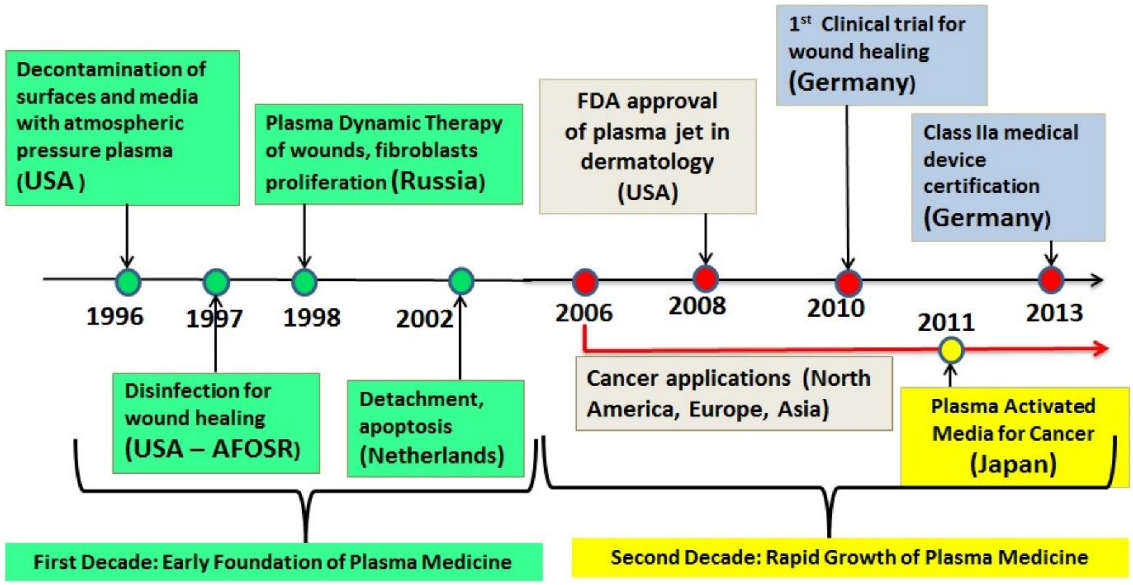

Figure 1.3 Timeline showing some milestones of the new field of the medical applications of ACP (Laroussi, 2018)

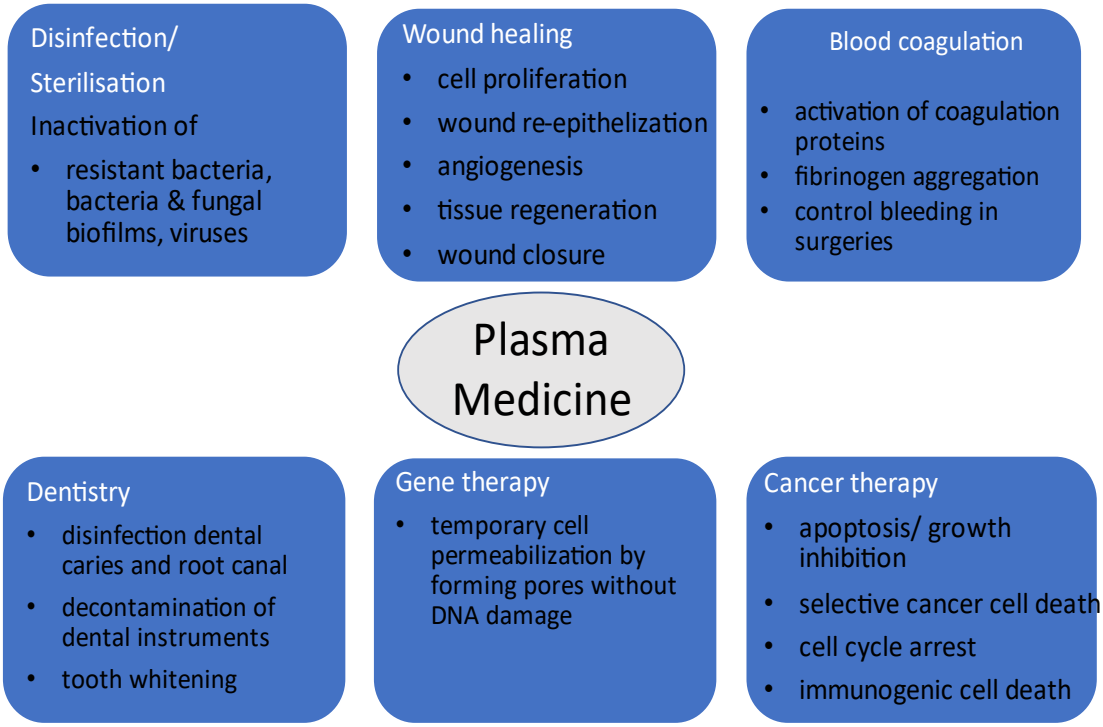

Figure 1.4 Applications of Plasma Medicine

1.3.1 Plasma Disinfection/Sterilisation

Bacterial contamination presents severe challenges in the healthcare sector, linked to hospital acquired infections caused by antibiotic resistant bacteria, such as *Enterococcus faecium, Staphylococcus aureus (S. aureus), Klebsiella pneumonia, Acinetobacter baumannii, Pseudomonas aeruginosa, Enterobacter* spp. acronymically dubbed 'the ESKAPE pathogens'. Factors that raise the risk of HAIs are catheters, surgeries, injections, and inadequate sterilization/decontamination of health care settings resulting in communicable diseases passing between patients and healthcare personnel (La Fauci *et al.*, 2019). Cold plasma is therefore considered as a novel technology that could be successfully applied to help solve some of the challenges described above.

Plasma disinfection has become one of the most widely studied biological applications of non-thermal plasma in the last decade. Studies have shown that different plasma

sources, working gases, experimental setups can inactivate a broad spectrum of microorganisms both in planktonic and biofilm forms (Ziuzina *et al.*, 2014; Patange *et al.*, 2019; Smet *et al.*, 2019). Formation of biofilms are more resistant to disinfectant agents than their planktonic forms. Daeschlein et al. observed that plasma generated by jet or DBD was effective in eradicating physiological and artificially contaminated flora on fingertips, making plasma an ideal candidate for skin disinfection and hand hygiene (Daeschlein *et al.*, 2012). Plasma's potential to inactivate multi drug resistant bacteria such as methicillin-resistant *S. aureus* isolates has also been reported (Napp *et al.*, 2016). Moreover, plasma has the potential to cause reduction in fungal biofilms. Direct treatment of *Candida albicans* biofilms with surface microdischarge plasma for 10 minutes resulted in 6 log reduction (Maisch *et al.*, 2012). Smet et al. reported that the food structure influences the cell inactivation behavior and bactericidal efficacy of cold plasma (Smet *et al.*, 2017).

In addition to bactericidal and fungicidal effects, virucidal effects of non-thermal plasma *in vitro* have been demonstrated (Filipić *et al.*, 2020). The inhibition of the human immunodeficiency virus (HIV) in cell culture, by a He plasma jet increased with increasing voltage and time of treatment. The highest voltage of 12 kV at 240 s caused virus inhibition; however, the cytotoxicity on the HeLa cell line was higher with increasing of voltage and time (Amiran *et al.*, 2016).

ACP technology has also been tested as an anti-adenoviral therapy for different human adenovirus species. All species were treated with plasma, and then the virus containing solution was added to eukaryotic cells and the viral load was determined. Results showed that ACP has a type-dependent effect on human adenoviruses and infectivity can even be increased for certain adenovirus types. Potential capsid proteins oxidized by ACP leading to different protein structure changes could be the cause of the

different response of adenoviruses subtypes (Bunz *et al.*, 2018). Argon plus 1% O_2 plasma treatment could cause more than a 6.0 $\log_{10}$ reduction of Feline calicivirus, a surrogate of norovirus virus after 15 s of exposure (Aboubakr *et al.*, 2015). The oxidation of viral capsid proteins by plasma generated by reactive oxygen and nitrogen species was thought to be responsible for the virucidal effect.

1.3.2 Plasma Cancer Treatment

Cancer is one of the main causes of death worldwide and many research studies have focused on finding new therapies to reduce the side effects caused by conventional therapies. Cancer progression is characterised by heterogeneous tumours which create a population of cells with different molecular features. Even if there have been significant advances in molecular testing and the discoveries of new therapeutics, promising treatments for cancer are still needed.

New innovative technologies for cancer therapy include use of nanomedicine, extracellular vesicles which can be used as drug delivery vehicles, natural antioxidants, gene therapy and expression of genes triggering apoptosis and wild type tumour suppressors, thermal ablation of tumours and magnetic hyperthermia (Pucci, Martinelli and Ciofani, 2019).

ACP's main advantage compared with conventional therapies could be a potential of selectivity toward cancer cells (Yan, Sherman and Keidar, 2017; Guerrero-Preston *et al.*, 2014; Mateu Sanz *et al.*, 2021), though this remains to be fully established.

Different cellular responses have been demonstrated following plasma treatment on cancer cells. Apoptosis, growth inhibition, selective cancer cell death, cell cycle arrest, DNA and mitochondrial damage, selective increase of ROS, or even immunogenic cell death have been suggested (Dubuc *et al.*, 2018) . Compared with normal cells, the

increased expression of reactive-species channels such as aquaporins and the lowered expression of catalase in cancer cells may cause such a selective rise of ROS in cancer cells (Yan, Sherman and Keidar, 2017).

The anticancer effects of cold plasma have been suggested by numerous groups in plasma medicine field, by using several cancer cell lines (Yan, Sherman and Keidar, 2017; Tanaka *et al.*, 2016). Brain, skin, breast, lung cancer, osteosarcoma, cervical cancer, chemotherapy resistant cancer cells such as glioblastoma cells are some of them. The growth of subcutaneous xenograft tumours or melanoma in mice can be halted after plasma treatment (Keidar *et al.*, 2011). Plasma treatment can also activate the immune response to attack tumours in *in vivo* experiments (Miller, Lin and Fridman, 2016).

Plasma is capable of production of cell based chemical reactive species such as hydrogen peroxide, which may affect eukaryotic cells through channel-facilitated transmembrane diffusion and corresponding ROS-based death pathways (Kim and Chung, 2016). One of the theories suggested regarding the selectivity of cancer cells to plasma exposure, is that cancer cells which express the p53 gene mutation are more sensitive to ACP treatment by activating ROS stress-response pathways (Ma *et al.*, 2014).

1.3.3 Plasma-induced Blood Coagulation

Blood coagulation is a natural response of the body in order to establish haemostasis following blood vessel injury. According to Bekeschus et al. platelets play a key role in regulation of plasma mediated haemostasis using the kINPen MED for *ex vivo* and *in vivo* experiments (Bekeschus *et al.*, 2017a). In another study, a DBD plasma treatment enhanced blood coagulation *in vitro* by activating coagulation proteins and

subsequent fibrinogen aggregation and by increasing Ca^{2+} ion concentration via a redox mechanism caused by hydrogen ions generated in plasma (Fridman *et al.*, 2006). Heslin et al. reported that the clotting of anticoagulated blood, and of anticoagulants-treated blood in particular, with plasma suggests that plasma-assisted coagulation is not dependent on Ca^{2+} ions (Heslin *et al.*, 2015). Interestingly, Yan et al. suggested that cold plasma can be an effective modality to control bleeding during surgical operation such as hepatectomy (Yan *et al.*, 2018). For these experiments, a pulsed cold plasma jet stimulated blood coagulation rapidly and effectively, by inducing a transparent white membrane mostly composed of platelet aggregation on the whole blood surface.

1.3.4 Plasma Dentistry

ACP technology has been applied in various fields of dentistry including surface modifications of dental implants, adhesion, caries treatment, endodontic treatment and tooth bleaching. The idea of using ACP for innovative dental procedures was first proposed by Sladek et al. in 2004, where the disinfection potential of a plasma needle against *Escherichia coli (E. coli)* was examined (Sladek et al., 2004*)*. In 2006, the same group demonstrated the antimicrobial effects of plasma against *Streptococcus mutans (S. mutans)* at conditions that would be attractive for dental clinical treatment. *S. mutans* is the most important microorganism for causing dental caries (Goree *et al.*, 2006).

Plasma has also been used for root canal disinfection. Plasma containing He/O_2 (20%) gas has a high rate of killing of *Enterococcus faecalis* (which is responsible for failure of root canal treatment due to biofilms) in *in vitro* dental root canal (Pan *et al.*, 2013). Dental caries, gingival, periodontal diseases, and oral mucositis can be caused due to the formation of biofilms on the tooth surface. ACP technology has been found to be

more efficient in killing of bacteria present in the dental biofilm *in vitro* than other conventional techniques such as chlorhexidine (Koban *et al.*, 2011). Plasma gas cleaning offers a safe and effective method for decontamination of dental instruments (Whittaker *et al.*, 2004). The effectiveness of ACP for sterilization of various dental instruments and equipment made of metals, rubbers, and plastics inoculated with *E. coli* and *B. subtilis* has been studied by Sung et al. (Sung *et al.*, 2013).

Park et al. demonstrated that the use of non-thermal plasma helium jet combined with 30% H_2O_2 significantly increases tooth whitening compared to 30% H_2O_2 application by itself, which is a conventional method for tooth whitening, without any thermal damage (Park *et al.*, 2011). Nam et al. used a plasma jet and reported that ACP has a greater capability for effective bleaching of teeth than carbamide peroxide alone and a combination of carbamide peroxide and diode laser without causing any thermal damage to the tooth (Nam *et al.*, 2013).

1.3.5 Plasma Applications in Wound Healing

Wound healing is a complex process involving inflammation, cell proliferation/migration, and skin remodelling. It is associated with the presence of a balanced content of chemical reactive species in which oxygen-dependent, redox-sensitive signalling represents an essential step in the healing cascade (Schmidt *et al.*, 2019b).

Effects of exposure of plasma on the wound for short time include blood coagulation and reduction of the microbial load in the area allowing the healing process to begin. *In vitro* studies have revealed that exposure to plasma has the potential to induce wound healing by the stimulation of cell proliferation and angiogenesis and

stimulation of tissue regeneration and wound closure, with reports on reduced scarring (Haertel *et al.*, 2014; Hasse *et al.*, 2016).

Ermolaeva et al. used Argon plasma and observed that a 5 day daily plasma treatment reduced bacterial loads on infected wounds of animals earlier than the control (Ermolaeva *et al.*, 2011). Nastuta et al. conducted experiments on a burn wound model on Wistar rat's skin and used a He APPJ to stimulate the wound healing process. Results showed that polyurethane wound dressing in combination with plasma assisted epithelization were positive for the induction of wound healing on burned skin (Nastuta *et al.*, 2011).The kINPen argon plasma jet device has been used for the treatment of full-thickness ear wounds in a murine model. A significant acceleration of wound re-epithelization was observed in days 3–9 (Schmidt *et al.*, 2017).

The beneficial effects of cold plasma have already been reported in clinical dermatology. Using the kINPen, pilot studies or case reports have been undertaken, showing a reduction of bacteria on wound surface (Daeschlein *et al.*, 2012), a skin recovery after laser-induced skin lesion (Metelmann *et al.*, 2013b; Metelmann *et al.*, 2013a), ulcer's wound healing (Ulrich *et al.*, 2015), and treatment of psoriasis vulgaris (Klebes *et al.*, 2014). Another clinical trial was conducted using the MicroPlaSter® to determine the bacterial load reduction on wounds (Isbary *et al.*, 2012), and treatment of infected skin blisters (Isbary *et al.*, 2011). Results for both studies showed significant microbial reduction on wounds.

Cold plasma modulates numerous cellular processes related to redox signaling and it is useful for targeting a plethora of specific, wound healing-related pathways (Bekeschus *et al.*, 2016). Schmidt et al. recently identified a number of targets such as

Nrf2, heme oxygenase, NAD(P)H quinone oxidoreductase 1, from gene and protein expression profiling that regulated accelerated wound healing (Schmidt *et al.*, 2019b).

1.3.6 Plasma for Gene Therapy

Introduction of genetic material into target cells is an important step for achievement of gene therapy. ACP has been tested as a novel transfection system for eukaryotic cells. Sakai et al. transfected different cell lines with pEGFP-C1 plasmid using a miniature atmospheric non-thermal plasma source producing an afterglow jet in helium, which is capable of creating pores between 4.8 and 6.5 nm in radius in the cell membrane (Sakai *et al.*, 2006). Leduc et al. reported the transfection of HeLa cells with the hrGFP-II-1 plasmid with a glow discharge torch, and reported that plasma could induce temporary cell permeabilization by forming pores ranging between 4.8 to 6.5 nm without any DNA damage (Leduc *et al.*, 2009).

1.4 Plasma Activated Liquids

Under *in vivo* conditions, living cells and tissue are surrounded by a liquid environment. Cold plasma affects biological targets not only directly but also indirectly through the medium, which has broadened the potential applications of cold plasma in medicine (Jablonowski and von Woedtke, 2015). One of the new challenges in the field of plasma medicine, is the biological activity of these plasma treated solutions. Based on discharge type, working gas, and the chemical composition of the surrounding environment, various chemical reactions induced by plasma can be initiated, with a number of resulting primary and secondary reactive chemical species penetrating or dissolving into the aqueous environment (Bruggeman *et al.*, 2016). After plasma treatment, plasma activated solutions are enriched with reactive oxygen and reactive nitrogen chemical species with lifetimes ranging from seconds to months,

with further use for potential biomedical applications (Shen *et al.*, 2016). These types of solutions are known as plasma-activated liquids, plasma-treated liquids or plasma-functionalized liquids. The solution obtained after the plasma treatment acts as a bioactive solution which can be transported to a target for specific biomedical applications, including places where plasma generation is not possible, such as cavities or body organs that cannot be exposed directly to plasma.

Different working gases can by utilised for generation of PAL, such as atmospheric air, nitrogen, oxygen and their mixtures in order to modulate the generation of the reactive chemical species in the liquid phase. In particular, plasma jets have been extensively studied for generation of PAL. These jets can generate PAL with and without ground electrodes (Laroussi, Lu and Keidar, 2017; Winter, Brandenburg and Weltmann, 2015).

In order for PAL to be efficient for biomedical applications, the delivery of chemical species through plasma needs to be sufficient and successful. This delivery can happen in two ways: (a) outside the liquid environment and (b) inside the liquid environment. In the first instance where the plasma source is operated outside the liquid environment, the solution can be placed below the plasma source (Norberg *et al.*, 2014), the chemical species are generated in the gas phase and then subsequently dissolve into the liquid. In the second case the liquid is in contact with the plasma, and additional reactive species generated through the plasma-liquid interactions are delivered directly into the solution. The concentrations of chemical species are higher in this setup, as the excited/ionized atoms combine with both ambient gas molecules and water molecules (Kaushik *et al.*, 2018). Many studies, have agreed that longer plasma treatment time of liquids can result in higher concentrations of long-lived chemical species (Chen *et al.*, 2016).

1.4.1 Reactive species in PAL

In the liquid phase, reactive species with a relatively long lifetime, such as hydrogen peroxide, nitrites, and nitrates, are produced by plasma–liquid interactions. In addition to these species other potentially less stable reactive species and different concentrations that vary depending on the target liquid solution type are important for their biological effects. Different PAL such as non-buffered and buffered solutions may carry different concentrations of reactive chemical species and maintain diverse antimicrobial properties and cytotoxic effects and may offer approaches for future targeted applications (Tsoukou *et al*., 2018). These differences can be based on the different composition of the liquids and antioxidants within the solutions as well as the plasma device and discharge conditions.

Hydrogen peroxide is taken as a general parameter for generation of ROS whereas nitrite and nitrate are representative parameters for generation of RNS/RONS. pH measurements are necessary for the characterization of the reactive conditions in the liquid phase. Consequently, these species are considered to be representative for more complex reactions chains with the participation of other ROS and RNS which are induced in solutions after exposure to plasma.

1.4.1.1 pH and ORP

pH is the measure of the hydrogen ion concentration of a solution. The pH value of plasma treated water decreases with increase of plasma treatment time and is one of the key players in the biochemical pathways of PAL. Oehmigen et al. reported that stable molecules like nitrous oxide, ozone, carbon dioxide, and traces of nitric acid and/or peroxynitrous acid were measured in plasma-gas phase by using Fourier-transform infrared spectroscopy. One of the theories for the reduction of pH in liquid

is that chemical reactions of the molecules mentioned from the gas phase with the liquid phase can result in acidification and generation of hydrogen peroxide and or peroxynitrite, respectively (Oehmigen *et al.*, 2011).

To evaluate the concentration of oxidizers in PAL, an indicator is required, and this is the oxidation reduction potential (ORP). ORP is the potential between the oxidation reaction occurring at the (positive) anode and the cathode (negative) reduction reaction in the electrochemical cell. ORP has been proposed as a real time monitor of the antimicrobial potential of a solution: the higher the ORP value, the higher the oxidation ability of a solution to take the electrons from the cell membrane of the bacteria (Ma *et al.*, 2015). As a result, cell membrane damage occurs and bacteria become unstable and leaky, resulting in cell death. The ORP value of PAL increases with plasma treatment time, indicating that the longer the plasma activation time, the higher the ROS level generated in the solution and the higher the antimicrobial potential (Xu *et al.*, 2016). These findings were also confirmed by OES experiments for investigation of the main excited active chemical species generated by plasma in liquids.

1.4.1.2 ROS

Numerous types of chemical analytical techniques with different selectivity, sensitivity and precision are used in the investigation of the chemical composition of PAL. Hydrogen peroxide (H_2O_2) is one of the most stable and easily detectable among the reactive oxygen species generated in PAL. Colorimetric measurements utilizing spectrophotometric assays are based on measuring the intensity of a color complex formed by reaction of the particular species with the relatively specific colorimetric reagent. One of the most common quantitative chemical analytic methods for measurement of H_2O_2 is the titanylsulfate assay. H_2O_2 reacts with titanium oxysulfate

($TiOSO_4$) to a yellow colour and then absorption can be measured by a spectrophotometer. The reaction between H_2O_2 with potassium iodide to iodine is another analytical colorimetric method of measurement of hydrogen peroxide concentration but this method is not specific for hydrogen peroxide but detects other ROS as well (Boehm *et al.*, 2016). Moreover, other commercial kits exist for detection of hydrogen peroxide such as the Amplex UltraRed reagent Fluorescence which is determined at λex 530 nm and λem 590 nm using a microplate reader (Tanaka *et al.*, 2016; Freund *et al.*, 2019b).

H_2O_2 is a ROS which plays a significant role in the antimicrobial properties of some PAW. Factors influencing the hydrogen peroxide generation can be the type of plasma discharge, working gas, applied voltage and discharge duration (Stará and Krcma, 2004). PAW generated by a helium APPJ contained 1.4 mM H_2O_2 after 180 s of activation, (Ikawa, Kitano and Hamaguchi, 2010) when in other studies H_2O_2 was estimated to be 22.4μM after 20 min of plasma treatment time (Shen *et al.*, 2016).

Hydrogen peroxide is an end-product of more or less complex reactions with the participation of other reactive oxygen species. Therefore, to obtain a more detailed insight into the ongoing oxygen chemistry in PAW, other species need to be identified. The precursors of hydrogen peroxide are hydroxyl (OH) and superoxide anion (O_2^-) radicals, but because of their radical character, they exist for a short time, thus making their detection in PAW more difficult. Moreover, generation and reactivity of hydroxyl radicals depends on pH of PAL (Tampieri, Ginebra and Canal, 2021). High concentration of nitrites and ROS such as hydrogen peroxide are thought to be important for the antibacterial activity, through the creation of reactive chemical species, such as peroxynitrous acid (Ikawa *et al.*, 2016).

1.4.1.3 RNS

Nirite can be detected by the Griess assay, which is based on the reaction with sulfanilic acid and N-(1-naphthyl)-ethylene diamine hydrochloride. Nitrate concentration can be detected by 2, 6-dimethyl phenol, and also measured via Griess assay (Wende *et al.*, 2015; Von Woedtke *et al.*, 2012). Nitrite and nitrate in aqueous solutions can also be measured by UV–visible absorbance spectroscopy with absorbance near 300 nm for nitrate and 360 nm for nitrite (Pavlovich *et al.*, 2014).

Reactive species generated in the liquid during plasma treatment can react to secondary products post-discharge. The post-discharge reactions between nitrites and hydrogen peroxide occurring in PAW can result in the generation of peroxynitrite (Lukes *et al.*, 2014) and nitrate and could be one of the reasons for a decrease in hydrogen peroxide concentration observed in some studies (Burlica *et al.*, 2010). Lukes et al. used phenol as a chemical probe to detect hydroxyl radicals (Lukes *et al.*, 2014). Phenol can react with hydroxyl radicals, ozone, nitric monoxide and nitrogen dioxide radicals, giving very specific oxidized or nitrated phenol products, detected by high performance liquid chromatography. In this study, peroxynitrite chemistry was shown to significantly participate in the bactericidal effects of PAW (Lukes *et al.*, 2014).

Machala et al. investigated peroxynitrite concentration in buffered and non-buffered solutions by the reaction with 2,7-dichlorodihydrofluorescein diacetate (H_2DCFDA) that converts to dichlorofluorescein under the action of ROS (Machala *et al.*, 2013). The measured fluorescent signal in PAW was significantly higher than the signal induced in plasma activated buffered solution.

1.4.2 Plasma activated Water (PAW)

Water is the least complex solution that can be treated by plasma. Water consists of H_2O and dissolved air species e.g. molecular oxygen or nitrogen. Water activated by cold plasma generates a low pH solution containing reactive oxygen and nitrogen species, known as PAW. PAW has been investigated for many applications such as disinfection, cancer therapy, wound healing.

1.4.3 Plasma activated Saline (PAS)

For the generation of plasma activated saline (PAS) different plasma systems have been reported such as DBD and plasma jets (Jablonowski *et al.*, 2013a). The chemical composition of PAS is very similar to PAW. Hydrogen peroxide, nitrites and nitrates are the most common long lived chemical species found in these solutions. Jablonowski et al. measured the related oxygen free radicals, hydroxyl and superoxide anion, in PAS, by using electron paramagnetic resonance spectroscopy, which offers a specific detection of free radicals in liquids (Jablonowski *et al.*, 2013a; Oehmigen *et al.*, 2011). Pavlovich et al. investigated ozone by the use of indigo dye (Pavlovich *et al.*, 2014). Several publications indicated that PAS is an effective solution for inactivation of microorganisms (Zhang *et al.*, 2019; Chen, Su and Liang, 2016).

In sodium chloride solution the chloride could be an origin of hypochlorite or hypochlorous acid formation as it is suggested in the literature for an argon and oxygen plasma jet (Wende *et al.*, 2015). In this research formation of hypochlorite caused by atomic oxygen is assumed ($Cl^- + O \rightarrow OCl^-$). Hypochlorite is a strong oxidant and has intense antimicrobial properties. More recently, in a study investigating PAS chemistry it was mentioned that the HeAPPJ did not cause ionic chloride to convert to harmful ionic chloride compounds, such as sodium hypochlorite and hypochlorous acid, because the pH did not change after plasma treatment (Cheng *et al.*, 2017).

1.4.4 Plasma activated Buffered solutions (PAPB/PAPBS)

In buffered solutions, hydrogen peroxide, nitrite and nitrate can be found after exposure to plasma. Phosphate buffered saline (PBS) is an example of a simple buffered solution. The more complex the liquid becomes, the more potential reaction partners need to be considered. Plasma-treated PBS (PAPBS) contains hydrogen peroxide and superoxide-like reactive species or/and their products which are responsible for strong antimicrobial properties (Yost and Joshi, 2015). PAPBS can induce severe oxidative stress in *E. coli* cells and reactive-oxygen species scavengers, α-tocopherol and catalase, protect *E. coli* from cell death (Yost and Joshi, 2015). The anti-cancer capacity of PAPBS has been evaluated by several groups in the plasma medicine field (Van Boxem *et al.*, 2017; Boehm *et al.*, 2016; Wende *et al.*, 2015; Yan *et al.*, 2017). Yan et al. showed that PAPBS is more stable than Plasma activated media (PAM), which is an advantage for the storage of this PAL solution (Yan *et al.*, 2016).

Dobrynin et al. investigated the chemical composition of PAPBS by measuring concentrations of hydrogen peroxide, superoxide (O_2^-), peroxynitrite, and singlet oxygen (Dobrynin, Fridman and Starikovskiy, 2012). Superoxide (O_2^-) was indirectly measured by hydrogen peroxide concentration in the presence of superoxide dismutase. Singlet oxygen was measured using the fluorescent dye Singlet-Oxygen Sensor Green reagent. Peroxynitrite, which is not only a free radical but also a powerful oxidant and is a product of the reaction of superoxide with nitric oxide, was measured using 2,7-Dichlorodihydrofluorescein.

1.4.5 Plasma activated Cell culture media (PAM)

ACP has been shown to have killing effects on cancer cells both *in vitro* and *in vivo*. One of the approaches in treating mammalian cells with ACP is through plasma activated media (PAM). PAM is produced by exposing cell culture media to plasma

and then applied onto the cells, so the cells interact only with RONS produced in the PAM. The effect on cells has been tested in various experimental setups aiming to find the most effective way of PAM production.

Dulbecco's modified Eagle's medium (DMEM) has been used extensively for generation of PAM (Adachi *et al.*, 2015; Höntsch *et al.*, 2012; Arjunan and Clyne, 2011; Yan *et al.*, 2017; Yan *et al.*, 2016). Yan et al suggested that high concentration of hydrogen peroxide in PAM was lost after 26 h at 8 °C and 22 °C (Yan *et al.*, 2016). The hydrogen peroxide decrease in PAM is due to the combined effect of the natural degradation of H_2O_2 in aqueous solution and the reaction between H_2O_2 and the components in DMEM such as cysteine and methionine. Arjunan et al. measured concentrations of H_2O_2, $^{\bullet}OH$, $ONOO^-$, $O_2^{\bullet-}$, $^1O_2$ and NO_2^- in DMEM (Arjunan and Clyne, 2011).

Jablonowski et al. used Rosewell Park Memorial Institute (RPMI) 1640 cell culture medium (Jablonowski *et al.*, 2015; Jablonowski *et al.*, 2013b; Jablonowski *et al.*, 2013a). In these studies hydroxyl radicals and superoxide anion radicals as well as hydrogen peroxide and nitrite were determined. Bekeschus et al. observed hydrogen peroxide and nitrite concentrations in the plasma treated RPMI 1640 medium (Bekeschus *et al.*, 2014). Different cell culture media have been regarded as a carrier for the dissolved plasma generated chemical species (Boehm *et al.*, 2016; Judée *et al.*, 2016; Kumar *et al.*, 2016).

Summarizing, this part gives an overview of reactive species detected in different liquids after plasma treatment. It can be stated that the detection of hydrogen peroxide, nitrite and nitrate as well as pH measurements are now established as basic parameters to characterize results of plasma–liquid interaction in general. As most important

precursors of hydrogen peroxide as well as nitrite and nitrate, hydroxyl radicals (OH), and superoxide anion radicals (O_2-), singlet oxygen ($^1O_2$), and nitric oxide (NO) were detected in different plasma treated liquids. It has to be stated that some or all of these ROS and RNS were identified in general in all liquids including water, buffered and non-buffered saline solutions and cell culture media but also after treatments with different plasma sources using different working gases, however concentrations varied greatly with plasma, treatment parameters and liquid composition.

1.5 Potential of PAL for biomedical applications

PAL generation is a promising new tool in the world of plasma medicine. PAL has shown some very promising results in relation to living tissue decontamination, blood coagulation, the destruction of cancer cells, and many other medical applications, such as wound healing, as a medical disinfectant for equipment, and even as a type of mouthwash for dental problems. It is a novel application because it offers the advantages of storability and ease of application. Some factors that can influence the efficacy of different PAL are the plasma exposure time, the plasma source, gas used, volume of solution, nature of solution, storage duration, and the storage temperature. The subsequent section discusses the potential of PAL for use in healthcare and the medical sector.

1.5.1 PAL as disinfectant

The search for novel techniques for microbial decontamination is currently the subject of a considerable number of investigations. Non-thermal plasma is a new approach to microbiological safety. Previous work has demonstrated that non-thermal plasmas can efficiently inactivate a wide range of microorganisms, including bacteria, fungi, viruses, bacterial spores and biofilms as discussed earlier. Plasma treated solutions have been demonstrated as disinfectants against bacteria such as *B. subtilis* (Sun et al.,

2012), *S. aureus* (Shen *et al.*, 2016) and also native microflora of food produce (Schnabel *et al.*, 2021). DBD was used to activate water for the decontamination of *E. coli* (J Traylor *et al.*, 2011), *Candida albicans* and *S. aureus* (Ercan *et al.*, 2014).

All artificial surfaces used in clinical practice and public health are prone to develop biofilms, and therefore present a source or risk of infections. Ercan et al. demonstrated a range of plasma-activated chemical solutions such as methionine, threonine, glucose, proline heparine which inhibited biofilm formation by multidrug-resistant bacterial pathogens such as carbapenem-resistant *Acinetobacter baumannii*, methicillin-resistant *S. aureus*, metallo-β-lactamase (NDM1)-positive *Klebsiella pneumoniae*, and *Enterococcus faecalis*, and prevented the formation of biofilms by about 70%. In conclusion, PAL such as plasma treated N-acetyl-cysteine, methionine, threonine, glucose, cysteine and proline could be used against planktonic cells and biofilm of various bacteria as a broad-spectrum agent that can inhibit biofilm formation on inanimate surfaces (Ercan et al., 2014).

Balan et al. demonstrated that PAW could be a high-level disinfection agent and an alternative method of disinfection for duodenoscope reprocessing, after current-standard manual cleaning (Balan *et al.*, 2018). For this study, the antimicrobial activity of PAW generated by a glide arc (GA) was investigated on four bacterial species (*E. coli, K. pneumoniae, A. baumannii,* and *P. aeruginosa*) that are usually involved in endoscopic retrograde cholangiopancreatography procedure-related infections and significant reductions in bacterial populations were achieved after 30 minutes of PAW treatment.

Dasan et al. reported the decontamination effect of a GA system on selected artificially contaminated surfaces (Dasan *et al.*, 2016). Kamgang-Youbi et al. showed that water

activated for 5 min with GA plasma contained high amounts of nitrites, peroxynitrite and hydrogen peroxide and showed strong bactericidal effects against 4 different microorganisms on different surfaces (Kamgang Youbi *et al.*, 2018). Pawlat et al. investigated the bactericidal effects of plasma activated water and phosphate buffer solutions and observed that non buffered solutions showed higher bactericidal activity (Pawlat *et al.*, 2019).

The efficacy of each PAL depends on the species of microorganism and the reactive species produced in the PAL. It has been suggested that direct exposure to plasma can be more effective against Gram-negative bacteria than Gram-positive bacteria, which might be attributed to the different cell wall structures (Mai-Prochnow *et al.*, 2016). Ji et al. reported that plasma treatment of bacterial suspension indicated that *E. coli* was more susceptible than *S. aureus* (Ji *et al.*, 2018). More recently, Xiang et al. supported the same statement by using PAW for inactivation of *E. coli* O157:H7 and *S. aureus* (Xiang *et al*., 2019). Laroussi et al. reported morphological changes in *E. coli* and not in *B. subtilis* using scanning electron microscopy after exposure to direct plasma treatment (Laroussi, Mendis and Rosenberg, 2003). The thick peptidoglycan layer of the Gram-positive bacteria poses a barrier for plasma reactive species to penetrate through the cell wall and affects its antimicrobial efficacy.

1.5.1.1 Antimicrobial stability and storability of PAL

The stability of the reactive species in solutions is one of the most important issues to determine the inactivation effectiveness and shelf-life of PAL. Studies using different gases and plasma systems have shown that PAL chemistry of long lived chemical species can be retained stable up to a period of 30 days after the generation of the solutions (Vlad and Anghel, 2017; Boehm *et al.*, 2016). Traylor et al. have shown that distilled water, which was plasma treated for 20 min retained its antibacterial activity

for 7 days. Storage conditions are important factors affecting the chemical composition and antimicrobial potential of PAL, but little information has been published about PAL's stability. Shen et al. investigated the bactericidal effects of PAW stored at four different storage temperatures: 25 °C, 4°C, −20°C, −80°C against *S. aureus* (Shen *et al.*, 2016). PAW stored at −80 °C caused approximately 4 log reduction after a 30-day period, with nitrites and hydrogen peroxide contributing synergistically to microbial inactivation. The storage temperature did not exert significant influence on pH and conductivity of plasma activated reverse osmosis water over 96 h storage time at 3°C or 24°C (Figueira *et al.*, 2018).

1.5.1.2 Fungicidal and virucidal effects of PAL

Except of the bactericidal effects of PAL, the fungicidal and virucidal effects of PAL have been reported recently as well. Comparison of antimicrobial activity of PAW between *Staphylococcus epidermidis*, *Leuconostoc mesenteroides* (as models of Gram-positive bacteria), *Hafnia alvei* (a Gram-negative type of bacteria) and *Saccharomyces cerevisiae* as a yeast model showed that PAW was more effective against bacteria than yeast (Vlad and Anghel, 2017).

More recently, Su et al. explored the efficacy of distilled water, NaCl, and H_2O_2 treated with plasma for 10 min against Newcastle disease virus, as an antiviral solution (Su *et al.*, 2018). The authors demonstrated that reactive oxygen and nitrogen species detected in different plasma activated solutions, including short-lived $OH^{\cdot}$ and $NO^{\cdot}$ and H_2O_2 may be able to change the morphology, destroy the RNA structure, and degrade the protein of the virus, thus resulting in virus inactivation.

1.5.2 Anticancer effects of PAL

New cancer therapies are needed to avoid the side effects commonly seen with traditional surgery, chemotherapy, and radiation therapy and address the problem of cancers unresponsive to current treatment methods. Indirect treatment of cancer cells using PAL has been recently proposed as an important new chemotherapy approach for resistant cancer cell lines that respond poorly to other anticancer treatments and also by avoiding surgeries and allowing multiple local administrations (Solé-Martí *et al.*, 2021).

Plasma activated media or plasma stimulated media have been reported to have anti-tumour effects against several types of cancer such as glioblastoma brain tumour cells (Tanaka *et al.*, 2011), ovarian (Utsumi *et al.*, 2014), pancreatic (Hattori *et al.*, 2015), lung carcinoma (Adachi *et al.*, 2015), head and neck squamous cell carcinoma (Chauvin *et al.*, 2018), and osteosarcoma (Mateu Sanz *et al.*, 2021) (Mateu Sanz *et al.*, 2020) . Intraperitoneal administration of PAM decreased the formation of peritoneal metastatic nodules by 60% in the mouse model in a study using a peritoneal metastasis in gastric cancer mouse model (Takeda *et al.*, 2017).

Both plasma activated media and other solutions such as PBS are able to cause inhibition of cancer cell growth. Hydrogen peroxide has been reported as one of the key plasma generated reactive species that contributes to the cancer inhibition potential of cold plasma (Bekeschus *et al.*, 2014; Boehm *et al.*, 2016).

The anti-cancer effects of PAM and PAPBS on pancreatic adenocarcinoma cells and glioblastoma cells have been compared by Yan et al (Yan *et al.*, 2017). The effect of different PAL on cancer cells is cell-dependent and dose-dependent. Specifically, pancreatic and brain cell lines were vulnerable to PAM and PAPBS respectively. The

concentrations of intracellular ROS of two cell lines in different PAL showed that the different cellular responses to each PAL might cause the different vulnerabilities of cells to PAL.

Cell culture media usually is a complex liquid, consisting of many components, and the reaction between plasma and media results in a more complicated solution, probably unsuitable for clinical use. To simplify the ingredients of PAM, solutions with simpler compositions, such as PBS, Ringer's lactate solution or saline might be more suitable for cancer applications. Tanaka et al. demonstrated a tumourigenicity inhibition effect of plasma activated Ringer's lactate solution on human glioblastoma cells (Tanaka *et al.*, 2016). Of the four components in Ringer's lactate solution, only lactate was found to exhibit anti-tumour effects through activation by plasma, which leads to the generation of acetyl and pyruvic acid-like groups. The antitumour effects of plasma activated lactated Ringer's solution have also been demonstrated on pancreatic cancer cells *in vitro* and *in vivo* by Sato et al. (Sato *et al.*, 2018). Intraperitoneal injection of PAL in mice which had been injected with pancreatic cancer cells before, showed that PAL can inhibit peritoneal metastases.

1.5.3 Role of PAL in blood coagulation

Very few studies have been conducted in the field of plasma activated liquids for blood coagulation. The facilitation of blood coagulation by non-thermal plasma-generated water is a novel method that could be especially useful for control of oozing bleeding and prevention of postoperative complications due to decreased tissue coagulation (Ikehara *et al.*, 2015).

1.5.4 PAL in Dentistry

Most commonly, chlorhexidine is used as a mouthwash, but it can cause tooth stains and erosion, and new antimicrobial dental solutions are needed. Li et al. investigated the antimicrobial effects of PAW as a novel mouthwash (Li *et al.*, 2017). For that study, the antimicrobial activity of PAW was tested against three oral pathogens which were: *S. mutans*, *Actinomyces viscosus (A. viscosus)* and *Porphyromonas gingivalis (P. gingivalis)*. The results showed reduction of *S. mutans* within 60 sec, of *A. viscosus* within 40 s, and of *P. gingivalisin* less than 40 s after exposure to PAW.

Tooth bleaching is a common cosmetic dental treatment worldwide. Cheng et al. performed tooth bleaching by using a He APPJ with saline solution to avoid ozone and hydrogen peroxide harm and achieved high bleaching efficacy (Cheng *et al.*, 2017). No harmful ionic chloride compounds in the solution were found, making ACP technology a promising and portable tooth bleaching solution.

1.5.5 PAL for wound healing

Evidence for therapeutic effects of PAL in wound healing is limited for both *in vitro* and *in vivo* animal studies. PAL might be more convenient as it can retain ROS and RNS and has similar biological effects to direct plasma treatment without the need for a plasma device on site. At the moment, studies investigating the application of PAL for wound healing are limited and further research is needed to reveal its potential in clinical trials in dermatology.

Xu et al. investigated the effects of plasma treated tap water on skin wound healing in full-thickness skin wounds of mice (Xu *et al.*, 2020). 100 mL of tap water were activated by a portable DBD for 5 min before being used to treat the infected wounds of mice by applying 10 mL of PAW to the wound area. PAW was efficient in the

inactivation of *Pseudomonas aeruginosa*, *E. coli*, *S. aureus* and *Salmonella paratyphi-B*, which are bacteria that commonly infect wounds. It was also reported that wounds had completely healed on day 17, while the wounds of the control group healed on day 23. The number of inflammatory cells reduced after treatment with PAW and results of biochemical blood tests including liver function, kidney function, blood lipids, blood glucose, inorganic ions, or antioxidants and histological analysis of major internal organs (heart, liver, spleen, lung, and kidney) in the mice showed that PAW had no obvious side effects.

For wound healing, antiseptic and tissue regenerating properties are needed. Lou et al. studied the generation of a particular composition of gases for treatment of cell culture media for wound closure (Lou *et al.*, 2020). Briefly, authors treated media with He and He/Ar plasma for evaluation of HaCaT cell proliferation, migration, and protein expression. He/Ar plasma treated media possessed more potent activity than He PAM for promoting keratinocyte migration. Results showed that the He/Ar plasma PAM, which consisted of reactive nitrogen and oxygen species, reduced E-cadherin and triggered p-ERK, cyclin D1, and Cdk2 expression, which are crucial factors for cell proliferation, resulting in promotion of keratinocyte proliferation and migration and the acceleration of cutaneous wound healing.

1.6 Mechanisms of interaction of PAL

1.6.1 Effects of PAL on bacterial cells

1.6.1.1 Effects of ROS

Water activated by non-thermal plasma near room temperature and at atmospheric pressure will generally consist of aqueous reactive species such as hydrogen peroxide, nitrite and nitrate ions, acidic pH values and a high oxidation potential (ORP) which

may play a crucial role in the microbial inactivation potential of PAW (Shen *et al.*, 2016; Tian *et al.*, 2015).

Although the exact changes that occur are not yet fully known, the interaction of the chemical species formed in the plasma with the cells begins at the surface of the cell where the chemical destruction of the cell wall, membrane and associated components can occur. The structural complexity of the cell wall and differences between Gram-positive and -negative bacteria adds another layer of complication to the investigation of bacterial membrane oxidation. ROS such as O, OH and O_2 are the key inactivation agents in direct plasma inactivation, and plasma-induced oxidative stress is believed to cause cell damage and death (Laroussi and Leipold, 2004). The bacterial membrane which is primarily composed of organic compounds, such as lipids, proteins and polysaccharides, plays an important role in susceptibility to biocidal challenges. The release of intracellular components such as nucleic acids and proteins is an indicator of membrane damage. Lukes et al. reported that the generation of ROS in PAW and their transport into the microbial cells is able to cause damage in cells through breakdown of nucleic acids, destruction of proteins and other internal components of the cells (Lukes, Locke and Brisset, 2012). The antimicrobial effects of hydrogen peroxide have been reported in numerous papers, and it involves the formation of OH● through the Fenton or Haber-Weiss reaction resulting in oxidative damage by stimulating DNA strand breaks and damage to other cellular components (Martins and Meneghini, 1994).

Tian et al. investigated the inactivation effects of PAW generated by a direct current atmospheric pressure cold plasma microjet beneath the water surface. Results showed that the cell membrane integrity and membrane potential of *S. aureus* were destroyed by PAW (Tian *et al.*, 2015). Moreover, the authors investigated the formation of ROS

in PAW and reported that a significant increase of intracellular ROS was induced by PAW, and consequently cause of oxidative stress in cells and contribution to their death. Recently Li et al., reported that the active species such as atomic oxygen, hydroxyl radical, and hydrogen peroxide, generated in PAW caused changes to the permeability of the bacterial cell membrane, and resulted in a dramatic leakage-release of intracellular DNA and proteins from *S. mutans*, *Actinomyces viscosus*, and *Porphyromonas gingivalis* which are three pathogenic species of the oral cavity (Li *et al.*, 2017). The leakage of intracellular DNA and proteins was lowest from *S. mutans* of all three species, which indirectly suggests the importance of the cell wall in the inactivation effects of the three bacteria. Scanning and transmission electron microscopy images showed that the normal cell morphology was changed by varying degrees. The interaction of important ROS generated by plasma with bacterial peptidoglycan by means of reactive molecular dynamics simulations was investigated by Yusopun et al. (Yusupov *et al.*, 2013). The authors showed that ROS could break bonds of peptidoglycan of the bacterial cell wall, which consequently lead to the destruction of the cell wall.

Lipids are the macromolecules most vulnerable to oxidation in the cell membrane. The membrane and lipids are attacked by ROS that can abstract a hydrogen atom from a methylene group, thus resulting in the cross-linking of fatty-acid chains to form transient pores in cell membrane. The hydroxyl radical is an important ROS which primarily targets the outer membrane of the microbial cells and can initiate lipid peroxidation of the lipid bilayer in the cell membrane (Ayala, Munoz and Arguelles, 2014). Lipid oxidation is a chain reaction that produces chemical products, such as malondialdehyde (MDA), as its final product. Lipid reactions with •OH radicals proceed mainly via H abstraction from the unsaturated carbon bonds of the fatty acids,

which in the presence of oxygen, causes lipid peroxidation and subsequent formation of MDA. Dolezalova et al. has reported the effect of plasma jet on bacterial cells suspended in liquid to increase bacterial inactivation and proposed an increasing concentration of MDA in the plasma-treated water (Dolezalova and Lukes, 2015). According to Joshi *et al*. who investigated bacterial cells in phosphate buffer saline solution, ROS such as singlet oxygen generated during plasma treatment, were responsible for membrane lipid peroxidation, and scavengers, such as α-tocopherol, were able to significantly inhibit lipid peroxidation and oxidative DNA damage of *E. coli* cells (Joshi *et al.*, 2011). The bactericidal effects correlated again with the oxidative stress induced in cell membranes, and indicated that cell membrane peroxidation by ROS is an important mechanism in plasma disinfection (Machala *et al.*, 2013).

Generally, intracellular RONS can accumulate through two pathways (Kaushik *et al.*, 2018). The first is that by which RONS produced extracellularly by plasma can move into the cell by active transport across the bilayer or the transient pores in the bacteria's cell membranes. The second is the external oxidative stress, which can induce oxidative stress in the cell, with consequent increase of intracellular RONS. Furthermore, protons in PAW can also flow into the cell via the damaged bacterial cell membrane and decrease the intracellular pH.

1.6.1.2 Effects of RNS on bacterial cells

Nitrates and nitrites are generated in PAW through the dissolution of nitrogen oxides that are formed in the ambient air plasma by gas-phase reactions of dissociated N_2 and O_2 or H_2O (Lukes *et al.*, 2014; Pavlovich *et al.*, 2014). The table below describes current challenges in bactericidal activity of PAL and highlights the chemical species

responsible for these inactivation processes performed in plasma medicine research (Table 1.1).

Peroxynitrite (ONOO-) has been suggested to play an important role in the biological effects of PAL. Machala et al. reported that the bactericidal effects correlate with the relative amount of the formed peroxynitrite, which is well-known for its high antimicrobial effectivity (Machala *et al.*, 2013). These qualitative measurements indicated an important role of ONOO in microbial inactivation and a correlation to lipid peroxidation of bacterial cell membranes. The estimated concentrations of peroxynitrites were, however, too low to claim their effect as the key player in bactericidal inactivation. Recently, the peroxynitrite concentration of PAW treated for 30 min with plasma was reported at 20.2 μM and identified to have a crucial role in the microbial inactivation originating from the synergistic plasma effects against *E. coli* (Zhou *et al.*, 2018). Lukes et al. reported that peroxynitrite chemistry in PAW had significant effects on the antibacterial properties of PAW and that despite being short its half-life was sufficient to diffuse into cells and lead to bactericidal inactivation (Lukes *et al.*, 2014). Additionally, ONOOH participates in the formation of peroxynitric acid (O_2NOOH) by the reaction with hydrogen peroxide which can also contribute to the bactericidal properties of PAW (Ikawa *et al.*, 2016).

Oehmigen et al. also investigated the possible formation mechanisms of peroxynitrite or peroxynitrous acid, which were assumed to exist in PAL as suggested by means of theoretical considerations (Oehmigen *et al.*, 2011). Initially, it was shown that a 30 min delay between plasma treatment of the liquid and addition of the bacterial suspension caused a bactericidal effect which was reduced but still detectable. Thus, it was concluded that a more or less stable chemical modification of the liquid environment might be the cause for the reduced antimicrobial efficacy after 30 minutes

in PAW and sodium chloride solution. It is possible that chemical reactions in liquid phase will have peroxynitrite or peroxynitrous acid as transient products in some stage of the reactions (Oehmigen *et al.*, 2011).

As mentioned earlier, depending on the nature of the discharge gas (argon, helium, air, oxygen, nitrogen or their mixtures), RONS are generated in the gas or liquid phase, after which they are dissolved in the liquid. The antibacterial effect of PAW generated by N2 + 0.5 wt% nitric acid vapour plasma was recently reported to be more efficient for the inactivation of bacteria and also contained larger amounts of RNS and ROS, compared to PAW generated without vapor system, indicating that a high concentration of both nitrites and hydrogen peroxide is important for the antibacterial activity, through the creation of other RONS, such as peroxynitric acid and O2•− (Shaw *et al.*, 2018). Ikawa et al. reported that O2•− is mainly responsible for the bactericidal activity of PAW (Ikawa *et al.*, 2016). Moreover, the authors also reported that the generation of O2•− does not require the presence of oxygen, as it is produced by peroxynitric acid.

1.6.1.3 Synergistic effects of chemical species on bacteria

In 2008, the group of Chen et al. studied the pH decrease for inactivation of *E. coli* (Wei Chen, Lee and Chang, 2008). It has been demonstrated that the antibacterial efficiency of an acidified solution consisting of NO_2^-, NO_3^- ,and H_2O_2 can be equal to that of PAW prepared by glide arc discharge (Naïtali *et al.*, 2010). Acidification of water is mostly attributed to formation of nitric and nitrous acid from RNS generated during plasma discharge (Vlad and Anghel, 2017). According to literature, both ROS and RNS are important for the bactericidal activity (Shaw *et al.*, 2018). The synergistic effect of nitrates, nitrites, and H_2O_2 in an acidic environment has been shown by Xiang et al., who reported the lethal effects of PAW on *Pseudomonas deceptionensis* CM2

(Shen *et al.*, 2016). PAW treatment disrupted the outer and cytoplasmic membranes of the bacteria, which was accompanied by leakage of intracellular components such as nucleic acids and proteins from the cells. High RONS contents led to bacteria killing through inhibition of the antioxidant machinery, which damages the membrane protein repair chaperone, as well as DNA repair cascade (Vatansever *et al.*, 2013). Consequently, these long-lived chemical species were considered to be responsible for reactions induced in liquids by plasma and subsequent microbial inactivation.

Table 1.1 Role of chemical species in bactericidal effects of different plasma activated liquids.

PAL	**Important chemical species**	**Experimental findings**	**References**
PAW	ROS	Cell damage through breakdown of nucleic acids. Destruction of intracellular components of the cell	(Lukes, Locke and Brisset, 2012)
PAW	ROS	Destruction of cell membrane integrity and membrane potential	(Tian *et al.*, 2015)
	atomic oxygen, hydroxyl radical hydrogen peroxide	Altered permeability of cell membrane. Leakage-release of intracellular DNA and proteins	(Li *et al.*, 2017)
PAPBS	singlet oxygen	Membrane lipid peroxidation	(Joshi *et al.*, 2011)
	ROS	Oxidative stress	(Machala *et al.*, 2013).
	Peroxynitrite	Importance of peroxynitrite and correlation to lipid peroxidation of cell membranes	(Machala *et al.*, 2013).
PAW	Peroxynitrite	Importance of peroxynitrite role in *E.coli* inactivation	(Zhou *et al.*, 2018)
PAW	peroxynitric acid	Peroxynitric acid contributes to the bactericidal properties of PAW	(Ikawa *et al.*, 2016)
PAW	RNS	Bacterial inactivation is enhanced by reactive nitrogen species	(Shaw *et al.*, 2018)
PAS	Acidic pH	When pH exceeded 3–4, the antibacterial effectiveness dropped	(Oehmigen *et al.*, 2011)
PAW	cocktail solution	Antibacterial efficiency of an acidified solution consisting of NO_2^-, NO_3^- and H_2O_2 can be equal to that of PAW	(Naïtali *et al.*, 2010).
PAW	RONS	Disruption of the outer and cytoplasmic membranes of the bacteria. Leakage of intracellular components	(Shen *et al.*, 2016)

1.6.2 Effects of PAL on mammalian cells

In connection with basic research on the role of liquid phases for the transmission of biological plasma effects to mammalian cells it was found that by plasma treatment liquids can acquire biological activity. Research in this field is mainly focussed on the applicability of PAL to inactivate cancer cells e.g. in the case of disseminated tumours in the abdomen (Tanaka *et al.*, 2015). However, the understanding of the mechanism of plasma-assisted processes is still limited.

1.6.2.1 Effects of RONS on mammalian cells

Cytotoxicity of PAL results from the generation of ROS and RNS in the plasma discharge and their subsequent transfer to the liquid environment (Table1.2). Incubation with PAL can result in increased oxidative stress in cells. Plasma generated reactive chemical species can cause altered mitochondrial dysfunction, caspase activation, cell cycle arrest, apoptosis, senescence or necrosis (Hirst *et al.*, 2016).

A dominant function for H_2O_2 in the cytotoxic effects PAL has been established through a number of studies but, importantly it has also been shown that this compound is not the only chemical species that causes the cytotoxic effects. Hydrogen peroxide can induce DNA damage, cause cell cycle arrest and trigger apoptosis and its toxicity is determined largely by the cellular anti-oxidant status. Hydrogen peroxide can diffuse freely through the cell membrane without disturbing it (Kaushik *et al.*, 2018). Hydrogen peroxide can cooperate with other products such as organic peroxides and subsequently interfere with the membrane structure and increase the permeability of the cell membrane, and then induce cell injury, followed by the influx of extracellular reactive species from PAL.

The role of plasma chemical species may be more accurately investigated in experiments using simple non-buffered or buffered solutions as they are devoid of amino acids, vitamins and other compounds, such as glucose or serum, which are normally found in different cell culture media. The presence of these nutrients might interfere with the formation of ROS such as hydrogen peroxide, during/after exposure to plasma discharges.

Boehm and colleagues investigated the cytotoxic effects of PAW and reported that cell growth reduction was similar between two cancer cell lines and two non-cancer cell lines (Boehm *et al.*, 2018). Moreover, cytotoxic effects of PAW and PAPBS were correlated with the hydrogen peroxide concentration (Boehm *et al.*, 2016; Boehm *et al.*, 2018). Cytotoxic effects of PAW exceeded those of the corresponding hydrogen peroxide concentrations (Azzariti *et al.*, 2019). Girard et al. investigated the role of long-lived chemical species in PAPBS and reported that hydrogen peroxide could not account alone for the toxicity in healthy and cancer cell lines, but nitrites and hydrogen peroxide synergistically were able to trigger cell death (Girard *et al.*, 2016).

The reduction of pH in solutions after exposure to plasma has been established through a number of studies. In acid liquids such as PAL, peroxynitrous acid can be generated by the interaction of nitrites and hydrogen peroxide (Brisset and Pawlat, 2015; Starodubtseva, Cherenkevich and Semenkova, 1999). In the two previous studies the pH of PAL was acidic, so it is reasonable to think that peroxynitrite could be formed. Peroxynitrite can induce cell death by both cellular apoptosis and necrosis. Cell death depends on the production rates and endogenous antioxidant levels (Szabo, Ischiropoulos and Radi, 2007) The cytotoxic effects of other plasma induced RONS cannot be excluded and could contribute, to a lesser extent, to plasma toxicity.

1.6.2.2 Mechanisms of cell damage and Apoptosis

ROS cause a reduction in cell proliferation, and it is known that ROS can kill cells through either apoptosis or autophagy (Santos *et al.*, 2018). Recently, Azzariti et al. reported that PAM might inhibit proliferation through various cell death mechanism such as apoptosis and autophagy and lead to immunogenic cell death (Azzariti *et al.*, 2019). In a study investigating six different PAL for their anticancer potential against colorectal cancer, it was found that incubation with PAL resulted in reduction of metabolic activity and created distinct morphological alterations and a reduction in cell motility (Freund *et al.*, 2019a). PAM, containing hydrogen peroxide and RNS, has been reported to initiate the apoptotic cascade in mammalian cells with selectively higher cytotoxicity in cancerous cell lines (Adachi *et al.*, 2015). Plasma treated RPMI-1640 had anti-proliferative effect in parallel with intracellular ROS up-regulation on chemo-resistant cells as well as parental cells, and PAL with NAC treatment reversed the anti-tumour effects, suggesting that most of its effects are attributable to ROS (Utsumi *et al.*, 2013). NAC has been widely used as an antioxidant and is well investigated for its reactivity for ROS. Different cells have different redox-buffering systems to maintain intracellular redox homeostasis, and disruption of the balance leads to transient or permanent cell cycle arrest and induces cell apoptosis (Barrera, 2012; Pelicano, Carney and Huang, 2004). The presence of FBS in cell culture medium was found to play a protective role in cancer cells, probably due to the scavenging effects of ROS, resulting in lower ROS levels in the culture medium (Yan, 2014).

RONS present in PAL can cause damage to the DNA structure by alteration of the hydrogen bonds between the complementary bases in DNA. This DNA oxidation is associated with activation of poly(ADP-ribose) polymerase-1 (PARP) (Kaushik *et al.*,

2018). Adachi et al. reported that hydrogen peroxide and/or its derived or cooperating reactive oxygen species in PAM reduced the mitochondrial membrane potential, downregulated the expression of the anti-apoptotic protein Bcl2, activated poly (ADP-ribose) polymerase-1, and released apoptosis-inducing factor from mitochondria with endoplasmic reticulum stress. Caspase-independent apoptosis in cells by induction of a spiral apoptotic cascade, involving the plasma membrane was also reported (Adachi *et al.*, 2015). Moreover, it is possible that membrane injuries by hydrogen peroxide-cooperating charged species could also increase the permeability of membranes to extracellular reactive species.

In 2011, Tanaka et al. reported that PAM induced apoptosis in glioblastoma cells via a caspase 3/7 pathway (Tanaka *et al.*, 2011). Induction of apoptotic cell death is beneficial compared to induction of necrosis, another type of cell death, because necrosis often causes inflammation. The authors showed that incubation of cancer cells with PAM resulted in downregulation of both total AKT expression and phosphorylated AKT (at Ser 473). AKT activation is partially responsible for inhibiting apoptosis (Haanen and Vermes, 1995), suggesting that apoptosis was induced in PAM-treated cells through downregulation of the activity of the PI3K/PTEN-AKT signal transduction pathway.

Table 1.2 Effects of different plasma activated liquids on healthy and cancerous mammalian cells.

PAL	**Cell line(s) used/species**	**Plasma system**	**Effects**	***In vitro/in vivo***	**References**
H_2O	HeLa U373MG HaCaT CHO-K1	DBD	Cytotoxic effects	+/-	(Boehm *et al.*, 2018)
PBS	CT26 MC38 PDA6606 HaCat Balb/C	kINPeN	Apoptosis, cell cycle arrest, upregulation of ICD markers in vitro, morphological changes elevated numbers of intratumoural macrophages increased T cell activation	+/+	(Freund *et al.*, 2019b)
PBS	A375, B16, A172	DBD	strong reduction of proliferation in	+/-	(Daeschlein *et al.*, 2018)
PBS	NHSF MRC5Vi HCT116	jet	Synergistic Effect of H_2O_2 and NO_2 in Cell Death	+/-	(Girard *et al.*, 2016)
H_2O, PBS, Saline, PB	CHO-K1	DBD	Distinct cytotoxic effects, depending on chemical composition of each solution	+/-	
hydroxyethyl starch, NaCl, glucose, electrolytes, Ringers Lactate, Gelafundin	CT26	kINPen	Reduction of metabolic activity Distinct morphological alterations Reduction in cell motility	+/-	(Freund *et al.*, 2019a)

DMEM	U251SP	jet	Downregulation of: -ERK signaling pathway -mTORC1 signaling pathway -CD44	+/-	(Tanaka *et al.*, 2012)
DMEM	PDAC PANC-Hmel1 MM HBL MM	DBD	Apoptosis/autophagy ICD markers: increase in calreticulin exposure, ATP release	+/-	(Azzariti *et al.*, 2019)
DMEM	C57BL/6 mice	kINPen MED	ICD markers: increase in T cells calreticulin	-/+	(Liedtke *et al.*, 2018a)
DMEM	A549 HepG2 MCF-7	jet	Caspase-independent apoptosis Disturb the mitochondrial–nuclear network	+/-	(Adachi *et al.*, 2015)
RPMI1640 or DMEM	SK-Mel 28, MNT-1, Capan-1, Panc-01, HT-29, SW-480, MCF-7, MDA-MB-231	kINPen	Hmox1 Upregulation Chemokine/cytokine secretion Reduction of metabolic activity ICD markers -increase of HSP90	+/-	(Bekeschus *et al.*, 2018a)
RPMI-1640	TOV21G SKOV3	jet	Apoptosis: inner nucleosomal DNA strand break, shrinking, rounding, detachment from dishes	+/-	(Utsumi *et al.*, 2014)
RPMI-1640	NOS2 NOS3 / BALB/C	jet	Apoptosis: Morphological changes, activation of caspase-3/7, intracellular ROS detection Histological differences in the tumoru sections Reduction of tumours, Loss of papillary growth, Central necrosis	+/+	(Utsumi *et al.*, 2013)

1.6.2.3 Immunogenic cell death and stimulation of the immune system

Determining the impacts of the immune system on cancer cells is important for the development of cancer treatments. The identification of immunogenic cell death (ICD) *in vitro* relies on detection of damage associated molecular patterns (DAMPs). These are molecules that are exposed or released by dying cells and let the immune system know the existence of a menace to the organism (Fuchs and Steller, 2015; Zhou *et al.*, 2019a). During the cell death process of ICD, immunogenic dead cells expose different hallmarks on the cell surface and release different substances to interact with antigen presenting cells or other immune cells. After direct ACP exposure, tumour cells expose complexes with the DAMP calreticulin (CRT) on the extracellular side of their plasma membrane at a pre-apoptotic stage (Van Loenhout *et al.*, 2018). Another DAMP is the release of ATP from dying cells, which in turn activates macrophages (Lin *et al.*, 2018).

Azzariti et al. investigated the role of PAM on metastatic melanoma and pancreatic cancer and observed an increase in CRT and ATP release, suggesting the potential use of PAL as an inducer of immunogenic cell death via activation of the innate immune system (Azzariti *et al.*, 2019). Bekeschus et al. observed that colon cancer cells underwent apoptosis, which was accompanied by exposure of CRT (Bekeschus *et al.*, 2017b). Lin et al. investigated the extracellular ATP on CT26 colorectal carcinoma cell line ATP levels and reported that ATP levels increased 70-fold (582.1 nM) following direct plasma treatment (Lin *et al.*, 2018). Increased exposure of CRT on tumour cells in a murine model of peritoneal spread of pancreatic cancer was reported by Liedtke et al., who used DMEM treated by a plasma jet (Liedtke *et al.*, 2018a). A significant increase in T cells was also reported in the same study. According to the

authors T cells could be antigen specific and tumour material could be phagocytosed and presented prior to T cell influx.

Increased immunogenicity was recently reported by Freund et al. who observed an increased amount of intratumoural macrophages and increased T cell activation following incubation of plasma-treated saline solution with CT26 cells *ex vivo* (Freund *et al.*, 2019b). Murine colon cancer cells showed cell cycle arrest and upregulation of ICD markers *in vitro*. DAMPs such as heat-shock protein 70 and high-mobility-group-protein B1 were found to be increased on the tumour cell surface with oxidizing treatment. The high-mobility-group-protein B1 can bind to several receptors like TLR2, TLR4, RAGE, and Tim3, which are known for their immunogenic signaling cascades. The authors reported increased secretion of several immunomodulatory mediators in the supernatant of cancer cells such as interleukin (IL) 1β, IL6, IL12p70, cc-chemokine ligand 4, tumour necrosis factor α, IL2, c-x-c motif ligand 9, monocyte chemotactic protein 1 interferon γ (IFNγ). This was accompanied by marked morphological changes with re-arrangement of actin fibres and reduced motility.

Bekeschus et al. investigated the effects of tumour-static PAM on eight human cancer cell lines (Bekeschus *et al.*, 2018a). The authors reported that while plasma generated ROS/RNS were of modest toxicity, heme oxygenase 1 (*hmox1*) was upregulated in all cell lines after treatment with PAM. *Hmox1* is an important target in cancer therapy although its expression is linked to both tumour proliferation and cell death (Was, Dulak and Jozkowicz, 2010). Oxidative stress is a known inducer of HO1 (protein) in human cells (Poss and Tonegawa, 1997), underlining the role of ROS and RNS being components of PAL. Research in plasma medicine has shown that cells such as human keratinocytes and human monocytes upregulate *hmox1* after treatment with plasma generated ROS/RNS (Bekeschus *et al.*, 2015; Poss and Tonegawa, 1997).

The immune-modulatory role that PAM may exert in macrophage cells has been investigated by Bekeschus et al. (Bekeschus *et al.*, 2018b). The authors exposed differentiated macrophage cells to PAM and observed a more pronounced NOS2 expression in several macrophage subtypes. NOS2 is a marker associated with a rather pro-inflammatory, antitumour phenotype. When stimulated with supernatants of pancreatic cancer cells, these macrophages released significantly increased amounts of immune-stimulatory molecules in response to PAM. Liedtke et al. investigated the cellular and molecular events in the tumour microenvironment of peritoneal cancer lesions of mice treated with PAM (Liedtke *et al.*, 2018b). Tumour nodes were stained with fluorescently labeled antibodies targeting myeloid cells and strong and significant influx of murine macrophages was observed. Macrophages were positive for CD206, a marker associated with anti-inflammatory M2 macrophages. As apoptosis was observed only on the tumour side exposed to the peritoneal cavity, macrophages likely influxed from that site.

1.6.2.4. Cytokines

Cytokines are small molecular weight proteins which act as soluble mediators and as 'messengers' secreted by one cell to alter its own behaviour or that of another cell. Cytokines are very important in the host defence system and play a critical role in protection against bacterial and viral infections. As such, they are regulators of immune responses, working within the immune system and between the immune system and other complex cellular networks within other tissues in the body (Zhang and An, 2007). Cytokines are also involved in the pathogenesis and development of symptoms in infections (Imanishi, 2000). Moreover, cytokines are relevant biomarkers for early stages of wound healing and can manipulate the inflammatory phase of wound healing (Shah *et al.*, 2012).

PAL application is innovative as it could be modulated to target two effects: cleaning the infected area of wound and inactivation of bacteria in it and stimulation of tissue regeneration such as fibroblast and skin cell growth. The application of plasma technology in wound healing has been studied for stimulation of epithelial and immune cells. Plasma increases translation of genes related to wound healing such as cytokines and growth factors and potentially promotes angiogenesis, proliferation or cell adhesion with subsequent promotion of the wound healing process (Barton *et al.*, 2014).

1.7 Antimicrobial agents for disinfection and antisepsis

Biocide is a term describing an active chemical agent, with broad antimicrobial spectrum. Biocides range in antimicrobial activity, so other terms may be more specific, including "-static," referring to agents which inhibit and "-cidal," referring to agents which kill the microorganism. Different types of pathogens vary in their response to antiseptics and disinfectants. This is due to different cellular structure, composition, and physiology.

Antiseptics and disinfectants are used extensively in hospitals and other health care settings for a variety of topical and hard-surface applications. They play an important role in infection control practices and aid in the prevention of nosocomial infections. Antisepsis is a process of removal of germs from the skin and antiseptics are chemical agents able to prevent or stop pathogens actions by inhibition of their functions or by destroying them in or on living tissue (e.g. health care personnel handwashes and surgical scrubs); and disinfectants are similar but generally are products or biocides that are used on inanimate objects or surfaces.

The widespread use of antiseptic and disinfectant products has prompted some speculation on the development of microbial resistance, in particular cross resistance to antibiotics (Mc Carlie, Boucher and Bragg, 2020). Thus, new alternative solutions and technologies are needed to fight nosocomial pathogens and antibiotic resistant strains.

1.7.1 Disinfectants for surfaces/medical instruments

Disinfectants are classified by their chemical nature and each class has its unique characteristics, hazards, toxicities and efficacy against various microorganisms. Environmental conditions, such as the presence of organic matter, pH or water hardness can also impact the action of a disinfectant. The major classes of chemical disinfectants and their characteristics follow.

1.7.1.1 Alcohol

In the healthcare setting, alcohol refers to ethyl alcohol and isopropyl alcohol. These alcohols are effective against vegetative forms of bacteria, fungi and viruses and they are also tuberculocidal and they are found mainly in gels, hand rubs, and foams (Sauerbrei, 2020; Goroncy-Bermes, Koburger and Meyer, 2010; Kampf et al., 2010).

The spectrum of virucidal activity of ethanol at 95% covers the majority of clinically relevant viruses, whereas for bactericidal effects the optimum concentration is 60%–90% solutions in water (Kampf, 2018). The mode of action of alcohol is denaturation of proteins.

Alcohols are not recommended for sterilizing medical and surgical materials because they lack sporicidal action. Ethanol toxicity is related to respiratory depression, which can cause respiratory arrest, hypothermia, arrhythmia, and possibly cardiac arrest (Gormley *et al.*, 2012).

1.7.1.2 Chlorine and Chlorine Compounds

Hypochlorites, which are the most widely used of the chlorine disinfectants, are available as liquid (sodium hypochlorite) or solid (calcium hypochlorite). The most prevalent chlorine products are aqueous solutions of 5.25%–6.15% sodium hypochlorite, usually called household bleach (Kampf et al., 2020).

Hypochlorites have a broad spectrum of antimicrobial activity (Chia Shi Zhe et al., 2016), and can remove dried or fixed organisms and biofilms from cleaning medical devices and surfaces (Merritt, Hitchins and Brown, 2000; Huang *et al.*, 2019). Chlorine can inactivate microorganisms by oxidation of amino acids and enzymes (McDonnell and Russell, 1999). Side effects could be poisoning, corrosive gastrointestinal injury, skin and irritation, burns, dermal hypersensitivity, irritation of the upper airways (Slaughter et al., 2019; Chia Shi Zhe et al., 2016).

1.7.1.3 Formaldehyde

Formaldehyde is used as a disinfectant and sterilant (Nikolic, Mudgil and Whitehall, 2019). Formaldehyde is used as a water-based solution called formalin, which is 37% formaldehyde by weight. It can cause inactivation of bacteria, fungus, viruses and spores. It has also been the classic inactivating agent for polio vaccine from 1954 till now (Abd-Elghaffar *et al*., 2020). Formaldehyde inactivates microorganisms by alkylating the amino and sulfhydryl groups of proteins and ring nitrogen atoms of purine bases.

Ingestion of formaldehyde can be fatal, and long-term exposure to low levels can cause asthma, respiratory problems, and skin irritation. It can be corrosive and absorbed by all surfaces of the body, and cause dermatitis and itching (Pandey *et al*., 2000).

1.7.1.4 Glutaraldehyde

Glutaraldehyde-based solutions are commonly used in healthcare facilities due to excellent antimicrobial effects even in the presence of organic matter. Alkaline glutaraldehyde solutions are effective against vegetative bacteria in less than 2 min, Mycobacterium tuberculosis, fungi, and viruses in under 10 min, and spores (McDonnell and Russell, 1999; Rutala and Weber, 2004). The biocidal activity of glutaraldehyde results from its alkylation of sulfhydryl, hydroxyl, carboxyl and amino groups, (McGucken and Woodside, 1973; Rutala and Weber, 2004). Inhalation of glutaraldehyde for long exposure affects the nose and respiratory tract (Takigawa and Endo, 2006).

1.7.1.5 Hydrogen Peroxide

Hydrogen peroxide is used in the medical field due to high biocidal activity for hard surface and medical devices disinfection. It has broad-spectrum activity with bactericidal, virucidal, sporicidal, and fungicidal properties (Linley *et al.*, 2012; Molloy-Simard *et al.*, 2019). The mode of action of hydrogen peroxide is the production of destructive hydroxyl free radicals which attack lipids on cell membranes, genetic material, and other cell components (Finnegan et al., 2010). Ingestion of 3% hydrogen peroxide can cause mild gastrointestinal irritation and also cause portal vein thrombosis (Ghafoor et al., 2021).

1.7.1.6 Iodophors

Iodine solutions have been used by health professionals due to their excellent antiseptic properties as antiseptics on skin or tissue. Different concentrations of iodine solutions have been tested from <0.001% to 10% for inactivation of Gram positive and negative bacteria and viruses such as enveloped model viruses as well as against

some nonenveloped human viruses, (adenovirus and polyomavirus) and poliovirus as a high-level disinfectant (Sauerbrei and Wutzler, 2010).

1.7.1.7 Ortho-phthalaldehyde

Ortho-Phthalaldehyde (OPA) is used as a high-level disinfectant for medical equipment and interacts with amino acids, proteins, and microorganisms. OPA is effective against a wide range of microorganisms, including *E. coli* (Lerones et al., 2004) and glutaraldehyde-resistant mycobacteria and *B. atrophaeus* spores (Walsh, Maillard and Russell, 1999). Disadvantages of OPA are that repeated exposures of OPA aerosols can result in functional and structural changes of airway cultures, higher mucin production and changes of tissue morphology (Wang *et al.*, 2021b).

1.7.1.8 Peracetic Acid

Peracetic acid is an oxidizer widely used for the sterilization of equipment in hospitals. Peracetic acid is characterized by rapid action against all microorganisms and it is mainly used for disinfection and has biofilm-cleaning effects (Kampf, Fliss and Martiny, 2014). Peracetic acid based formulations can be easily inactivated by organic material (Kampf, Fliss and Martiny, 2014). Peracetic acid can oxidize proteins, enzymes and other metabolites (Ruddy and Kibbler, 2002). Peracetic acid can corrode copper, brass, bronze, plain steel, and iron.

1.7.1.9 Phenolics

Phenolic based disinfectants are able to destroy or eliminate fungi, viruses, bacteria, and spores (Cueva *et al.*, 2010; Merkl *et al.*, 2010; Herrera, 2004). Phenolics are also efficient against antibiotic resistant *S. aureus*. Phenolics penetrate and disrupt the bacterial cell wall and can precipitate the cell proteins. In the past there was an outbreak of neonatal hyperbilirubinemia, where infants had been placed in bassinets

where excessive concentrations of phenolic disinfectant detergent were used (Wysowski *et al*., 1978).

1.7.1.10 Quaternary Ammonium Compounds

The quaternary ammonium compounds are widely used as disinfectants for noncritical surfaces, such as floors, furniture, and walls. The quaternaries are generally efficient against bacteria, fungi, biofilms and viruses (Liu *et al.*, 2019; Padnya *et al.*, 2021; Makvandi *et al.*, 2018). Their bactericidal action has been attributed to the inactivation of energy-producing enzymes, denaturation of proteins, and disruption of the cell membrane. These solutions lose their effectiveness when in contact with organic matter such as blood, urine, faecal matter or soil.

1.7.2 Topical antimicrobial agents in wound care

From a microbiological point of view, healthy skin's function is the control of microbial populations that live on the skin, prevention of colonization and invasion by potential pathogens in tissues. Wounds can provide a moist, warm, and nutritious environment for microorganisms and enhance their colonization and proliferation. Factors that influence the quantity and variety of microorganisms in a wound can be: wound type, wound depth, location and the ability of the host to control the bacterial community (immune response).

Wound pathogens can originate from three main sources: the environment, the surrounding skin (normal skin microflora) and from endogenous sources (Duerden, 1994). The normal microflora can be very diverse and abundant in the gut, the oral cavity, and the vagina, and these areas can supply the majority of microorganisms that colonize wounds.

The progress from wound colonization to infection depends on the quantity, species and virulence factors of bacteria in the wound, the synergistic interactions between the different species and the host immune response. Bacteria in chronic wounds survive in formed biofilms which offer them protection from host defences and develop antibiotic resistance (Edwards and Harding, 2004). Bacteria can rapidly form biofilms following their attachment to a surface. When a biofilm becomes a stable community, interaction of aerobic and anaerobic bacteria increases their net pathogenic effect and enhances the likelihood of infection in the wound site and delay of wound healing. Infection leads to inflammatory response, resulting in release of free radicals and lytic enzymes which effects negatively the cellular processes involved in the wound healing process.

1.7.2.1 Antiseptic solutions

After a debridement procedure in wound care, an antiseptic solution is applied for prevention of infection and formation of biofilm. Antiseptics are commonly used in health care settings for topical applications. Nowadays, there are numerous antiseptic solutions but both their antimicrobial efficacy and cytotoxicity to healthy tissue surrounding the wound site should be taken into account. Water and saline have also been widely used for wound cleaning/washes but are ineffective in reduction of microbial populations.

1.7.2.1.1 Chlorhexidine

Chlorhexidine is widely used as an antiseptic for decontamination of skin before surgery to decrease the surgical site infection with or without the addition of other antiseptics (Sidhwa and Itani, 2015). Nevertheless, several *in vitro* studies have reported cytotoxicity on cultured cells, while *in vivo* and clinical data seem to show

more controversial results (Abdel-Sayed *et al.*, 2020). Their effect on the healing wound can further cause serious burn injuries and damage to new tissues (Sivathasan, Ramamurthy and Pabla, 2010). .

1.7.2.1.2 Sodium hypochlorite

Sodium hypochlorite is widely used as an antiseptic for cleaning of infected wounds in 0.5% w/v concentration. The main active agent in the solution is created when the chlorine in the solution reacts with water to form hypochlorous acid. Hypochlorous acid produces the potent antibacterial effect. The low cost and effectiveness of it make it very popular in the healthcare field (Duarte *et al.*, 2017). It is highly antimicrobial effective against bacteria, viruses, fungi, and spores (Schmidt *et al.*, 2018) (Levine, 2013). The main side effects of this solution include redness, swelling, and skin irritation, allergic reactions, skin hypersensitivity, impaired wound healing and fibroblast toxicity.

1.7.2.1.3 Iodine

Iodine-based compounds are the most significant microbicidal solutions used in the clinic. Iodine powder can be applied to the wound site; it is rapidly bactericidal, fungicidal, tuberculocidal, virucidal, and sporicidal with molecular iodine being primarily responsible for antimicrobial efficacy (Rutala and Weber, 2015). Although, it demonstrates good skin tolerance and low cytotoxicity, iodine solutions have been reported for allergies, ineffective penetration, and toxic effects on host cells, irritation and excessive staining (Bigliardi *et al.*, 2017).

1.7.2.1.4 Silver

Silver ion has a broad-spectrum antimicrobial activity, and causes inactivation in bacteria, yeast and viruses (Dakal *et al.*, 2016). Silver ions can bind to nucleic acids

and proteins, causing protein and nucleic acid denaturation, membrane permeability, and poisoning of the respiratory chain (McDonnell and Russell, 1999). It can cause high local toxicity, without providing the sustained silver levels necessary for microbicidal activity and it can cause pain when applied topically (Khansa *et al.*, 2019).

1.7.2.1.5 Octenidine dihydrochloride

Another antimicrobial topical wound surfactant with high broad spectrum is octenidine dihydrochloride. It has been proven to be effective in oral hygiene, preventing plaque and gingivitis, and also as a body wash for methicillin-resistant *S. aureus* decolonization (Rohr *et al.*, 2003) and for skin disinfection of premature newborn infants (Bührer *et al.*, 2002). It has been shown to be less toxic to keratinocytes and fibroblasts than silver, leading to faster wound healing (Krasowski *et al.*, 2015).

1.7.2.1.6 Polihexanide

Polihexanide is a topical solution used in the management of infected wounds as a cleaning agent with strong activity against Methicillin-resistant *S. aureus*, Vancomycin-resistant *Enterococcus*, and *Candida albicans* (Kramer *et al.*, 2018). Polyhexanide has been reported for allergic reactions and clinical cases of severe anaphylaxis (Lachapelle, 2014).

1.7.2.1.7 Hydrogen peroxide

Hydrogen peroxide is a topical antiseptic used in wound cleaning. Hydrogen peroxide used in clinics is 3% (975 μM) and has not been reported to be beneficial in promoting wound healing (Spear, 2011). Antimicrobial effects of hydrogen on pathogenic bacteria like *Pseudomonas aeruginosa* is doubtful because these bacteria contain

catalases (Thomas *et al.*, 2009). Uncontrolled production or decomposition of hydrogen peroxide can result in tissue injury and increased susceptibility to diseases due to the unbalanced redox homeostasis.

1.7.2.2 Wound Dressings

Wound dressings were created for supplying a moist environment and optimal environment for wound healing and consequently protect it. By incorporation of the therapeutic agents into the dressings, it is possible to repair the wounds more quickly and better (Rezvani Ghomi *et al.*, 2019). The dressing is selected based on the type, depth, location, and extent of the wound, the amount of discharge, infection in wound site, and wound adhesion.

Systemic administration of antimicrobials is not thought to be necessary nor useful for the management of local wound infections, since (a) the drugs may not penetrate well into the wounds because of the poor blood flow and the presence of dead tissue around the wound, (b) would need to be used in high concentrations to treat organisms growing in biofilms, (c) systemic administration has not been shown to prevent bacterial colonisation (Stone, 1966). Furthermore, inappropriate use of systemic antibiotics can be associated with problems such as allergy, toxicity and more importantly development of resistance in non-target organisms.

Different antimicrobial agents can be incorporated in dressings such as silver, iodine, chlorhexidine, antibiotics (bacitracin, neomycin, polymyxin, mupirocin, and fusidic agents), medical-grade honey, essential oils (cinnamon, lemongrass and peppermint (Liakos *et al.*, 2015)).

1.8 Advantages and limitations of PAL

The complexity of atmospheric pressure plasma devices, differences in design and operations can lead to different reaction compounds with different mechanisms of action. The chemistry of gas plasma is not simple, and the control of the chemical reactions is a major challenge. The gaseous plasmas generated at atmospheric pressure involve many active species (charged particles, radicals, atomic and molecular species, UV radiation) and also electric fields. These reactive chemical species and radicals are interesting since they can efficiently affect many kinds of living biological tissue or surfaces because they can easily penetrate small pores, spread over rough surfaces, and reach for instance prokaryotic or/and mammalian cells. However, plasma can be applied on accessible surfaces such as skin but not as easily for instance to internal organs in an animal or human body. PAL consists of many reactive short and long living oxygen and nitrogen species, which can be applied for the treatment of accessible surfaces but may also reach inaccessible surfaces for instance through injections using syringes. Moreover, PAL have the potential to be used as a surface decontaminant that can be used in washing/cleaning procedures, thus making it more similar to 'conventional' disinfectants. PAL can be generated in the lab, stored and transported to parts where plasma cannot be generated. The characteristics of the PAL can be optimized by the plasma treatment conditions like working gas, target solution, treatment time etc. Moreover, it is important that a person without any knowledge of plasma but having knowledge of the medical field could use it e.g. for decontamination of a wound.

Another limitation is the short half-life of the reactive species like OH, or singlet oxygen produced in the PAL. It is very difficult to differentiate between the various physico-chemical properties of PAW responsible for microbial inactivation or

cytotoxic effects, respectively. In order to use PAL as a disinfectant agent, the complete diagnostics of the plasma treated solution needs to be performed which requires different radical diagnostic methods. Moreover, the chemical composition and the end reaction products of the liquid, depend on the gas used for plasma generation. The use of different gases for the plasma generation increases the operating costs.

1.8.1 Biosafety concerns

While, the generation of intracellular ROS can lead to cell apoptosis, and subsequently it is beneficial for tumour treatment, it may also pose risks for causing oxidative stress-induced genetic and epigenetic alterations involved in human carcinogenesis (Ziech *et al.*, 2011) or inducing inflammation or other side effects.

Direct exposure to plasma and indirect treatment (through use of plasma activated liquids) have been investigated in *in vivo* experiments. Utsumi et al. reported administration of PAM via sub-cutaneous injection to subcutaneous xenograft tumours of ovarian cancer cells in mice (Utsumi *et al.*, 2013). Mouse weights, survival, and behaviour showed no toxic effects and no anaphylaxis or skin necrosis were detected after plasma treatment. The MicroPlaster β plasma device has been investigated in a wound model in mice. Different pro-inflammatory cytokines and collagen were increased in the dermal tissue. Negative side effects such as infection, swelling oozing, or erythema were not observed (Arndt *et al.*, 2013).

Clinical studies have already been conducted, in the dermatological field where plasma is used for microbial disinfection and promotion of wound healing. No adverse side effects such as sensitization or allergic reaction were reported. Patients of laser

lesions treated by plasma did not show any pre-cancerous skin features after a 12-months follow-up study (Metelmann *et al.*, 2013b).

In a study investigating the bactericidal efficacy of direct exposure to plasma discharge, the mutagenic potential of plasma was tested (Boxhammer *et al.*, 2013). A standardized test system called 'hypoxanthine guanine phosphoribosyl transferase assay' was tested with V79 cells, for measurements of eukaryotic cell mutagenesis induced by external factors. The authors reported that no mutations beyond naturally occurring spontaneous mutations at the Hprt locus were induced in the V79 cells.

The mutagenic potential of the MicroPlaSterβ plasma device, which has been used efficiently in humans for treating chronic and acute wounds, was investigated using the same mutagenic assay with V79 Chinese hamster cells and no mutagenic potential was detected (Maisch *et al.*, 2017). Boehm et al. investigated the cytotoxic and mutagenic effects of plasma treated FBS and observed increased mutagenic potential at the hprt locus in CHO-K1 cells exposed to this solution over a 39 day cultivation period as determined using the mammalian HPRT assay (Boehm *et al.*, 2016).

Increase in micronuclei formation along with loss in cell viability and clonogenicity were observed after plasma treatment of brain cancer cells treated by a DBD system (Kaushik, Uhm and Choi, 2012). DNA damage has been reported in HaCaT cells exposed to plasma (Blackert *et al.*, 2013) and also in mouse leukocytes (Morales-Ramirez *et al.*, 2013). DNA damage induced by a helium plasma needle was assessed in both prokaryotic and eukaryotic cells using the chromotest and comet assays, respectively. Results showed no genotoxic effects in *E. coli*, while HeLa cells showed DNA breakage (Garcia-Alcantara *et al.*, 2013).

ATP release and exposure of calreticulin to the surface of cancer cells has been reported after treatment with PAL (Bekeschus *et al.*, 2017b). Immunogenic potential of treatment with plasma needs to be further investigated in case undesirable immune reactions against benign host cells could potentially be triggered or inflammatory responses elicited.

1.8.2 Environmental considerations

Generation of wastewater is one of the main environmental sustainability issues across food sector industries and of growing concern in the healthcare sector. Wastewater streams are the subject of microbiological and chemical criteria and can have a significant eco-toxicological impact on the aquatic life. Ecotoxicological testing provides an overall direct estimation of the environmental hazard of effluents, by the exposure of selected test species on the respective samples and the determination of certain end-points, such as lethal effect or growth ability. The generation of PAL at large volumes and ultimate discharge to the environment via wastewater streams therefore also needs to be considered under ecotoxicological aspects.

Patange et al. evaluated the role of ACP for reduction of key microbial targets encountered in complex and nutritious wastewater effluents and the eco-toxicological impact of plasma treatment on aquatic species (Patange *et al.*, 2018). Results showed reduction and complete inactivation of key indicator microorganisms in model dairy and meat wastewater effluent. Moreover, *Daphnia magna* was used as a model for acute toxicity tests. Plasma treatment reduced the toxicity of the food sector effluents up to 24 h exposure, but a prolonged contact of up to 48 h was toxic to *Daphnia magna*.

A wider variety of *in vitro* tests such as AlgalTox test, Zebrafish embryos test and Microtox test are needed in order to build a better understanding of toxic effects of

PAL and their chronic effects in aquatic environments. The effects of long-term exposure of PAL on reproduction, growth, and survival over one or more generations of tested organisms could provide a holistic approach in establishing safe environmental concentrations of PAL before release into the environment.

1.9 Objectives of the study

Following the golden era of antibiotic development, when several antibiotic classes were discovered, the effective role of antibiotics for bacterial infections was taken for granted. Nowadays, the spread of antimicrobial resistance has been recognised as a significant threat and is eroding our ability to control bacterial infections with traditional techniques. Despite new intervention tactics targeting bacterial infections, this threat remains relevant on a global scale and there are scientific challenges to develop new technologies and approaches focussing on efficient antimicrobial treatments.

Interaction of cold plasma with aqueous solutions is a relevant topic of study to the field of plasma medicine. Mammalian cells and tissues are surrounded or covered by biological fluids, therefore, the plasma-induced chemistry in the liquid phase is crucial and usually dictates the biological outcomes. Achievements have been reported on the application of PAL, but important questions remain. This research aims to build an understanding of PAL mediated biological effects and establish how PAL may be harnessed as a technology in its own right as anti-microbial decontamination and/or disinfection agent to provide the basis for new antimicrobial technologies for prevention or treatment of bacterial infections. The research outcomes will help to define both the efficacy and safety of the potential uses of this technology.

The specific objectives of the study are:

- To investigate the role of the composition of the liquid on the resultant chemistry of Plasma Activated Liquids and the impact this has on their antimicrobial and cytotoxic effects. To this end 4 different liquids which differ with regards to buffering capacity and chloride ion – water, saline, phosphate buffer and phosphate buffered saline – are treated using a high voltage DBD system (Chapter 3). *E. coli* (Gram negative) and *S. aureus* (Gram positive) are used as model pathogenic microorganisms for antimicrobial assays in order to investigate the antimicrobial activity of different PAL against Gram positive and negative bacteria while cytotoxic effects are assessed in the mammalian cell model CHO-K1.
- To assess the effects of process and storage conditions such as temperature and storage time on the chemical composition and antibacterial effects of PAW and PAS (Chapter 4). Different sub-ambient and supra-ambient temperatures are investigated in order to determine the stability of reactive species and their biological activity and realise which condition would result in the longest retention of bactericidal effects.
- To elucidate the role of ROS and RNS in bacterial inactivation and cytotoxic effects using ROS-rich and RNS-rich plasma activated water generated using a reactive species selective spark and glow discharge set-up. Chapter 5 focuses on the effects of treatment time, mode of discharge and contact time of PAW on the same bacterial strains. These results provide a primary understanding of how ROS and RNS affect different biological targets.
- To assess anti-cancer effects of ROS- and RNS-rich PAW, respectively. Chapter 6 focuses on investigating the cytotoxic properties of PAW on colorectal cancer, glioblastoma, squamous carcinoma and melanoma cell lines.

- To evaluate the antibacterial efficacy of plasma activated saline in a co-culture model with human HaCaT cells as a more complex challenge which better reflects an infected wound setting (Chapter 7). Chapter 7 also examines the cellular response to exposure with PAS in this set-up and elucidates the mechanisms by which cellular stress and cell death pathways are activated. The effects of PAS on cytokine secretion after exposure of HaCaT cells are also investigated.

Chapter 2: Materials and Methods

2.1 Plasma Sources Evaluated and Sample treatment

2.1.1 DBD-120 system

For the generation of PAL, a high voltage DBD atmospheric cold plasma system (DBD-120) custom built at Technological University Dublin was used (Figure 2.1). The DBD-120 has a maximum voltage output of 120 kV_{rms} at 50 Hz in air. DBD-120 consists of two 15 cm diameter aluminium disk electrodes which are separated by a rigid polypropylene container (310 × 230 × 22 mm), which serves as a sample holder and as a dielectric barrier with wall thickness of 1.2 mm. Below the top electrode there is a primary dielectric barrier, which is a 10 mm Perspex layer, placed on top of the sample holder. The distance between the two electrodes was equal to the height of the polypropylene container, which served as sample holder and as the di-electric barrier. The voltage of DBD-120 is transformed onto the top electrode, i.e. the top electrode is the main output voltage carrier, and the bottom is the ground electrode. Moiseev et al. has investigated concentrations of the reactive chemical species generated in the gas phase in that system of DBD-120 plasma system (Moiseev *et al.*, 2014).

2.1.1.1 Treatment of liquids with DBD system

Liquid samples, i.e. 10 mL of distilled water, PBS (137 mM NaCl, 2.7 mM KCl and 10 mM phosphate buffer solution), saline (137 mM NaCl, 2.7 mM KCl), and 10 mM phosphate buffer (100mM KH_2PO_4, 100mM K_2HPO_4), were added separately to a sterile petri dish of 90mm diameter and placed without a lid at the centre of the polypropylene plastic container and then sealed in a high barrier polypropylene bag (Cryovac, B2630, USA). The plastic containers were placed at the centre between the electrodes of DBD-120 and treated for 0, 1, 5, and 10 min at a voltage of 80 kV_{rms} and

50 Hz using atmospheric air as the inducer gas. In order to maximize the retention of plasma generated reactive species over time, samples were stored at room temperature for 24 hours post treatment storage time (PTST) following the treatment times at room temperature. Liquids without any plasma treatment were kept as negative controls (0 minutes) and stored under the same conditions throughout the study.

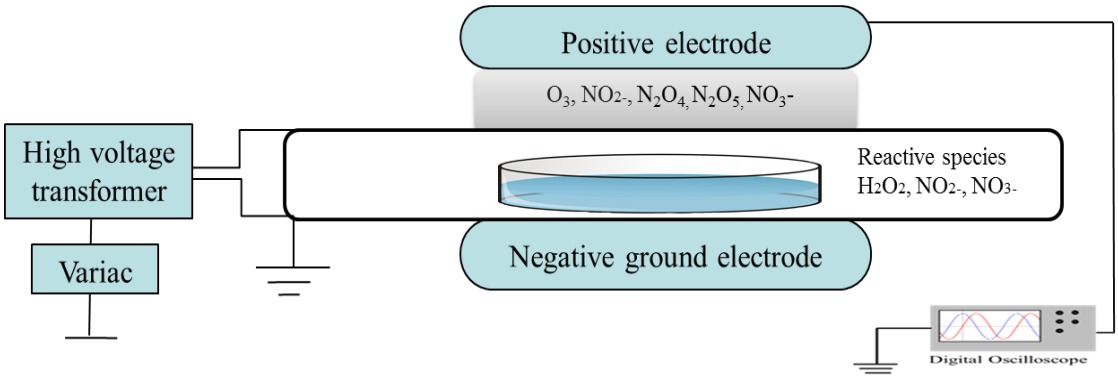

Figure 2.1 Schematic of the experimental setup of the DBD-120 plasma generator.

2.1.2 Reactive Species specificity (RSS) system

Two different types of electrical discharge configurations have been set up for this plasma system (Lu *et al.*, 2017a; Lu *et al.*, 2017b). In both setups, a stainless-steel needle served as the high voltage electrode and it was fixed perpendicular to the solution's surface. The distance between the high voltage needle tip and the liquid's surface was fixed to 5 mm for all experiments.

To realize two different discharge modes, the ground electrode connection was adjusted in the two setups. In Figure 2.2 (a), the plastic petri dish was placed on a stainless-steel plate which was connected to the ground (spark discharge); in Figure 2.2 (b) a thin ground electrode rod was submerged into the water contained in the small petri dish (glow discharge). Both types of discharges were operated in atmospheric

air. The power supply used for driving the plasma discharges was a HV half bridge resonant inverter circuit (PVM500, INFORMATION UNLIMITED). Its maximum output voltage was 20 kV with a variable frequency of 20–65 kHz depending on the plasma load capacitance (Lu *et al.*, 2017a; Lu *et al.*, 2017b).

2.1.2.1 Treatment of liquids with RSS system

For each treatment of the liquid sample, 10 mL volume deionized water or saline were added into a plastic petri dish (55 mm inner dimeter), which corresponded to a water layer of about 4.2 mm depth.

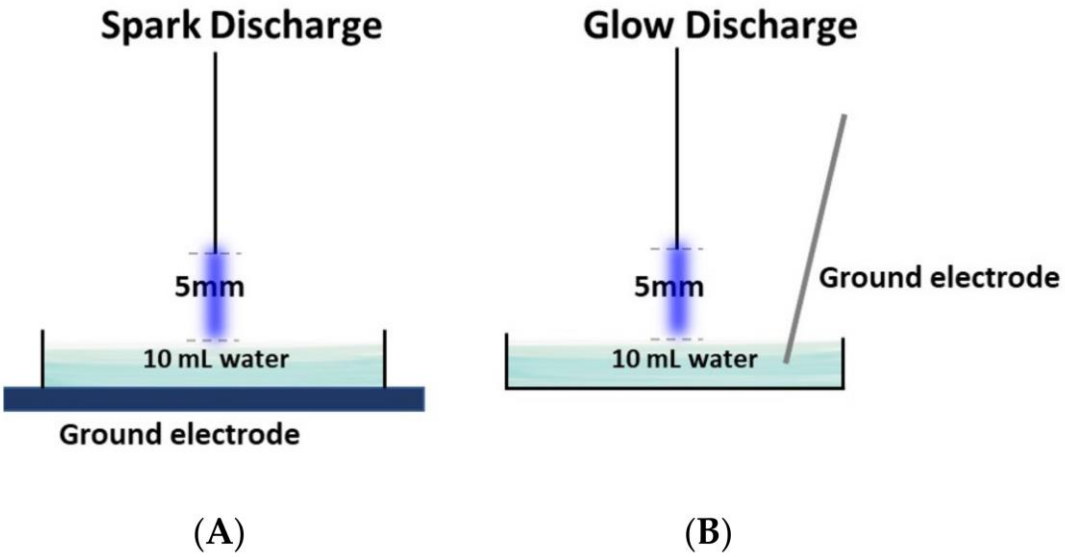

Figure 2.2 Schematic of air discharge in contact with water showing configuration of electrodes, (a) spark discharge, (b) glow discharge (Lu et al., 2017a).

2.2 Antimicrobial efficacy

2.2.1 Bacterial strains and growth conditions

The bacterial strains *Escherichia coli* NCTC 12900, *S. aureus* ATCC 1803 and *S. aureus* ATCC 25923 were obtained from the microbiology stock culture of the School of Food Science and Environmental Health of the Technological University Dublin, maintained at -80°C using protective beads (Technical Services Consultants

Ltd, UK). One protective bead of the selected strain was streaked onto tryptic soy agar (TSA, Biokar, France), incubated for 24 h and further maintained at 4°C. A single colony of the culture was used to inoculate tryptic soy broth (TSB, ScharlauChemie, Spain) and incubated at 37°C for 18 h.

2.2.2 Preparation of cell suspensions

The cells were harvested by centrifugation at 10,000 rpm for 10 minutes, washed three times in PBS and finally re-suspended in PBS. Finally, 30µl of bacterial suspension was diluted in 970µl of PBS and this was the bacterial working solution. For the determination of each plasma activated solution's antimicrobial effect, 10% bacterial suspension was added to 90% PAL and incubated at room temperature for 15, 30 and 60 min (contact time).

2.2.3 Microbiological analysis

After each contact time, a concentrated PBS (4.5xPBS concentration) solution was added to the bacterial solution to neutralize the pH and cells were diluted in Maximum Recovery Diluent (MRD; Merck, Ireland). Dilutions were made to 10^{-3} and three 10 µl droplets were placed on TSA plates. The plates were incubated aerobically at 37°C for 24 h, after which colonies were counted to determine the number of viable cells. In order to detect any subsequent increase in visible colonies, the plates were further incubated for 2 days. Results obtained are represented as surviving bacterial population in log10 colony forming unit (CFU)/mL units with error bars representing standard deviation.

2.2.4 Adjusted pH experiments

In order to investigate if the antimicrobial efficacy of PAL depends on the pH of the solutions, hydrochloric acid solution was added to buffered solutions such as PAPBS

and PAPB in order to reduce their pH, whereas 4.5x concentrated PBS was added to non-buffered liquids such as PAW and PAS to increase their pH to neutral. Serial dilutions of hydrochloric acid solution 1 M were made and few drops were added to PAPBS and PAPB. The pH values of the acidified solutions were measured continuously, until reaching the desired pH value. For these experiments the tested solutions were plasma treated for 5 minutes.

2.3 Effect of Temperature on PAL stability

2.3.1 PAL heated to supra-ambient Temperatures

Waterbath

2.5 mL of PAL generated by DBD system were transferred to 20 mL sterile tubes, and heated in a waterbath at 50, 60, 70, 80, 90, 100°C for 5 min. The bottles were closed during the heating, to avoid loss of liquid due to high temperature. After the heating times, the samples were placed on ice for 5 min to stop heating process. A control sample was stored in room temperature.

Bunsen Burner

PAW samples generated by RSS system were heated to 100 °C in a boiling water bath over a Bunsen burner for 5, 10, or 15 min. PAW samples of 2.5 mL were placed in 15 mL sterile tubes and heated while the tubes were closed, to avoid loss of liquid due to high temperature. After each heating time, the samples were placed on ice for 5 min to halt any thermal effects.

Autoclave

PAW generated by RSS system was autoclaved for 20 min at 121°C/15 pounds per square inch by an autoclave (MP25, Rodwell Scientific Instruments, Basildon, UK).

A control sample was stored at room temperature. After cooling, all samples were stored at room temperature prior to chemical and antimicrobial assays.

2.3.2 PAL stored in sub-ambient temperatures

After 24 h PTST , 1.5 mL of PAW or PAS made by DBS system were transferred to sterile microtubes and stored at five different storage temperatures: room temperature, 4 °C (standard fridge, Zanussi, Dublin, Ireland), −16 °C (standard freezer, Zanussi), −80 °C (ultra-low temperature freezer, Innova U535, Eppendorf New Brunswick, Hamburg, Germany) and −150 °C (cryogenic ultra-low temperature freezer, MDF-1156ATN, Sanyo, Osaka, Japan). After 1, 3, 6 and 18 months of storage period, the samples were thawed at room temperature, vortexed and tested for chemical composition and antimicrobial activity as described below. The samples were at room temperature when tested for all assays.

2.4 Investigation of the chemical composition of PAL

2.4.1 Quantification of Hydrogen Peroxide using Titanium Oxysulfate

Hydrogen peroxide concentrations were quantified employing the titanium oxysulfate (TiOSO4, Sigma-Aldrich, Arklow, Ireland) colorimetric method. Quantification of H_2O_2 concentrations in PAL was determined by incubating a total of 10 µl $TiOSO_4$ to 100 µl of PAL in the dark for ten minutes producing the yellow pertitanic acid. This absorbance was measured at 405 nm using a spectrophotometric microplate reader (Biotek, Swindon, UK). Standard curves of known hydrogen peroxide concentrations were included on each plate and used to convert absorbance into concentrations. All measurements of hydrogen peroxide were measured immediately after the PTST. To prepare the calibration curve, 30% hydrogen peroxide standard solution was diluted

into a concentration range of 0, 2×10^{-4} %, 3×10^{-4} %, 5×10^{-4} %, 1×10^{-3} %, 2×10^{3} %, 3×10^{-3} %, and 5×10^{-3} % (1% = 0.3263 M).

2.4.2 Quantification of Peroxides using potassium iodine

The quantification of peroxide concentrations in PAL were performed by oxidation of potassium iodide to yellow iodine and spectrophotometric measurement. 50 µl of PAL or standard curve samples were added to 50 µl of phosphate buffer solution (10mM) or deionised water and 100 µl 1M potassium iodide (Sigma-Aldrich, Arklow, Ireland) in a 96 well microtiter plate at room temperature, incubated for twenty minutes and the absorbance was read at 390 nm (Boehm *et al.*, 2016). All measurements of peroxides were taken immediately after the PTST. To prepare the calibration curve, 30% hydrogen peroxide standard solution was diluted into a concentration range of 0, 2×10^{-4} %, 3×10^{-4} %, 5×10^{-4} %, 1×10^{-3} %, 2×10^{-3} %, 3×10^{-3} %, and 5×10^{-3} % (1% = 0.3263 M).

2.4.3 Determination of Nitrite

Concentration of nitrites was determined using Griess reagent (Sigma-Aldrich, Arklow, Ireland). A total of 50 µl of Griess reagent was added to 50 µl of PAL/ standard curve sample. Absorbance was read at 548 nm, after 30 min of incubation, and compared to a sodium nitrite standard curve. A range of known concentrations of sodium nitrite (0, 40, 50, 60, 80, 100, 200µM) was used to prepare the nitrite calibration curve and to convert absorbance into nitrite concentration.

2.4.4 Determination of Nitrate

Nitrate (NO_3^-) concentrations were determined photometrically by 2,6-dimethyl phenol (DMP) using the Spectroquant® nitrate assay kit (Merck Chemicals, Darmstadt, Germany) adapted to a 96-well plate format. Sulfamic acid was used for

pre-treatment of PAL for elimination of nitrite interference. 200 µl of reagent A, 25 µl of treated sample and 25 µl reagent B was added into a microtube and incubated for 20 min. After incubation period, 100 µl of the total mixture was added to a fresh 96 well plate microtiter plate and absorbance was read at 340 nm. A set of standard concentrations of sodium nitrate 0, 0.1, 0.2, 0.5, 1, 2, 4, and 5 mM was prepared to make a nitrate standard curve.

2.5.5 pH and conductivity measurements

The pH of PAL was measured by an Orion pH meter (model 420A, Thermo Electron Corporation, USA) and conductivity measurements were performed after plasma treatment of the solutions by a Jenway conductivity meter (model 4520, Jenway, UK).

2.4.6 Temperature measurements

Temperatures of samples stored in different storage temperatures were measured by non-contact infrared thermometer with laser pointer (N75KH, PresicionGold, USA). The temperature of samples during freezing was measured using a dual channel thermocouple data logger (Lascar Electronics, Wiltshire, UK) with measurements taken at 10 s intervals.

2.5 Mammalian Cell Culture

2.5.1 Eukaryotic cell lines

The Chinese hamster ovarian cell line (CHO-K1) was kindly provided by Professor Mohamed Al-Rubeai (School of Chemical and Bioprocess Engineering, UCD, Dublin, Ireland). The immortal human keratinocyte cells (HaCaT) were obtained from Professor Fiona Lyng (Radiation and Environmental Science Centre, Technological University Dublin). The A375 human malignant melanoma, A431 human epidermoid carcinoma, SW480 human colorectal, U373mg glioblastoma cell lines were kindly

provided by Professor James Curtin (School of Food Science and Environmental Health, Technological University Dublin).

All cell lines were cultured in Dulbecco's modified Eagle's medium/Ham's F-12 Nutrient Mixture (DMEM/F12, Sigma-Aldrich, Arklow, Ireland), supplemented with 2 mM L-glutamine and 10 % (v/v) foetal bovine serum (FBS, Sigma-Aldrich, Arklow, Ireland). Cells were grown at 37°C and 5% carbon dioxide (CO_2) in a humidified incubator, sub-cultured using trypsin-EDTA (Sigma-Aldrich, Arklow, Ireland), cell concentrations and viability were assessed using trypan blue counting.

2.5.2 Analysis of cytotoxicity

2.5.2.1 Exposure to PAL in media - Crystal Violet

For cytotoxicity assays, 20µl of cells of $2.5x10^4$ cells/mL concentration were supplemented with 60µl of DMEM-F12+10% FBS, and 20µl of PAL. PAL had been filter sterilized through a 0.2 µm filter. Cells were incubated at 37° and 5% CO_2 in a humidified incubator for two days and cell growth was assessed.

Cell growth was assessed by using a crystal violet colourimetric growth assay in a 96-well plate. For the crystal violet staining, the culture supernatant was aspirated and adherent cells were fixed with 70% methanol (Sigma-Aldrich, Arklow, Ireland) for 1 min. Then, the methanol solution was removed and cells were stained with 0.2% crystal violet solution (Sigma-Aldrich, Arklow, Ireland) for 10 min. Excess stain was rinsed off with tap water, plates were air-dried and the dye bound to the adherent cells was resolubilized with 10% acetic acid (Sigma-Aldrich, Arklow, Ireland) and absorbance measured at 560 on a spectrophotometric microplate reader (Biotek, Winooski and Thermofisher, Massachusetts, United States). Cell growth was expressed as percentage of control cells.

2.5.2.2 Exposure of cell layer directly to PAL – Resazurin

HaCaT cells were seeded at a density of $5x10^6$ cells/mL into 96 well cell culture plates in 100 µL/well DMEM supplemented with foetal bovine serum (FBS; 10%) and L-glutamine, to reach a confluent layer after 24 h. The cell culture medium was removed and 100 µL of PAS were added to each well for 15-60 min contact time at room temperature. After each interval time, PAS was removed, the wells were washed with sterile phosphate buffer solution (PBS) and fresh medium was added to the wells and incubated in a humidified atmosphere of 5% CO_2 at 37°C. Three replicate wells per contact time were examined.

Cell viability was analysed using the resazurin dye (Sigma-Aldrich, Arklow, Ireland), a redox indicator that generates fluorescent signal by metabolic reduction and the reducing environment of living cells causes the indicator to change colour from the blue oxidized-form to the red reduced form. For resazurin solution 10 mg mL^{-1} resazurin sodium salt was dissolved in PBS and 8 µL mL^{-1} of it was diluted in DMEM/F12 without FBS. After culture supernatant or PAL were aspirated, wells were washed with warm PBS, 100 µL resazurin solution was added to each well and plates were incubated for 2 h at 37°C. Absorbance was measured at 570 nm and 600 nm using a plate reader.

2.5.2.3 Analysis of apoptosis

Cells were treated and harvested as described above (2.5.2.2). Annexin V-7AAD apoptosis detection kit was used as described by the manufacturer in dilution 1:10 for Annexin V (Thermofischer, Massachusetts, United States). After PBS wash, the cells were stained and then analysed by flow cytometry (CytoFlex, Beckmann Coulter, Brea, CA, USA).

2.5.2.4 Detection of intracellular reactive oxygen species

For intracellular ROS measurements, the cells were plated at a density of $5x10^6$ cells/mL and after 18 hours of adherence, HaCaT cells were loaded with 100 µL 2′,7′-dichlorodihydrofluorescein diacetate (H2DCFDA, 50 µM) for 45 min at 37 °C and 5% CO_2. Subsequent treatment with different percentages of PAS followed and intracellular ROS levels were then detected using a plate reader (excitation, 485 nm; and emission, 535 nm; Varioskan, ThermoScientific, Waltham, MA, USA). Triplicates were run for each condition.

2.5.2.5 Mitochondrial membrane potential analysis

After 18 h of cell adherence of cells seeded at $5x10^6$ cells/mL on 96 well-plates, media was removed and cells were washed with warm PBS and PAS treatment followed. 100 µL of 2 µM of JC-1 dye were added and plates were incubated at 37 °C, 5% CO_2 for 30 min. After incubation, the dye was removed, wells were washed and 100 µL of PBS were added to each well. Mitochondrial membrane potential was detected using a plate reader (Ex 535 nm, Em 595 for the aggregates and Ex 485 nm, Em 535 nm for the monomers; VarioSkan Lux, ThermoScientific, Waltham, MA, USA). The ratio was determined between the aggregates fluorescence and the monomers fluorescence. Analyses were performed in triplicate for each condition.

2.5.2.6 Glutathione measurements

Cells were seeded and treated as mentioned before. For total glutathione measurements, samples were washed, trypsinised and collected in tubes, deproteinized with 5% sulfosalicylic acid (SSA) (Sigma) and diluted with assay buffer to 1% SSA according to manufacturer's instruction (Thermofischer, Massachusetts, United States). To measure GSSH, samples were initially treated with 2-vinylpyridine

solution (Sigma) following the same procedure. Absorbance was measured utilizing a microplate reader at 405 nm (MultiSkan GO, ThermoScientific, Waltham, MA, USA).

2.5.2.7 Lipid peroxidation

Cells were seeded, treated as described above and collected by trypsinisation. Cells were then centrifuged at 100 g for 5 min and homogenized by sonication (Sonics, vibracell, Connecticut, United States). 100µL homogenate were added into a tube with 200 µL ice cold 10% trichloroacetic acid and incubated for 15 min on ice and then samples were centrifuged at 2200 g for 15 min at 4°C. Then, 200 µL supernatant or standards were added to 200 µL 0.67% (w/v) thiobarbituric acid (Sigma-Aldrich, Arklow, Ireland). and incubated in a boiling water bath for 10 min. The samples were then cooled for 10 min and 150 µL were transferred in 96 well plate and absorbance was read at 532nm. Standards were prepared by different dilutions of 1,1,3,3-tetramethoxypropane (Sigma-Aldrich, Arklow, Ireland) from 0.625 µL to 50 µL.

2.5.3 Protein expression analysis

PAS induced cytokine and chemokine signalling protein expression profile of HaCaT cells was quantified by an ELISA Array Kit to analyse the human interleukins (IL): IL1α, IL1β, IL2, IL6, IL8, IL10, IL12, IL17A, and IFNγ, TNFα and granulocyte macrophage colony-stimulating factor (GM-CSF) (Qiagen, Manchester, UK) according to the manufacturer's instructions.

HaCaT cells were seeded at $5x10^5$ cells/ml in 6 well plates with DMEM/F12 and 10% FBS and after 18-24 h when cells were 90% confluent, media was removed. Cells were washed with sterile PBS and then treated with PAS. After specific contact time with PAS, PAS was removed and 100 µl serum free DMEM/F12 media was added in and incubated for 18 hours.

Briefly, after 18 hours incubation the media was centrifuged to remove any particulates. 50 µl of assay buffer was added to each well and 50 µl of each sample or 50 µl of standard was then added to the selected wells. The plate was incubated for 2 hours at room temperature and then the well contents were aspirated and discarded. Wells were washed three times with 350 µl wash buffer. 50 µl of assay buffer were added to each well followed by 50 µl of the detection antibodies. The plate was then incubated for 1 hour at room temperature. Wells were washed as previously described. 100 µl Avidin-HRP was added to each well and incubated for 30 minutes at room temperature. Wells were then washed 4 times. 100 µl of development solution was added to each well and incubated in the dark for 15 minutes at room temperature. The reaction was terminated by adding 100 µl of stop solution to each well. The absorbance was measured within 30 minutes of stopping the reaction utilizing a microplate reader at 450 nm and a reference wavelength of 570 nm, and protein concentration was calculated from respective standard curves.

2.6 Co-culture model setup

2.6.1 Microbial inactivation in co-culture model

A confluent layer of HaCaT cells grown on 96 well plates were used. The cell culture medium was removed, and wells were washed with sterile PBS. Then, 10 µL of bacteria suspension were added to each well, followed by 90 µL of the test solution to each well. After each contact time (15, 30, 40 or 60 min), 30 µL4.5x sterile PBS was added to the bacterial solution and serial dilutions were then prepared in MRD; 10 µl of the liquid suspension of each dilution was plated in triplicate on TSA plates. The CFU were counted after 24-48 h of incubation at 37°C.

2.6.2 Antibiotic Invasion assay

After microbial inactivation, the number of internalised bacteria was measured using the antibiotic invasion assay. The bacteria's ability to invade cells can be easily assayed using this method, while antibiotics cannot penetrate eukaryotic cells. *E. coli* is susceptible to gentamicin and *S. aureus* is susceptible to lysostaphin.

After HaCaT monolayer was grown as described before, media was removed and 10 μL of *E .coli* or *S. aureus* were added in each well and 90 μL PAS was added on top . After 60 min contact time, the PAS supernatant (containing bacteria) was discarded, the wells were washed with sterile PBS and replaced with 200 μL DMEM without serum supplemented with 100 μg mL^{-1} gentamicin for *E. coli* or 10 μg mL^{-1} lysostaphin for *S. aureus* (Brannon *et al.*, 2020; Münzenmayer *et al.*, 2016). Plates were incubated at 37°C in 5% CO_2 for 1 h to inactivate all extracellular bacteria. After incubation, wells were washed with sterile PBS and 200 μL of 0.1% TritonX100. The cells were gently homogenized by repeat pipetting and incubated for 10 min at room temperature. Bacteria that penetrated the cells and remained alive are now released, and they are plated. Controls of wells containing only PAL and bacteria were similarly tested. After incubation, the liquid suspension was plated onto TSA as described above.

2.6.3 Disinfectants testing

Common chemical disinfectants were tested as positive controls and to compare their bactericidal efficacy and cytotoxicity with PAS. Iodine 10% w/w Cutaneous Solution was purchased from a local pharmacy and was diluted in sterile saline according to manufacturer to make 1% povidone iodine solution. Hibiscrub 4% w/v chlorhexidine cutaneous solution was bought from a local pharmacy and diluted to 1% chlorhexidine. 0.045% NaClO was made by dilution of bleach consisting of 4.5% w/w sodium hypochlorite. 2% formaldehyde, 2% glutaraldehyde, 70% ethanol and 3% H_2O_2 were

prepared through dilution of solutions in water purchased from Sigma (Sigma-Aldrich, Arklow, Ireland).

All chemical disinfectants were tested using same conditions and contact times as used for PAL.

2.7 Statistical analysis

Results are presented as means with standard deviations using Excel (Microsoft, Redmond, WA, USA) and GraphPad Prism (GraphPad, San Diego, CA, USA). Comparisons between different groups were analysed by ANOVA.

Chapter 3: Bactericidal and Cytotoxic Effects of PAL by DBD-120

Part of this Chapter has been published.

E. Tsoukou, P. Bourke, D. Boehm (2018). Understanding the differences between antimicrobial and cytotoxic properties of plasma activated liquids. Plasma Medicine 8(3), 299-320

DOI : 10.1615/PlasmaMed.2018028261E

Plasma activated liquids are a promising new technology, as an alternative to conventional sterilization techniques, which is considered to be useful for applications in numerous settings (food industry, agriculture, medicine) (Judée *et al.*, 2016; Schnabel *et al.*, 2015; Tanaka *et al.*, 2016; Boehm *et al.*, 2016). Liquid phase processes have been identified to be the main key to understanding detailed mechanisms of atmospheric pressure plasma effects on living systems (Jablonowski and von Woedtke, 2015).

In order to establish PAL as a technology for medical applications, the understanding of liquid-mediated effects is required. The aim of this study was to investigate the bactericidal and cytotoxic effects of four different PAL: plasma activated water (PAW), plasma activated PBS (PAPBS), plasma activated saline (PAS) and plasma activated phosphate buffer solution (PAPB), in order to understand which liquid would offer high bactericidal effects and low cytotoxic effects. These solutions consisted of two buffered and two non-buffered solutions, with different compositions in order to realise how that would affect both mammalian and microbial cells. The synergistic effects of acidic pH, hydrogen peroxide, nitrate and nitrite anion concentrations on the inactivation processes and the stability of bactericidal efficiency of PAL were assessed after plasma activation of the liquids. PAL's antimicrobial efficacy against *E. coli* and *S. aureus* was examined by CFU count for up to 2 days after creation and the Chinese hamster ovary K1 (CHO-K1) cell line was used for the cytotoxicity assay.

3.1 Chemical properties of PAL

3.1.1 pH measurements of PAL

Figure 3.1 shows the pH decrease in PAL as a function of plasma treatment time of the liquids increased up to 10 min. As is observed, the pH of the buffered solutions seemed to decrease linearly with treatment time, while the non-buffered showed a sharp drop in pH after 1 minute exposure to plasma and were almost stable after that. PAW and PAS, which are the non-buffered solutions, had lower pH values than the buffered solutions. Specifically, the pH value of the PAW and PAS decreased exponentially from 3.75±0.6 and 4.35±0.1 to 2.73±0.3 and 2.8±0.13 respectively, after 10 min of plasma activation time. The decrease in pH may be due to the nitrogen oxides produced in the plasma interacting with liquids and producing nitric and nitrous acids.

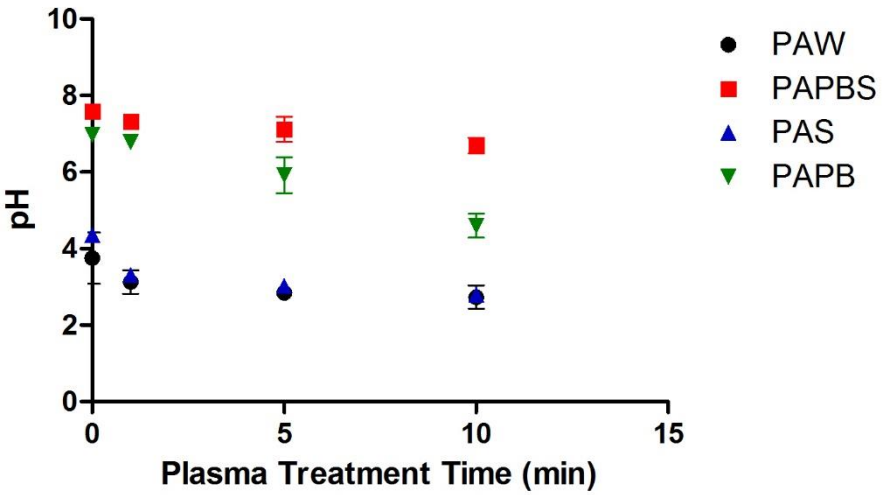

Figure 3.1 Dependence of pH on time of activation for various PAL (n=3). PAL was exposed to DBD for up to 10 min as described in Materials & Methods section 2.1.1.1 and their pH was measured using a pH meter.

3.1.2 Chemical composition of PAL

Measurement of the ROS/RNS concentrations and an understanding of their role in antimicrobial and cytotoxic activity of PAL are important for any possible application. Slopes of the graphs show a time dependent hydrogen peroxide concentration increase as plasma treatment time increases (Figure 3.2 A). H_2O_2 concentration increased up to 925 µM for PAW after 10 min of treatment and 524 µM for PAPBS. The highest concentrations of peroxide were obtained for PAS and PAPB, which were 1300 µM and 2300 µM, after 10 min plasma exposure, respectively. Of note, while concentrations generally ranged between 500 and 1500 µM in all samples after 10 min of treatment, up to 5500 µM were reproducibly measured in set 3 of PAPB, resulting in the much higher average concentration.

Formation of nitrite in PAL was investigated using a colorimetric assay. As shown in Figure 3.2 B, the concentration of nitrite in PAPBS and PAPB increased with activation time to around 38 µM and 27µM, respectively, while there was no detectable NO_2^- concentration for PAW and PAS after 10 min of plasma treatment. An increase of nitrate concentration with treatment time was also detected in all PAL after plasma exposure, reaching 0.5-1 mM after 10min. High concentrations of up to 3.7 mM were observed in PAPB treated for 10 min in data set 3, resulting in an average concentration of about 2 mM (Figure 3.2 C).

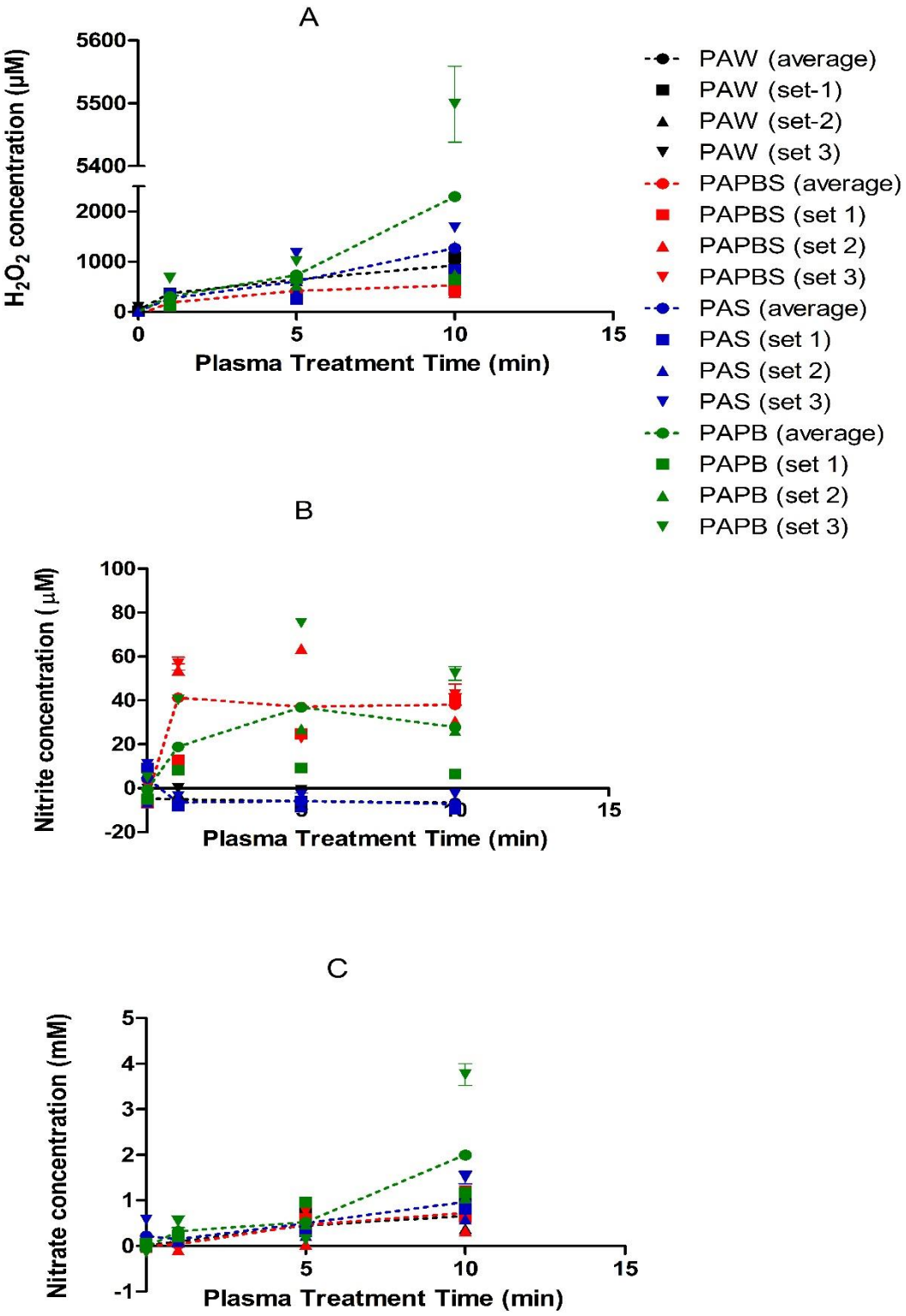

Figure 3.2 Changes in chemical composition of PAL generated after 1, 5, 10 min DBD plasma activation times at 80kV. (A) Generation of hydrogen peroxide, (B) nitrite and

(C) nitrate concentrations (n=3). Graphs represent averages of 3 independent plasma treatments (circles + lines), with the individual data sets represented as symbols only.

3.2 Antimicrobial Activity and Stability of PAL

3.2.1 Bacterial inactivation of PAL

In this section, 3 different sets are presented individually e.g. *E.coli* 1, *E. coli* 2, *E. coli* 3, *S. aureus* 1, *S. aureus* 2, *S. aureus* 3, due to differences between the sets. Pure microbial strains of *E. coli* and *S aureus* were incubated with PAL for periods up to 60 min. Compared to the control group sample (0 min PAL treatment time), considerable inactivation was observed for both bacteria. Figure 3.3 and Tables 3.1-4 present the microbial inactivation of PAW, PAPBS, PAS, PAPB obtained on the first day, expressed in log10 CFU /ml. Generally speaking the bactericidal activity of all PAL increased with increasing contact time between the bacterial suspensions and liquids, with 60 >30 >15 min obtained for reduction of bacterial growth. Specifically, PAW treated for 1, 5 or 10 min caused ≥5 log reduction to both bacteria after 30 min of contact time (Figure 3.3 A, B). One minute treated PAS was capable of causing a reduction of *E. coli* population to undetectable levels after 15 min of contact time (Figure 3.3 E), whereas 10 min of plasma activation time was needed for inactivation of *S. aureus* (Figure 3.3 F). With regards to PAPBS, 1 min of liquid exposure to plasma was not sufficient to cause any significant log reduction at any of the contact times for *E. coli*, but 10 min of treatment combined with 30 or 60 min contact time caused inactivation of *E. coli* below the detection limit (Figure 3.3 C) and decreasing contact time to 15 min was sufficient for inactivation of *S. aureus* (Figure 3.3 D). PAPB treated with plasma for 10 min was able to reduce *S. aureus* levels below the detection limit after only 60 min contact time (Figure 3.3 H), but no inactivation was obtained for *E. coli* (Figure 3.3 G). Of note, PAPB set 3 which had displayed exceptionally high

concentrations of H_2O_2 and nitrate only showed slightly higher antimicrobial activity than sets 1 and 2 (Table 3.3).

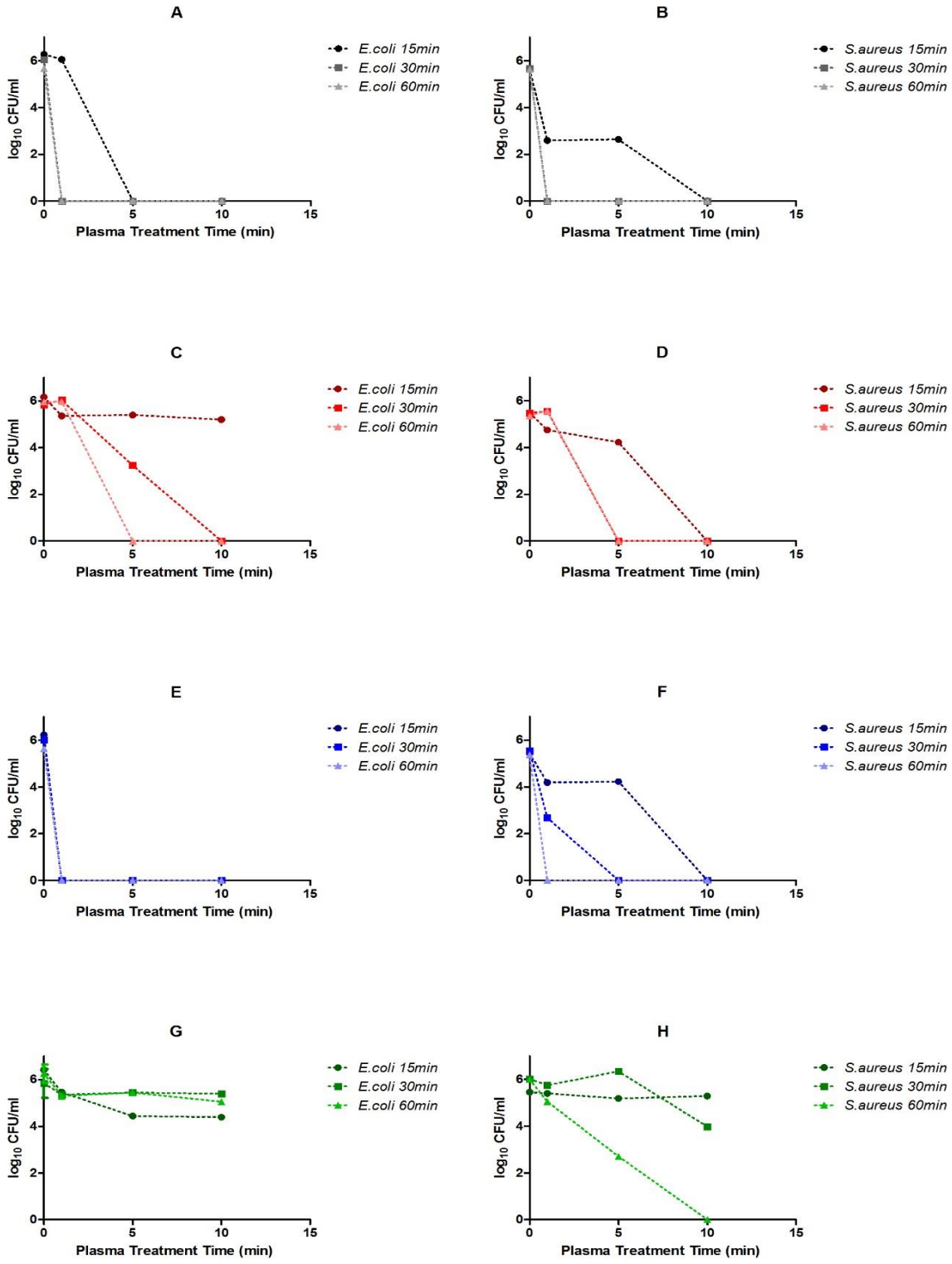

Figure 3.3 Surviving bacterial cells in response to PAL exposure after 1, 5, or 10 min plasma treatment. All bacteria cells were exposed to PAL for 15 min, 30 min or 60 min contact times and bacterial counts after different contact times were measured as described in Materials & Methods, Section 2.2.3 (A) PAW- E.coli, (B) PAW-S. aureus,

(C) PAPBS-E. coli, (D) PAPBS- S. aureus, (E) PAS- E. coli, (F) PAS-S. aureus, (G) PAPB - E. coli , (H) PAPB-S. aureus (set 2).

Table 3.1 E. coli and S. aureus planktonic inactivation efficacy by PAW. Limit of detection: 2 log10 CFU/mL. 3 different sets are presented individually e.g. E.coli 1, E. coli 2, E. coli 3, S. aureus 1, S. aureus 2, S. aureus 3 correspond to PAL Set 1, PAL Set 2 and PAL Set 3 due to differences in chemical composition between the 3 Sets.

Day	Contact time (min)	Treatment time (min)	*E. coli* 1		*E. coli* 2		*E. coli* 3		*S. aureus* 1		*S. aureus* 2		*S. aureus* 3	
			Cell density	SD	**Cell density**	SD	**Cell density**	SD	**Cell density**	SD	**Cell density**	SD	**Cell density**	**SD**
1	15	0	5.39	0.056	6.26	0.045	5.63	0.072	5.06	0.048	5.63	0.072	5.18	0.073
		1	ND	-	6.05	0.029	3.21	1.19	ND	-	2.59	-	2.84	0.153
		5	ND	-	ND	-	ND	-	ND	-	2.63	0.072	4.46	0.048
		10	ND	-	ND	-	ND	-	ND	-	ND	-	ND	-
	30	0	5.61	0.041	6.05	0.029	5.21	0.173	4.94	0.128	5.67	0.072	5.15	0.039
		1	ND	-	ND	-	ND	-	ND	-	ND	-	2.95	0.062
		5	ND	-	ND	-	ND	-	ND	-	ND	-	ND	-
		10	ND	-	ND	-	ND	-	ND	-	ND	-	ND	-
	60	0	5.70	0.022	5.67	0.072	5.21	0.173	5.24	0.018	5.63	0.072	4.44	0.043
		1	ND	-	ND	-	ND	-	ND	-	ND	-	ND	-

		5	ND	-	ND	-	ND	-	ND	-	ND	-	ND	-
		10	ND	-	ND	-	ND	-	ND	-	ND	-	ND	-
2	15	0	5.65	0.049	6.15	0.039	6.03	0.151	5.52	0.043	6.01	0.054	5.24	0.064
		1	ND	-	ND	-	3.33	0.053	4.16	0.021	5.59	-	4.19	0.036
		5	ND	-	ND	-	3.37	0.083	4.16	0.057	5.47	0.101	2.78	0.055
		10	ND	-	ND	-	1.40	1.220	ND	-	5.57	0.151	ND	-
	30	0	5.27	0.060	5.63	0.072	5.31	0.173	5.35	0.038	6.11	0.043	6.18	0.073
		1	3.57	0.030	ND	-	ND	-	ND	-	4.46	0.061	2.69	0.173
		5	ND	-	ND	-	ND	-	ND	-	ND	-	ND	-
		10	ND	-	ND	-	ND	-	ND	-	ND	-	ND	-
	60	0	6.24	0.082	6.12	0.092	6.26	0.065	5.46	0.048	6.53	0.068	5.05	0.029
		1	0.70	1.220	ND	-	1.60	1.394	ND	-	ND	-	4.30	0.076
		5	ND	-	ND	-	2.43	0.275	ND	-	ND	-	ND	-
		10	ND	-	ND	-	ND	-	ND	-	ND	-	ND	-
	15	0	6.64	0.028	6.19	0.036			5.62	0.047	6.21	0.020		
		1	6.59	0.044	6.05	0.029			5.50	0.027	5.88	0.073		
		5	5.51	0.034	5.59	-			5.28	0.029	6.05	0.029		
		10	ND	-	6.25	0.031			3.35	0.083	6.01	0.054		
		0	6.50	0.061	5.59	-			6.31	0.054	6.28	0.058		

3	30	1	5.83	0.045	5.21	0.173			5.52	0.033	6.03	0.029		
		5	5.28	0.074	5.83	0.045			ND	-	4.59	-		
		10	ND	-	ND	-			ND	-	5.31	0.027		
	60	0	6.23	0.081	6.03	0.029			6.64	0.044	5.47	0.101		
		1	6.32	0.066	ND	-			ND	-	2.77	0.101		
		5	ND	-	ND	-			ND	-	ND	-		
		10	ND	-	ND	-			ND	-	ND	-		

Table 3.2 E. coli and S. aureus planktonic inactivation efficacy by PAPBS. Limit of detection: 2 log10 CFU/mL. 3 different sets are presented individually e.g. E.coli 1, E. coli 2, E. coli 3, S. aureus 1, S. aureus 2, S. aureus 3 correspond to PAL Set 1, PAL Set 2 and PAL Set 3 due to differences in chemical composition between the 3 Sets.

Day	Contact time (min)	Treatment time (min)	*E. coli* 1		*E. coli* 2		*E. coli* 3		*S. aureus* 1		*S. aureus* 2		*S. aureus* 3	
			Cell density	SD	**Cell density**	SD	**Cell density**	SD	**Cell density**	SD	**Cell density**	SD	**Cell density**	**SD**
1	15	0	6.36	0.048	6.16	0.021	6.33	0.128	5.56	0.031	5.48	0.028	6.49	0.072
		1	6.12	0.023	5.36	0.027	6.12	0.092	4.47	0.051	4.74	0.020	5.24	0.064
		5	5.88	0.073	5.39	0.033	5.31	0.173	4.16	0.021	4.22	0.033	6.20	0.138
		10	6.17	0.075	5.20	0.053	ND	-	4.08	0.069	ND	-	2.47	0.101
	30	0	6.29	0.061	5.83	0.045	6.38	0.069	5.53	0.025	5.46	0.039	6.24	0.049
		1	6.40	0.079	6.03	0.029	5.53	0.101	5.28	0.029	5.55	0.024	5.97	0.088
		5	4.78	0.055	3.23	0.038	ND	-	4.39	0.033	ND	-	4.37	0.075
		10	5.62	0.047	ND	-	ND	-	3.47	0.037	ND	-	ND	-
		0	6.47	0.058	5.95	0.062	5.46	0.048	5.30	0.043	5.35	0.037	5.46	0.039

	60	1	5.25	0.062	5.97	0.088	ND	-	ND	-	5.56	0.038	4.15	0.117
		5	4.36	0.027	ND	-	ND	-	ND	-	ND	-	ND	-
		10	5.25	0.031	ND	-	ND	-	ND	-	ND	-	0.70	1.22
2	15	0	6.12	0.092	5.34	0.025	4.24	0.048	5.56	0.038	5.34	0.025	4.99	0.090
		1	6.20	0.053	5.46	0.043	4.18	-	5.56	0.045	5.46	0.043	4.20	0.102
		5	6.36	0.014	5.33	0.067	4.34	-	5.55	0.046	5.33	0.067	4.15	0.079
		10	6.25	0.031	5.31	0.027	4.16	-	5.68	0.024	5.31	0.027	2.83	0.045
	30	0	6.30	0.016	6.08	0.069	4.49	0.036	5.56	0.015	6.08	0.069	4.96	0.135
		1	6.56	0.032	5.83	0.045	4.26	0.065	5.57	0.031	5.83	0.045	3.92	0.130
		5	6.35	0.053	6.11	0.043	3.92	0.105	5.59	0.070	6.11	0.043	3.70	0.111
		10	5.97	0.088	5.78	0.055	ND	-	5.43	0.041	5.78	0.055	4.19	0.114
	60	0	6.63	0.072	5.83	0.045	5.06	0.098	5.44	0.050	5.44	0.031	6.65	0.066
		1	6.63	0.072	5.74	0.055	4.16	0.083	5.66	0.032	5.36	0.014	6.29	0.061
		5	7.15	0.039	5.90	0.102	ND	-	5.48	0.028	5.43	0.056	6.41	0.136
		10	7.05	0.029	5.59	-	ND	-	5.37	0.050	5.49	0.049	5.11	-

Table 3.3 E. coli and S. aureus planktonic inactivation efficacy by PAS. Limit of detection: 2 log10 CFU/mL. 3 different sets are presented individually e.g. E.coli 1, E. coli 2, E. coli 3, S. aureus 1, S. aureus 2, S. aureus 3 correspond to PAL Set 1, PAL Set 2 and PAL Set 3 due to differences in chemical composition between the 3 Sets.

Day	Contact time (min)	Treatment time (min)	*E. coli* 1		*E. coli* 2		*E. coli* 3		*S. aureus* 1		*S. aureus* 2		*S. aureus* 3	
			Cell density	SD	**Cell density**	SD	**Cell density**	SD	**Cell density**	SD	**Cell density**	SD	**Cell density**	**SD**
1	15	0	6.20	0.053	6.22	0.033	4.90	0.021	5.48	0.046	5.43	0.020	5.99	0.033
		1	ND	-	ND	-	ND	-	ND	-	4.18	0.092	1.40	1.220
		5	ND	-	ND	-	ND	-	ND	-	4.22	0.033	ND	-
		10	ND	-	ND	-	ND	-	ND	-	ND	-	ND	-
	30	0	6.03	0.029	6.01	0.054	5.83	0.045	5.22	0.067	5.55	0.024	5.06	0.712
		1	ND	-	ND	-	3.31	0.082	ND	-	2.67	0.72	1.40	1.220
		5	ND	-	ND	-	ND	-	ND	-	ND	-	ND	-
		10	ND	-	ND	-	ND	-	ND	-	ND	-	0.70	1.220
	60	0	5.67	0.072	5.63	0.072	5.67	0.072	5.36	0.027	5.36	0.024	6.09	0.050
		1	ND	-	ND	-	2.11	-	ND	-	ND	-	ND	-

		5	ND	-	ND	-	0.70	1.22	ND	-	ND	-	ND	-
		10	ND	-	ND	-	ND	-	ND	-	ND	-	ND	-
2	15	0	5.91	0.038	6.03	0.276	5.47	0.101	5.49	0.028	5.86	0.045	4.95	0.062
		1	ND	-	5.36	0.027	4.88	0.073	5.15	0.039	6.05	0.029	5.25	0.031
		5	ND	-	ND	-	2.37	0.241	4.08	0.069	4.05	0.029	4.47	0.101
		10	ND	-	ND	-	ND	-	4.26	0.045	ND	-	4.41	-
	30	0	5.95	0.062	5.86	0.045	5.45	0.054	5.52	0.045	5.97	0.033	5.31	0.173
		1	ND	-	4.63	0.072	3.03	0.029	ND	-	5.63	0.072	4.63	-
		5	ND	-	ND	-	ND	-	ND	-	5.47	0.101	ND	-
		10	ND	-	ND	-	ND	-	ND	-	ND	-	ND	0.013
	60	0	6.25	0.079	6.05	0.029	4.97	0.033	5.74	0.055	6.43	0.041	5.31	0.173
		1	ND	-	ND	-	ND	-	ND	-	5.97	0.033	ND	-
		5	ND	-	ND	-	ND	-	ND	-	ND	-	ND	-
		10	ND	-	ND	-	ND	-	ND	-	ND	-	3.18	0.073
	15	0	6.21	0.053	5.67	0.072			6.35	0.038	6.23	0.049		
		1	5.39	0.045	5.36	0.024			6.26	0.075	5.48	0.028		
		5	5.60	0.028	5.41	0.085			6.40	0.034	5.29	0.061		
		10	5.28	0.058	ND	-			6.08	0.069	5.48	0.046		
		0	6.39	0.033	5.53	0.101			6.21	0.053	6.19	0.036		

3	30	1	6.27	0.060	5.30	0.100			5.97	0.033	5.47	0.101		
		5	5.63	0.072	5.42	0.174			5.53	0.101	5.59	-		
		10	5.27	0.270	ND	-			5.21	0.053	5.23	0.018		
	60	0	6.24	0.064	6.25	0.031			6.28	0.058	5.97	0.033		
		1	ND	-	ND	-			ND	-	3.27	0.101		
		5	ND	-	ND	-			ND	-	2.78	0.055		
		10	ND	-	ND	-			ND	-	1.40	1.22		

Table 3.4 E. coli and S. aureus planktonic inactivation efficacy by PAPB. Limit of detection: 2 log10 CFU/mL. 3 different sets are presented individually e.g. E.coli 1, E. coli 2, E. coli 3, S. aureus 1, S. aureus 2, S. aureus 3 correspond to PAL Set 1, PAL Set 2 and PAL Set 3 due to differences in chemical composition between the 3 Sets.

Day	Contact time (min)	Treatment time (min)	*E. coli* 1		*E. coli* 2		*E. coli* 3		*S. aureus* 1		*S. aureus* 2		*S. aureus* 3	
			Cell density	SD	**Cell density**	SD	**Cell density**	SD	**Cell density**	SD	**Cell density**	SD	**Cell density**	**SD**
1	15	0	6.18	0.102	6.41	0.021	6.10	0.125	6.05	0.029	5.44	0.011	5.26	0.045
		1	6.11	0.043	5.45	0.019	5.27	0.275	6.22	0.033	5.39	0.033	4.61	0.109
		5	6.36	0.024	4.43	0.020	6.24	0.082	5.19	0.114	5.18	0.021	4.41	0.086
		10	6.48	0.028	4.39	0.022	1.40	1.220	4.18	0.102	5.28	0.029	ND	-
	30	0	6.35	0.038	5.83	0.623	5.59	-	6.21	0.053	6.01	0.054	4.53	0.101
		1	6.43	0.041	6.35	0.014	5.31	0.173	5.49	0.049	5.74	0.055	5.52	0.075
		5	6.39	0.033	5.44	0.043	5.57	0.151	5.05	0.029	6.34	0.025	5.51	0.084
		10	5.95	0.062	5.39	0.038	0.70	1.220	3.09	0.050	3.97	0.033	5.23	0.114
	60	0	6.48	0.046	6.26	0.038	5.21	0.173	6.28	0.029	5.99	0.033	4.74	0.055
		1	6.3	0.038	5.29	0.033	5.21	0.173	5.06	0.048	5.05	0.029	4.37	0.241

		5	5.11	-	5.44	0.043	3.37	0.241	4.23	0.070	4.05	0.029	ND	-
		10	ND	-	5.05	0.029	ND	-	ND	-	ND	-	ND	-
2	15	0	6.32	0.066	6.23	0.049	5.51	0.173	6.29	0.061	5.93	0.038	5.53	0.101
		1	6.08	0.066	6.19	0.036	5.51	0.173	6.25	0.052	5.74	0.055	5.47	0.101
		5	6.26	0.045	5.81	-	5.53	0.101	6.14	0.023	5.86	0.045	5.03	0.078
		10	6.14	0.023	6.08	0.026	4.67	0.072	6.08	0.069	6.15	0.039	3.23	0.049
	30	0	6.15	0.039	5.83	0.045	5.03	0.151	6.29	0.036	5.78	0.055	5.70	0.111
		1	6.01	0.054	5.74	0.056	5.47	0.101	6.25	0.054	5.86	0.045	5.80	0.088
		5	6.25	0.031	5.88	0.073	5.21	0.173	6.14	0.069	5.67	0.072	5.11	0.043
		10	5.78	0.055	5.93	0.038	ND	-	6.08	0.050	5.80	0.088	ND	-
	60	0	6.14	0.023	6.19	0.036	5.61	0.173	6.17	0.143	6.19	0.036	5.04	0.079
		1	6.22	0.033	5.97	0.033	5.27	0.275	6.20	0.041	6.05	0.029	5.24	0.120
		5	6.06	0.098	5.97	0.033	4.74	0.055	6.09	0.050	5.83	0.045	2.51	0.173
		10	5.78	0.055	5.83	0.045	2.07	1.797	6.34	0.051	5.83	0.045	ND	-

3.2.2 Antibacterial stability of PAL

The antimicrobial testing experiments were repeated the second day after post treatment storage time (PTST) to investigate the bactericidal stability of PAL by the same methods (Figure 3.4). Overall, PAL had lower antimicrobial activity after 1 day of storage at 4°C and it was observed that loss of bactericidal activity in PAW and PAS was less compared to PAPBS and PAPB, which were able to cause microbial inactivation only on the first day. The non-buffered solutions retained bactericidal activity against *E. coli* and *S. aureus* up to the second day. It is important to note that PAW and PAS treated with plasma for 5 minutes were still able to cause 6 log reduction for *E. coli* after 1 day of storage at 4°C or all the different contact times. The antibacterial variations between the different PAL might be explained by differences in the physicochemical properties of PAL in the same conditions. Among all four PAL investigated in this study, the non-buffered solutions seem to be ideal candidates as antimicrobial agents, as they can retain their antimicrobial properties for several days. In addition, the best conditions to generate antimicrobial solutions are longer plasma activation times and contact times (30 min and 60 min).

A number of studies have reported that Gram-positive bacteria are more resistant than Gram-negative bacteria to direct treatment by plasma discharge (Ermolaeva *et al.*, 2011; Lee *et al.*, 2006). Han et al. reported two different mechanisms of microbial inactivation between Gram-negative and Gram-positive bacteria. Specifically, the same strain of *E. coli* (Gram negative) as was studied in these experiments was inactivated mainly by cell leakage and low-level DNA damage, whereas *S. aureus* was inactivated by intracellular damage (Han *et al.*, 2015). In this study, PAL were effective against both *E. coli* and *S. aureus*, on the first day of the experiment, but on the second day some of the liquids were less effective against *S. aureus*. This could be

explained through oxidative stress exerted by ROS and RNS generated in the liquids by plasma, on bacterial components, attacking the membrane's macromolecules, such as lipopolysaccharides, and thus making Gram negative bacteria more vulnerable to plasma reactive species.

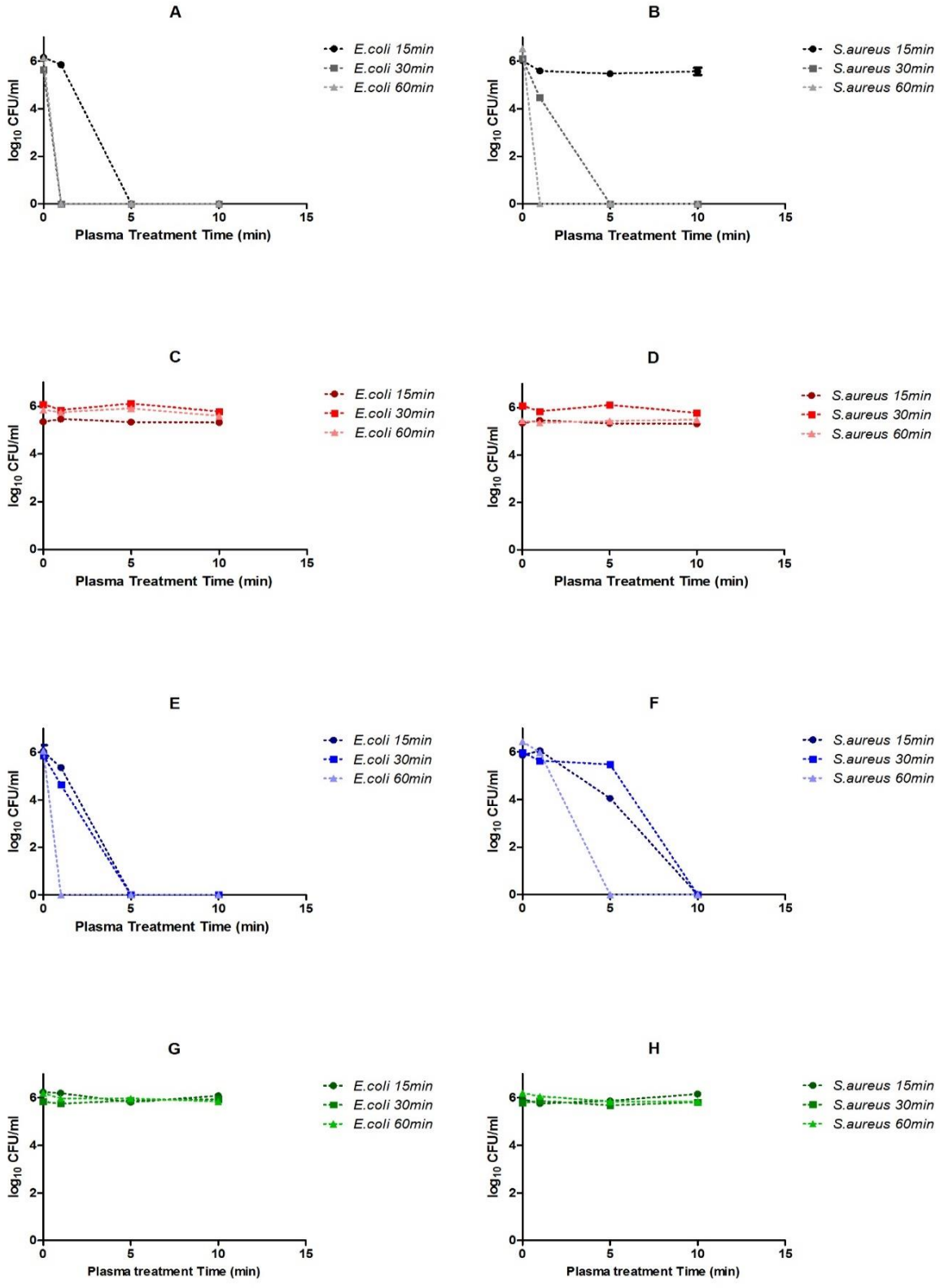

Figure 3.4 Antibacterial stability in response to PAL exposure after 1, 5, or 10 min plasma treatment on day 2. All bacteria cells were exposed to PAL for 15 min, 30 min or 60 min contact times and bacterial counts after different contact times were

measured as described in Methods, Section 2.2.3. (A) PAW- E. coli, (B) PAW-S. aureus, (C) PAPBS-E. coli, (D) PAPBS- S. aureus, (E) PAS-E. coli, (F) PAS-S. aureus, (G) PAPB - E. coli , (H) PAPB-S. aureus (set 2).

3.2.3 Effects of pH on antimicrobial activity

PAW and PAS plasma treated for 5 min were adjusted to the pH of corresponding PAPBS and PAPB by addition of 4.5x PBS as described in Section 2.2.4. (Figure 3.5). Whereas PAPBS and PAPB were pH adjusted to the pH of PAW and PAS, respectively by addition of diluted acidic hydrochloric acid with pH 1-2. Different contact times were tested, but only 30 and 60 min contact time resulted in bacterial inactivation to undetectable levels (Figure 3.6- 3.7). Generally, buffered PAW and PAS had lower bactericidal efficacy against both *E. coli* and *S. aureus* compared to PAW and PAS, whereas acidified PAPBS and PAPB could cause higher inactivation than PAPBS and PAPB.

With regards to buffered PAW, differences were observed after 60 min contact time with bacterial suspension. Normal PAW caused complete *E. coli* inactivation, whereas buffered PAW did not cause any inactivation (Figure 3.6 A). Similarly, buffered PAW showed no effect on *S. aureus* whereas PAW reduced concentrations by 2 $\log_{10}$ CFU/mL (Figure 3.7 A). PAS could cause higher logarithmic reductions than PAW, with effects seen after 30 min of contact time for both bacteria. Specifically, PAS caused complete microbial inactivation for both bacteria but the increase of pH reversed the bactericidal effects (Figure 3.6 C, 3.7 C).

PAPBS and PAPB did not cause any bacterial reduction compared to non-plasma treated solutions (controls). Acidified PAPBS, however, led to almost complete

inactivation of *E. coli* (after 30 and 60min) and *S. aureus* (after 60 min) (Figure 3.6 B, 3.7 B). Acidified PAPB caused higher inactivation compared to PAPB for both bacteria (Figure 3. 6 D, 3.7 D).

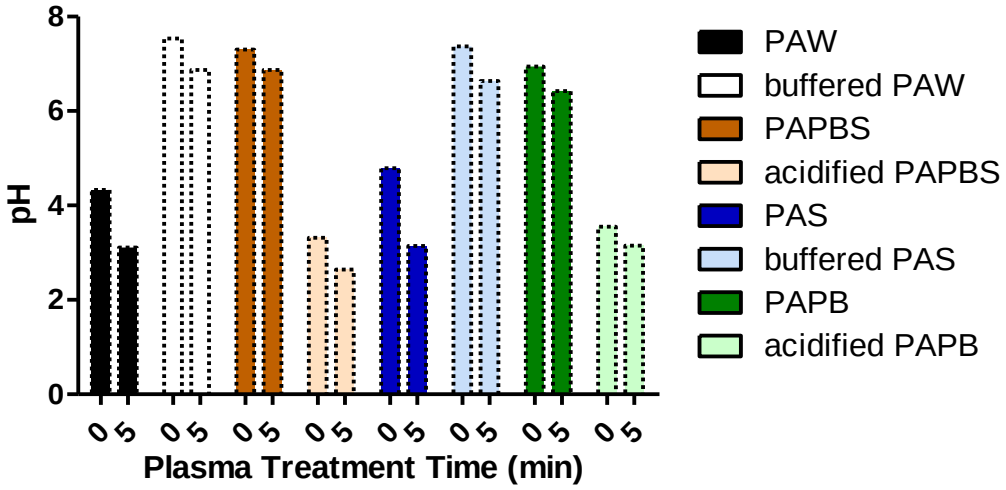

Figure 3.5 pH measurements of pH-adjusted PAL. Liquids were exposed individually to plasma for 5 min. All pH measurements were carried out as described in Section 2.2.4.

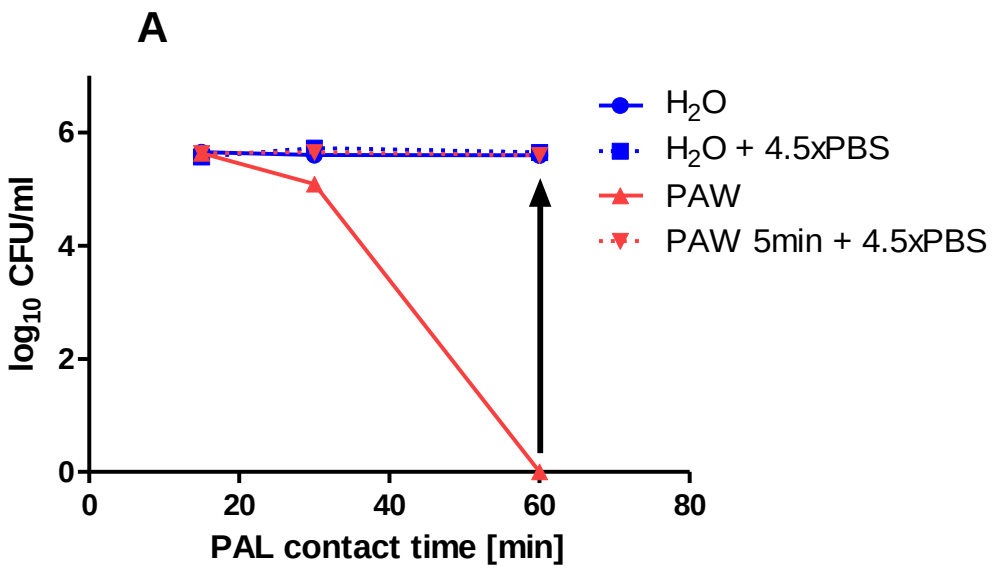
A
log10 CFU/ml
0
2
4
6
0
20
40
60
80
PAL contact time [min]
H2O
H2O + 4.5xPBS
PAW
PAW 5min + 4.5xPBS

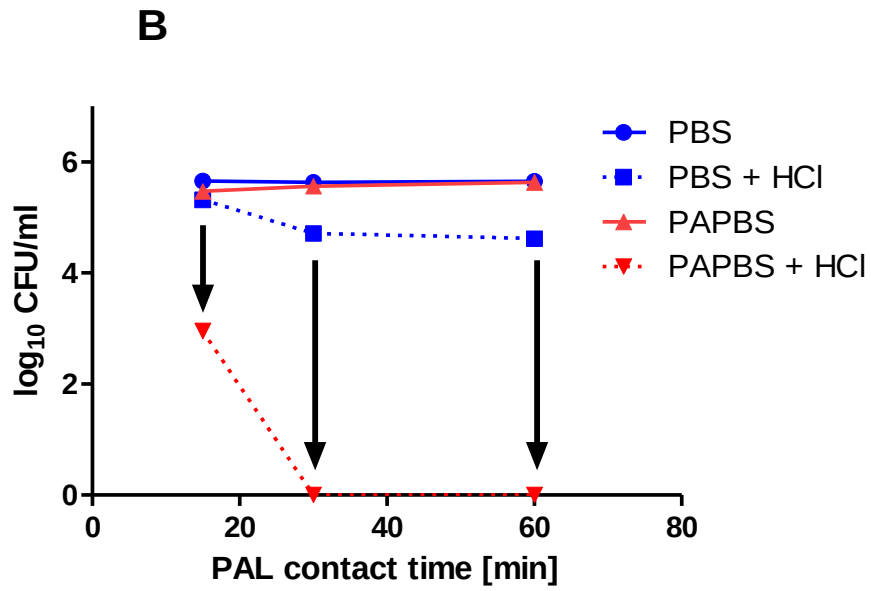
B
log10 CFU/ml
0
2
4
6
0
20
40
60
80
PAL contact time [min]
PBS
PBS + HCl
PAPBS
PAPBS + HCl

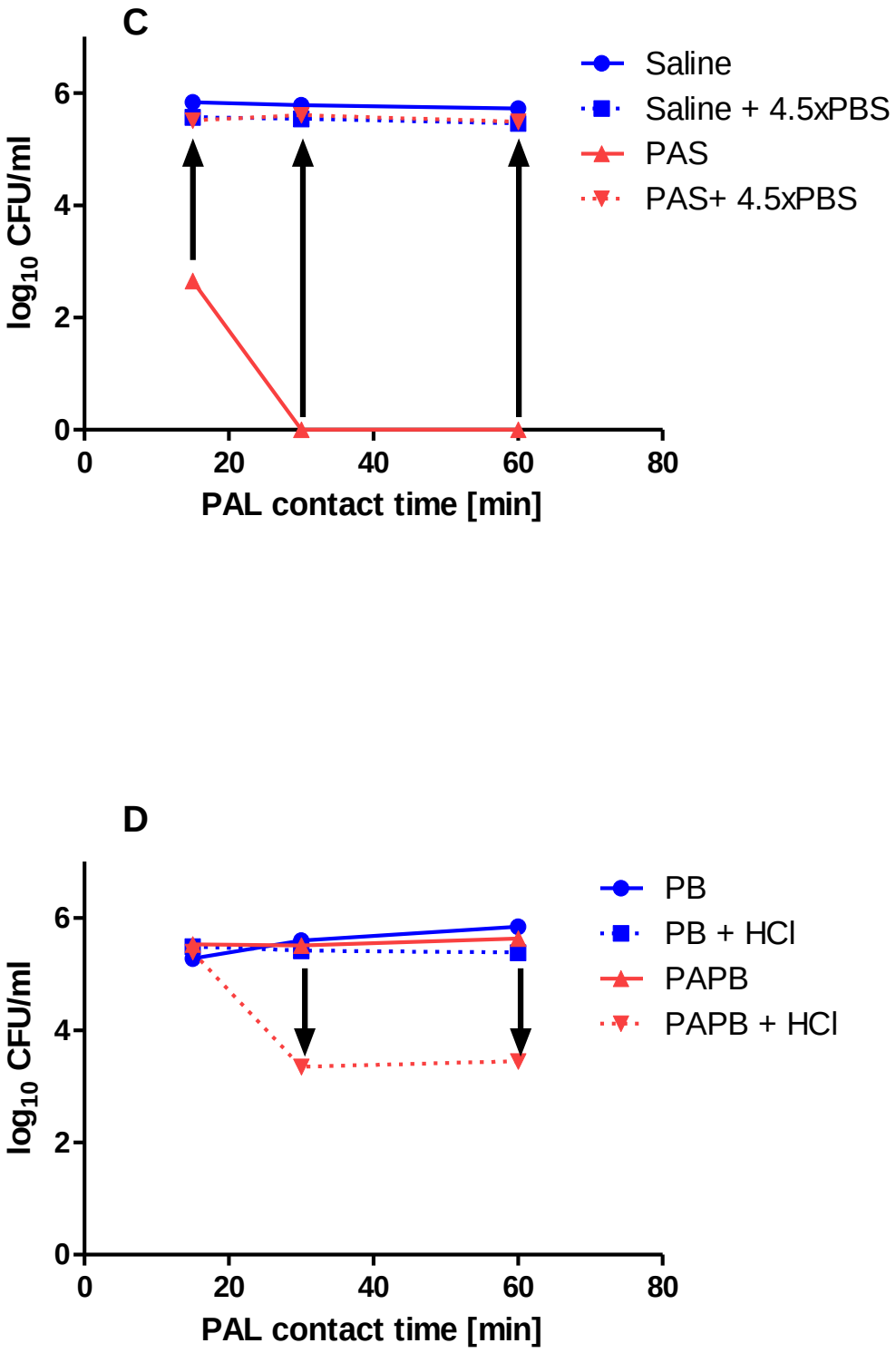

Figure 3.6 Effects of adjusted pH PAL on microbial inactivation of E. coli. Bactericidal effects of plasma treated and non-plasma treated (controls) (A) water and buffered water, (B) PBS and acidified PBS, (C) saline and buffered saline (D)

phosphate buffer solution and acidified phosphate buffer solution. The arrows represent the enhanced/reversed antibacterial effects of acidified/buffered PAL.

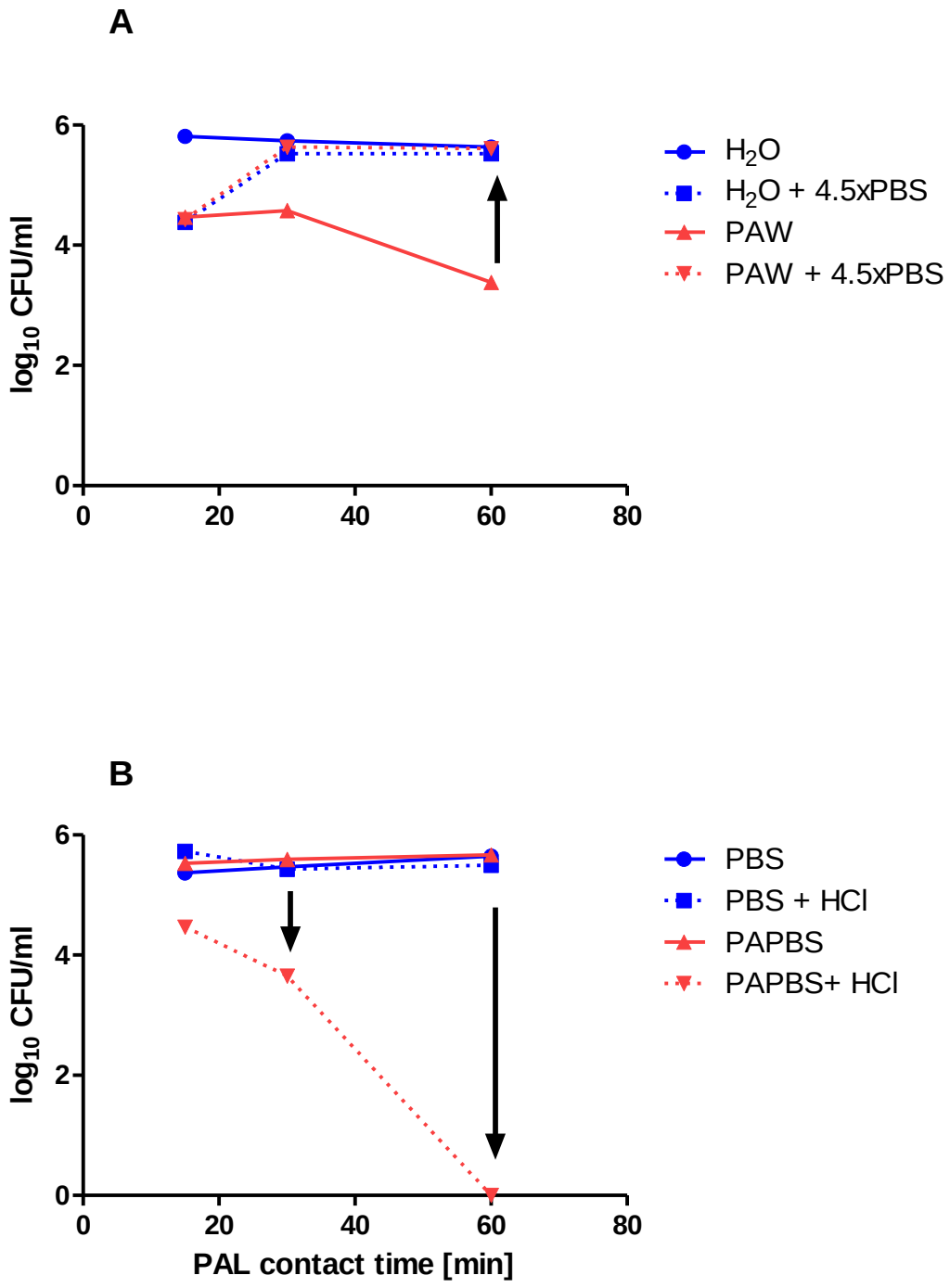

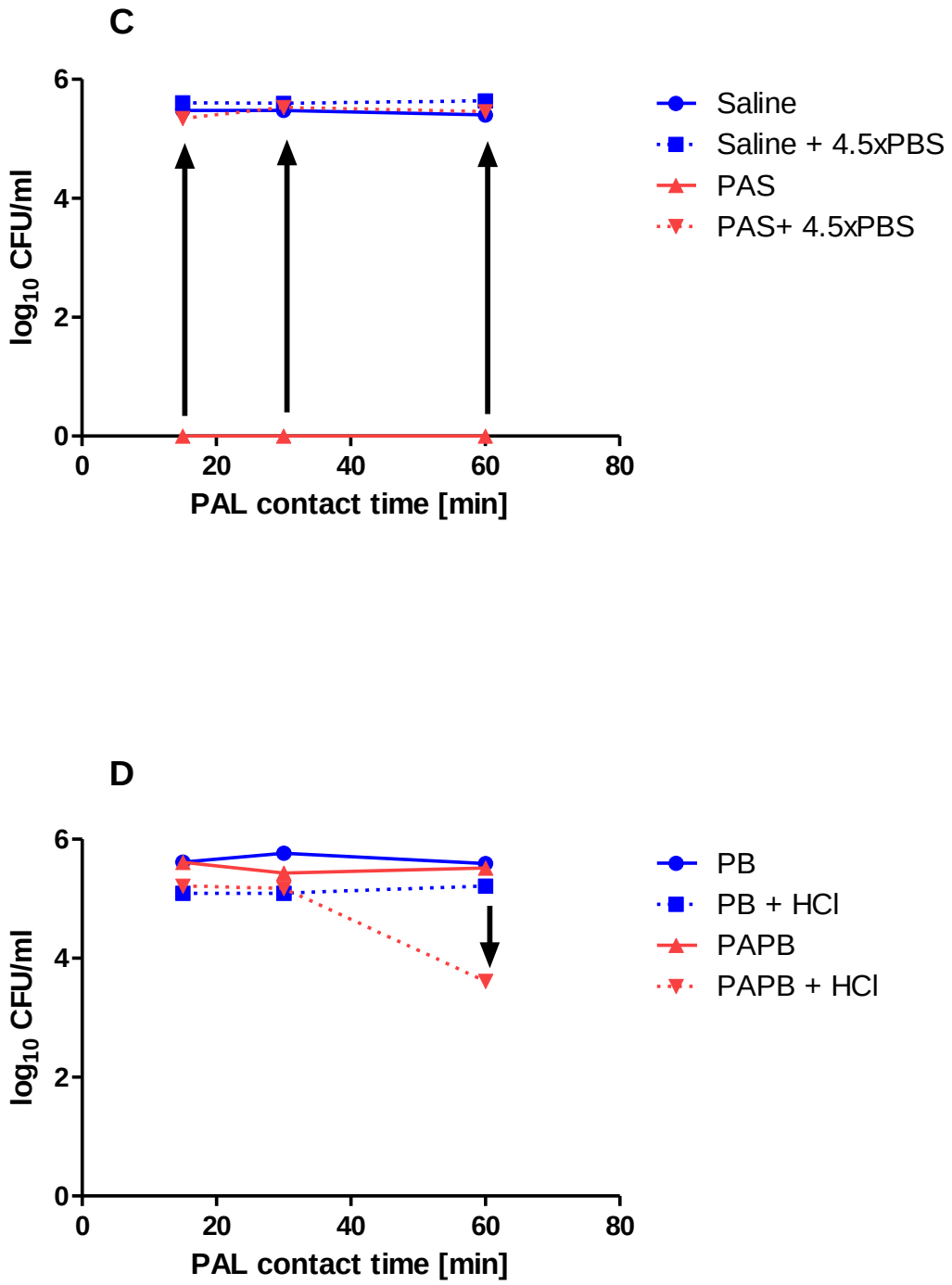

Figure 3.7 Effects of adjusted pH PAL on microbial inactivation of S. aureus. Bactericidal effects of plasma treated and non-plasma treated (controls) (A) water and buffered water, (B) PBS and acidified PBS, (C) saline and buffered saline (D) phosphate buffer solution and acidified phosphate buffer solution. The arrows represent the enhanced/reversed antibacterial effects of acidified/buffered PAL.

3.2.4 Effects of chemical composition on antimicrobial effects

As antibacterial efficacy is influenced by chemical characteristics of PAL, the influence of the buffering solutions needs to be taken into consideration. From results in the previous Section 3.2.3, it was observed that buffered PAW and PAS were not as bactericidal as normal PAW and PAS, whereas acidified PAPBS and PAPB became more efficient against both bacteria populations. These results indicate that bactericidal efficacy of PAL depends on the pH values of the solutions. A number of studies have shown that microbial inactivation of PAL depends on the pH of the solutions but the exact mechanism is still not fully understood (Naïtali *et al.*, 2010; Schnabel *et al.*, 2016; Niquet *et al.*, 2017). Moreover, it is possible that the pH value governs the generation of other active compounds. In acidic conditions, nitrites can be converted into nitrous acid. Nitrous acid is an unstable, monobasic acid and spontaneously disproportionates to nitrates and nitric oxide, which exerts broad-spectrum antimicrobial activity (Fang, 1997).

The antimicrobial effects of hydrogen peroxide have been reported in the past as well (Raffellini *et al.*, 2011). Hydrogen peroxide in acidic environments can react with nitrites to form peroxynitrite and further by-products (Oehmigen *et al.*, 2011). Therefore, higher concentrations of hydrogen peroxide in relation to nitrites could enhance the production of peroxynitrite. Hänsch et al. had shown that plasma treated saline had strong antibacterial effects against *E. coli* (NCTC 10538) and it was largely due to the interaction between nitrite, nitrate, and hydrogen peroxide generated in liquids (Haensch *et al.*, 2015). Therefore, the effects on biological systems are more likely to be caused by multiple agents with different targets which possibly lead to synergistic effects.

3.3 Cytotoxic evaluation of PAL

In this study, we used the CHO-K1 cells as a well-established mammalian epithelial model. Cells cultured in 20% PAL, which had been activated with plasma for 1, 5 or 10 min demonstrated a treatment-time dependent reduction in cell growth compared to controls, indicating that PAL have cytotoxic effects. Figure 3.8 presents the percentage of cell growth as plasma activation time of liquids increases. As it is observed PAW, PAPBS and PAPB activated for 10 min have stronger effects on the cells than PAS, than shorter activation times with minimum cell growth 61% ± 16, while other PAL caused higher cytotoxicity.

It is widely known, that air plasma results in formation of a variety of ROS and RNS and both induce oxidative or nitrosative stress in mammalian cells (Machala *et al.*, 2013). When the concentration of hydrogen peroxide increased due to plasma treatment, higher cytotoxicity was obtained, which is in accordance with other publications (Van Boxem *et al.*, 2017; Graves, 2012), thus hydrogen peroxide plays one of the major roles in cell cytotoxicity. It is yet unclear why PAS, which had a high concentration of hydrogen peroxide and a similar chemical composition to PAW, had the lowest cytotoxic activity. The generation of hypochlorite (OCl-) might be possible in plasma activated saline solution but it has not been investigated in this study. Of note, exceptionally high concentrations of H_2O_2 in PAPB set 3 of 5500 µM did not show cytotoxic effects beyond those observed in the other samples.

Nitrites were not generated in detectable concentrations in non-buffered solutions in contrast to buffered solutions and other PAL generated using jet-based systems in other studies (Chauvin *et al.*, 2017; Reuter, von Woedtke and Weltmann, 2018). Boehm et al. previously reported that cell cultures supplemented with high concentrations of nitrite, did not show cytotoxic effects on the CHO-K1 cell line under

the same conditions (Boehm *et al.*, 2018). Concentrations of nitrate were generated in all PAL, however no cytotoxic effects of nitrate were found in 10-fold higher concentrations in the mammalian cells tested according to the same study. In agreement with numerous studies, these results confirm that mammalian cytotoxicity correlates with hydrogen peroxide content in PAL but that this does not, however constitute the only cytotoxic factor. Moreover, hydrogen peroxide in liquids can react with oxygen to form hydrogen peroxide radicals (HOO·), which then can form protons and superoxide anion (O2·) leading to generation of other ROS, which should not be excluded from plasma cytotoxicity.

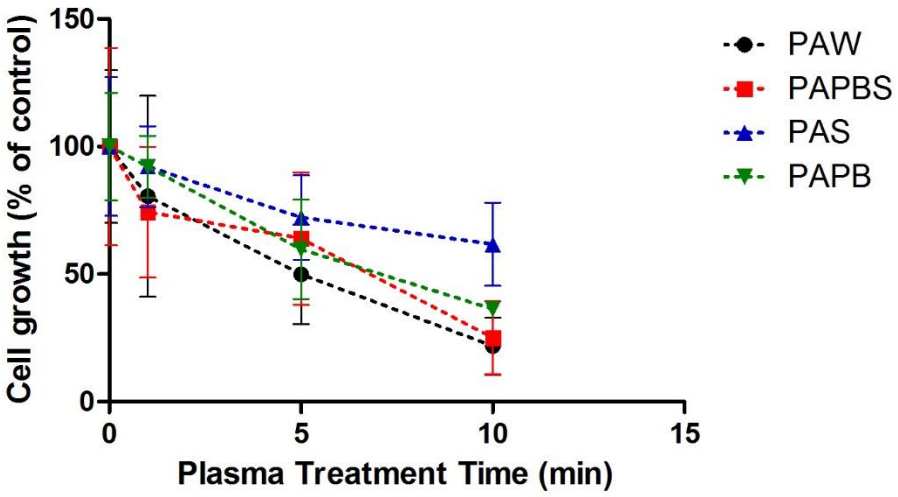

Figure 3.8 Growth inhibition of PAL on CHO-K1 cells. PAL were exposed to plasma for 1, 5 or 10 min and CHO-K1 cells were grown as described in Section 2.5.2.1

3.4 Conclusion

The concentrations of some representative long-lived chemical species in PAL increased as plasma treatment time advanced. Large differences in cytotoxicity and antimicrobial activity were found among the different PAL. We demonstrated that non-buffered PAL exerted strong bactericidal activity that persisted up to 2 days after PAL's generation. Of the studied PAL, PAW and PAS were antimicrobially stable up

to the second day, in contrast to PAPBS and PAPB which lost their antimicrobial activity the second day after the PTST. Cytotoxicity experiments showed that PAW, PAPBS and PAPB activated with plasma for 10 min were able to cause cell death in more than 50% of cells, while it is interesting to note that PAS was less cytotoxic and showed significant antimicrobial effects on both kinds of microbes, thus potentially making it a novel candidate for microbial decontamination. These results highlight the complexity of PAL solutions where multiple chemical components exert varying biological effects. As a broad measure of adverse biological responses, cytotoxicity is a useful metric to gauge the health impacts of disinfectant agents. Our results showed that different PAL may have different concentrations of chemical species, maintain diverse antimicrobial properties and cytotoxic effects and may offer approaches for future targeted applications in medicine.

Chapter 4: Effects of process and storage conditions on PAL efficacy and stability

Part of this Chapter has been published

E. Tsoukou, P. Bourke, D. Boehm (2020). Temperature Stability and Effectiveness of Plasma-Activated Liquids over an 18 Months Period. Water, 12(11), 3021

DOI: 10.3390/w12113021

The threat of antibiotic resistance has attracted a lot of interest in the 21st century, leading to antimicrobial stewardship programs and research on alternative antimicrobial therapies, as existing antibiotics are becoming a limited resource. Conversely, significantly less consideration has been given to the directly related issue of resistance toward antiseptics and biocides (Kampf, 2016). There is a need for an "antiseptic stewardship" initiative and for effective disinfection methods in a variety of sectors. Such technology should be sustainable in terms of energy efficiency, and safe for both human and environment.

Whether storage conditions affect chemical composition and antimicrobial potential of PAL is an important factor in determining their suitability for applications in decontamination and disinfection but little information has been published about PAL's stability over extended storage periods. The stability of the reactive species in solution is one of the most important issues to determine the inactivation effectiveness and shelf-life of PAL. Plasma-treated water has been shown to retain its antibacterial activity for 7 days (Traylor *et al.*, 2011) when stored at room temperature or a fridge. PAW stored at −80 °C caused approximately 4 log microbial load reduction 30 days

after its generation, with nitrites and hydrogen peroxide contributing synergistically to microbial inactivation (Shen *et al.*, 2016).

In Chapter 3 we reported that PAW and PAS can maintain their antimicrobial activity against *E. coli* and *S. aureus* for several days (Chapter 3). The current work constitutes a follow-on study using the same plasma system with optimal treatment parameters for highest microbial inactivation, to establish the stability of these PAL at different process and storage conditions, such as high temperatures or long-term storage, and determine suitable application and storage conditions.

In the first part of this chapter the influence of heating of PAW and PAS on their antimicrobial efficacy was evaluated, by using the same strains as before. In this study PAL's chemical composition was examined as well.

The objective of the second part is the evaluation of the physicochemical properties and bactericidal activities of PAW and PAS stored in sub-ambient temperatures at storage times up to 18 months, in order to ensure effective disinfection.

4.1 Effect of supra-ambient temperatures on PAL by DBD-120

4.1.1 Antimicrobial effects

To ascertain the effect of temperature increase on the antimicrobial efficacy of PAW and PAS, overnight cultures of *E. coli* and *S. aureus* were grown in TSB and used at a 10^6 CFU/mL working concentration. Deionised water and saline were plasma treated for 10 min and after 24 post-treatment storage-time (PTST), PAL were heated for 5 min between 50°C-100°C with 10°C increments. The liquids were cooled to room temperature approximately 16°C and their antimicrobial activity and chemical composition were analysed.

The colony count assay was employed to assess the bactericidal effects of PAL samples heated at different temperatures. The PAL stored at RT and solutions heated at 50°C, 60°C showed antibacterial activity against both *E. coli* and *S. aureus*; however, this property was lost after the temperature was increased ≥70°C.

PAW incubated with bacteria for 15 min were not able to cause more than 2 log reduction for either of these two bacteria (Figure 4.1 A, B). By increasing the heating temperature, the antimicrobial activity of PAW was found to be decreasing. Regarding 30 min contact time, only PAW stored at RT and PAW heated at 50°C led to microbial inactivation below the limit of detection which was 2 log (Figure 4.1C, D). As demonstrated in Figure 4.1, PAW could retain its antimicrobial activity only when it was stored at RT or heated at 50°C and 60°C and had 60 min contact time with bacteria suspensions. These solutions resulted in 4-6 log reduction for both *E. coli* and *S. aureus*, whereas PAW heated at higher temperatures achieved around 2 log reduction (Figure 4.1).

Similar antimicrobial efficacy was observed for PAS (Figure 4.2). 15 min contact time did not cause any reduction even for unheated PAS (Figure 4.2 A, B). Only PAS incubated for 60 min with bacteria showed a remarkable decrease and microbial inactivation to undetectable levels and this efficacy was retained at temperatures below 70°C (Figure 4.2 E, F). Antimicrobial activity of PAS heated at temperatures higher than 60°C was lower compared to heated PAS at lower temperatures. In conclusion, by increasing heating temperature of PAL, the bactericidal potential reduces.

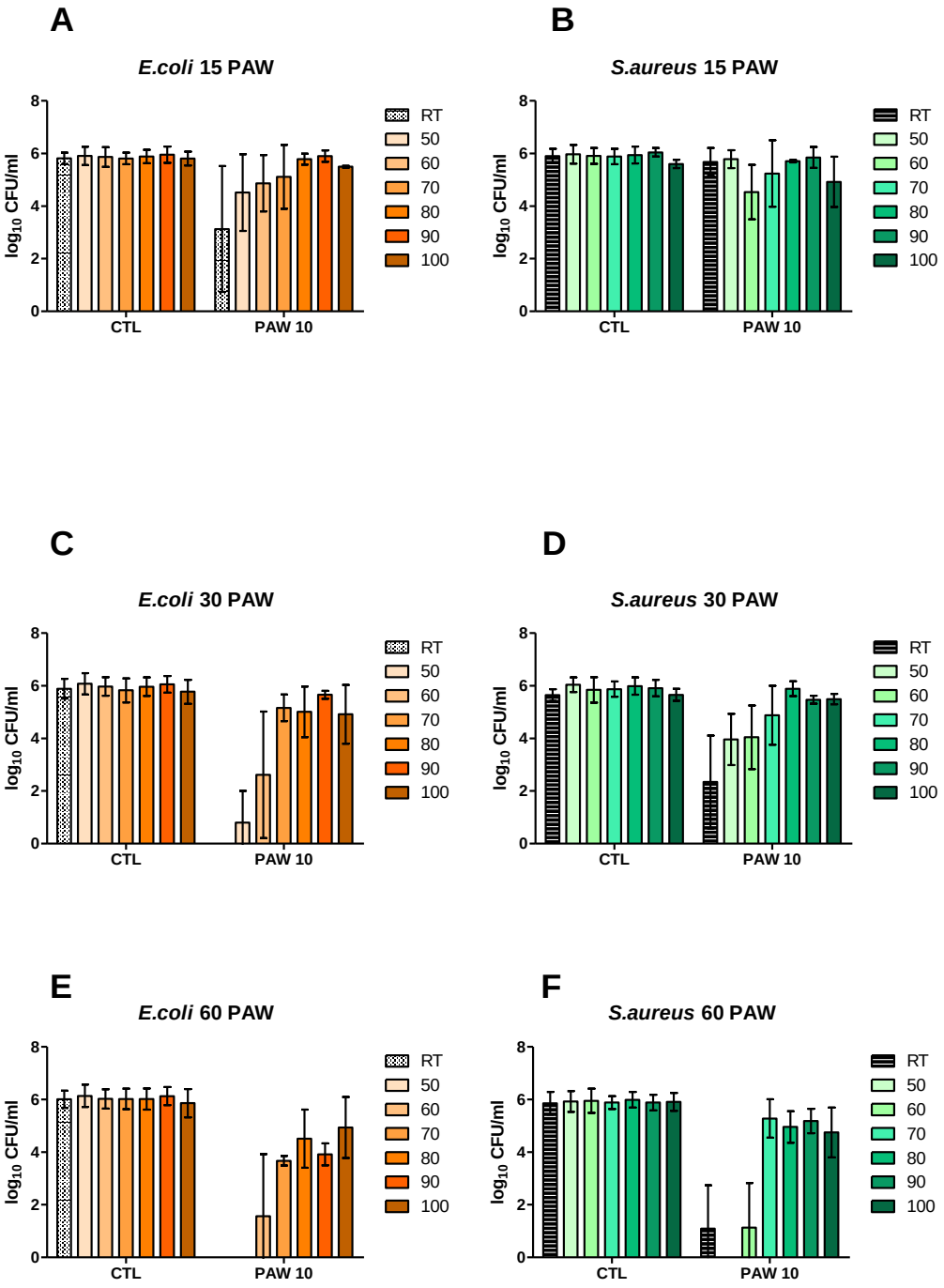

Figure 4.1 Bactericidal activity in response to heated PAW after 10 min plasma treatment and 15, 30 or 60 min contact times. PAW were heated at 50, 60, 70, 80, 90, 100°C for 5 min and then cooled at room temperature before exposed to bacteria. (A) PAW- E. coli 15 min contact time, (B) PAW-S. aureus 15 min, (C) PAW-E. coli 30 min, (D) PAW-S. aureus 30 min, (E) PAW-E. coli 60 min, (F) PAW-S. aureus 60 min. PAL were heated as described in Materials & Methods section 2.3.1 .Graphs represent averages of 3 independent plasma treatments.

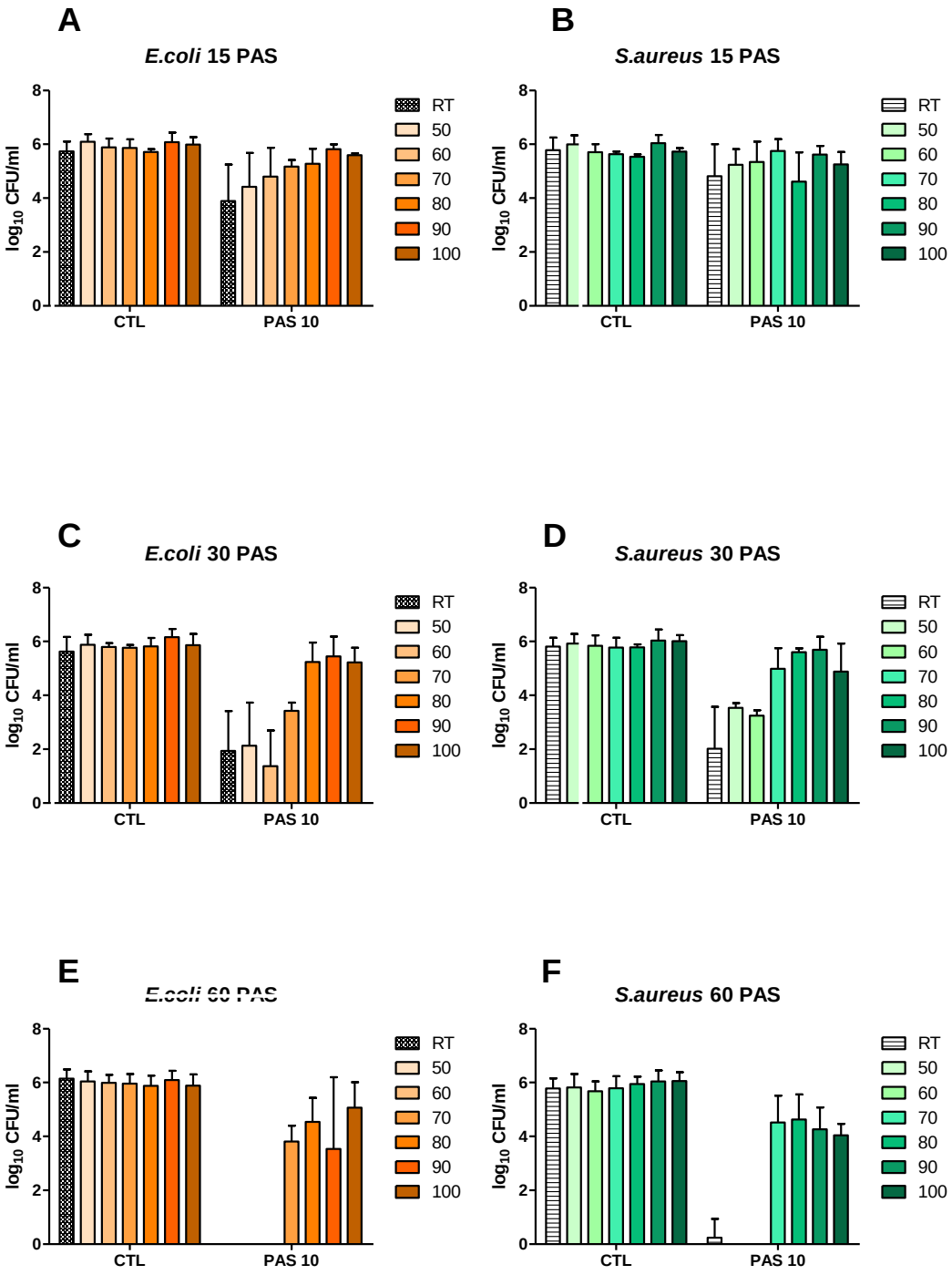

Figure 4.2 Bactericidal activity in response to heated PAS after 10 min plasma treatment and 15, 30 or 60 min contact times. PAS were heated at 50, 60, 70, 80, 90, 100°C for 5 min and then cooled at room temperature before exposed to bacteria (A) PAS- E. coli 15 min contact time, (B) PAS-S. aureus 15 min, (C) PAS-E. coli 30 min, (D) PAS-S. aureus 30 min, (E) PAS-E. coli 60 min, (F) PAS-S. aureus 60 min. PAL

were heated as described in Materials & Methods section 2.3.1.Graphs represent averages of 3 independent plasma treatments.

4.1.2 Chemical characterisation

As shown in Figure 4.3 A, B, pH measurement of different PAL suggested that pH of the solutions was not affected by the temperatures and remained essentially stable independent of temperature. The pH value of PAL remained around 3 regardless of heating temperature.

No significant difference in peroxide concentration of PAW and PAS was observed after heating times. Specifically, concentration of peroxides of PAW stored at RT was 1308±164μM and PAW heated at 100°C was 1328±190 μM (Figure 4.3 C, D). The concentration of peroxides for PAS stored at RT was found to be 1128 ±109 μM, and PAS 100 °C was 1150±94 μM (Figure 4.3 C, D).

Anova results for nitrate and peroxides showed that temperature did not have any significant effect on nitrate or hydrogen peroxide concentrations. Nitrite concentration was not detected for any of the solutions.

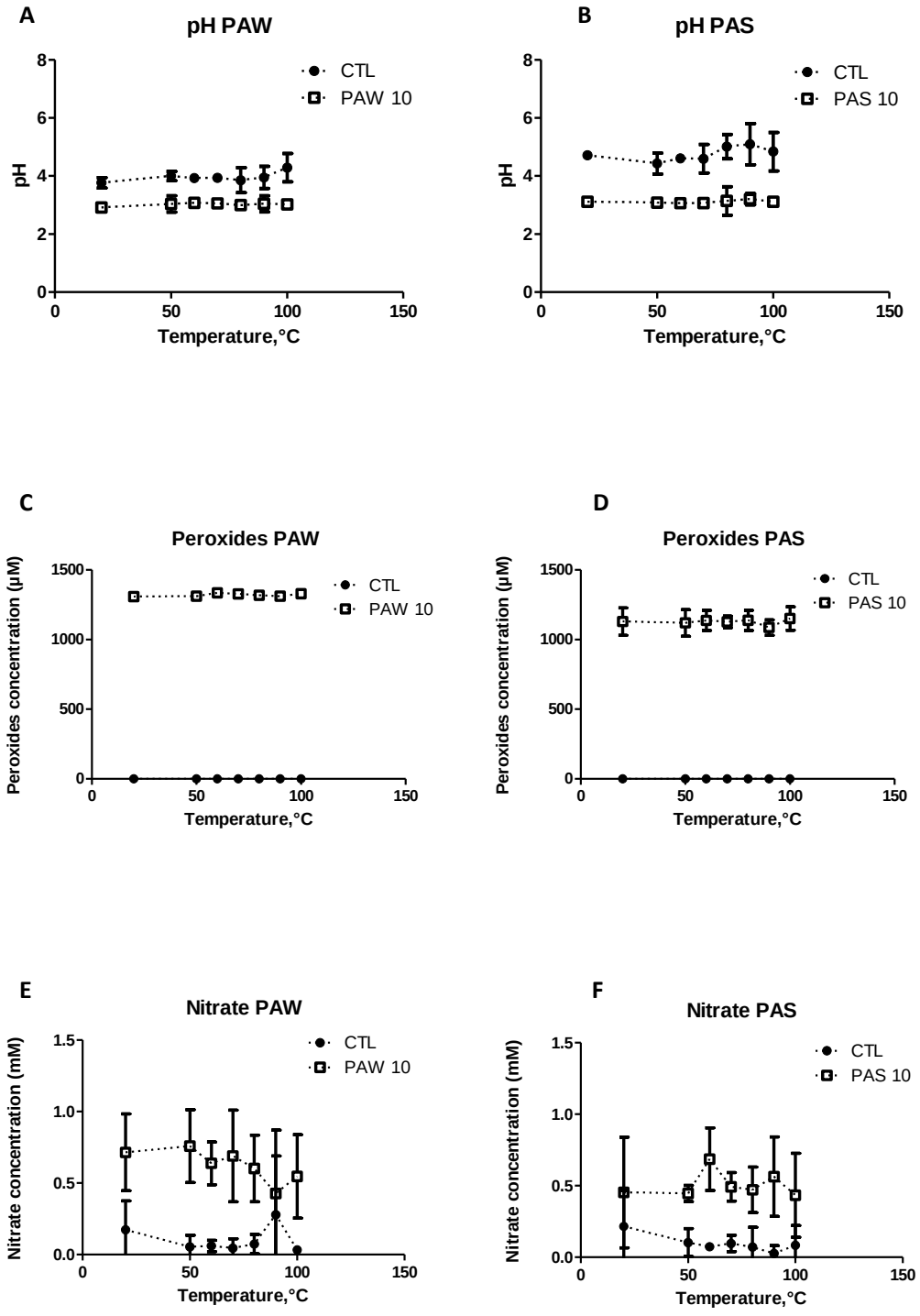

Figure 4.3 Chemical composition of PAW and PAS heated at 50, 60, 70, 80, 90, 100°C for 5 min and then cooled at room temperature before tested for concentration of different chemical species.. (A, B) pH measurements, (C, D) generation of peroxides measured by buffered KI, (E, F) nitrate concentrations) (n=3). PAL were heated as

described in Materials & Methods section 2.3.1. Graphs represent averages of 3 independent plasma treatments.

4.2 Discussion

This study aimed to evaluate the heat stability of PAL under a short-term heating scenario by characterization of their chemical composition and subsequent changes in antimicrobial activity. It was shown that higher temperature reduced the antibacterial properties of PAL. Although, PAL seemed to be stable up to 60°C, its antimicrobial activity was lost upon heating to >60 °C, due to possible degradation of unidentified chemical species in PAL.

Increase in temperature results in higher levels of energy for molecular vibrations and consequently a solution's molecules may dissociate more easily. In this study, temperature did not affect significantly the pH values of either PAW and PAS solutions, the concentrations of hydrogen peroxide or nitrate.

Hydrogen peroxide solutions are used for cleaning and disinfectant applications. Hydrogen peroxide is a quite stable substance in low and moderate pH. The increase in temperature and also pH adversely affects the stability of hydrogen peroxide (Yazici and Deveci, 2010). The decomposition of hydrogen peroxide at high temperatures yields oxygen and water. In this study there was not any statistically significant reduction of peroxides after PAL were heated at high temperatures, so in this case presumably, sufficient changes occur in other reactive oxygen or reactive nitrogen chemical species that are not detected in this study (such as peroxynitrite, peroxynitrous acid, hypochlorous acid) and permit such a loss in antimicrobial activity.

Generally, temperature can have an effect on the inactivation of bacteria especially through nucleic acid denaturation and the use of disinfectants at elevated temperature may therefore enhance their antibacterial effect. In this case bacteria were exposed to room temperature liquids but the stability of these liquids to temperature increases was evaluated. To the best of our knowledge, previous reports have not answered whether temperature has a significant effect on the bactericidal activity of PAL. Previous studies have suggested that antibiotics such as sulfamethazine oxacillin, chloramphenicol, aminoglycosides, quinolones, clindamycin, novobiocin, trimethoprim, vancomycin, and azlocillin are heat-stable (P. Papapanagiotou, J. Fletouris and Psomas, 2005; Traub and Leonhard, 1995). On the other hand, several β-lactams such as penicillin G, ampicillin and amoxicillin appear heat-labile (Traub and Leonhard, 1995). Antibiotics of the same class have been reported to have different heat stabilities depending on different types of matrices and heating treatments involved (Franje *et al.*, 2010).

Peracetic acid is a chemical disinfectant used mainly in the food industry, where it is applied as a cleanser and as a disinfectant. A peracetic acid sanitizer containing peracetic acid and hydrogen peroxide was stored at constant temperatures (25, 35, 40 and 45°C) and results showed that the decomposition rate constant of the solution was affected by temperature (Kunigk *et al.*, 2001). Another disinfectant is glutaraldehyde, which is usually applied successfully in the field and commonly shows a broad range of microbial killing. Cross-linked chitosan-glutaraldehyde which had been heated in sterile water at 40 °C, 70 °C and 100 °C for 2 h showed antibacterial activity against antibiotic-resistant *Burkholderia cepacia* although the inhibitory effects varied with different temperatures (Li *et al.*, 2013).

The effects of heating treatments have been investigated in antimicrobial activity of natural drug sources such as garlic. The antimicrobial activity of garlic decreased as the heating temperature increased up to 100 °C for various microorganisms (Kim *et al.*, 2002). Antimicrobial activity in garlic samples is produced by a reaction, where an enzyme and substrates are involved. This implies that alliinase (the enzyme) can be heat inactivated and cannot convert alliin into allicin. The antibiotic properties of ginger against human pathogenic bacteria such as *Klebsiella pneumoniae, E. coli and S. aureus* have been reported to decrease as well when heated at boiling water conditions (100°C) (Sah *et al.*, 2012).

These results focus on providing a potential industrial or commercial use of PAL to a wide range of products, which require treatments, such as fumigation applications or when disinfecting an instrument with an automated reprocessor, where the device will heat the disinfectant to the required temperature. Since the exposure to temperature equal or higher than 60°C reduced the antimicrobial activity of PAL, further research is needed for applications were higher processing temperatures are needed such as fumigation.

4.3 Sub-ambient Temperature Stability and Effectiveness of PAL over 18 Months

4.3.1 Antimicrobial effects

The practical application of PAL in biomedical, food or processing sectors would benefit from an ability to generate these liquids off-site, and retention of functional stability over long-term storage. The effects of storage at different sub-ambient temperatures over periods of up to 18 months on the antibacterial effects were therefore investigated. PAW and PAS were the liquids of interest as they demonstrated

high antimicrobial activity in our previous study (Chapter 3) and present suitable liquids for a range of bio-decontamination applications. The antimicrobial effects and the chemical composition of four independent sets of PAW and PAS were analysed and two different scenarios were observed in the chemical measurements.

Our results showed that bactericidal stability of both PAL was affected by storage temperature. It is worthwhile to mention that when microbial inactivation was assessed, all PAL were completely thawed and at room temperature. The bactericidal stability of both PAL increased with lower storage temperature with -150 ≥ −80 > −16 > 4 ≥ 20°C showing a descending order for bacterial inhibition of *E. coli* and *S. aureus,* and solutions stored at RT or 4°C showed complete loss of antibacterial activity (Figures 4.4 – 4.7). As observed in previous experiments using the same microbial targets (*E. coli* and *S. aureus*), longer contact times (i.e. 60min) between bacteria and PAL were more effective than short contact time (i.e. 15 min showed very little antibacterial effect). The retention of antibacterial effect over storage time at different temperatures is presented for 60 min contact time in figures 4.4 – 4.7 with detailed data (log CFU/mL ± SD) for all contact times available as tables in supplementary data (Table S1-3). Untreated deionized water samples controls were stored at all of the storage temperatures and their average is represented in figures 4.4 – 4.7.

Generally, antimicrobial efficacy of PAW and PAS was very similar: Fresh PAW and PAS could cause a log reduction of up to 6 cycles for both bacteria tested (Figures 4.4 – 4.7). However, after a week of PAL storage at RT, 4, -16, −80 or -150°C the bactericidal efficacy for some of the liquids decreased from 3 to 6 log, particularly at the higher storage temperatures. PAW and PAS stored at RT and 4°C no longer reduced bacterial growth. Conversely, PAW and PAS stored at −80°C and -150°C retained similar bactericidal efficacy to the fresh PAL and were able to inhibit bacterial

growth after 60 min contact time (Figures 4.4 – 4.7). Specifically, after 1 week of storage, PAW that had been stored at -16 °C could cause 3-4 log reduction for *S. aureus*, whereas after 2 weeks the same solutions stored at these conditions did not inactivate the bacteria (Figure 4.6 B). Regarding PAS under the same conditions, the solutions could cause a 6 log reduction of *S. aureus* after 1 week of storage, declining to an approximate 2 log reduction after 2 weeks (Figure 4.7B). With increasing storage time, the antimicrobial efficacy of PAL stored at -16°C was lost and antimicrobial assay results after 1, 3, 6 and 18 months of storage were quite similar for both bacteria. All PAL stored at −80°C and -150°C could still cause 6 log reduction of bacterial concentrations. These findings indicate that PAW and PAS retained efficient content of reactive species after 18 months of storage time at -80°C and -150°C, and consequently bactericidal activity. However, bactericidal activity of these PAL was unstable at -16°C, with activity lost in the range of weeks.

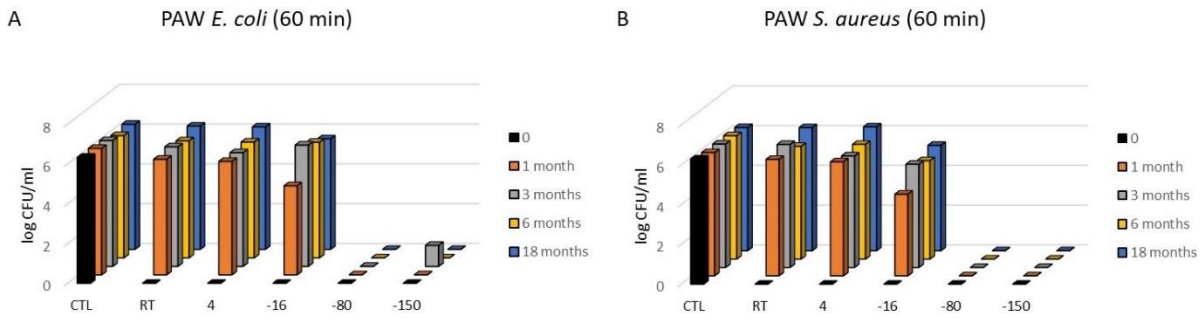

Figure 4.4 Microbial inactivation of E. coli and S. aureus at 60 min contact time, treated with PAW stored at different temperatures for up to 18 months. PAW were plasma treated for 10 min and stored as described in Materials & Methods section 2.3.2. Graphs represent averages of 2 independent plasma treatments (Set 1 and 2).

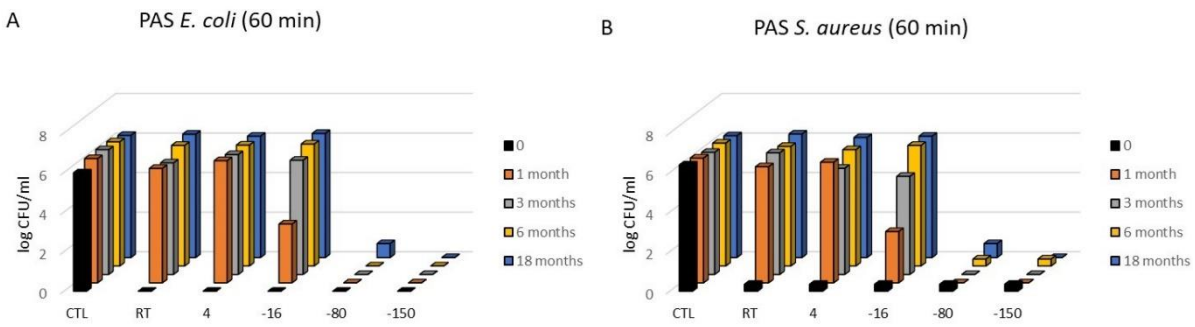

Figure 4.5 Microbial inactivation of E. coli and S. aureus at 60 min contact time, treated with PAS stored at different temperatures for up to 18 months. PAS were plasma treated for 10 min and stored as described in Materials & Methods section 2.3.2. Graphs represent averages of 2 independent plasma treatments (Set 1 and 2).

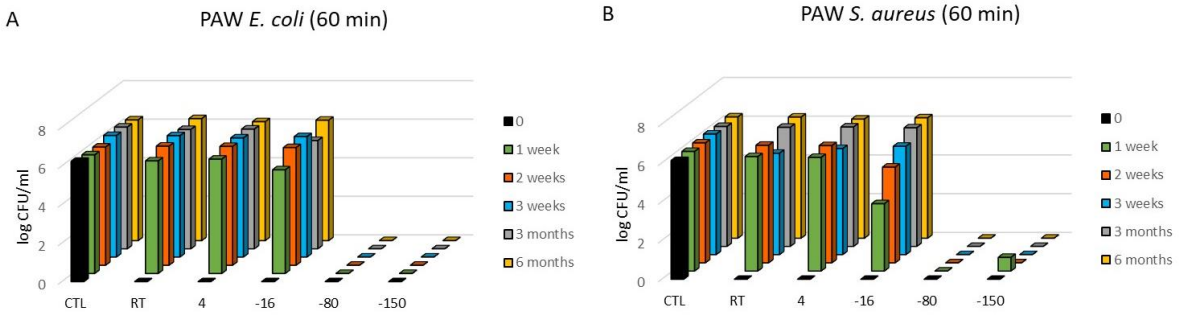

Figure 4.6 Microbial inactivation of E. coli and S. aureus at different contact times, treated with PAW stored at different temperatures for up to 6 months (Set 4). PAW were plasma treated for 10 min and stored as described in Materials & Methods section 2.3.2.

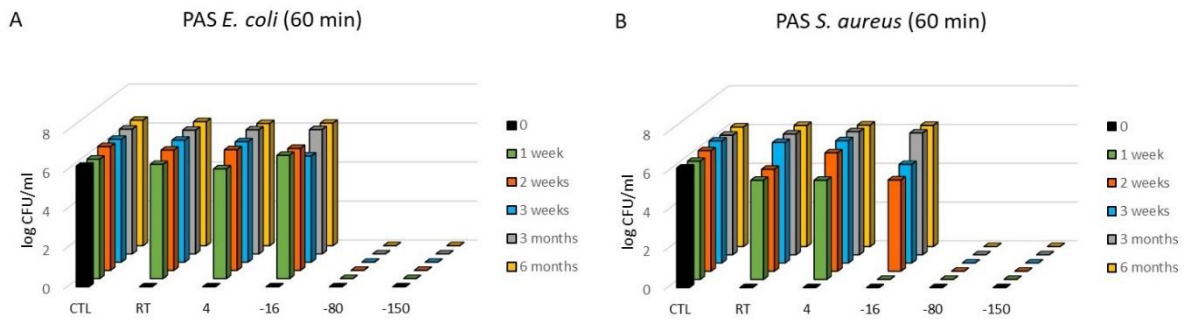

Figure 4.7 Microbial inactivation of E. coli and S. aureus at 60 min time, treated with PAS stored at different temperatures for up to 6 months (Set 4). PAS were plasma treated for 10 min and stored as described in Materials & Methods section 2.3.2.

4.3.2 Chemical characterisation of PAL

Untreated PAL (controls) were stored in all different conditions and no difference was found between different storage times or storage temperatures (controls are not represented in the figures). Figure 4.8 shows the decline in the pH of PAW and PAS (on the first day of their generation) from 4.7 to 2.9 and from 4.7 to 3, respectively, and pH appeared to be unaffected by storage in different ambient and sub-ambient temperatures, remaining stable during the storage time.

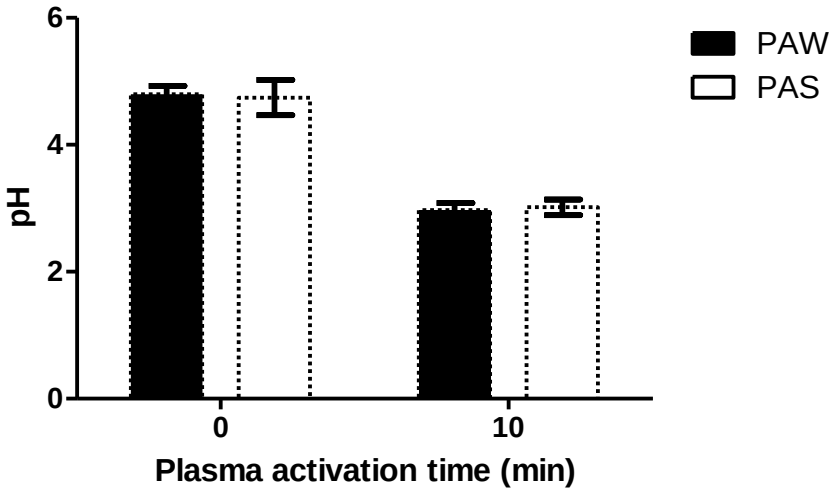

Figure 4.8 pH measurements of PAW and PAS the first day of their generation. PAL were generated by exposure to DBD for 10 min and are compared to the pH of an untreated control.

Generally, the chemical properties of PAW and PAS after storage in different storage conditions displayed changes when compared to freshly prepared solutions. The graphs below show the evolution of ROS and nitrate in PAW and PAS from the day of their generation over storage time (Figure 4.9, 4.10) and was divided into 4 different phases. 4 sets of PAL are represented individually due to differences in concentrations of chemical species. Phase I showed a strong decrease of ROS concentrations within the first month of storage in all conditions. In phase II (1-3 months) concentrations increased in sets 1 and 2 (scenario a) at all storage temperatures except -16°C while remaining constant in sets 3 and 4 (scenario b). Phase III showed relatively stable concentrations of ROS, which decreased post 6 months of storage (phase IV only analysed for sets 1 and 2). Anova indicated that ROS concentrations were significantly affected by storage temperature and storage time (3 months and 6 months) by comparison with PAL stored at RT ($P<0.001$).

In sets 1 and 2 the concentration of ROS measured by KI assay (see Materials & Methods, Section 2.4.2) the first day of PAL generation was around 1000 μM for PAW and PAS. Both PAW and PAS experienced a decrease of ROS concentration over the storage at different storage temperatures over a period of a month (Figure 4.9, 4.10). ROS concentration for both PAL after a month storage time varied between 300-700 μM, except of PAL stored at -16 °C, which consistently had the lowest concentration around 200 μM. After 3 months of storage, measurements showed that ROS concentrations increased in all PAL- due to possible chemical reactions between ROS and RNS which led to generation of oxidising species -except for PAL stored at -16 °C, which was the only liquid with unchanged concentration after 1 month storage. Highest concentration of ROS was observed for PAL stored at 20 °C (room temperature) with a peak of around 1300 μM for PAW, and 1500 μM for PAS. Similar trend lines followed for measurements after 6 months storage time. ROS were also measured after 18 months of storage and all PAL had decreased ROS, similar to concentrations found after 1 month of storage. Regarding set 3 and set 4, the starting concentrations of ROS were up to three times higher for PAW and up to 5 times higher for PAS (Figures 4.9, 4.10). For this reason, hydrogen peroxide measurements were performed, which showed that only around 620 -1000 μM of the total ~3000 μM ROS in PAW from sets 3 or 4 were hydrogen peroxide (Figure 4.11). The measurements were repeated at 1, 2, 3 weeks and 1 month post storage for set 4 and showed a gradual decrease of ROS. This remained stable after 3 months of storage at the same conditions, similar to solutions in set 1 and set 2. No changes were observed in hydrogen peroxide concentration (Figure 4.11).

Nitrite concentration was not detectable for any of the solutions. With regards to nitrate, plasma treatment increased PAW nitrate concentrations for set 1 and set 2 to

around 600-800 μM and for PAS to 500 μM after 10 min plasma treatment (Figure 4.9, 4.10). Nitrate concentrations were variable; in almost all sets concentrations increased after a month, and nearly doubled in some cases, with a following decrease after 3 months, and a subsequent gradual increase in concentration to 6 months of storage. As for storage temperature, no significant differences in nitrate concentrations among various storage conditions were obtained. Generally, PAL stored at RT had slightly higher nitrate concentrations for all storage times compared to other conditions. Set 3 and set 4 both showed higher concentrations of nitrate the first day of their generation for PAW, whereas PAS had lower concentration in set 3 but higher for set 4.

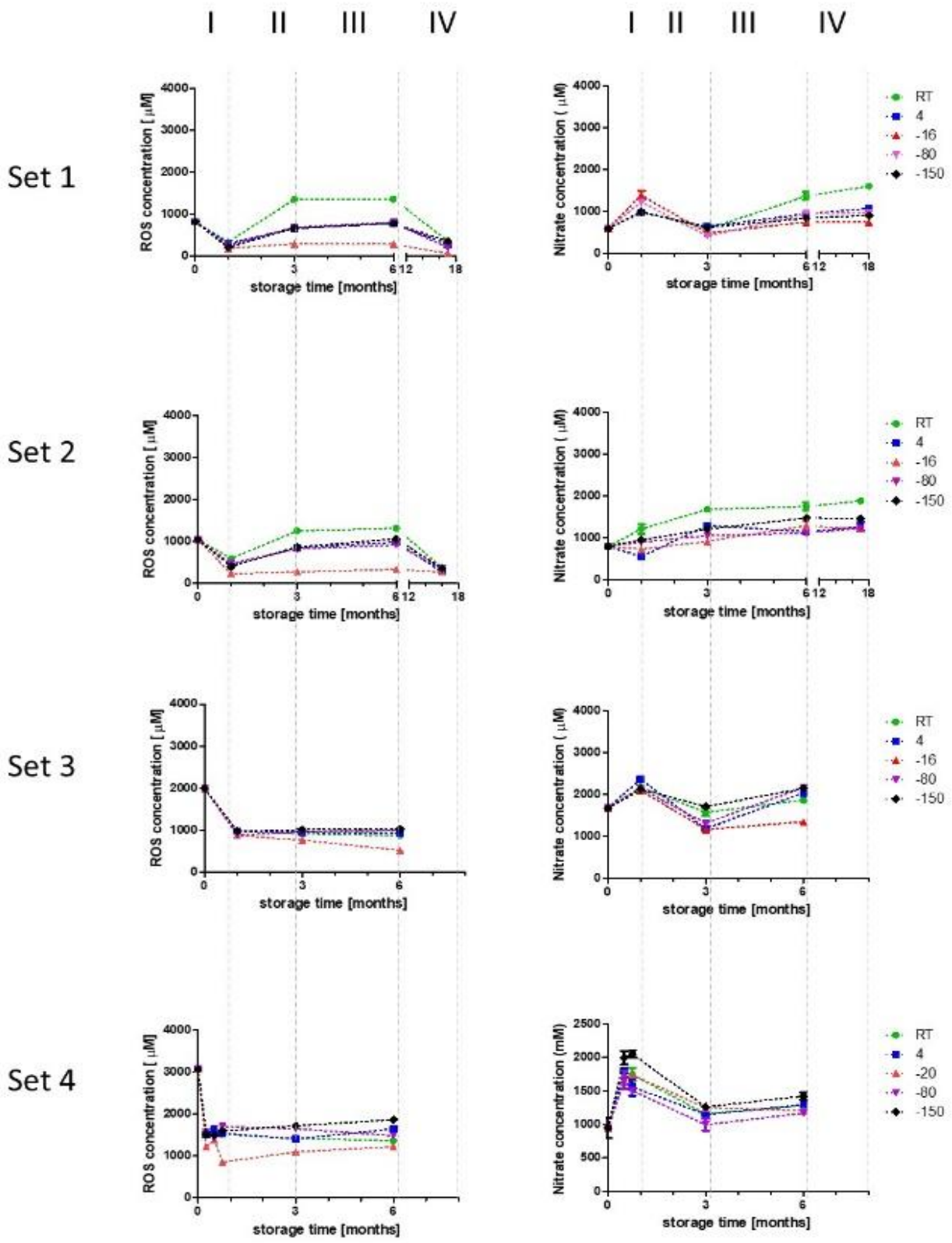

Figure 4.9 Chemical properties of PAW stored at different temperatures for 6 - 18 months showing ROS concentrations in the column on the left and nitrate concentrations in the column on the right. Samples were analysed after 1, 3 and 6

months and 18 months (set 1 and 2). Set 4 was also analysed after 1, 2 and 3 weeks of storage.

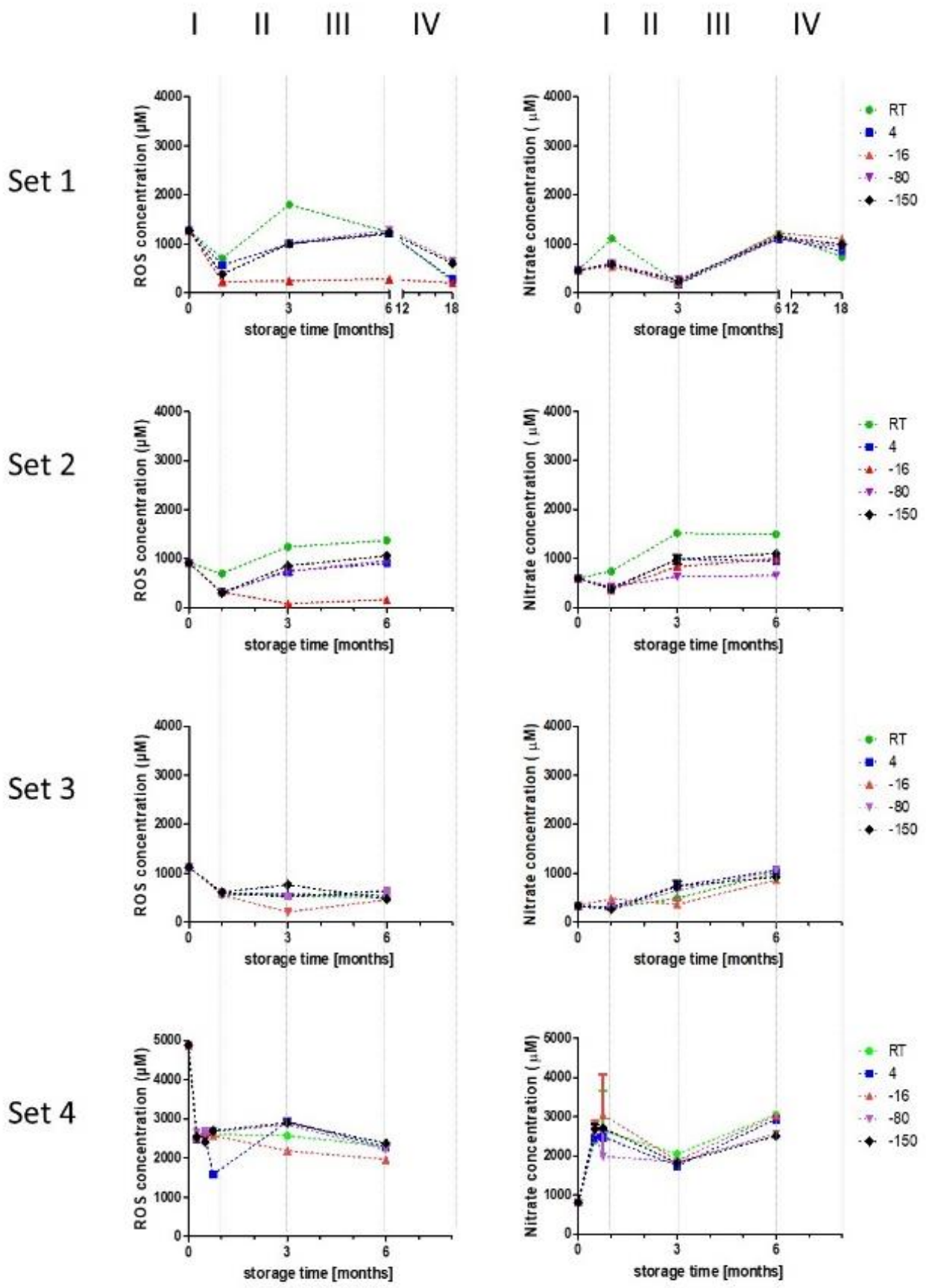
I II III IV
I II III IV
Set 1
Set 2
Set 3
Set 4
ROS concentration (µM)
Nitrate concentration (µM)
storage time [months]
RT
4
-16
-80
-150

Figure 4.10 Chemical properties of 4 different sets of PAS stored at different temperatures for 6 - 18 months showing ROS concentrations in the column on the left and nitrate concentrations in the column on the right. Samples were analysed after 1, 3 and 6 months and 18 months (set 1 and 2). Set 4 was also analysed after 1, 2 and 3 weeks of storage.

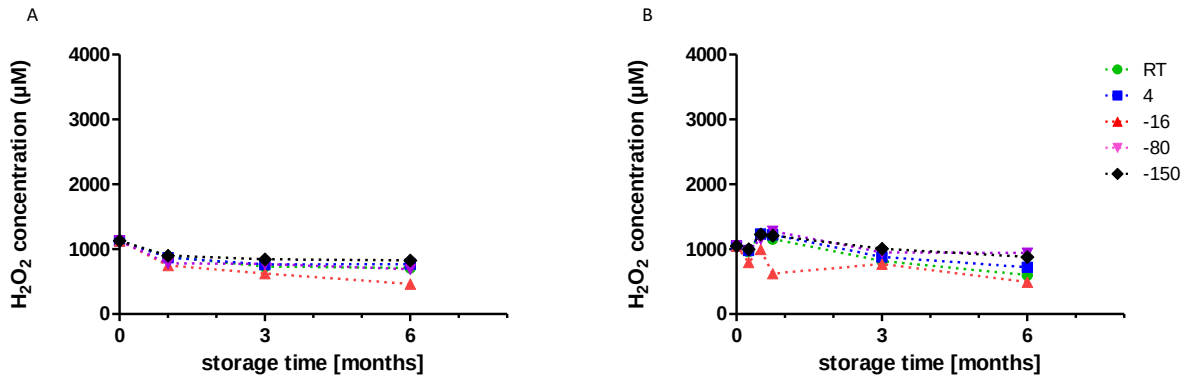

Figure 4.11 Hydrogen peroxide concentrations of PAW set 3 (A) and set 4 (B) stored at different temperatures for 6 months.

4.3.3 Freezing behaviour

The instability of PAL during storage at -16°C suggests a degradation of the relevant reactive species and differences to other conditions were observed in the chemical analyses. Freezing and nucleation behaviour of PAW stored at -16 °C was investigated in order to determine if the PAL stored at this temperature were fully frozen, or if they were still partly in aqueous phase. Generally, liquid freezing is usually divided into three stages as shown in Fig. 4.12: (1) supercooling, (2) crystallization and (3) solid freezing. Generally, in the supercooling stage, nucleation of liquid may occur at any time. In the crystallisation phase, most of the solution turns into solid and during solid freezing the temperature of the solid solution drops until it reaches the end temperature. In this study, 3 sets of PAW were investigated and no major changes to nucleation and freezing points of PAW were observed with a nucleation point between -5.7 and -4.8°C and a freezing point of -0.1 to 0°C (Figure 4.13). Plasma reactive

species did not show major effects on liquid supercooling and did not cause a depression of the freezing point. Of the samples analysed, one closely resembled deionised water in freezing behaviour, while the others were more closely aligned with the curves observed for solutions of H_2O_2 and $NaNO_3$ at concentrations similar to those found in PAW. Differences to control water were seen in the crystallization phase where the temperature of PAW samples continuously decreased from the freezing point. This suggests the concentration of solutes (ROS/RNS) in the aqueous phase as water froze out of solution.

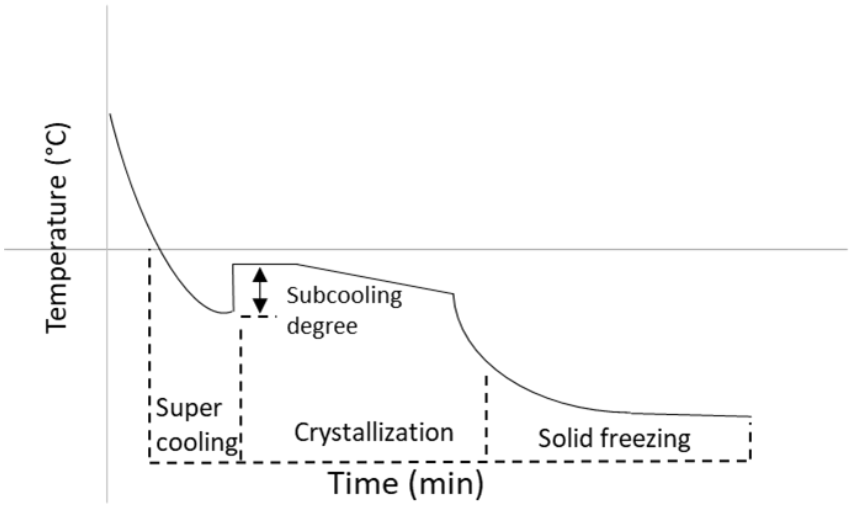

Figure 4.12 Schematic of typical freezing curve.

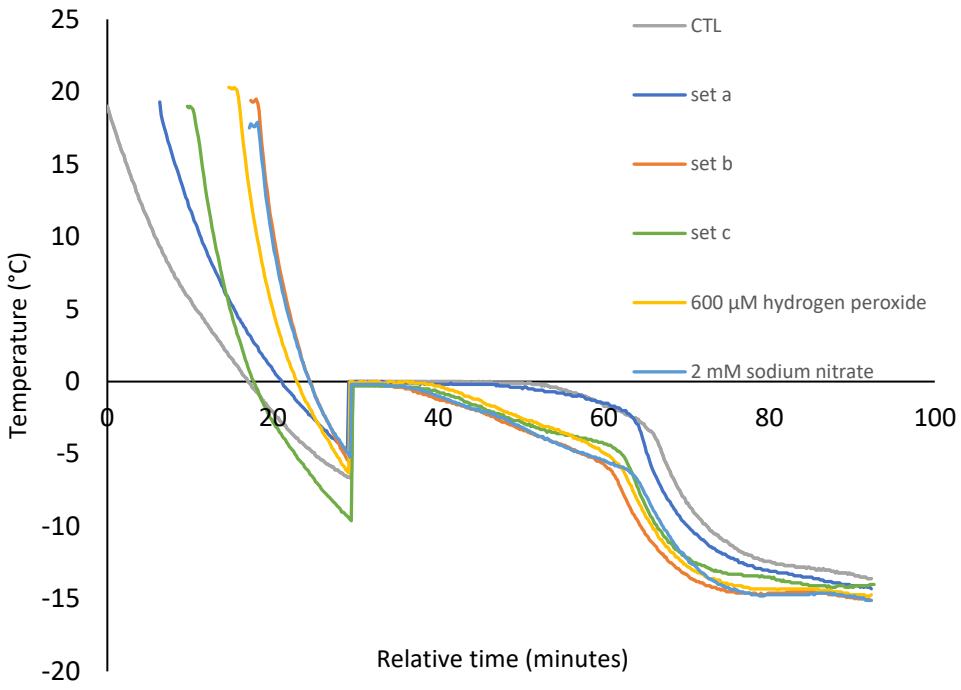

Figure 4.13 Freezing curve of PAW. Temperatures of different PAW sets, aliquots of hydrogen peroxide and sodium nitrate were measured by non-contact infrared thermometer with laser pointer (Materials & Methods Section 2.4.6)

4.4 Discussion

When selecting the best disinfectant and optimal conditions for maximum efficacy for a particular use, the most important factors to consider are the active ingredient concentration in the solution, temperature of use, contact time and side effects. Temperature could be an important factor to influence the efficiency of the bactericidal agents (Wei *et al.*, 2005). Our results revealed that the effect of storage temperature on preserving bactericidal activity of PAW and PAS was in the order of 20<4<-16<-80=-150 °C. The differences of the different storage conditions of PAL might be explained by differences in the physicochemical properties of PAL in different temperatures.

Peroxides measurements showed that there was a decrease after a month of storage time for all PAL and increase after 3 months. These results indicate that peroxides in PAL had possibly reacted with other chemical species such as RNS substances under these conditions. Bactericidal activity of PAL decreased with storage time for liquids stored in higher temperatures such as 20°C, 4°C, - 16°C. Hydrogen peroxide is a strong oxidizer especially in acidic environments. The lowest concentration of peroxides was always observed for PAW and PAS kept at -16°C.The liquids stored in the higher sub-ambient temperature started losing their antimicrobial activity completely after 1 month of storage time. The reduction in the concentration of peroxides in PAL may be correlated with the loss of bactericidal efficacy observed. Interestingly, PAW stored at -80 °C and -150 °C after 1 month (306-360 μM), had peroxides concentrations as low as PAW stored at -16°C after 6 months (307±29 μM). However, these liquids still retained their efficacy against bacteria after 6 months of storage, indicating that peroxides are not the only factors affecting microbial killing. The synergistic effects of hydrogen peroxide, nitrates and values of ORP have been proposed to affect microbial inactivation of PAW over storage time stored at 25°C, 4°C and -20°C (Shen *et al.*, 2016). In this study PAW stored at -80°C was the only solution with stable hydrogen peroxide and nitrite concentrations and retention of its bactericidal efficacy.

In previous studies, it has been mentioned that storage temperature did not exert significant influence on pH and ORP values of acidic and basic electrolyzed oxidizing water stored at 4°C or 25°C (Fabrizio and Cutter, 2003). Plasma activated reverse osmosis water stored at 3°C or 24°C did not show any difference in pH values and conductivity after 96 hours storage time (Figueira *et al.*, 2018). Moreover, pH of 20 min plasma treated water remained essentially stable during a 30-day storage in different conditions reaching up to -80°C (Shen *et al.*, 2016).

In this study the concentrations of hydrogen peroxide and nitrate increased after plasma exposure. Nitrite concentration was not detectable, and the pH was acidic. An increase of nitrate after one month of storage time at different conditions can also support the scenario that chemical reactions between the detectable peroxides and RNS occur and subsequently result in the formation of nitrate. Zhou et al reported that nitrite can be converted into unstable HNO_2 in acidic conditions and subsequent decomposition to other nitric oxide species (1-3) (Zhou *et al.*, 2018). Moreover, nitrites can also react with hydrogen peroxide in acidic environment and form peroxynitrite (4) (Lukes, Locke and Brisset, 2012).

$$NO_2^- + H^+ \rightarrow HNO_2 \quad (1)$$

$$HNO_2 + H^+ \rightarrow NO^+ + H_2O \quad (2)$$

$$2HNO_2 \rightarrow NO^{\bullet} + NO_2^{\bullet} + H_2O \quad (3)$$

$$NO_2^- + H_2O_2 + H^+ \rightarrow O{=}NOOH + H_2O \quad (4)$$

Antibacterial studies have indicated peroxynitrite as a crucial factor responsible for the bactericidal potential of PAL. A decrease in the storage temperature could significantly improve the final concentration of peroxynitrite, for instance 2.2 and 4.6 μM for 4°C and −16°C, respectively, over a 24 hour post-discharge period in one study (Zhou *et al.*, 2018). Based on this statement, we can hypothesize that in our study the concentration of peroxynitrite in PAL might be higher at lower temperatures such as -80 and -150 °C compared to PAW stored at higher temperatures and explain why these solutions could retain their antimicrobial efficacy. Peroxynitrite is a highly reactive species that gives rise to both oxidative and nitrosative stresses in bacteria. In acidic conditions, peroxynitrite can cross the lipid bilayer of the cell membrane of the bacteria cell and then initiate lipid and protein peroxidation and nitration directly or

by its decomposition to one-electron oxidants like • OH and NO2 • (Jia *et al.*, 2016) (Huie and Padmaja, 1993). The chemical reactions between the chemical species and the membrane enhance the permeability of the cell by formation of pores on the membrane in favour of more reactive chemical species penetrating into the cell (Zhang *et al.*, 2016).

Interestingly, PAL stored at -16°C was the only liquid stored at sub-ambient temperature that did not retain its antimicrobial activity. From a thermodynamically point of view, one of the reasons this happened could be that the freezing point of these solutions might have been lower than -16°C, so that there was still (relative) motion of molecules/atoms. When liquids freeze, the molecules slow and settle into place. Moreover, it needs to be noted that frozen PAL at -16°C was observed to be <softer> than PAL stored -80°C or -150°C and the controls which were untreated water/saline stored in the same conditions, when removed from freezers.

Water's phase diagram displays great complexity with currently 17 experimentally-confirmed polymorphs of ice and several more predicted computationally (Salzmann, 2018). The great complexity comes from the hydrogen-bonded networks of the various polymorphs of ice. In our case, crystals of ice could be in random places and the solutions may be inhomogeneous. Due to the content of different reactive chemical species in PAL, the chemical dimensions of PAL different phases should be more complex than normal water.

4.5 Conclusion

Although environmental surface disinfectants are generally used under ambient conditions, there can be differences in air temperature from place to place and at the same site, depending on season, climate, and air-handling systems. The results in this

chapter provide a basis for PAL storage and practical applications in disinfection and food preservation. A better understanding of the effects of temperature on the bactericidal activity of PAL will also contribute to an improved classification of PAL for use in the biomedical sector.

In the first part of this study, the effects of supra-ambient temperatures on bactericidal activity and chemical composition of PAW and PAS was investigated. Increase of temperature up to 100°C decreased the bactericidal efficiency of PAL, whereas temperature up to 60°C could retain it. In the second part, it was demonstrated that storing non-buffered PAL at −80 °C or −150 °C may be a good method to remain their bactericidal activity over long-term storage time. A better understanding of the effects of the temperatures on the chemical species found in PAL could lead to an improved classification of PAL in the context of conventional disinfectants.

Chapter 5: Biological effects of plasma activated water generated with spark and glow plasma discharges

Part of this Chapter has been published

E. Tsoukou, M. Delit, L. Treint, P. Bourke, D. Boehm (2021). Distinct Chemistries Define the Diverse Biological Effects of Plasma Activated Water Generated with Spark and Glow Plasma Discharges. Applied Sciences, 11(3), 1178

DOI: 10.3390/app11031178

PAL obtained after the plasma treatment acts as a bioactive solution which may be delivered to a target for specific biomedical applications such as cancer treatment, disinfection and bio-decontamination, including places where direct plasma generation is less feasible or undesirable, such as cavities or body organs (Kaushik *et al.,* 2018). Differences in reactive species chemistry and biological effect between various PAL can derive from different composition of the liquids, or antioxidants (depending on the liquid) within the solutions as well as the plasma device and discharge conditions.

The search for novel techniques for improved microbial decontamination of environmental objects and surfaces in hospital rooms and healthcare facilities is currently the subject of a considerable number of investigations (e.g. UV light, hydrogen peroxide systems, ozone) (Dancer, 2014). PAL have been proposed as an alternative method of disinfection for medical devices such as duodenoscope reprocessing after current-standard manual cleaning (Balan *et al.*, 2018) and as a novel mouthwash against oral pathogens (Li *et al.*, 2017).

The efficacy of each PAL depends on the reactive species produced in the PAL, the type of microorganism and phenotype (Ng *et al.*, 2020b).

The aim of this study is to assist the development of PAL which could be used as wound disinfectants, hand sanitizers or for washing at surgical sites. Ideally, PAL should retain high level antimicrobial activity, but cause minimal or acceptable cytotoxicity in surrounding or exposed tissues. Plasma activated water, as the simplest form of a plasma activated liquid, generated using a spark (SD) and a glow (GD) cold atmospheric plasma discharge, with ROS- or RNS-rich chemistry, respectively, was investigated for its antimicrobial properties on gram negative and gram positive

bacteria. The PAW was characterized in terms of its chemical composition and stability of the chemistry and antibacterial effect to a high temperature and pressure. The impact on mammalian cell growth was also determined.

5.1 Chemical Composition of PAW

Water samples were plasma treated for 5, 10 or 15 min in atmospheric air to generate a range of PAW. The PAW were chemically characterised immediately after plasma treatment (Day 0) and 7 days (week 1) post generation. The pH of both types of PAW decreased, from neutral to acidic, to levels of 3.03 and 2.7 after 5 min exposure to plasma for spark discharge (SD) PAW and glow discharge (GD) PAW, respectively. There was little further decrease with additional treatment time up to 15 min (Figure 5.1 A). The conductivity of SD and GD PAW increased with plasma treatment time, up to 2800 µS for both types of PAW (Figure 5.1 B).

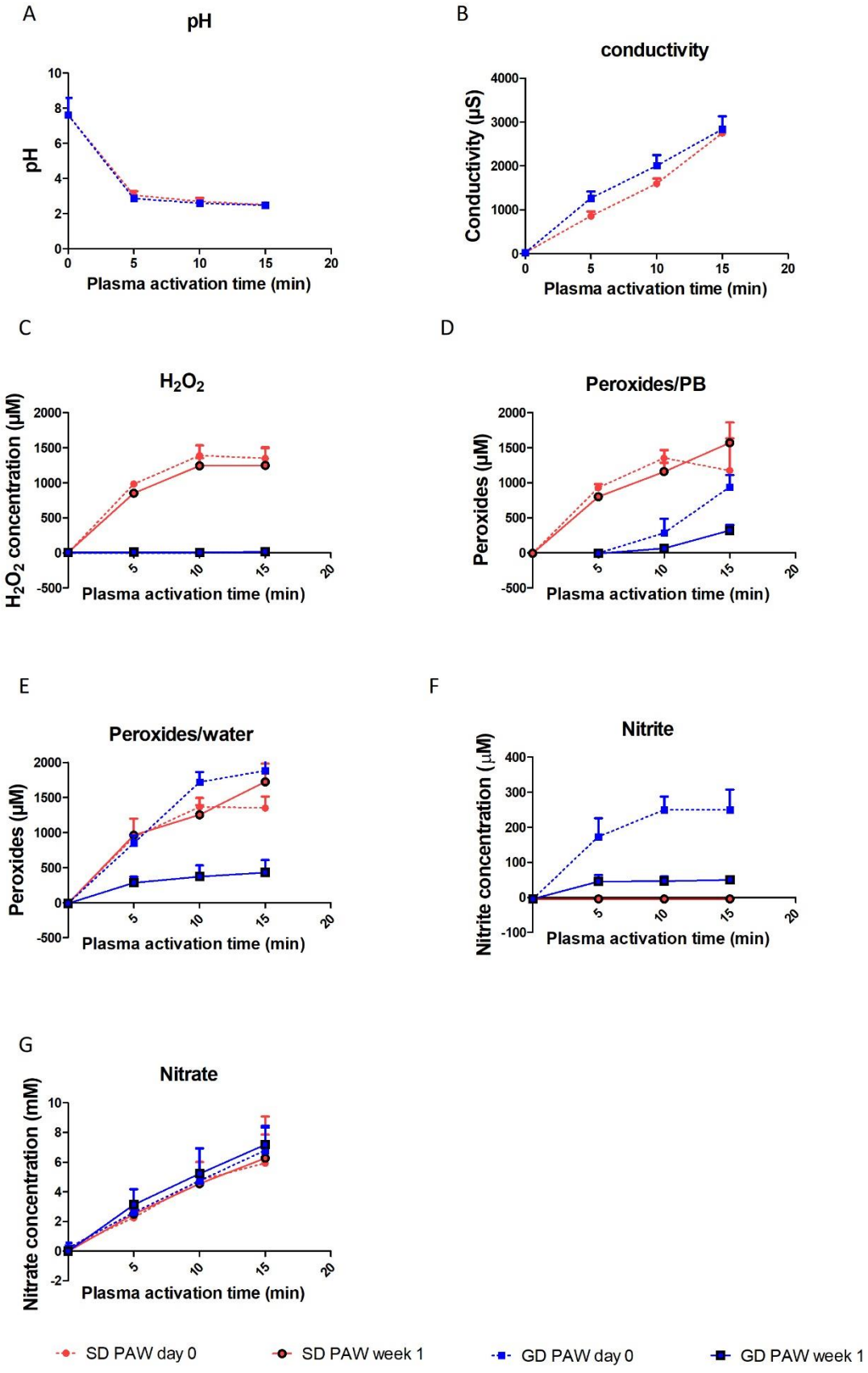
A
pH
pH
Plasma activation time (min)
B
conductivity
Conductivity (µS)
Plasma activation time (min)
C
H2O2
H2O2 concentration (µM)
Plasma activation time (min)
D
Peroxides/PB
Peroxides (µM)
Plasma activation time (min)
E
Peroxides/water
Peroxides (µM)
Plasma activation time (min)
F
Nitrite
Nitrite concentration (µM)
Plasma activation time (min)
G
Nitrate
Nitrate concentration (mM)
Plasma activation time (min)
SD PAW day 0
SD PAW week 1
GD PAW day 0
GD PAW week 1

Figure 5.1 Chemical composition of PAW made by spark and glow discharges on the day of generation (Day 0) and after 1 week storage. (A) pH, (B) conductivity measurements, (C) hydrogen peroxide measured by $TiOSO_4$, (D) peroxides measured by KI buffered with PB, (E) peroxides measured by KI and water, (F) nitrite concentration, (G) nitrate concentration (n=3 experiments with measurements performed in triplicate. All chemical species were measured immediately after generation of PAL and aftern1 week storage. Concentrations of chemical species were measured as described in Materials & Methods section 2.4.

Hydrogen peroxide was only detectable for SD PAW and not for GD PAW. Measurements on the day of PAW generation showed that H_2O_2 for SD PAW plasma treated for 10 min increased up to approximately 1500 µM and after 15 min plasma treatment, the concentration plot seemed to approach a plateau (Figure 5.1 C). Similar concentrations of peroxides (measured by KI with phosphate buffer or water) for the same samples of SD PAW were measured on Day 0, indicating that the peroxide was almost exclusively hydrogen peroxide (Figure 5.1 D, E). After 1 week, hydrogen peroxide and overall peroxide concentrations remained at comparable levels for most SD PAW samples. As previously reported for this plasma set-up, no hydrogen peroxide was detectable in GD PAW by $TiOSO_4$, but reaction with potassium iodide indicated the presence of other peroxides/oxidative species. After treatment for 5 min no detectable concentration of peroxides was observed, whereas 938 µM of peroxides were detected after 15 min exposure to plasma (Figure 5.1 D). After 1 week of storage, GD PAW 10 and 15 had lost more than half of the peroxide concentration compared to Day 0 (Figure 5.1 D). Concentrations of peroxides were also measured by KI with addition of water instead of phosphate buffer solution in order to measure peroxides in non-buffered environment (Figure 5.1 E). Comparison between Figures 5.1 D and 5.1 E shows that SD PAW concentrations of peroxides in buffered and non-buffered

conditions were similar, whereas GD PAW measured by KI with water had about three times higher concentration of peroxides than measured with KI with phosphate buffer solution. This indicates that there is a higher amount of oxidative species in non-buffered GD PAW and suggests that neutralization of the pH by phosphate buffer leads to loss of some plasma reactive species. After one week of storage, both measurements showed substantial peroxide loss for GD PAW.

Nitrites were only detected for GD PAW having concentrations up to 254 µM for GD PAW 15 min (Day 0) (Figure 5.1 F). Measurements after 1 week, showed that nitrite had decreased for all GD PAW samples (50µM). Nitrate concentrations increased in both SD PAW and GD PAW with plasma activation time up to 5.9 mM and 6.7 mM, respectively and after 1 week, no significant change in concentration of nitrates was observed for all PAW (Figure 5.1 G).

5.2 Bactericidal efficacy of PAW

The bactericidal effects of PAW were tested against gram negative *E. coli* and gram positive *S. aureus* strains using four different contact times: 15 min, 30 min, 60 min and 24 h (Figure 5.2). Generally, by increasing contact time, higher bactericidal activity was observed. Specifically, 15 min contact time was able to reduce *E. coli* concentrations by approximately 4 log when incubated with GD PAW plasma treated for 15 min but showed very little effect on *S. aureus* (Figure 5.2 A, B). *S. aureus* was less susceptible, even after 30 min of contact time, whereas *E. coli* was inactivated below the limit of detection (log 2 CFU/mL), when incubated with SD PAW 15min, GD PAW 5, 10 and 15 min at 30 min contact time (Figure 5.2 C, D). Increasing contact time to 60 min increased inactivation efficacy. *E. coli* was reduced by 6 log by all PAW generated for longer than 10 mins, whereas only GD PAW generated for 15 min was able to cause 6 log reduction for *S. aureus* (Figure 5.2 E, F), and only on prolonged

contact. 24 h contact time reduced bacteria below the detection limit (approximately 6 log reduction) for all PAW generation times.

Comparison of PAW generated with the different discharge modes, showed that overall GD PAW was more efficient than SD PAW in reducing microbial counts for *E. coli* but showed no difference for *S. aureus* at shorter contact times, and increased antimicrobial efficacy of GD10 and GD15 was observed with extended contact time only.

In Figure 5.3, the bactericidal stability of PAW after 1 week is presented. For these experiments only 30 and 60 min contact times were investigated. After 1 week of storage, the bactericidal activity of PAW had decreased and none of the PAW samples were able to reduce *S. aureus* to undetectable levels (Figure 5.3 B, D). Only the solutions plasma treated for 15 min retained the functionality to cause 4 log and 6 log reductions for *E. coli*, respectively, after 30 min contact time. Prolonging contact time to 60 min did enhance antimicrobial efficacy, indicating that the bactericidal activity of the liquids was reduced but not completely lost after the storage time.

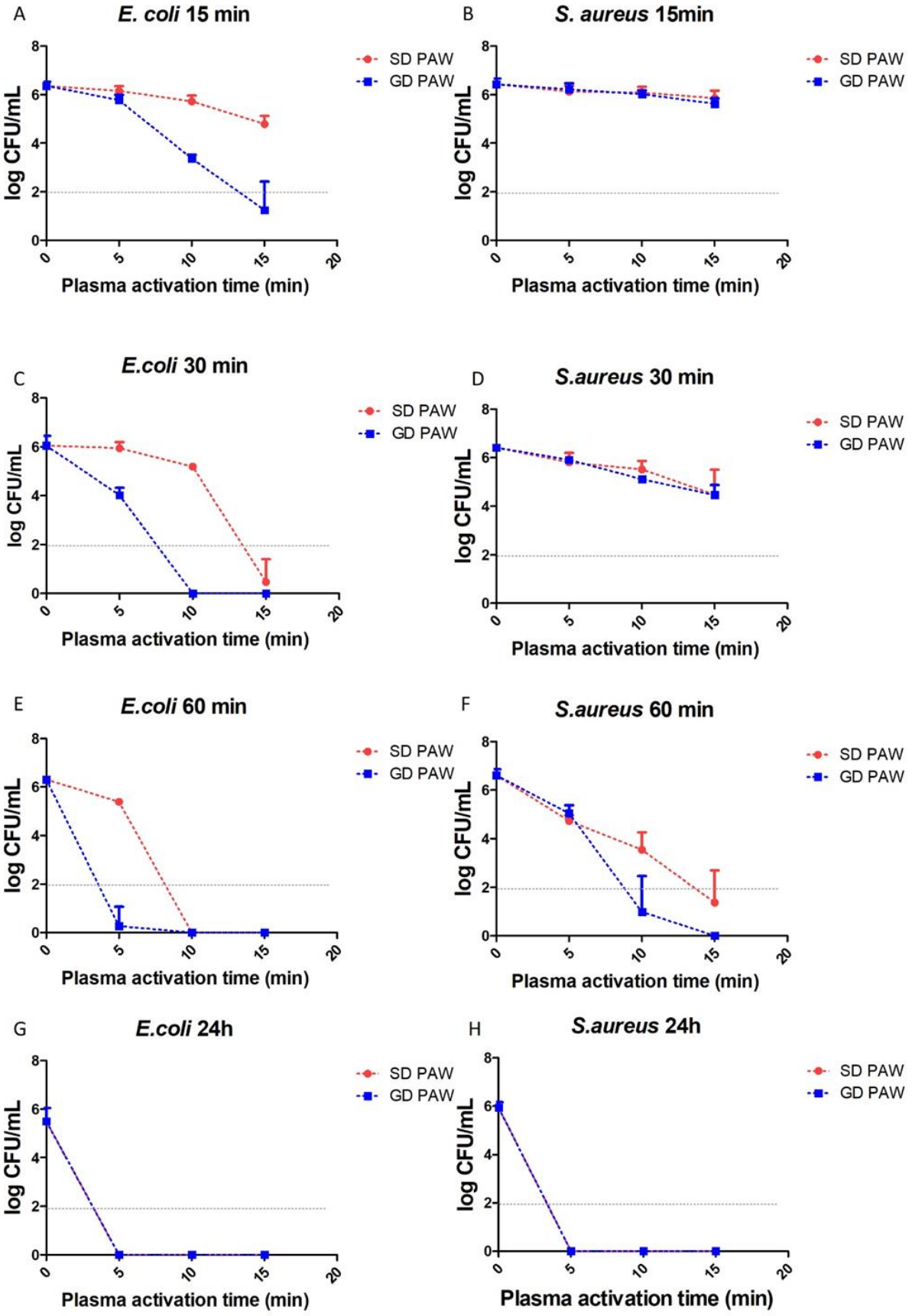
A
E. coli 15 min
B
S. aureus 15min
C
E.coli 30 min
D
S.aureus 30 min
E
E.coli 60 min
F
S.aureus 60 min
G
E.coli 24h
H
S.aureus 24h
SD PAW
GD PAW
log CFU/mL
Plasma activation time (min)

Figure 5.2 Bactericidal effects of PAW after 5, 10 or 15 min plasma activation, made by spark and glow discharges, on E. coli and S. aureus with contact times of 15, 30, 60 and 24 h on the day of PAW generation. (A) E. coli-15 min, (B) S. aureus-15 min, (C) E. coli-30 min, (D) S. aureus-30 min (E) E. coli-60 min, (F) S. aureus-60 min, (G) E. coli-24 h, (H) S. aureus 24 h (average of 3 experiments). Limit of detection: 2 log_{10} CFU/mL.

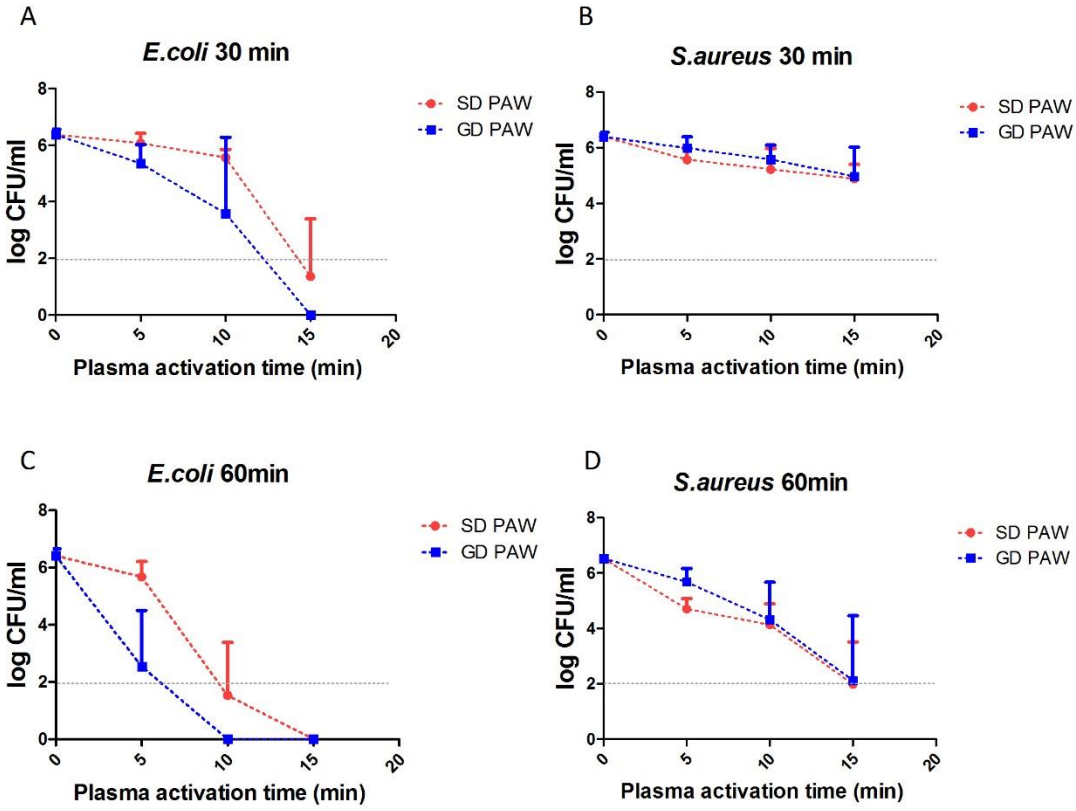

Figure 5.3 Bactericidal stability of PAW after 5, 10 or 15 min plasma activation, made by spark and glow discharges on E. coli and S. aureus with 30 and 60 min contact time a week after PAW generation. (A) E. coli-30 min, (B) S. aureus-30 min, (C) E. coli-60 min, (D) S. aureus-60 min (average of 3 experiments). Limit of detection: 2 log_{10} CFU/mL.

5.3 Heat stability of plasma activated water by spark and glow discharges

High stability of the bactericidal activity of PAW at supra-ambient temperatures was recorded. Both SD15 and GD15 PAW heated to between 50 and 100 °C for 5 min retained the ability to reduce bacterial concentrations below the limit of detection (data not shown). Similar peroxide concentrations were recorded between the heated and non-heated PAW. There were no adverse effects of heating SD15 and GD15 PAW at 100 °C for different time periods (5 min, 10 min or 15 min) on the retention of antimicrobial efficacy (Figure 5.4 A). Hydrogen peroxide concentration of SD PAW was observed to be relatively stable, for the different heating times (Figure 5.4 B). Peroxide concentration was similar to that of hydrogen peroxide for SD PAW, indicating that the peroxides present are almost exclusively hydrogen peroxide (Figure 5.4 B). Regarding GD PAW, hydrogen peroxide was not detected, but the concentration of peroxides indicated similar amounts as measured in SD PAW, which decreased slightly as the heating times increased. However, in non-buffered conditions, an increase in peroxides was found (Figure 5.4 B).

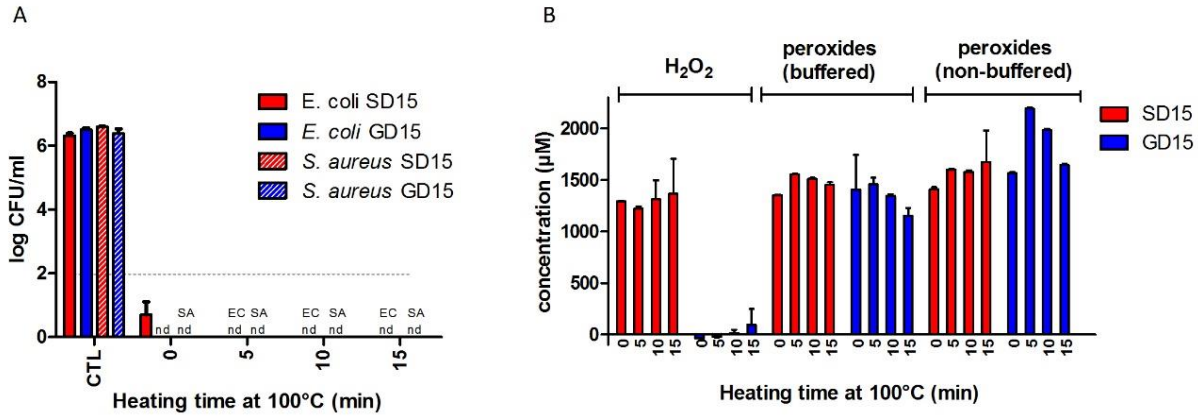

Figure 5.4 Effect of heating at 100 °C and heating time duration on retention of antimicrobial efficacy of PAW (SD15, GD15). (A) Bactericidal effects after 60 min

contact time. (B) Chemical composition of hydrogen peroxide measured by TiOSO4, peroxides measured by buffered KI and non-buffered KI. nd = no colonies detected. Limit of detection: 2 log_{10} CFU/mL.

Based on the high temperature stability observed at 100°C, PAW samples were further heat treated by autoclaving at 121°C, 15 psi for 20 minutes and their chemical composition and antibacterial effects analysed. The liquids showed remarkable stability to high temperature and pressure in terms of their bactericidal activity. Autoclaved samples of SD15 showed comparable or even enhanced antibacterial activity to the original PAW for all contact times (Figure 5.5). Autoclaved PAW GD15 on the other hand retained a similar ability to reduce *E. coli* and *S. aureus* in some cases but demonstrated reduced antibacterial efficacy in others, thus 3 different sets are represented in Figure 5.5 and not their averages. Analysis of hydrogen peroxide and other peroxides in these samples indicated a strong reduction in the concentrations of these species but the extent of reduction varied significantly between the 3 sets of PAW analysed (Table 5.1).

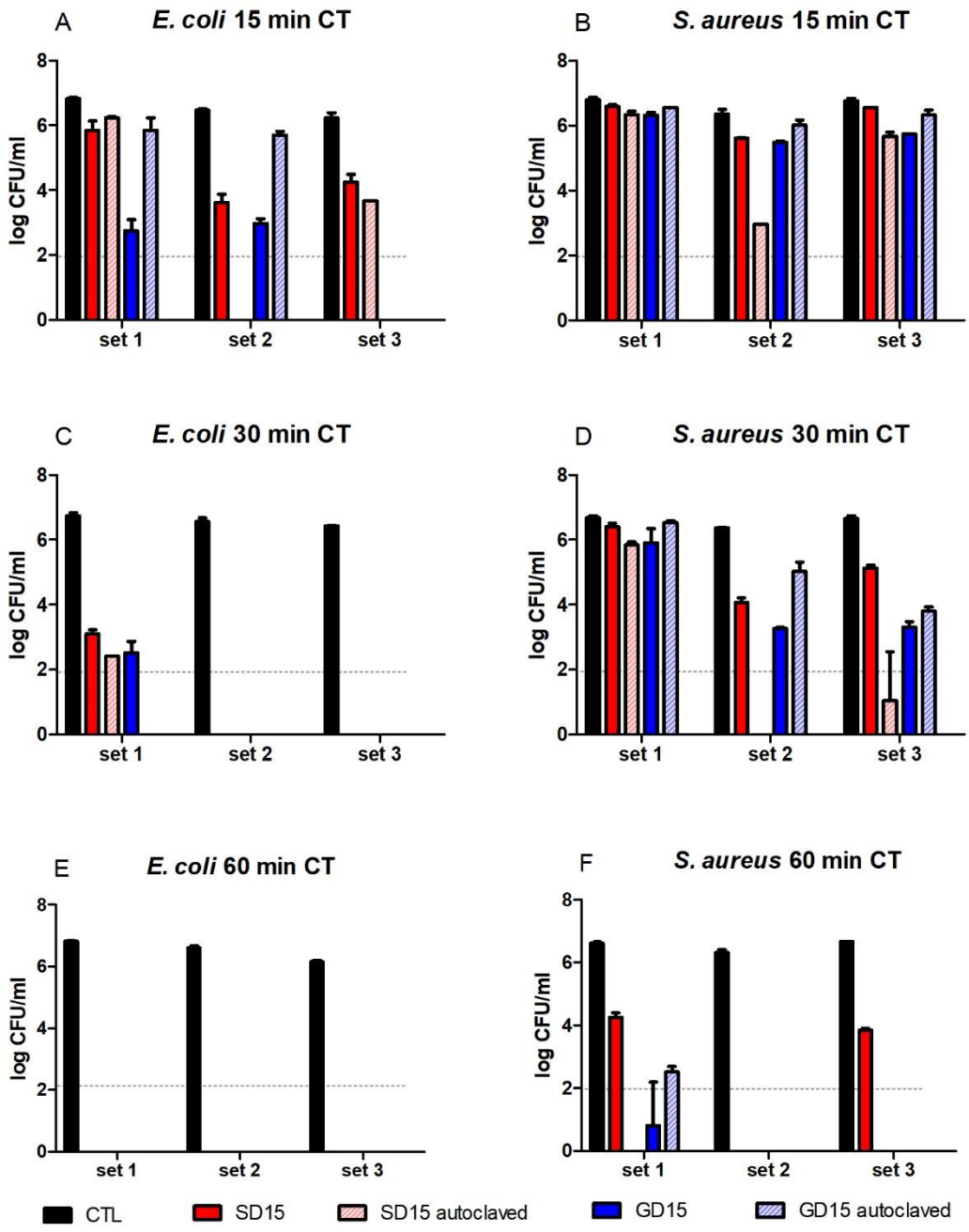

Figure 5.5 Effect of autoclaving on retention of antimicrobial activity of SD15 and GD15 PAW over 15-60 minute contact time (CT). (A) E. coli-15 min, (B) S. aureus-15 min, (C) E. coli-30 min, (D) S. aureus-30 min (E) E. coli-60 min, (F) S. aureus-60 min (n=3). Limit of detection: 2 log_{10} CFU/mL.

Table 5.1 Chemical composition of SD15 PAW and GD15 PAW, before and after autoclaving. ND = not detected. Set 1 and 2 correspond to sets 1 and 2 in figure 6, set 4 is an additional set, which is not shown in Figure 6.

	H_2O_2 (μM)		Peroxides (Buffered) (μM)		Peroxides (Non-buffered) (μM)	
	SD15	**SD15 Autoclaved**	**SD15**	**SD15 Autoclaved**	**SD15**	**SD15 Autoclaved**
Set 1	1150 ± 12	78 ± 2	1235 ± 3	92 ± 2	1269 ± 56	99 ± 6
Set 2	1064 ± 16	774 ± 6	1121 ± 10	850 ± 2	1136 ± 18	868 ± 2
Set 4	770 ± 22	494 ± 74	891 ± 3	550 ± 8	929 ± 4	550 ± 4
	GD15	**GD15 Autoclaved**	**GD15**	**GD15 Autoclaved**	**GD15**	**GD15 Autoclaved**
Set 1	ND	ND	1444 ± 11	357 ± 17	1836 ± 9	386 ± 15
Set 2	ND	ND	985 ± 90	286 ± 21	1592 ± 30	334 ± 4
Set 4	ND	ND	785 ± 3	339 ± 3	1349 ± 15	450 ± 7

5. 4 Cytotoxic effects of PAW

Incubation of CHO-K1 and HaCaT cells grown as described in Section 2.2.3 with 20% PAW exposed to plasma for 5, 10 or 15 min demonstrated that both types of PAW possessed cytotoxic effects, with SD PAW exhibiting higher cytotoxicity than GD PAW for both cell lines under the same conditions. Specifically, SD 5 PAW resulted in approximately 90% cell inhibition for both cell lines tested and extending PAW generation time to 10 and 15 minutes led to complete cell growth inhibition (Figure 5.6 A, B). In contrast, for GD PAW there was no direct correlation with plasma

activation time observed and a minimum of 66-74% cell growth was maintained for both cell lines.

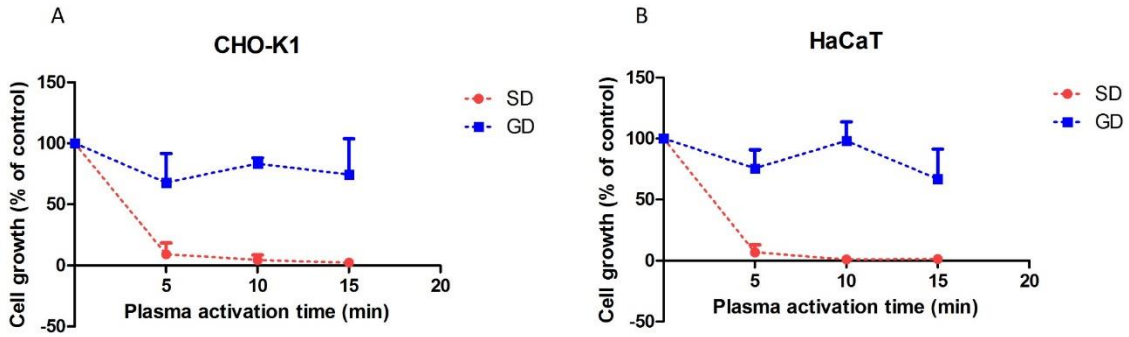

Figure 5.6 Cell growth of CHO-K1 (A) and HaCaT (B) cell lines exposed to PAW generated by SD and GD discharge at 20% (v/v) as plasma activation time of PAW increases (n=3). Cells growth o of cell lines after exposure to PAW is described in Section 2.5.2.1.

5. 5 Discussion

Different discharge modes above liquids can give rise to generation of different reactive chemical species. The impact of PAW on the reduction of bacterial and mammalian growth depends on its chemical composition. The bactericidal effects of PAW generated by SD and GD revealed that both of these PAW were more effective against *E. coli* than *S. aureus*. Gram-positive bacteria have been reported to be more resistant than Gram-negative bacteria when exposed directly to plasma discharges (Ermolaeva *et al.*, 2011; Lee *et al.*, 2006). Comparing SD and GD PAW, for the same plasma activation times, GD PAW caused higher microbial inactivation, with spark discharge resulting in generation of hydrogen peroxide and nitrate in PAW, whereas glow discharge contained nitrite, nitrate and other oxidative species.

Synergistic effects of ROS and RNS are important for bactericidal activity (Shaw *et al.*, 2018). Studies on the bactericidal effects of PAW on Gram negative cells showed

that nitrates, nitrites, and H_2O_2 in acidic solution can lead to lethal activity (Shen *et al.*, 2016). PAW caused damage to the outer and cytoplasmic membrane of *Pseudomonas*, which was accompanied by leakage of intracellular components such as nucleic acids and proteins. Plasma-induced chemical species can cause bacterial death through inhibition of the antioxidant machinery, which disrupts the membrane protein repair chaperone mechanism, and also DNA repair cascade (Vatansever *et al.*, 2013). Interaction between nitrite, nitrate, and hydrogen peroxide generated in PAL, showed strong antibacterial effects against *E. coli* (Haensch *et al.*, 2015). Therefore, the plasma-induced effects on living organisms are likely to be caused by several agents with multiple targets which possibly lead to synergistic inactivation effects.

Peroxynitrite concentration in PAW was reported to have a crucial role in the microbial inactivation of *E. coli*, where despite the short half-life, this was sufficient to diffuse into cells and lead to bactericidal effects (Zhou *et al.*, 2019b; Lukes, Locke and Brisset, 2012). In our study, this conclusion could correlate with PAW made by glow discharge, which was more efficient than SD PAW and lacked hydrogen peroxide, whereas measurements with potassium iodide indicated high concentrations of ROS which could be peroxynitrite. According to Oehmigen et al. peroxynitrite or peroxynitrous acid as transient products could be formed at some stage of the chemical reactions in the liquid phase (Oehmigen *et al.*, 2011). With regard to Gram positive bacteria, simulation studies have shown that plasma generated chemical species such as hydrogen peroxide, atomic oxygen and hydroxyl radicals can interact with the bacterial peptidoglycan of *S. aureus* and lead to breakage of bonds of peptidoglycan of the cell wall, and result in bacterial cell destruction (Yusupov *et al.*, 2013).

Bactericidal solutions to be used as antiseptics should possess potent activity and a long-lasting effect. According to Traylor et al., 20 min PAW, generated by a surface

micro-discharge plasma system in air, retained its antibacterial activity for 7 days (J Traylor *et al.*, 2011). Our study is in agreement with these results as we observed that SD PAW and GD PAW plasma treated for 15 min, retained their antimicrobial activity after 1 week of storage at 4°C, thus making PAW a candidate for biomedical use. Concentrations of chemical species were altered in the same storage period, indicating that the chemical reactive species in PAW may have reacted to form other secondary products. According to Lukes et al., post-discharge reactions between nitrites and hydrogen peroxide can occur in PAW and result in formation of peroxynitrite (Lukes *et al.*, 2014) and nitrate (Burlica *et al.*, 2010).

PAW has the potential to be formulated for use in a variety of clinical applications, such as disinfection, blood coagulation, oncotherapy or wound healing. Formulations used in clinical settings or as carriers for therapeutics normally undergo terminal sterilization, which may be mediated by heat and pressure. The PAW generated here has the potential to be used in a setting requiring sterilization, but might undergo chemical decomposition through a number of pathways at the elevated temperatures used for its sterilization. A widely used method for sterilization, is moist heat in the form of saturated steam under pressure. The basic principle of steam sterilization, as accomplished in an autoclave, is to expose each item to direct steam contact at high temperature and pressure for a specific time. Thus, there are four parameters of steam sterilization: steam, pressure, temperature, and time.

In this study different temperatures and heating times were applied to PAW, and results showed that this PAW retains antimicrobial efficacy. In some cases, autoclaving actually increased the antimicrobial efficacy by comparison with unheated PAW. From a reactive species point of view, hydrogen peroxide and peroxides of SD15 PAW were strongly reduced post autoclaving. Reduction of peroxides post

autoclaving was also observed for GD15 PAW, which also retained antimicrobial effects at longer contact times. This suggests that other chemical species were primarily responsible for the bactericidal effects of PAW. The differences in the concentrations and/or structure of chemical species measured in this study could be caused by autoclave sterilization because of the high pressure and steam. Moreover, stability of hydrogen peroxide can be altered by increase of temperature (Yazici and Deveci, 2010) and result in its decomposition to yield oxygen and water. In conclusion, these results show that PAW can be generated to provide strong disinfectant efficacy and retain its stability in different conditions, including high temperatures and pressure. In addition, the possibility of post-plasma modifications of plasma activated liquids to alter their chemical composition and biological effects arises and presents an exciting avenue for further investigations.

Cytotoxicity results demonstrated that GD PAW had a better safety profile than SD PAW; using the same plasma activation times, a significantly higher cytotoxicity was observed by SD PAW for both cell lines. Hydrogen peroxide in SD PAW seems to be a central player in the cytotoxic effects but a role of nitrite and nitrate concentration or other reactive species (GD PAW) in cytotoxicity cannot be excluded as GD PAW showed growth inhibition in the absence of hydrogen peroxide. Several publications have reported hydrogen peroxide as a principle cytotoxic reactive species in PAL. Reduction of cell growth and viability of CHO-K1 and HaCaT cells showed a linear correlation to the concentration of peroxide in PAL in previous studies (Boehm *et al.*, 2016; Winter *et al.*, 2014). Moreover, Lu et al. investigated the cytotoxic effects of SD PAW combined with GD PAW and observed that cytotoxicity was reduced by GD treatment in line with the reductions of hydrogen peroxide concentrations (Lu *et al.*, 2017b). In the same study, PAW containing only nitrates of approximately 1.5 mM

showed minor cytotoxicity, suggesting that nitrite could play a role in cell death attributed to GD PAW, even though the addition of nitrite and nitrate concentrations up to 1.2 mM showed no cytotoxic effects on HeLa cells in another investigation (Boehm *et al.*, 2018).

Other chemical reactive species, including less stable transient species, may also be responsible for inhibition of cell growth. Peroxynitrous acid can be formed by the interaction of nitrites and hydrogen peroxide, in weakly acidic to acid solutions (Brisset and Pawlat, 2015). The plasma treatment of water led to a decrease of pH, generating an acidic environment, which can promote peroxynitrous acid formation. Peroxynitrite/peroxynitrous acid can cause cell death by inducing both cellular apoptosis and necrosis (Szabo, Ischiropoulos and Radi, 2007).

5.6 Conclusion

In this study, the biological effects and the influence of heating temperature on the bactericidal effects of PAW generated by two different discharges were investigated. We established that PAW solutions may be suitable disinfectant solutions in terms of potent and stable bactericidal efficacy as well as biological safety to non-target cells. Investigation of the chemical composition of two types of PAW, showed that PAW consisted of different long-lived chemical species. PAW were able to retain their bactericidal effects against both Gram positive and Gram negative bacteria post generation for up to one week at refrigerated temperature. PAW heated for varying times showed that PAW could retain its bactericidal activity on both *E. coli* and *S. aureus* even when it had been autoclaved. A better understanding of the mechanisms of the biological activity of PAW will lead to an improved classification and more

targeted applications and may provide post-plasma modifications as further means of modulating the chemistry and biological effects of these liquids.

Chapter 6: Effects of PAW on cancerous cell lines

ACP technology has been reported to have potential selective anti-cancer effects both in *vitro* (Yan *et al.*, 2015b) and in *vivo* (Vandamme *et al.*, 2012) but other studies found no such selectivity. Recently, PAL were shown to exhibit significant anti-cancer activity against colorectal carcinoma (Griseti, Merbahi and Golzio, 2020), melanoma (Sersenová *et al.*, 2021), glioblastoma (Yan *et al.*, 2015a), lung (Adachi *et al.*, 2015) and urinary bladder cancer cells (Mohades *et al.*, 2015) similar to direct exposure to cold plasma. PAL was reported to cause selective cell inhibition in cancer cells rather than normal cells (Kumar *et al.*, 2016). Injection of PAL into mice has been observed to reduce the growth of tumours (Utsumi *et al.*, 2013), thus PAL offer the advantage in oncotherapy when ACP technology cannot reach tumours.

In previous chapters, high cytotoxic activity of PAL was observed which while undesirable for antimicrobial applications, could be exploited for other applications such as cancer treatment. For this reason, four different cancer cell lines were tested in order to investigate the anti-cancer potential of PAW.

In this chapter, chemistry of PAW used is the same as described in Chapter 5 (Figure 5.1).

6.1 Anticancer capacity of PAW

For this study, 4 cancer cell lines (A375 human malignant melanoma, A431 human epidermoid carcinoma, SW480 human colorectal, glioblastoma U373mg) were tested with regard to cytotoxic effects of SD and GD PAW (See section 2.5.2.1 for measurements of cytotoxicity of mammalian cells).

Incubation of cancer cells with 20% PAW, demonstrated that both SD and GD PAW possessed cytotoxic effects, with SD-PAW exhibiting higher cytotoxicity than GD PAW for all cell lines under the same conditions. Specifically, 5 min treated SD PAW resulted in approximately 90% cell inhibition for all cell lines tested (Figures 6.1 - 6.4). SD PAW treated for 10 and 15 min led to complete cell growth inhibition, indicating that SD PAW plasma treated for 5 min provided similar cytotoxic effects and higher plasma treatment times are not needed for cytotoxic effects. GD PAW treated with plasma for 5 min did not reduce cell growth for cell lines such as A375, A431, SW480 and thus the plasma treatment time of GD PAW was increased up to 15 min in order to investigate if higher exposure of liquids to plasma would lead to higher cytotoxic effects. 15 min treated GD PAW caused approximately 50% reduction in cell growth for A375 cells (Figure 6.1), whereas the other cell lines had cell growth higher than 70%.

Figure 6.5 shows the reduction of cell growth of all cancer cell lines as concentration of hydrogen peroxide, peroxides and nitrate increased in SD PAW. As mentioned in Chapter 5, concentrations of peroxides are exclusively all hydrogen peroxide. In Figure 6.5 A, hydrogen peroxide in PAW caused a 90% reduction in cell growth of all cancer cell lines when its concentration was around 110 μM.

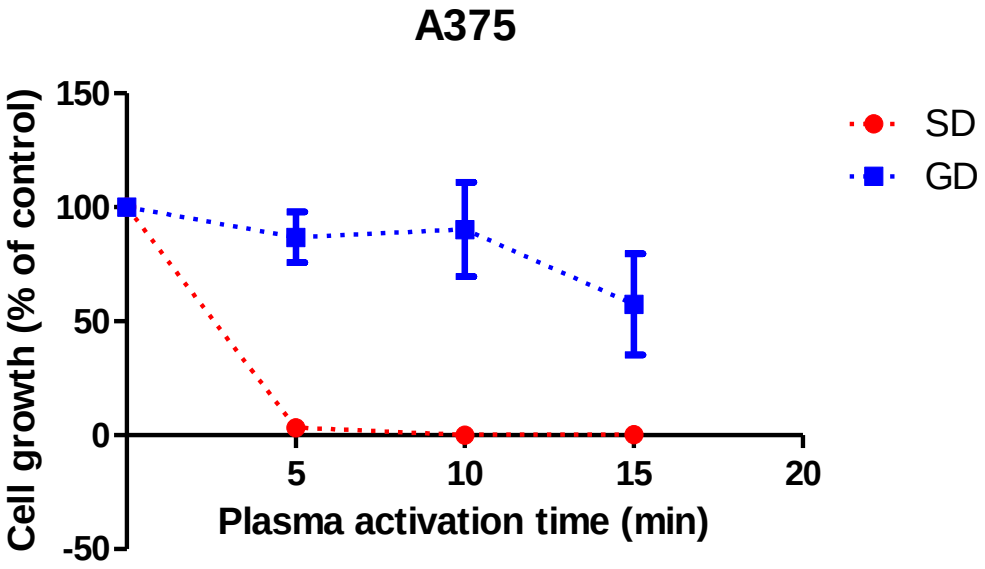

Figure 6.1 Cell growth of A375 cancer cell line as the plasma activation time of PAW increases. Cells growth of cancer cell lines after exposure to PAW is described in Section 2.5.2.1.

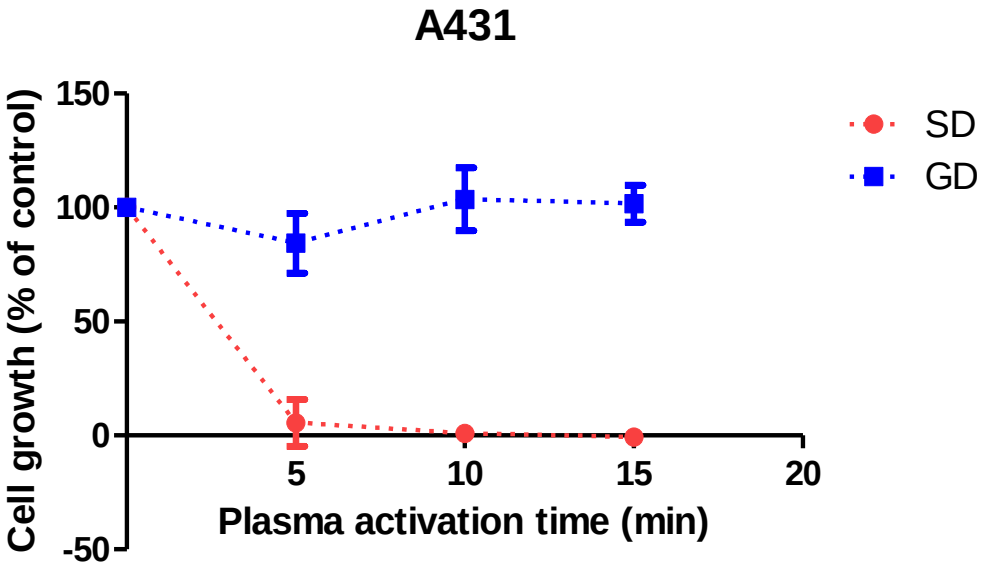

Figure 6.2 Cell growth of A431 cancer cell line as the plasma activation time of PAW increases. Cells growth of cancer cell lines after exposure to PAW is described in Section 2.5.2.1.

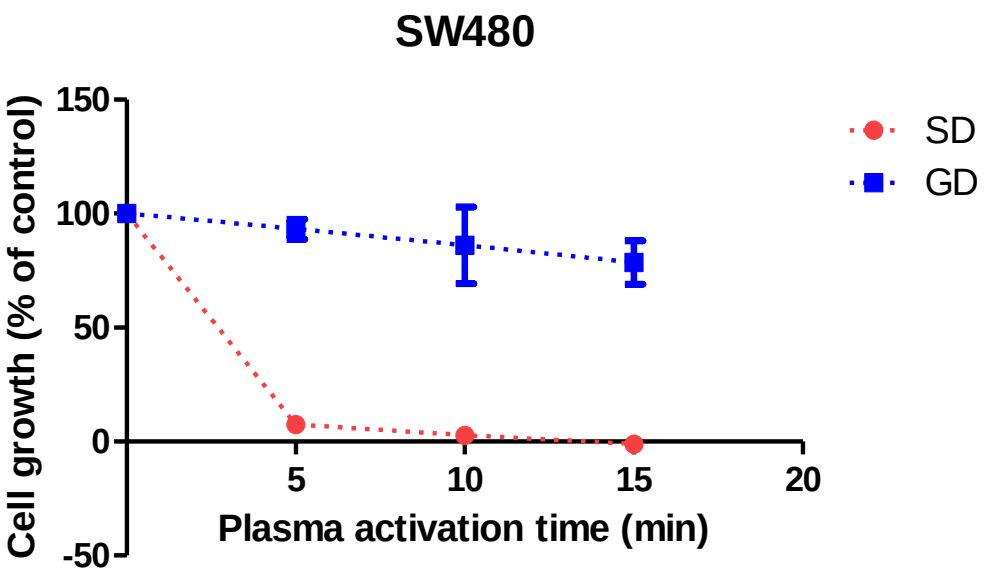

Figure 6.3 Cell growth of SW480 cancer cell line as the plasma activation time of PAW increases. Cells growth of cancer cell lines after exposure to PAW is described in Section 2.5.2.1.

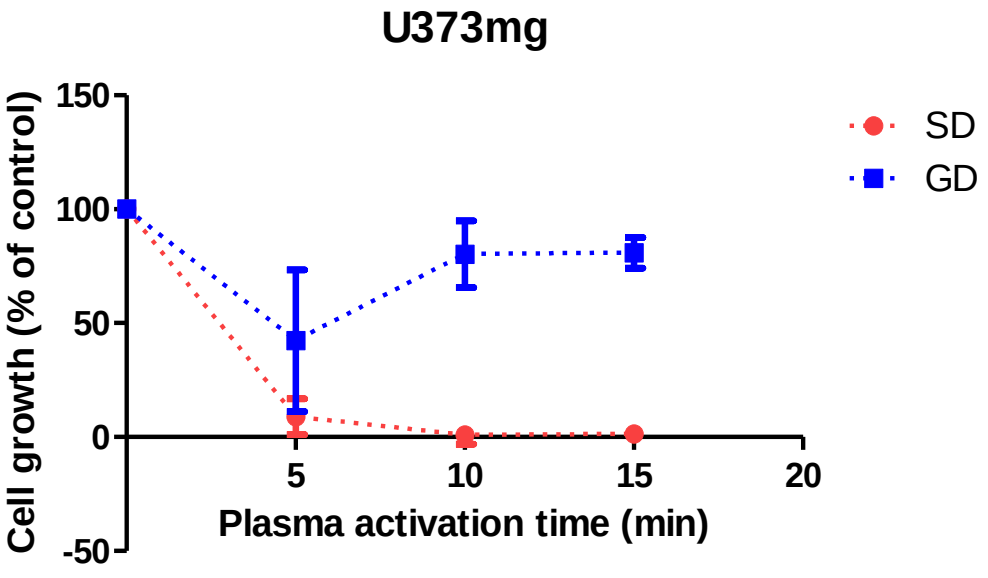

Figure 6.4 Cell growth of U373mg cancer cell lines as the plasma activation time of PAW increases. Cells growth of cancer cell lines after exposure to PAW is described in Section 2.5.2.1.

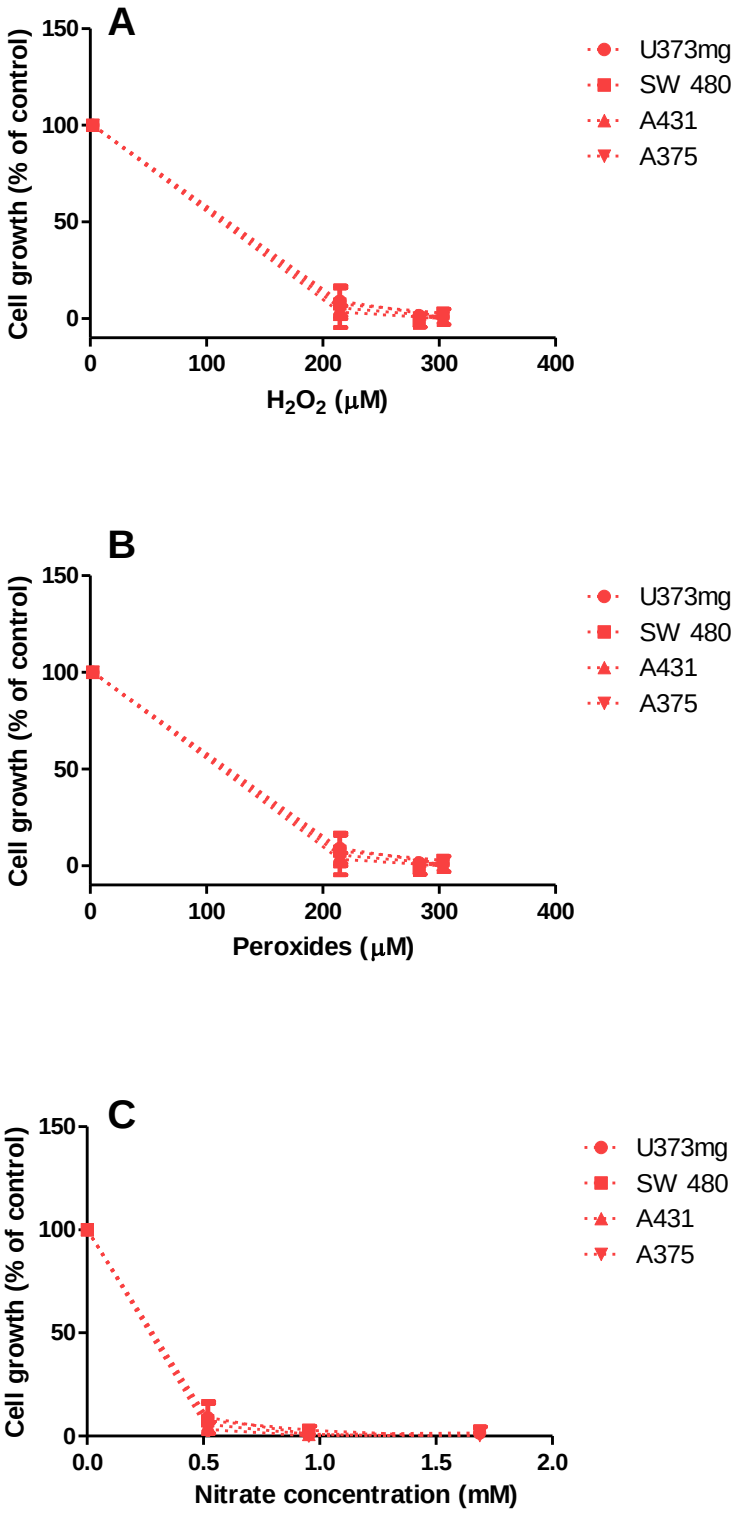

Figure 6.5 Cell growth of cancer cell lines relative to concentration of chemical species determined in SD PAW. (A) Concentration of H_2O_2 measured by $TiOSO_4$, (B) concentration of total peroxides measused by KI and (C) concentration of nitrate was

measured photometrically by 2,6-dimethyl phenol (DMP) using the Spectroquant® nitrate assay kit Chemical composition of PAW is described in Section 2.4.

6.2 Discussion

Different discharge modes above liquids can realize reactive chemical species specificity. The impact of PAW on the reduction of cell growth depends on its chemical composition. The cell growth of both SD PAW and GD PAW shows a plasma treatment time-dependent decrease. Higher cytotoxicity was observed for SD PAW than GD PAW for the same plasma treatment times. SD PAW consisted of hydrogen peroxide and nitrate, whereas GD PAW contained nitrite and nitrate as shown in Chapter 5 (Figure 5.1).

In this study SD PAW treated for 5 min caused more than 50% cell reduction to all cell lines tested. Increased plasma treatment time of deionised water up to 15 min resulted in higher to complete cell inhibition. Actual concentrations of SD PAW exposed to plasma for 15min according to Chapter 5 consisted of: approximately 1500 μM peroxides which were hydrogen peroxide and 8.4 mM nitrate, whereas nitrite was not detected. GD PAW treated for 15 min consisted of 1040 μM peroxides which were not hydrogen peroxide, 8.1mM nitrate and 140 μM nitrites Hydrogen peroxide in SD PAW seems to be a central player in this inactivation process, nonetheless, we cannot exclude a role of nitrite and nitrate concentration or other reactive species (GD PAW) in cytotoxicity as GD-PAW shows growth inhibition in the absence of hydrogen peroxide. Several publications have reported that hydrogen peroxide has been regarded as a main cytotoxic reactive species in PAL. Boehm et al. reported that reduction of cell growth of CHO-K1 cells showed a linear correlation to the

concentration of peroxide in PAL (Boehm *et al.*, 2016). Winter et al. reported that the amount of hydrogen peroxide produced in PAM correlated with reduced viability of HaCaT cells (Winter *et al.*, 2014).

Hence, H_2O_2 is quite an important molecule in plasma medicine concerning cell activity. Other chemical reactive species, that could be less stable transient species, may also be responsible for inhibition of cell growth. Peroxynitrous acid/peroxynitrite can be formed by the interaction of nitrites and hydrogen peroxide, in weakly acidic to acid solutions (Brisset and Pawlat, 2015). The plasma treatment of water led to decrease of pH, generating acidic PAW, leading possibly to peroxynitrite. Peroxynitrite can cause cell death by inducing both cellular apoptosis and necrosis (Szabó, Ischiropoulos and Radi, 2007). Acidic pH values were observed for both PAW, but addition of 20% v/v in buffered cell culture media did not exceed the buffering capacity of the medium after its addition. Thus, a direct contribution of pH to the cell inhibition is excluded.

With regards to GD PAW, cytotoxicity levels for all cell lines were lower compared to SD PAW. GD PAW consisted of nitrite and nitrate, thus these two long lived chemical species may contribute to cause a reduction in cell growth, as well. Actual concentrations of nitrites and nitrates in 20%v/v GD PAW in medium were 32 μM and 1.6 mM respectively. Boehm et al. reported that nitrite and nitrate concentrations up to 1.2 mM showed no cytotoxic effects on HeLa cells (Boehm *et al.*, 2018). Moreover, Lu et al. investigated the cytotoxic effects of SD PAW combined with GD PAW and observed that cytotoxicity was reduced by GD treatment in line with the reductions of hydrogen peroxide concentrations (Lu *et al.*, 2017b). Furthermore, in the same study PAW containing only nitrates of approximately 1.5mM showed minor cytotoxicity, suggesting that nitrite could play a dominant role in cell death in GD PAW. These

statements are in agreement with Girard et al. who measured the concentrations of long lived chemical species in PAPBS and reported that hydrogen peroxide and nitrite have a synergistic effect on the cytotoxic capacity of PAPBS, while nitrate did not play any role in cell reduction (Girard *et al.*, 2016). Van Boxem et al. reported that hydrogen peroxide is a more important species for the cytotoxic capacity of PAPBS than nitrite (Van Boxem *et al.*, 2017). Moreover, Yan et al. showed that nitrite alone did not cause cell reduction on cancer cells (Yan *et al.*, 2017).

Plasma is recognized as a promising tool for cancer therapy because of its ability to induce apoptosis in several types of cancer cells. In this study the route leading to cell death was not investigated, but it is reported from other studies that apoptosis is the main cell death pathway after PAL incubation with cancer cells. Cells which undergo apoptosis show morphological changes in cell shape (small and round), cell nuclei become aggregated and Caspase-3 and -7 are activated (Griseti *et al.*, 2019; Tanaka *et al.*, 2011). Moreover, plasma-activated saline solutions have been reported to induce cell death in human and mouse osteosarcoma cells due to increase of intracellular ROS which triggers DNA damage and subsequent apoptosis (Mateu Sanz *et al.*, 2020).

Analysis of p21 mRNA expression showed that ACP treatment leads to induction of p21 expression in p53 wildtype LoVo and HT29 colorectal cancer cells, but no changes were observed in SW480 cells at the p21 mRNA level compared to untreated control, suggesting that plasma is able to kill colorectal cancer cells independent of their p53 mutation status (Schneider *et al.*, 2018). Bekeschus et al. reported that SW480 had a strong increase in *hmox1* levels after incubation with PAM and some chemokines/cytokines/growth factors were also increased in response to PAM (Bekeschus *et al.*, 2018a).

In the current study, PAW treated by glow discharge for 15 min, did not cause any reduction for A431 cells, but caused 43% and 22% cell inhibition for A375 and SW480 cells, respectively. These results suggest that different cell lines display different sensitivities to PAL. It needs to be noted that different cell lines have different cell growth rates (Van Boxem *et al.*, 2017).

Generally, cancer cells are favourably more sensitive to plasma exposure compared to normal healthy cells (Babington *et al.*, 2015). Different cellular responses have been demonstrated following plasma treatment on cancer cells. Apoptosis, immunogenic cell death, reduction of cell growth, damage of DNA and mitochondria have been suggested in the last years (Dubuc *et al.*, 2018). Compared with normal cells, the increased expression of reactive-species channels such as aquaporins on their cytoplasmic membranes and the lowered expression of catalase in cancer cells may cause uptake of chemical species in cancer cells, which leads to anticancer effects (Yan, Sherman and Keidar, 2017; Yan *et al.*, 2015b). Hydrogen peroxide's toxicity is determined by the anti-oxidant status of mammalian cell and ability to detoxify H_2O_2 through catalase (Kaushik *et al.*, 2018). Moreover, H_2O_2 can react with other products and interfere with the cellular membrane structure and cause increase of the permeability of the cell membrane, and then induce cell injury, followed by the influx of extracellular reactive species from PAL.

To explain the differences between different studies, various parameters need to be taken into account such as the plasma systems used for generation of plasma, the concentration of chemical reactive species generated, the liquid composition and the cell line. Moreover, it is important that comparison between normal and cancer cells should be investigated from the same tissue for more reliable results.

6.3 Conclusion

This study describes the reduction of cell growth of multiple cancer cell lines using the SD and GD PAW. Differences in the reduction rate were obtained between the cell lines, demonstrating variable sensitivity to plasma reactive species between cancer cell lines and the need to select the right parameters for treating a specific cancer cell type. PAW effectiveness from cell line to cell line also depends on the anti-oxidants and radical scavengers in cells, which can protect them from reactive oxygen species. While these results are promising, molecular mechanisms of how PAW treatment effects cancer cells such as the induction of apoptosis, necrosis or senescence need to be investigated.

PAL treatment, which would be more akin to a drug therapy, would offer the advantage of being a flexible platform in cancer treatment, such as specific situations where ACP cannot reach tumours or when the plasma device cannot be portable.

Chapter 7: Efficacy and mechanisms of plasma activated saline in a co-culture infection control model

Part of this Chapter is under review in Scientific Reports E. Tsoukou, P. Bourke, D. Boehm (2021). Efficacy and mechanisms of plasma activated saline in a co-culture infection control model. Scientific Reports (under review).

Plasma activated liquids have demonstrated antimicrobial effects and receive increasing attention due to the potential to strengthen the armoury of novel approaches against antibiotic resistant bacteria. However, the bactericidal activity and cytotoxic effects of these solutions need to be understood and balanced before exposure to humans. In this study, the bactericidal effects of plasma activated saline (PAS) were tested against Gram negative and positive bacteria, and HaCaT keratinocytes were used for cytotoxicity studies. For the first time, a co-culture model between these bacteria and eukaryotic cells under the influence of PAS has been described. The aim of this study was to ascertain the relationship between antimicrobial efficacy and application safety of plasma activated saline (PAS), as a biomedically relevant solution for disinfection and thus its potential for use as an antiseptic or decontamination solution. Mammalian cell damage was investigated by examination of the HaCaT keratinocyte cell line as an indication of the effects on the skin and potential risks to a patient. The microbial inactivation efficacy in the presence of a keratinocyte cell layer was assessed, and the cell death pathway, oxidative stress and cytokines expression of HaCaT cells after exposure to PAS at different dilutions were investigated to identify if a balance between cytotoxic and microbial inactivation effects could be achieved in a co-culture model.

7.1 Hydrogen peroxide and nitrates are the main species detected in PAS

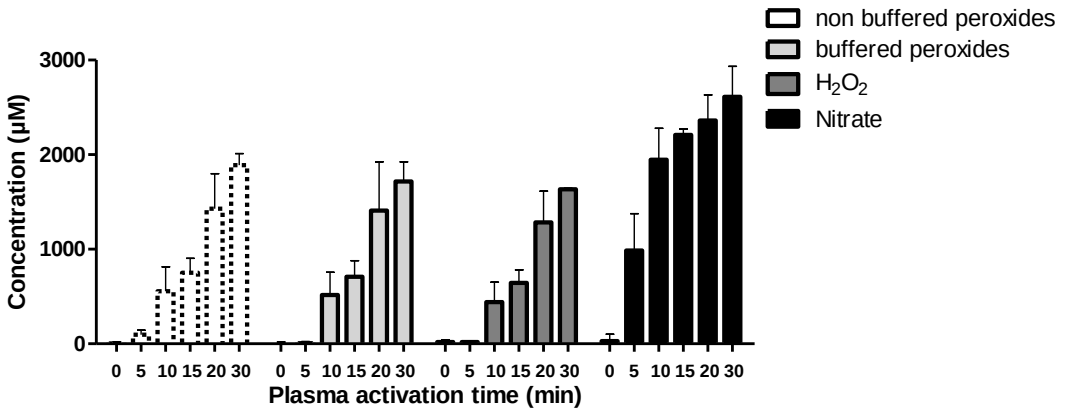

Figure 7.1 Chemical composition of PAS after exposure to spark plasma discharge for activation times of 0-30 min. The results are the mean ± S.D. of three determinations. Peroxide was determined as described in Materials & Methods section 4.2.2

Plasma treatment in liquids leads to the generation of chemical species such as reactive oxygen and nitrogen species, which mediate subsequent plasma-induced effects on prokaryotic and eukaryotic cells. The concentration of hydrogen peroxide increased within saline as a function of plasma treatment time, where 17 μM was recorded after 5 min plasma treatment, reaching 643 μM after 15 min, 1282 μM after 20 min and 1632 μM after 30 min treatment time (Figure 7.1). Similar trends to hydrogen peroxides were observed for non/buffered peroxides concentrations. Concentrations of buffered and non-buffered peroxides were similar to hydrogen peroxide, indicating that almost all peroxides generated and retained in PAS were hydrogen peroxide, which is in accordance with a previous study on PAW using the same plasma system (Tsoukou *et al.*, 2021). Nitrate concentration increased up to 900 μM after 5 min

exposure to plasma and doubled after 10 min, with 2610 μM reached after 30 min plasma treatment time. No nitrites were detected in agreement with previous studies using the same plasma system.

7.2 Bactericidal effects of PAS in co-culture model

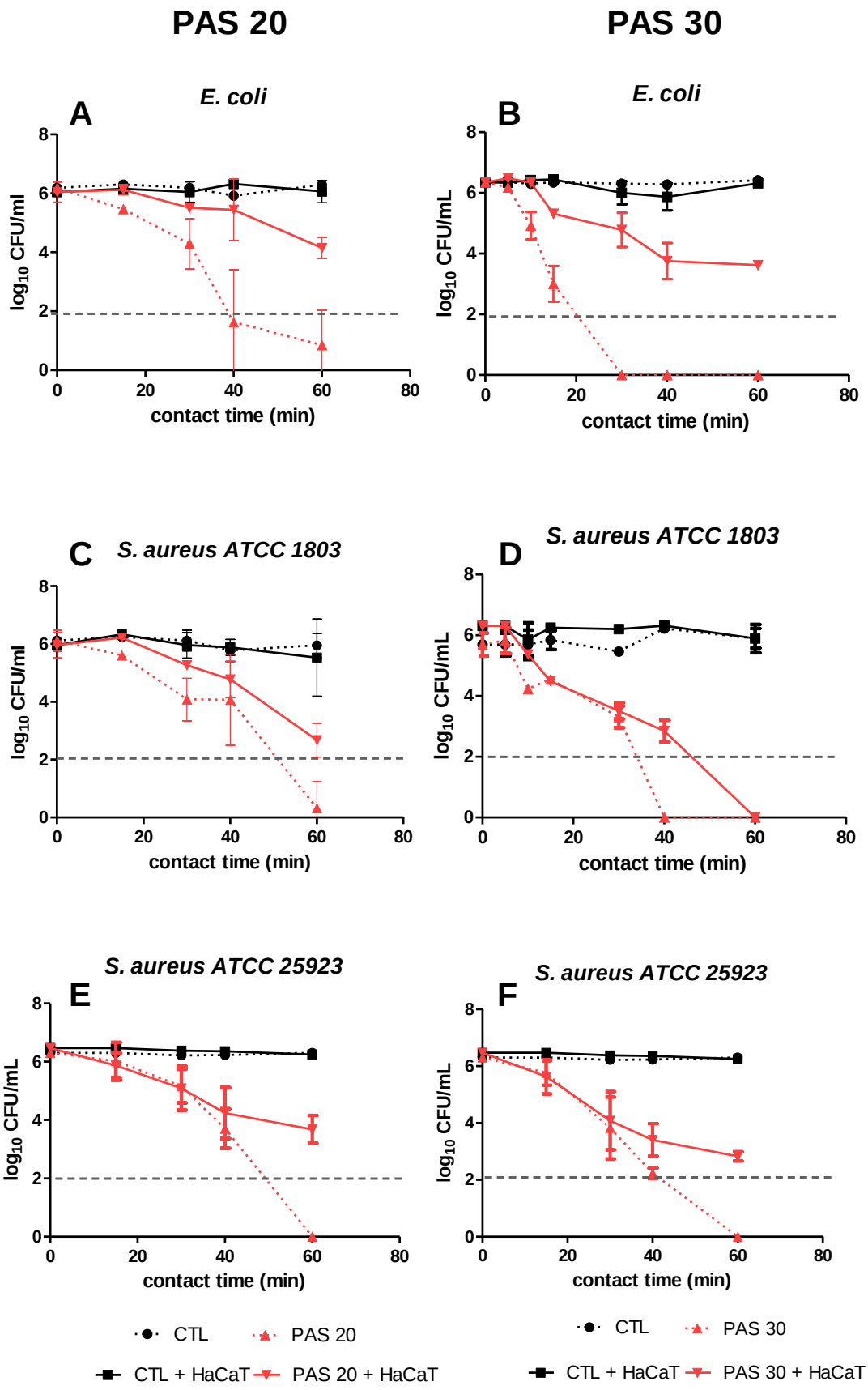

Figure 7.2 Bacterial inactivation in a co-culture model of HaCaT cells and E. coli or S. aureus under incubation with PAS 20 or PAS 30 as a function of contact time. (A) E. coli – PAS 20, (B) E. coli – PAS 30, (C) S. aureus ATCC 1803 – PAS 20, (D) S. aureus ATCC 1803- PAS 30, (E) S. aureus ATCC 25923 –PAS 20, (F) S. aureus ATCC 25923 - PAS 30. The results are the mean ± S.D. of three determinations. Antimicrobial assay was determined as described in Materials & Methods section 2.6.1.

The effect of PAS on both Gram-positive and Gram-negative bacteria, *Escherichia coli* and *Staphylococcus aureus,* was investigated. Initially PAS 10 and PAS 15 were tested for their bactericidal effects (data not shown) but due to limited bactericidal efficacy in the co-culture model, the plasma treatment time of saline was increased to 20 and 30 min (PAS 20 and PAS 30). Thereafter, the effect of contact time between bacteria and PAS were investigated. With regards to *E. coli*, PAS 20 was found to gradually reduce bacterial load as contact time increased, and a 6 log cycle reduction was achieved after 60 min contact time (Figure 7.2A). In the co-culture model, the bactericidal efficacy was reduced, and PAS 20 was not able to reduce *E. coli* to the same extent, and only 2 log cycle reduction occurred at the longest contact time of 60 min (Figure 7.2A). *S. aureus* ATCC 1803 was reduced by 2 log after 30 min contact time, and 6 log after 60 min contact time (Figure 7.2C). PAS 20 retained better efficacy against the Gram positive challenge in the co-culture model where, in the presence of the HaCaT monolayer, *S. aureus* ATCC 1803 was reduced by 3 log within a 60 min contact time.

The microbial inactivation of PAS 30 was also investigated to assess if the contact time could be reduced. *E. coli* was inactivated by 6 log after 30 min contact time with PAS 30, which was 10 min earlier than PAS 20, but when PAS 30 was challenged with the co-culture, the microbial load was not further reduced, even with extended

contact time (Figure 7.2B). PAS 30 reduced *S. aureus* ATCC 1803 by 6 log cycles after 40 min contact time (20 min earlier than PAS 20), and this effect persisted in co-culture, where PAS 30 reduced the microbial load by 6 log at 60 min contact time (Figure 2D). PAS 20 inactivation efficacy against *S. aureus* ATCC 25923 was similar to that observed for *S. aureus* ATCC 1803. However, PAS 30 led to 6 log reduction only after 60 min contact time and 3 log reduction in the co-culture set up (Figure 7.2 E, F).

7.3 Balancing cytotoxic and bactericidal effects

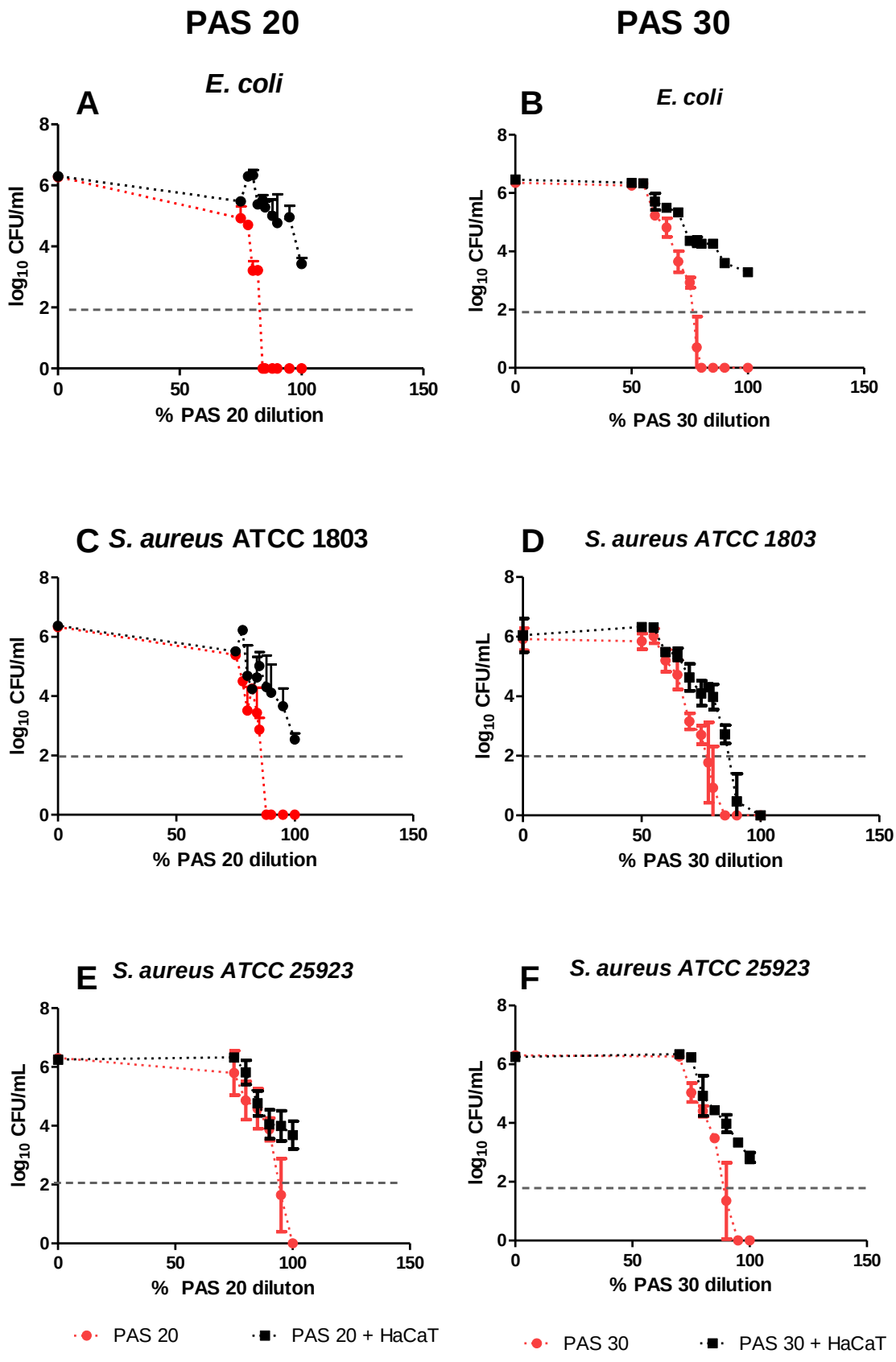

Figure 7.3 The antimicrobial efficacy of PAS 20 and PAS 30 within the co-culture model between HaCaT cells and E. coli or S. aureus and incubation with diluted PAS 20 or PAS 30 after 60 min contact time. (A) E. coli – PAS 20, (B) E. coli – PAS 30, (C) S. aureus ATCC 1803 – PAS 20, (D) S. aureus ATCC 1803 – PAS 30, (E) S. aureus ATCC 25923 – PAS 20, (F) S. aureus ATCC 25923 - PAS 30. The results are the mean ± S.D. of three determinations. Antimicrobial assay was determined as described in Materials & Methods section 2.6.1.

A useful balance between minimal cytotoxic and efficient antimicrobial effects could make these solutions ideal candidates as disinfectants or antiseptics. To investigate if this scenario was feasible, dilutions ranging from 70% to 100% PAS were made using sterile PBS and then tested against the same bacteria strains for 60 min contact time as this was the most effective process for microbial inactivation. Figure 3 shows that 75% PAS 20 can cause 1.5 log reduction for *E. coli* suspensions, 80-82% PAS 20 yields a 3 log reduction and 84-100% PAS 20 a 6 log reduction (Figure 7.3A). In contrast, when the bacteria were in the presence of a cell layer, a 6 log cycle inactivation was only achieved when 100% PAS was applied. *S. aureus* ATCC 1803 was reduced by approximately 3 log cycles when incubated with 85% PAS, whereas 88-100% PAS 20 solutions achieved 6 log reductions (Figure 7.3C). In the co-culture model, *S. aureus* ATCC 1803 was reduced by 3.5 log by 100% PAS 20, whereas 95% PAS 20 caused 2.5 log reduction. *S. aureus* ATCC 25923 seemed to be slightly more resistant than *S. aureus* ATCC 1803 (Figure 7.3E).

The same method was followed for PAS 30. Solutions of PAS 30 at higher than 78% and 80%, led to 6 log reduction for *E. coli* and *S. aureus*, respectively showing that PAS 30 has stronger bactericidal effects (Figure 7.3 B, D). The highest inactivation in the co-culture model was achieved with PAS 30 concentrations of 90% and 100%. A

2.5 log reduction was obtained for *E. coli* after 60 min. *E. coli* was further incubated up 24 hours in the co-culture setup to establish if inactivation was possible after longer contact time. A further decrease was noted after 4 hours, with complete inactivation after 6 hours of contact time (results not shown). When in co-culture, *S. aureus* was inactivated by 100% PAS 30, following the same trend as the inactivation trial without the monolayer. *S. aureus* ATCC 25923 was reduced by 6 log when incubated with 95% PAS 30 and 100% PAS 30, but the inactivation efficiency was reduced in the co-culture, and did not exceed 3 log cycles. The reduction factor decreased as PAS 30 dilution increased (Figure 7.3F).

7.4 Internalisation of bacteria to host cells

Table 7.1 Antibiotic invasion assay against E. coli, S. aureus ATCC 1803 and S. aureus ATCC 25923. Results are the surviving bacterial concentration in log CFU/mL shown as mean ± S.D. of three determinations. ND = not detected, limit of detection 2log. Antibiotic invasion assay was determined as described in s Materials & Methods section 2.6.1.

	CTL	**CTL+ HaCaT**	**S20**	**S20+ HaCaT**	**S30**	**S30+ HaCaT**
E. coli						
PAS	6.16 ± 0.12	6.27 ± 0.09	ND	4.07 ± 0.43	ND	3.11 ± 0.08
Gentamicin	ND	ND	ND	ND	ND	ND
1% Triton	ND	ND	ND	ND	ND	ND
***S. aureus* ATCC 1803**						

PAS	5.93 ± 0.34	6.31 ± 0.13	ND	2.91 ± 0.19	ND	ND
Lysostaphin	ND	ND	ND	ND	ND	ND
1% Triton	ND	ND	ND	ND	ND	ND
***S. aureus* ATCC 25923**						
PAS	6.30 ± 0.05	6.46 ± 0.07	ND	3.68 ± 0.47	ND	2.83 ± 0.16
Lysostaphin	ND	ND	ND	ND	ND	ND
1% Triton	ND	ND	ND	ND	ND	ND

To determine whether the reduction of bacterial counts was indeed the result of inactivation by PAS, we next investigated if bacteria were internalized into host cells using the gentamicin/lysostaphin invasion assay. This assay is used to quantify the ability of pathogenic bacteria to invade eukaryotic cells and allows counting them, while not destroying them Table 7.1 shows that gentamicin or lysostaphin were able to inactivate all bacteria in the wells after 1 h incubation time. Subsequent lysis of HaCaT cells by addition of Triton did not yield any colonies in the plates, indicating that bacteria did not invade into the keratinocytes, thus PAS reduced bacterial load.

7. 5 Comparison of PAS to disinfectants

Table 7.2 List of the chemical disinfectants used and their antimicrobial activity and HaCaT cell viability after 15 min contact time (ND=not detected, limit of detection 2log).

Disinfectant used	Bacterial concentration in co-culture [CFU/mL]			Cell viability of HaCaT [%]
	E. coli	***S. aureus* ATCC 1803**	***S. aureus* ATCC 25923**	
CTL	6.26 ± 0.1	6.17 ± 0.1	6.46 ± 0.07	100 ± 0.1
PAS 20	6.12 ± 0.1	6.21 ± 0.1	5.87 ± 00.4	32.1 ± 6.8
1% Povidone Iodine	ND	ND	ND	14.7 ± 0.1
1% Chlorhexidine	ND	ND	ND	11.2 ± 0.3
2% Formaldehyde	ND	ND	ND	13.6 ± 0.3
2% Glutaraldehyde	ND	ND	ND	ND
0.045% NaClO	ND	ND	ND	9.6 ± 5.3
70% Ethanol	ND	ND	ND	17.5 ± 0.7
3% H_2O_2	ND	ND	ND	16.1 ± 1.0

The antimicrobial efficacy of seven different chemical disinfectants from different classes of disinfectants applicable to the biomedical field were compared with PAS. Higher concentrations of these disinfectants were also tested, but only the lowest concentrations are shown here. All solutions tested (1% povidone iodine, 1% Chlorhexidine, 2% formaldehyde, 2% glutaraldehyde, 0.045% NaClO, 70% ethanol and 3% H_2O_2) had strong bactericidal effects and were able to reduce *E. coli* or *S. aureus* to undetectable levels after 15 min contact time (Table 7.2). Strong cytotoxic effects were also observed for all disinfectants with cell viabilities below 20% for all solutions tested.

7.6 Decrease of cell viability and cell death of HaCaT cells induced by PAS

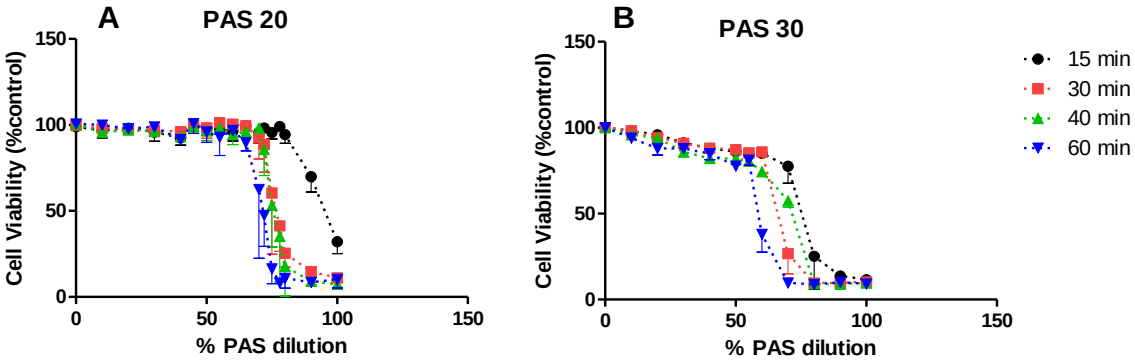

Figure 7.4 Cell viability of diluted PAS 20 (A) and PAS 30 (B) at 15 min, 30 min, 40 min and 60 min contact time. Cell cytotoxicity assay was determined as described in Materials & Methods section 2.5.2.2.

The resazurin assay (described in Section 2.5.2.2) was used to measure cell metabolic activity which served as an indicator of mammalian cell cytotoxicity. Pure plasma activated saline demonstrated strong cytotoxic effects on HaCaT cells, where the intensity of effects was a function of contact time duration and PAS concentration. Regarding PAS 20, 30% cells remained viable when incubated for 15 min with the undiluted PAS (100% PAS 20), whereas 30, 40 and 60 min contact time had stronger cytotoxic effects and no viable cells were observed. The effect of diluting PAS with PBS was therefore tested (Figure 7.4A). Generally, cytotoxicity increased as a function of PAS concentration. Figure 4B shows that 75% cytotoxicity on HaCaT cells occurred following incubation of 80% PAS 30 for 15 min and a 90% reduction in viability when incubated for longer contact time. For 60 min contact time, 60% PAS 30 caused 60% cytotoxicity and 70% PAS 30 resulted in complete loss of cell viability. Comparing diluted PAS 20 and PAS 30, PAS 30 seems to follow the same trendline as PAS 20, but with a 20% PAS dilution difference. For instance, for 15 min contact

time, cytotoxic effects start around 70% PAS 30 and 90% PAS 20 which both led to cell viability of 70%.

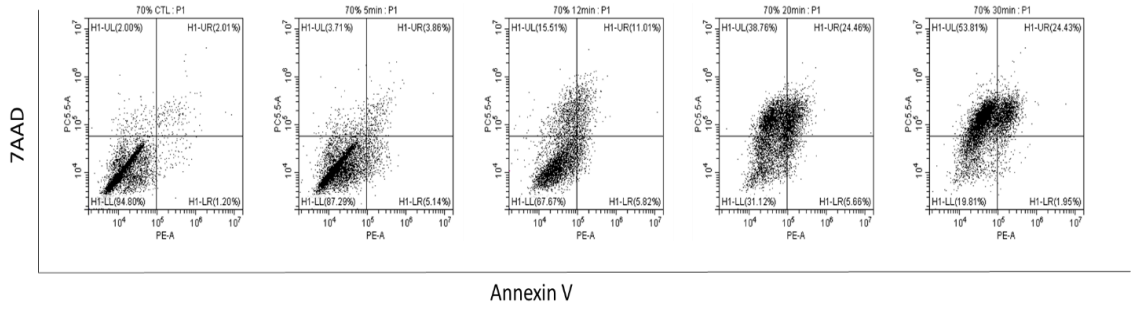

Figure 7.5 Apoptosis and lysis of HaCaT cells after incubation with 70% PAS at different contact times. Flow cytometry analysis was determined as described in Materials & Methods section 2.5.2.3.

We further explored the cell death of HaCaT cells after incubation with different % of PAS from 1 min up to 60 min contact time by flow cytometric analysis (Figure 7.5 and Table S.4 Supplementary material). The flow cytometry data showed that at low concentrations of PAS, HaCaT cells maintained high levels of viability, however, when these cells were treated with higher concentrations of PAS accelerated cell lysis occurred, probably due to acidic pH (Table S.4 Supplementary material). In more detail when HaCaT were incubated with 55% PAS a maximum 2% of cells appeared as Annexin V-/7AAD + after 60 min of incubation compared to control and a slight increase of AnnexinV+/7AAD- and AnnexinV+/7AAD+ (less than 5%) occurred. Generally, early apoptotic cell populations did not increase above 10% fraction for most of the samples, whereas the increase of late apoptotic and necrotic/lysed cells was higher. PAS concentrations such as 65% PAS led to >20% late apoptotic cells and 40% lysed cells after 60 min contact time. 70% PAS was more cytotoxic and acidic and caused >20% late apoptotic cells and 50% lysed cells within the shorter contact time of 30 min (Figure 7.5 and Table 7.1) and even shorter contact times (15 min)

caused similar effects using a 75% PAS solution. Changes in forward scatter/side scatter profile and microscopic observation indicated that the AnnexinV+/7AAD+ (normally considered late apoptotic) and AnnexinV-/7AAD+ populations represented severely damaged/lysed cells. The lack of progression of cells through the early apoptotic stage suggests that Annexin V+/7AAD+ cells are the result of phosphatidylserine on the inner side of the membrane becoming accessible for AnnexinV due to excessive membrane damage rather an apoptotic pathway.

7.7 Extracellular pH expected to be an important parameter influencing cell viability

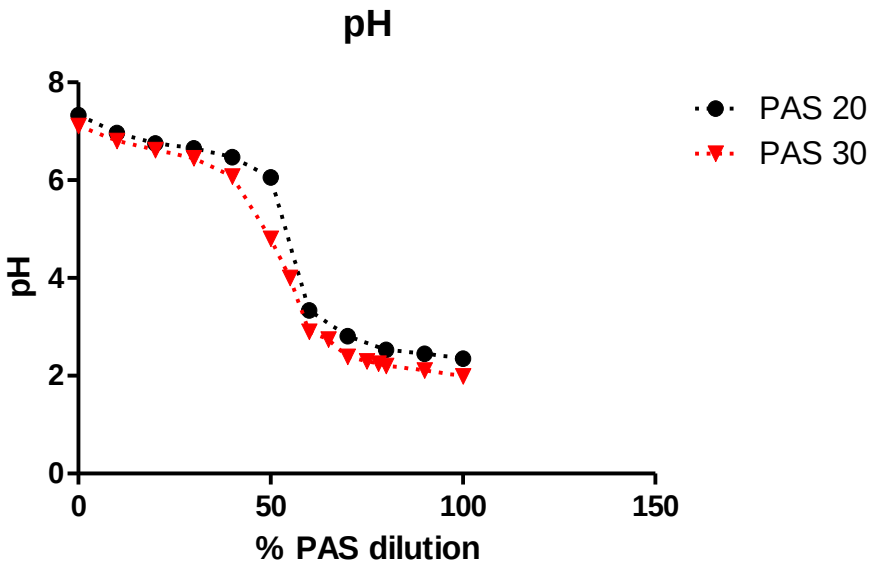

Figure 7.6 pH values of diluted PAS 20 and PAS 30.

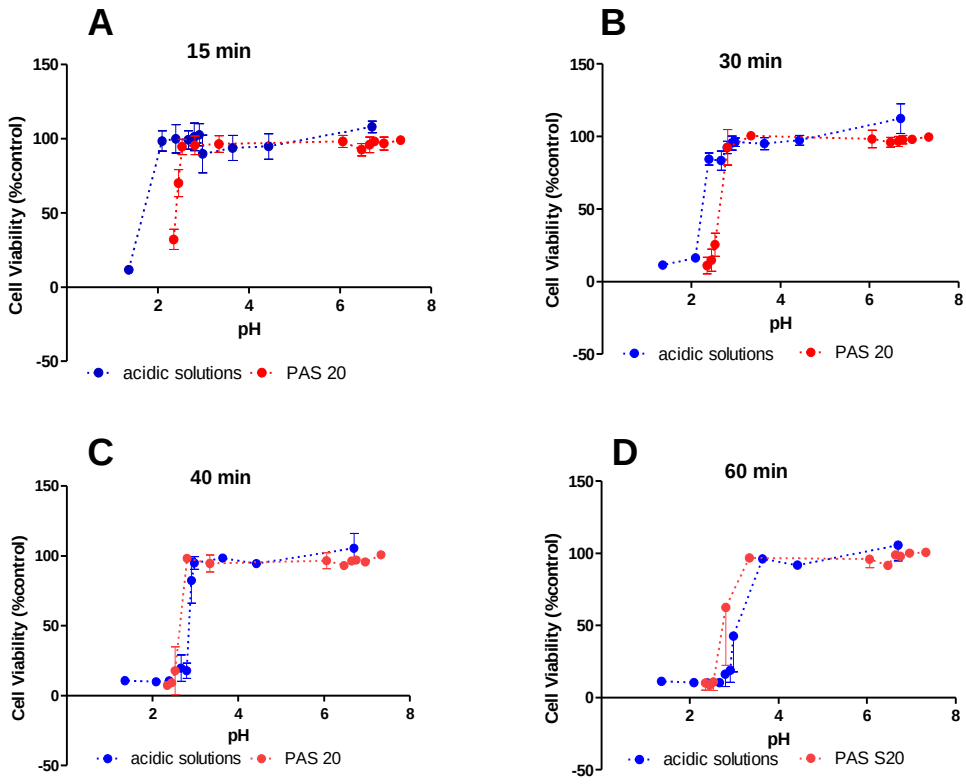

Figure 7.7 Cell viability of acidic solution at pH values similar to pH values observed for PAS 20, compared with different dilutions of PAS 20.

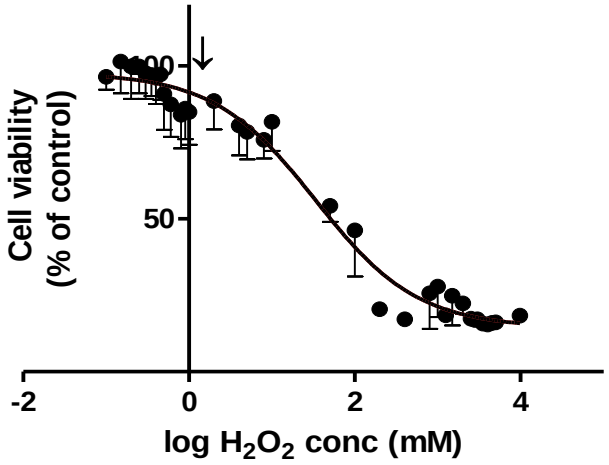

Figure 7.8 Cell viability of HaCaT cells at different concentrations of hydrogen peroxide after 60 min contact time. The arrow indicates the concentration of hydrogen peroxide measured in PAS 20. Cell cytotoxicity assay was determined as described in Materials & Methods section 2.5.2.2.

The low pH value of PAS seems to play a vital role in the cytotoxic effects of less diluted samples. Generally, the more diluted samples had higher pH values, which were also a function of plasma generation time, with PAS 30 dilutions being slightly more acidic than PAS 20 dilutions (Figure 7.6). However, pH level is only one aspect of the cytotoxicity mechanism, as shown with the pH controls. 100% PAS 20 with pH 2.35 was more cytotoxic than the acid control solution with pH of 2.39 for 15 and 30 min contact time (Figure 7.7A, B). Extended contact times of 40 min and 60 min had similar effects for both PAS and acidic control solutions (Figure 7.7C, D). Similar effects were observed for 90% PAS 20 and 80% PAS 20 with pH values 2.45 and 2.53, respectively, and both had higher cytotoxic effects than the pH control solution of pH 2.39. Acidic pH therefore potentiated the effects in cytotoxicity but the role of ROS and RNS cannot be excluded. Cell viability response to hydrogen peroxide was investigated to understand if hydrogen peroxide was responsible for the cytotoxic effects. The IC50 of hydrogen peroxide within the current setup with a contact time of 60 min was 33.57 mM (Figure 7.8). A hydrogen peroxide concentration up to 10 mM, which is almost 5-6 times higher than PAS 20 or PAS 30, was found not to be cytotoxic, indicating that hydrogen peroxide on its own is not able to cause comparable cytotoxicity.

More diluted samples which were less cytotoxic than the undiluted samples, had less acidic pH levels, but were also diluted with regards to their chemical composition.

7.8 Oxidative stress analysis

The mechanisms by which cellular stress are activated, were examined after exposure of HaCat cells to PAS 20, these consisted of measurements of mitochondria membrane potential, concentration of intracellular ROS and levels of total GSH and GSSH.

The JC-1 ratio of aggregates/monomers decreased as PAS 20 dilution decreased, with a peak happening around 55%-60% PAS 20, indicating that at these dilutions, the cell membranes may be disrupted and aggregate components of mitochondria were exposed extracellularly (Figure 7.9).

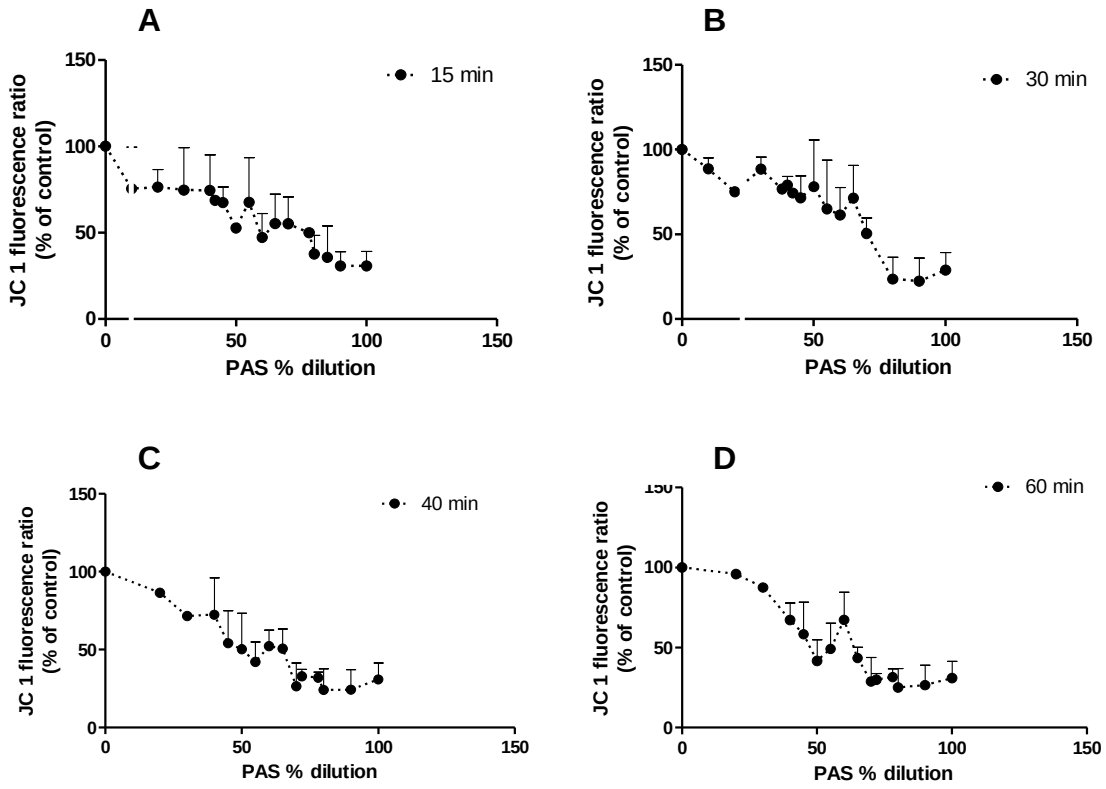

Figure 7.9 Mitochondrial membrane potential after incubation with PAS 20 for different contact times: (A) after 15 min, (B) 30 min, (C) 40 min, (D) 60 min contact time. Graphs represent averages of three independent plasma treatments. Mitochondrial membrane potential concentrations were measured as described in Materials & Methods section 2.5.2.5.

An increase of intracellular ROS in cells, with a peak at 50% PAS for all contact times occurred and then a decrease followed as PAS concentration increased. Similar trendlines occurred for all contact times, with longer contact times showing higher fluorescence values (Figure 7.10). The level of lipid oxidation following treatment

with dilutions of PAS between 10% PAS and 100% PAS with 10% increments, over a range of contact times (10 min to 60 min) was investigated. The levels of MDA did not increase (results not shown), and therefore lipid peroxidation was not detected for any contact time or solution. The same treatment was followed for analysis of glutathione and figure 7.11 shows that cells treated with up to 50% PAS have similar values for both total glutathione and oxidised glutathione (GSSH), with total glutathione (230 μM) having double concentration than GSSH (Figure 7.11). Contact with 60% PAS showed a decrease of total glutathione to 160 μM with further decrease as concentration increased. Similarly, GSSH levels decreased to half after incubation with 50% PAS and led to undetectable levels following more concentrated PAS, indicating cell lysis and leakage of intracellular components. In order to investigate if reduction of GSH and GSSH was due to acidic pH, 70-100% PAS were neutralized with NaOH and results showed that total GSH and GSSH concentration were similar to controls, indicating that acidic pH could cause lysis to cells.

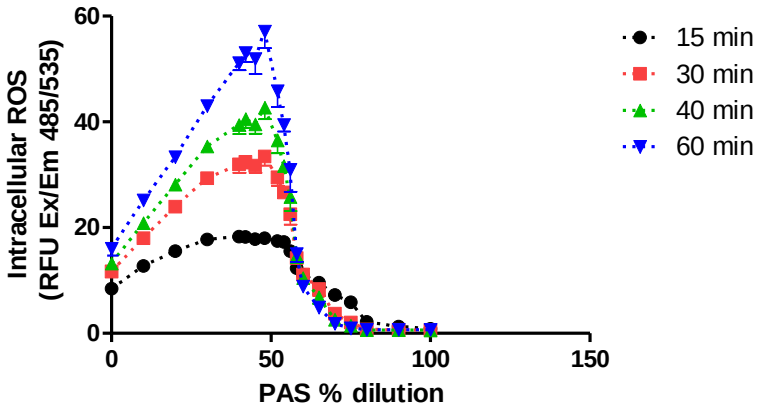

Figure 7.10 Detection of intracellular ROS after incubation of HaCaT with PAS 20 at different contact times. One representative experiment is represented.Intracellular

ROS concentrations were measured as described in Materials & Methods section 2.5.2.4.

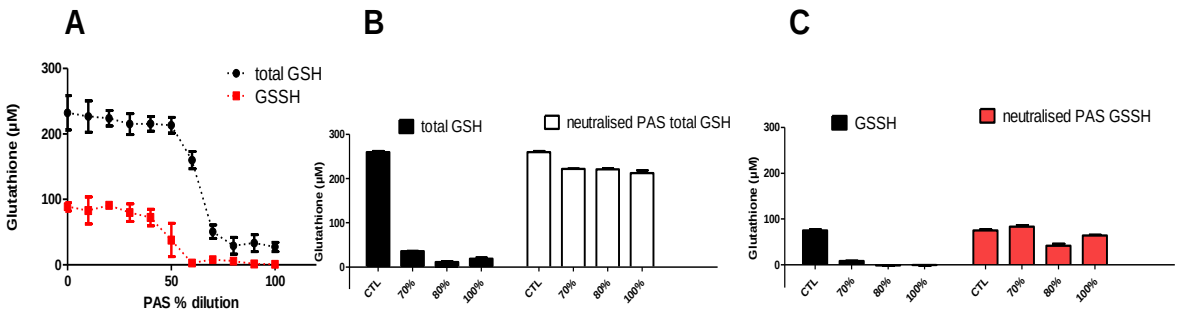

Figure 7.11 Measurements of total GSH and GSSH after 60 min exposure of PAS and neutralized PAS. Glutathione concentrations were measured as described in Materials & Methods section 2.5.2.6.

7. 9 Cytokine expression

Table 7.3 Cytokine analysis after treatment with 50% or 68% PAS. Results are shown as % of induced cytokine production compared to positive control. Protein expression analysis is described in Materials & Methods section 2.5.3.

Cytokines	**Solution**		
	CTL	**50% PAS 20**	**68% PAS 20**
IL1α	9.9 ± 0.1	13.8 ± 0.1	10.3 ± 2
IL1β	ND	5.9 ± 0.6	4.04 ± 0.2
IL2	ND	4.1 ± 0.7	ND
IL4	ND	ND	ND
IL6	ND	ND	ND
IL8	83.2 ± 0.1	102.9 ± 6.5	29.5 ± 2.5
IL10	ND	ND	ND

IL12	ND	ND	ND
IL17α	ND	ND	ND
IFNγ	ND	ND	ND
TNFα	3.3 ± 0.4	3.9 ± 0.1	ND
GM-CSF	3.8 ± 0.6	6.0 ± 0.2	ND

Cytokines and chemokines are major regulators of inflammation in wound healing. In order to realise changes in cells after PAS treatment, HaCaT cells were grown in 6 well plates, treated with 50% or 68% PAS for 60 min and then they were incubated with new media without serum for 24 hours. After incubation, cell culture supernatants were collected and prepared for qualitative ELISA analysis (Table 7.3). Positive controls were provided by the manufacturer and results are presented as % cytokine produced compared to positive control. 50% PAS and 68% PAS were chosen as solutions that caused no death or 90% cytotoxicity respectively, in order to test two different conditions. Generally, PAS induced production of IL1α, IL1β, IL2, IL8, TNFα and GM-CSF, with higher percentages observed for cells treated with 50% PAS, as cells were healthier in this condition. Except of IL8, all other induced cytokine production ranged between 3.9 and 13.8% of the positive control after 50% PAS treatment. Regarding IL8, the saline control was 83% of the positive control, 103% expression was detected after incubation with 50% PAS and 29.5% following incubation with 68% PAS.

7.10 Discussion

For a good wound healing response, the bacterial load of wounds needs to be optimally managed, as infection can delay the process of wound healing. The primary objective

of this study was to determine plasma treatment conditions which would provide a balance between cytotoxic and bactericidal effects of PAS in a co-culture set up, as a simplified model of infection control in a wound setting. PAL have been described to have antibacterial effects on different bacteria. In the current study, we confirm that PAS has high bactericidal effects against both Gram negative and positive bacteria. Bacterial loads of all 3 strains used in this study were reduced depending on the plasma treatment time of the solution and contact time of liquids with the cells. Most importantly, PAS showed strong bactericidal effects (a reduction of at least 99.9% (≥3 log10) of the total count of CFU/mL in the original inoculum) against bacteria in the co-culture setup and especially *S. aureus*, where a 3-6 log reduction was achieved after 60 min depending on the strain.

Acidification of PAL and the generation of short- and long-lived reactive chemical species play an important role in the antimicrobial effects of PAL (Zhou *et al.*, 2019b; Tarabová *et al.*, 2019). Acidic pH of PAL and reactive species such as nitrite and hydrogen peroxide can act synergistically and enhance antimicrobial activity of PAW (Hoeben *et al.*, 2019; Laurita *et al.*, 2015). The short-lived reactive species can be: nitric oxide, hydroxyl radicals, superoxide, peroxynitrite, and peroxynitrite (Mokhtar Hefny *et al.*, 2016). Interestingly, previous work showed the pH of PAL remained stable, whereas concentrations of long-lived chemical species can change after storage time, and bactericidal effects can be lost, showing that pH is not the only factor responsible for inactivation effects (Tsoukou *et al.*, 2020). Naïtali et al. showed that a synergistic effect of acidic pH, hydrogen peroxide, nitrite and nitrate can be similar to bactericidal effects of PAW (Naïtali *et al.*, 2010). Different bacterial species included in this study behave differently to PAL. For example, in our study, PAS consists of hydrogen peroxide and nitrates and in the co-culture model, *S. aureus* ATCC 1803

was inactivated by 6 log after incubation for 60 min, which was higher than *E. coli*. Hozak et al. showed that PAW inhibits *S. epidermidis* more efficiently than *E. coli* (Hozak *et al.*, 2018). Thus, bactericidal effects of PAL are due to synergistic effects of reactive chemical species and other unknown species which might be difficult to detect, and they cause different effects on different types of bacteria.

The development of the co-culture, encompassing the growth of monolayers of HaCaT cells and addition of another planktonic population (bacteria), enabled a more complex investigation of the bactericidal potential of PAS in a more challenging environment. This co-culture method gives a benefit from an application point of view and could be more realistic if it could be developed further into an infected wound model consisting of necrotic cells and biofilms of different bacteria. Bacterial biofilm has a decreased susceptibility to antimicrobial agents due to tolerance and/or resistance. Plattfaut et al. reported that no significant reduction in the bacterial load was detected in *S. aureus* biofilms after treatment with direct plasma, whereas weak antibacterial efficacy was found against planktonic *S. aureus*, confirming that inactivation of bacteria is more complex and difficult in biofilms which are more realistic clinical setups (Plattfaut *et al.*, 2021). PAW treatment was shown to downregulate expression of quorum sensing related virulence genes in biofilms of *E. faecalis in vitro* and lead to biofilm disruption and removal (Li *et al.*, 2019). Also, it has been reported that *S. aureus* primarily colonizes the region of wounds which is close to the surface, whereas Gram negative bacteria such as *P. aeruginosa* primarily colonizes the deeper regions and can keep the wounds arrested in a stage dominated by inflammatory processes (Fazli *et al.*, 2009), thus it is difficult to mimic a realistic infected wound model. *In vivo* experiments have shown that PAW can inactivate a variety of bacteria including *E.*

coli and *S. aureus* and also accelerate the healing of full-thickness skin wounds on mice (Xu *et al.*, 2020).

PAL can be stored for periods of 18 months retaining their bactericidal effects (Tsoukou *et al.*, 2020), are easy to transport and packed compared to direct exposure to plasma. Nevertheless, the acidic nature of these solutions needs to be investigated with regards to physiology and health of skin and wounds after repeated exposure to PAL, even if it is surrounded by necrotic tissue. It needs to be mentioned that pH of normal skin surface is acidic and skin surface becomes more alkaline by bacterial colonisation. Wound pH is an influential factor for the healing process and different pH ranges are required for certain distinct phases of wound healing (Schneider *et al.*, 2007). For example, during re-epithelialization of chronic wounds, the pH decreases closer to the values of normal skin surface (Lengheden and Jansson, 1995). Interestingly, antibiotics such as glycopeptide antibiotics have been shown to be less active against vancomycin resistant *Enterobacter* species in an acidic milieu with a pH value of 6.4 compared to pH values above 7.4 (Mercier, Stumpo and Rybak, 2002).

Studies have reported that antiseptics at specific concentrations such as povidone iodine solution may be beneficial in reduction of bacterial load in open wounds without trauma to the cells critical to wound repair (Doughty, 1994). On the other side, there have been antimicrobial agents that have been shown to predispose to sensitization, such as neomycin which highly predisposes patients to contact allergy (Menezes de Pádua *et al.*, 2005) and alcohol-based hand sanitizers which can induce irritant contact dermatitis and skin burns (Schick and Milstein, 1981), while trace amounts of chlorhexidine gluconate can also be absorbed through the skin (Chapman, Aucott and Milstone, 2012). PAS efficacy was compared with common chemical disinfectants and these were all more effective at shorter times than the contact time

needed for PAS, nonetheless they all had similar cytotoxic effects to PAS. Lee et al. recently reported comparison between cold plasma technology and peracetic acid and showed that peracetic acid had much higher and faster reduction rates (Lee *et al.*, 2021). Interestingly, *in vivo* experiments showed recently that PAW treatment can be more efficient on a wound healing processes than medical alcohol in mice, by the promotion of the release of pro-inflammatory factors and anti-inflammatory factors in the wound (Wang *et al.*, 2021a). Combining these data together, it seems that in the near future, PAL may still become a novel antimicrobial solutions in the field of hygiene.

Hydrogen peroxide was detected in PAS, however cytotoxic effects of hydrogen peroxide solution was not similar to PAS. According to literature, supplementation of cell cultures with nitrite or nitrate did not show cytotoxic effects on different cell lines tested by others (Boehm *et al.*, 2018; Wende *et al.*, 2015). These observations suggest that another factor such as acidic pH plays a crucial role in the effects observed here, with cell viability being decreased by more than 50% after incubation with PAS with pH 2.53-2.81. HaCaT cells were incubated with PAS for a maximum time of one hour, a time which was not enough for H_2O_2 to cause cytotoxic effects. Whereas in past reports hydrogen peroxide has been reported to be cytotoxic when cells were in contact with PAL for 2 or 3 days (Boehm *et al.*, 2016).

A general indication of the redox state of the cells was given by studying the changes in intracellular ROS, mitochondria depolarisation, GSH and lipid peroxidation after exposure of HaCaT to PAS. Results revealed that intracellular ROS was enhanced, and breakdown of mitochondrial membrane potential followed which was associated with slight increases in apoptosis for PAS concentrations below 50%. These results indicate that low % of PAS are responsible for oxidative stress through increased

intracellular ROS levels and the breakdown of mitochondrial membrane potential. A peak of fluorescence for intracellular ROS was observed around 50 % PAS with a sharp drop and complete loss of ROS signal for higher concentrations of PAS. Under the same conditions cell viability values were low too, suggesting that dead/lysed cells cannot produce intracellular ROS. Similar results have been obtained in studies investigating direct plasma exposure of fibroblasts and keratocytes (Brun *et al.*, 2012). Also, PBS treated for 5 min with either He plasma or He-N_2 plasma and predominant species H_2O_2 and nitrites lead to death in HaCaT cells after 1 hour of exposure (Dezest *et al.*, 2017).

Cells maintain a reducing intracellular environment to avoid genomic damage after induction of oxidative stress. Glutathione is the most important redox regulatory factor, subsequently essential for survival in mammalian cells. GSH is an important regulator of cell proliferation, apoptosis, and gene transcription (Rahman *et al.*, 2005) and its oxidation to glutathione disulfide (GSSG) is associated with oxidative stress. GSH depletion produced by different ways generates a low GSH/GSSG ratio leading to oxidative stress and apoptosis of cells by exacerbation of reactive oxygen species production (Xiao *et al.*, 2010). HaCaT cells are able to express the main enzymes involved in the glutathione cycle in a way that is comparable to that observed in healthy human skin (Hewitt *et al.*, 2013). Following application of a non-toxic concentration of PAS (lower or equal to 60%), the amount of total GSH was not depleted and levels were maintained similar to control, demonstrating an active GSH cycle in HaCaT cells. Incubation with PAS equal or higher than 70% caused an immediate decrease in total cellular glutathione concentration GSH with levels significantly lower than control. According to Klinkhammer et al., DBD plasma treatment on GSH resulted in oxidation of the sulphur atoms from thiols to S-O, S = O,

S-S and S-N = O groups, resulting in GSO_3H, GSSG and GSNO. GSO_3H was one of the most dominant final products which accumulated with longer plasma treatment times, whereas GSSG was the most prevailing molecule only after short treatment (Klinkhammer *et al.*, 2017). According to this theory, it is possible that decrease of GSH and GSSH at 60-70% PAS is due to transformation of these molecules to others such as GSO_3H after incubation with more concentrated solutions.

Moreover, in order to investigate if acidic pH was responsible for the decrease of GSH, solutions were neutralized by addition of NaOH and results revealed that the GSH decrease could be largely prevented, indicating that the dominant reactions are influenced by pH value (Klinkhammer *et al.*, 2017). Consideration needs to be taken of the fact that treatments were carried out for a maximum of 60 min, thus possible rupture of plasma membranes, and cell lysis with leakage of cell components such as glutathione through the damaged plasma membranes in necrotic cells might have happened. Following discard of PAS and washing, glutathione may have been removed before being tested, thus glutathione was not detected, due to intracellular leakage.

PAS which is not at a cytotoxic level, such as 50% PAS, potentially induces the secretion of cytokines and growth factors, thus can stimulate activation of the wound healing process. Cold plasma has been reported to induce epigenetic mechanism modifications that activate the expression of cytokines, chemokines and growth factors, explaining how it acts as an efficient tool in regenerative medicine to stimulate and activate proliferation of stem cells and immune cells, and to recover wounds (Park *et al.*, 2020). PAS treatment increased the expression of GM-CSF in HaCaT, which is in agreement with previous reports investigating plasma treatment on the same cell line (Schmidt *et al.*, 2019a; Barton *et al.*, 2014). Increase of chemokine IL-8 is in line

with work reported before, where two minutes direct exposure of keratinocytes or fibroblasts to plasma treatment resulted in increased secretion of proteins including IL-1 and IL-8 hence activating wound healing relevant molecules to improve wound healing (Arndt *et al.*, 2015; Arndt *et al.*, 2013).

Diffusion of RONS into the cell may be facilitated by lipid peroxidation caused by reactive species, which then leads to pore formation in the membrane. Membrane lipids such as the polyunsaturated fatty acids are sensitive to ROS, and that makes them vulnerable to lipid peroxidation. ROS extracts an H atom from polyun-saturated fatty acids which results in MDA formation as a final product. No increase in lipid peroxidation was detected by analyzing the accumulation of MDA, suggesting that changes in cell morphology were not due to oxidation of the membrane lipid. Lipid peroxidation product production in HaCaT cells was also not increased after exposure to three plasma devices, even if increase in DNA damage was detected (Dezest *et al.*, 2017). Moreover, accumulation of lipid peroxidation is one characteristic of ferroptosis, thus in our case we can exclude this type of cell death. In case of cancer cell lines such as melanoma and glioblastoma cells, PAM or direct exposure to plasma respectively caused an increase in the formation of MDA in cells as compared to the control (Adhikari *et al.*, 2019; He *et al.*, 2019). Lipid oxidation has also been reported for shrimps after PAW ice treatment (Liao *et al.*, 2018).

7.11 Conclusion

Taken together, our results suggest that PAS is highly antimicrobial in the co-culture model but leads to changes in HaCaT cells with increase of intracellular ROS as early sign of apoptosis, then breakdown of the mitochondrial membrane potential and subsequent cell lysis and leakage of intracellular components such as GSH as concentration of PAS increases. We conclude that if PAS is diluted enough (i.e., 40-

50%), cell viability remains unaffected with a minimal increase in early apoptotic cells, whereas undiluted PAS negatively influences the number of healthy cells with undesired effects of cell lysis. Our results demonstrate the difficulty in establishing a balance between antimicrobial efficacy and low cytotoxic effects since wound related cells such as HaCaT are affected negatively by incubation with PAS earlier than inactivation of bacteria. These findings may have implications for refining plasma activated liquids towards the design of a highly antimicrobial solution with low or moderate cytotoxic effects in surrounding tissues. Additional studies are required for determining the mechanism of action involved in the wound healing activity, and the elucidation of other chemical species in PAS in order to validate if PAS could be used in the field of hygiene as a novel antimicrobial agent.

Chapter 8: Conclusions and future recommendations

After plasma treatment, the plasma activated solutions are enriched with reactive oxygen and reactive nitrogen chemical species with lifetimes ranging from seconds to months, making them useful for potential biomedical applications. Plasma-activated liquids, prepared by cold atmospheric plasma treatment of liquids, have gained increasing interest as they can offer advantages and variable modes of delivery over direct exposure to plasma. Based on discharge type, working gas, and the chemical composition of the surrounding environment, various chemical reactions induced by plasma can be initiated, with a number of resulting primary and secondary reactive chemical species penetrating or dissolving into the PAL.

Overall, this work comprehensively investigated and advanced understanding of the relationship between biological activity, mechanisms and chemical composition of PAL. The specific objectives and conclusions obtained from these investigations are presented below:

To generate four PAL, which differed in respect to their buffering capacity and presence of saline, using a dielectric barrier discharge system, and investigate their bactericidal activity against Gram negative and positive bacteria, and their cytotoxic effects relative to the chemical composition (presented in Chapter 3).

Conclusions:

- The concentrations of hydrogen peroxide and nitrates in all PAL increased as plasma treatment time advanced, whereas pH decreased.
- Different PAL may carry different concentrations of chemical species, retain diverse antimicrobial properties and cytotoxic effects.

- Longer plasma treatment time in combination with longer contact time could achieve higher inactivation effects.
- PAW and PAS exerted bactericidal activity that persisted up to 2 days after PAL's generation. PAPBS and PAPB lost their antimicrobial activity on the second day.
- pH of PAL plays an important role in bactericidal efficacy.

In Chapter 3, antimicrobial and cytotoxic effects of buffered and non-buffered solutions were investigated using a DBD system. Using this lab-based system treatment volume was restricted to 10 mL of liquid each time and required 24 hours post treatment storage time as previous investigations had shown that 24 hours post treatment storage time allows higher concentration of chemical species and subsequent higher inactivation effects.

From an application point of view, the long post treatment storage time of PAL is a limitation of usage of the DBD system. It would be beneficial if a disinfectant could be generated, tested or used immediately.

Another limitation of the DBD system was that the samples were treated in a sealed package as described in Chapter 2. Historically, this system was built for testing the antimicrobial effects of cold plasma on food produce and packaging such as meat and strawberries. In our study, the decision for plasma treating liquids with this system, is due to the fact that the system is very well-studied in our group by previous members and it was used as a benchmark for this study. Results obtained with this system will further the basic understanding of PAL chemistry and biological effects which would be beneficial for future researchers in our group but also aid the development and scale-up of PAL for future applications.

The research area was expanded to understand the effects of process and storage conditions on PAW and PAS efficacy and stability as important factors to consider for PAL in a biomedical application. These experiments considered only PAW and PAS as these liquids were more bactericidal than buffered PAL (presented in Chapter 4).

Conclusions:

- In the first part of the study, heating of PAW and PAS and their bactericidal efficacy showed that antimicrobial activity was lost upon heating to >60 °C, with detected chemical species being unaffected.
- In the second part PAW and PAS stored in temperatures of -80°C or -150°C at storage times up to 18 months showed high bactericidal effects against *E. coli* and *S. aureus* strains, with big fluctuations in chemical species and unaffected pH values. Bactericidal effects of PAW were lost when solutions were stored at room temperature, fridge or -16°C.

A limitation in this study, was the fact that generation of larger volumes of PAL required days. Samples were stored in small volumes in microtubes for the storage study but the pH could not be measured at all time points as the volume was low in Eppendorf tubes and the pH probe would not fit in these tubes.

A reactive species selective spark and glow discharge set-up (RSS system) was then introduced for Chapter 5. This system provided the ability to control the generation of ROS- rich versus RNS-rich PAW and therefore investigate the role of this chemistry in defining the antibacterial and cytotoxic effects. The influence of heating temperature on the bactericidal effects of PAW generated by the two different discharges was also investigated. This study allowed us to compare the thermal stability profiles to different discharge modes.

Conclusions:

- Two types of PAW were investigated: spark discharge (SD) and glow discharge (GD) PAW. SD PAW consisted of hydrogen peroxide, nitrates and acidic pH, whereas GD PAW consisted of nitrites, nitrates and acidic pH. Long plasma treatment in combination with long contact times resulted in high bactericidal effects against bacteria, for both PAW.
- PAW were able to retain their bactericidal effects against both Gram positive and Gram negative bacteria post generation for up to one week at refrigerated temperature.
- PAW heated up to 100°C for up to 15 min could retain its bactericidal activity. PAW made by glow discharge was found to be highly bactericidal with low cytotoxic effects

While the cytotoxic activity of PAL observed on CHO-K1 and HaCaT cell lines were undesirable for potential antimicrobial applications, cell toxic effects of plasma activated liquids are of interest in other fields such as cancer research. The cytotoxic effects of ROS-rich or RNS-rich PAW against a range of different cancer cell lines were therefore investigated (Chapter 6).

Conclusions:

- Cytotoxic effects of SD and GD PAW on multiple cancer cell lines were observed, with SD PAW causing higher cell reductions than GD PAW. SD PAW contained hydrogen peroxide and nitrates, whereas GD PAW consisted of nitrites, nitrates and peroxides.

A limitation of this study is the fact that the cancer cell lines were not compared with their respective normal healthy control cell lines, in order to investigate potential selectivity of PAW.

Due to the fact that changes occurred to the RSS system as a result of replacement of power supply and electrodes, re-establishment of the identical chemistry was not possible. Thus, chemical characterisation of PAL is different between Chapter 5 and 6 and Chapter 7.

In Chapter 7, the bactericidal effects of PAS against a range of bacteria in the presence of a HaCaT layer were investigated. This Chapter also focused on the mechanistic pathways and cellular events which followed after exposure to PAS.

Conclusions:

- PAS treated by SD consisted of hydrogen peroxide, nitrates and acidic pH.
- Saline exposed to plasma for 20 or 30 min caused 6 log reduction for *S. aureus* after 60 min contact time, in the co-culture setup, with bacteria not being internalised in mammalian cells.
- High cytotoxic effects of PAS after 60 min contact time with PAS were attributed mainly to acidic pH.
- A series of molecular events happened for PAS concentrations below 60% including increase of intracellular ROS, mitochondrial membrane depolarization and induction of low levels of apoptosis while exposure to higher concentrations of PAS resulted in cell lysis.
- PAS induced production of IL1α, IL1β, IL2, IL8, TNFα and GM-CSF, with higher percentages observed for cells treated with 50% PAS, as cells were healthier in this condition compared to 68% PAS.

Future recommendations

The present study investigated the biological effects of PAL on bacteria and mammalian cells. The results show that there are differences in the activity and stability between buffered and non-buffered solutions, which were influenced by the acidity of the solution but not linked with the concentration of identified long lived chemical species. Moreover, in Chapter 4, temperature and storability studies of PAL showed that bactericidal effects were lost after PAL were stored at temperatures above -16°C, even if the solutions were still acidic. Additional research is needed to better understand the role of short-lived chemical species in different PAL, the resultant stable longer lived chemical species and their effects on different biological targets. For example, peroxynitrite chemistry has been reported to contribute in the bactericidal effects of PAL and it could be one of the candidates to start with. Its concentration in solutions could be measured by ion chromatography.

The current study investigated the bactericidal effects of PAS in combination with a layer of HaCaT cells, in order to mimic an infection model. The results show that PAS has strong bactericidal effects after 60 min contact time, but high lysis to mammalian cells is associated with it. Approaches for cellular response mechanisms of the mammalian cells could also be investigated to pinpoint the specific stress response pathways using the transcription and expression level, with reverse transcription polymerase chain reaction and protein analysis (such as actin).

The co-culture study suggests the need to employ a different PAL, which could offer a balance between cytotoxic effects and bactericidal effects. That could possibly be achieved by applying a different PAL for longer contact time which does not have such an acidic pH to cause lysis. Another suggestion would be to apply a strong

bactericidal PAL for a short time, to remove a large bacteria population, followed by one or multiple washes with less acidic pH. Approaches like these could assist to establish PAL based therapy as an antiseptic solution.

In order to understand the action of PAL on more complicated molecular structures and in complex physiological milieus, the effects of PAL on different biomolecules needs to be investigated. A range of biomolecule models of interest such as carbohydrates, proteins, and lipids could be researched in order to understand the underlying chemical modifications to the biological molecules which constitute the cellular building blocks. Moreover, additional research could be on testing different additives to PAL to investigate if cytotoxicity could be modulated. Plasma-treated aqueous biomolecule solutions showed differences in short-term cytotoxic effects with arachidonic acid and glucose being less cytotoxic than treated BSA or cholesterol (Heslin *et al.*, 2021). The antibacterial effects of PAL with additives such as these biomolecules could be tested, in order to realise if these inactivation effects would be modulated too. These experiments could be achieved by cytotoxicity and antimicrobial assays, as the ones used in this study.

A mechanistic insight for bacterial death could also be investigated by testing the metabolic activity, intracellular ROS, lipid peroxidation after expose to PAL and scanning electron microscopy imaging to help visualise the changes in bacterial morphology and attachment. For better understanding of the inactivation mechanisms of microorganisms by PAL and ensuring safety of PAL applications, resistance studies are needed against different bacteria. Potential of resistance development and resistance associated genes could be tested by genome expression analysis. The existence of viable but non-culturable microorganisms after exposure to PAL could be tested by PCR.

Bacteria can exist both in the planktonic and biofilm state. Biofilms are associated with the chronic microbial infections particularly in hospitalised patients using a medical device. Moreover, the biofilm lifestyle is the main reason why chronic wounds do not heal in a timely manner. In our research, we focus only on planktonic cells, moving towards the bactericidal effects of PAL in bacterial biofilms would be beneficial for a more realistic approach. The anti-biofilm effects of PAL are under investigation to reveal the full potential of these solutions for clinical applications.

As discussed, in this research PAL consist of chemical species such as hydrogen peroxide, nitrites, nitrates, acidic pH and show high cytotoxic effects in different mammalian cell lines. PAL have been reported to be mutagenic to the Chinese hamster ovarian cell line CHO-K1 using the mammalian HPRT assay. Moreover, it would be of particular interest to investigate if treatment of HaCaT cells with PAL could induce DNA damage. This could be detected by phosphorylation of the histone variant H2AX which is used to quantify accumulation of double strand DNA breaks. This could be achieved by using either western blot or by flow cytometric detection of levels of phosphorylated histone H2AX.

Toxicity and mutagenicity of PAL should be monitored in cells/tissues that are to be exposed to this new technology, to ensure acceptable levels for either decontamination, wound healing or cancer therapy. Our results were all based on *in vitro* experiments, such as cell experiments. Results can be more realistic and representative by doing *in vivo* experiments in models such as *Galleria mellonella* (Heslin *et al.*, 2021), or even animal studies such as mice. *In vivo* studies could provide answers about potential systemic toxicity of PAL to eukaryotic organisms and local toxic effects to surrounding tissues and organs at the point of application.

Future investigations should involve all of these features for the establishment of PAL in various applications such as medicine and healthcare. An important future consideration is the scalability of PAL production. PAL needs to meet industry standard production rates, with high volumes being generated in a controlled environment, retaining the same reproducibility and low cost.

Appendices

Appendix I Supplementary Information for Chapter 4

Table S1. Microbial inactivation of *E. coli* and *S. aureus* NCTC 1803 at 30 and 60 min contact time, treated with PAW or PAS stored at different temperatures for up to 18 months. Table represents averages of 2 independent plasma treatments (Set 1 and 2). ND = not detected.

Contact time (min)	**Storage time (months)**	**CTL**	**RT**	**4**	**-16**	**-80**	**-150**
		Cell density (log_{10} CFU/mL) ±SD					
***E. coli* PAW set 1 + set 2**							
30	0	6.49±0.14	1.68±1.84	1.68±1.84	1.68±1.84	1.68±1.84	1.68±1.84
	1	6.33±0.08	5.67±0.57	5.68±0.07	4.90±0.87	2.49±1.41	1.37±1.50
	3	6.28±0.05	6.09±0.08	5.99±0.15	6.26±0.07	2.02±1.00	4.32±1.38
	6	6.15±0.06	5.85±0.12	5.79±0.06	5.61±0.60	1.13±1.25	2.74±0.58
	18	6.16±0.08	6.15±0.08	6.14±0.09	6.13±0.57	ND	ND
60	0	6.32±0.11	ND	ND	ND	ND	ND
	1	6.34±0.08	5.80±0.37	5.69±0.57	4.47±1.65	ND	ND
	3	6.31±0.14	6.00±0.18	5.70±0.09	6.09±0.19	ND	1.05±1.15
	6	6.14±0.07	5.87±0.08	5.81±0.20	5.80±0.08	ND	ND
	18	6.28±0.05	6.19±0.08	6.14±0.16	5.55±0.12	ND	ND
***S. aureus* PAW set 1 + set 2**							
30	0	6.23±0.22	1.78±1.95	1.78±1.95	1.78±1.9	1.78±1.95	1.78±1.95
	1	6.25±0.08	5.74±0.51	5.61±0.34	3.85±0.75	0.70±1.09	2.04±1.66
	3	6.18±0.12	6.19±0.15	6.01±0.19	6.15±0.07	2.59±0.52	3.95±0.72
	6	6.05±0.03	5.60±0.19	5.87±0.12	5.92±0.16	2.04±1.03	2.76±0.35
	18	6.11±0.08	6.22±0.12	6.25±0.07	5.66±0.49	ND	ND
60	0	6.29±0.02	ND	ND	ND	ND	ND
	1	6.19±0.10	5.85±0.34	5.73±0.38	4.10±1.39	ND	ND
	3	6.20±0.08	6.18±0.30	5.60±0.10	5.18±0.48	ND	ND
	6	6.20±0.04	5.66±0.09	5.77±0.11	4.94±0.42	ND	ND
	18	6.19±0.07	6.18±0.06	6.23±0.12	5.30±0.28	ND	ND
***E. coli* PAS set 1 + set 2**							
30	0	6.36±0.09	ND	ND	ND	ND	ND
	1	6.23±0.15	5.78±0.23	5.71±0.20	1.55±1.70	ND	ND
	3	6.25±0.05	6.03±0.22	5.79±0.26	6.27±0.15	ND	ND
	6	6.25±0.04	6.05±0.09	6.21±0.15	5.65±0.48	ND	ND
	18	6.23±0.04	6.19±0.06	6.21±0.13	6.23±0.04	ND	ND
60	0	5.98±0.51	ND	ND	ND	ND	ND
	1	6.27±0.11	5.78±0.32	6.17±0.11	2.97±0.83	ND	ND
	3	6.30±0.07	5.63±0.47	6.05±0.28	5.77±0.72	ND	ND
	6	6.27±0.07	6.09±0.05	6.11±0.15	6.16±0.08	ND	ND
	18	6.17±0.05	6.23±0.04	6.13±0.10	6.27±0.06	0.70±1.22	ND

***S. aureus* PAS set 1 + set 2**							
30	0	6.45±0.27	ND	ND	ND	ND	ND
	1	6.25±0.07	5.58±0.09	5.84±0.11	4.4±01.2	ND	0.35±0.86
	3	6.14±0.09	6.12±0.11	5.30±0.28	5.81±0.38	1.05±1.15	ND
	6	6.26±0.04	5.85±0.25	6.00±0.16	5.98±0.34	ND	ND
	18	6.27±0.04	6.19±0.08	6.18±0.09	6.12±0.02	ND	ND
60	0	6.38±0.06	0.35±0.86	0.35±0.86	0.35±0.86	0.35±0.86	0.35±0.86
	1	6.30±0.04	5.86±0.35	6.09±0.08	2.59±1.50	ND	ND
	3	6.16±0.07	6.14±0.10	5.36±0.38	4.96±0.17	ND	ND
	6	6.21±0.10	6.04±0.11	5.87±0.27	6.09±0.10	0.35±0.86	0.35±0.86
	18	6.15±0.12	6.24±0.06	6.06±0.14	6.13±0.10	0.70±1.22	ND

Table S2. Microbial inactivation of *E. coli* and *S. aureus* NCTC 1803 at 30 and 60 min contact time, treated with PAW or PAS stored at different temperatures for up to 6 months. Table represents 1 independent plasma treatment (Set 3). ND = not detected.

Contact time (min)	**Storage time (months)**	**CTL**	**RT**	**4**	**-16**	**-80**	**-150**
		Cell density (log_{10} CFU/mL) ±SD					
***E. coli* PAW set 3**							
30	0	6.20±0.05	ND	ND	ND	ND	ND
	1	6.17±0.07	6.14±0.11	6.25±0.08	6.10±0.08	ND	ND
	3	6.38±0.06	6.28±0.05	6.30±0.07	6.22±0.09	ND	ND
	6	6.36±0.07	6.29±0.08	6.23±0.04	6.20±0.12	ND	ND
60	0	6.29±0.07	ND	ND	ND	ND	ND
	1	6.29±0.09	6.20±0.07	6.26±0.07	4.19±0.11	ND	ND
	3	6.31±0.06	6.24±0.03	6.30±0.05	6.13±0.12	ND	ND
	6	6.24±0.06	6.17±0.07	6.27±0.08	6.29±0.04	ND	ND
***S. aureus* PAW set 3**							
30	0	6.15±0.15	ND	ND	ND	ND	ND
	1	6.15±0.07	6.18±0.07	6.35±0.07	5.28±0.11	ND	ND
	3	6.20±0.07	6.19±0.11	6.12±0.09	6.22±0.11	ND	ND
	6	6.17±0.07	6.12±0.06	6.15±0.12	6.09±0.09	ND	ND
60	0	6.19±0.06	ND	ND	ND	ND	ND
	1	6.13±0.08	6.20±0.05	6.25±0.03	4.29±0.07	ND	ND
	3	6.28±0.08	6.20±0.07	6.17±0.09	6.06±0.04	ND	ND
	6	6.26±0.04	6.18±0.10	6.15±0.03	6.25±0.13	ND	ND
***E. coli* PAS set 6**							
30	0	6.17±0.09	ND	ND	ND	ND	ND
	1	6.26±0.04	6.17±0.05	6.14±0.13	6.25±0.05	ND	ND
	3	6.34±0.07	6.28±0.08	6.22±0.09	6.36±0.06	ND	ND
	6	6.06±0.04	6.17±0.05	6.30±0.07	6.13±0.16	ND	ND
60	0	6.25±0.06	ND	ND	ND	ND	ND
	1	6.37±0.05	6.21±0.06	6.20±0.10	5.10±0.10	ND	ND
	3	6.29±0.08	6.25±0.06	6.29±0.19	6.26±0.04	ND	ND
	6	6.22±0.09	6.16±0.09	6.12±0.14	5.68±0.05	ND	ND
***S. aureus* PAS set 6**							
30	0	6.18±0.06	ND	ND	ND	ND	ND
	1	6.20±0.07	6.30±0.07	6.16±0.05	6.17±0.05	ND	ND
	3	6.21±0.13	6.13±0.08	6.30±0.07	6.21±0.03	ND	ND
	6	6.23±0.07	6.10±0.08	6.32±0.09	6.40±0.05	ND	ND
60	0	6.27±0.04	ND	ND	ND	ND	ND
	1	6.18±0.10	6.12±0.06	6.31±0.05	5.23±0.10	ND	ND
	3	6.15±0.12	6.19±0.03	6.23±0.21	6.08±0.06	ND	ND
	6	6.13±0.06	6.25±0.06	6.13±0.08	6.35±0.08	ND	ND

Table S3. Microbial inactivation of *E. coli* and *S. aureus NCTC 1803* at 30 and 60 min contact time, treated with PAW or PAS stored at different temperatures for up to 3 months. Table represents 1 independent plasma treatment (Set 4). ND = not detected.

Contact time (min)	**Storage time (weeks/ months)**	**CTL**	**RT**	**4**	**-16**	**-80**	**-150**
		Cell density (log_{10} CFU/mL) ±SD					
***E. coli* PAW set 4**							
30	0	6.16±0.04	ND	ND	ND	ND	ND
	1	6.29±0.07	6.03±0.07	5.88±0.07	6.05±0.02	ND	ND
	2	6.28±0.02	6.13±0.01	6.16±0.13	6.24±0.06	ND	ND
	3	6.26±0.04	6.28±0.08	6.22±0.03	5.08±0.06	ND	ND
	3m	6.36±0.10	6.29±0.03	6.18±0.14	6.26±0.09	ND	ND
	6m	6.17±0.05	6.14±0.13	5.68±0.07	6.23±0.04	ND	ND
60	0	6.24±0.04	ND	ND	ND	ND	ND
	1	6.15±0.03	5.83±0.04	5.92±0.10	5.37±0.05	ND	ND
	2	6.13±0.12	6.17±0.04	6.16±0.08	6.10±0.10	ND	ND
	3	6.30±0.07	6.29±0.07	6.17±0.05	6.24±0.06	ND	ND
	3m	6.31±0.07	6.18±0.07	6.21±0.08	5.61±0.05	ND	ND
	6m	6.25±0.03	6.32±0.04	6.16±0.02	6.24±0.06	ND	ND
***S. aureus* PAW set 4**							
30	0	6.19±0.06	ND	ND	ND	ND	ND
	1	6.10±0.07	5.88±0.07	5.74±0.05	2.31±0.17	3.05±0.02	ND
	2	6.16±0.13	5.91±0.03	5.91±0.03	3.93±0.15	ND	ND
	3	6.28±0.08	6.20±0.07	6.16±0.08	5.10±0.10	ND	ND
	3m	6.41±0.11	6.27±0.06	6.24±0.06	6.22±0.03	ND	ND
	6m	6.27±0.04	6.20±0.07	6.18±0.16	6.47±0.05	ND	ND
60	0	6.12±0.02	ND	ND	ND	ND	ND
	1	6.17±0.11	5.90±0.10	5.86±0.04	3.47±0.03	ND	0.70±1.22
	2	6.18±0.07	6.06±0.15	6.04±0.05	4.93±0.15	ND	ND
	3	6.22±0.09	5.23±0.10	5.47±0.09	5.59±0.07	ND	ND
	3m	6.18±0.07	6.14±0.10	6.16±0.08	6.11±0.10	ND	ND
	6m	6.25±0.06	6.25±0.10	6.14±0.11	6.21±0.06	ND	ND
***E. coli* PAS set 4**							
30	0	6.25±0.03	ND	ND	ND	ND	ND
	1	6.17±0.05	5.83±0.10	5.83±0.04	4.44±0.04	ND	ND
	2	6.22±0.03	6.10±0.10	6.10±0.10	6.11±0.10	ND	ND
	3	6.18±0.07	6.15±0.17	6.25±0.06	5.65±0.05	ND	ND
	3m	6.35±0.05	6.26±0.06	6.38±0.06	6.43±0.06	ND	ND
	6m	6.37±0.05	6.43±0.05	6.28±0.08	6.27±0.04	ND	ND
60	0	6.18±0.07	ND	ND	ND	ND	ND
	1	6.12±0.02	5.86±0.08	5.63±0.07	6.32±0.05	ND	ND
	2	6.34±0.06	6.17±0.10	6.18±0.14	6.25±0.06	ND	ND
	3	6.30±0.08	6.25±0.06	6.17±0.14	5.44±0.08	ND	ND
	3m	6.40±0.07	6.35±0.03	6.36±0.04	6.37±0.15	ND	ND

	6m	6.43±0.06	6.36±0.12	6.26±0.04	6.28±0.07	ND	ND
***S. aureus* PAS set 4**							
30	0	6.22±0.08	ND	ND	ND	ND	ND
	1	6.14±0.12	5.21±0.17	5.31±0.17	6.01±0.05	ND	2.43±0.27
	2	6.23±0.04	6.12±0.06	6.14±0.11	6.26±0.06	ND	ND
	3	6.23±0.07	6.27±0.07	6.11±0.10	6.13±0.06	ND	ND
	3m	6.31±0.08	6.29±0.09	6.16±0.13	6.20±0.05	ND	ND
	6m	6.20±0.07	6.10±0.10	6.27±0.04	6.28±0.07	ND	ND
60	0	6.16±0.04	ND	ND	ND	ND	ND
	1	6.09±0.09	5.11±0	5.11±0	ND	ND	ND
	2	6.21±0.06	5.25±0.06	6.10±0.10	4.70±0.11	ND	ND
	3	6.28±0.05	6.21±0.06	6.30±0.07	5.08±0.06	ND	ND
	3m	6.16±0.05	6.22±0.13	6.34±0.08	6.27±0.03	ND	ND
	6m	6.16±0.13	6.24±0.04	6.26±0.09	6.24±0.03	ND	ND

Appendix II Supplementary Information for Chapter 7

Table S4. Apoptosis and lysis of HaCaT cells after incubation with different % PAS at different contact times.

Contact time (min)												
	0	**1**	**3**	**5**	**10**	**12**	**15**	**20**	**30**	**40**	**50**	**60**
Cell percentages (%)												
PAS 55%												
AnnV-/7ADD- Viable cells	86.7	78.8	87.9	93.9	92.6	91.3	92.7	89.4	95.1	91.3	86.5	91.3
AnnV+/7ADD- Early apoptotic	10.3	6.4	7.3	3.4	3.3	3.2	3.8	5.8	2.5	5.4	6.5	3.7
AnnV+/7ADD+ Late apoptotic	2.1	12.8	3.6	1.4	2.9	3.2	2.5	3.2	1.2	2.2	5.0	3.1
AnnV-/7ADD+ Necrotic/Lysed	0.8	1.9	1.0	1.3	1.1	2.1	0.8	1.5	1.1	1.0	1.9	1.8
PAS 60%												
AnnV-/7ADD- Viable cells	81.7	87.4	83.0	84.7	81.6	87.7	74.7	83.8	92.0	87.0	92.7	88.0
AnnV+/7ADD- Early apoptotic	14.0	7.4	11.4	8.1	12.6	5.9	2.7	5.5	4.1	7.6	4.3	7.1
AnnV+/7ADD+ Late apoptotic	2.5	3.1	3.5	4.3	3.5	4.1	6.6	7.4	2.3	3.6	1.6	2.3
AnnV-/7ADD+ Necrotic/Lysed	1.8	1.8	2.0	2.7	2.2	2.1	16.0	3.2	1.5	1.8	1.3	2.5
PAS 65%												
AnnV-/7ADD- Viable cells	84.5	66.9	81.9	88.1	88.2	87.9	85.2	80.3	61.2	58.4	56.2	33.1
AnnV+/7ADD- Early apoptotic	2.4	12.2	7.6	3.9	1.5	2.8	4.7	4.5	3.8	5.0	7.6	3.4
AnnV+/7ADD+ Late apoptotic	4.4	13.2	6.0	4.1	3.5	3.8	6.5	9.7	9.6	17.3	18.4	23.6
AnnV-/7ADD+ Necrotic/Lysed	8.5	7.5	4.4	3.8	6.7	5.4	3.1	5.3	25.2	19.3	17.8	39.7
PAS 70%												
AnnV-/7ADD- Viable cells	94.8	86.5	90.0	87.3	81.1	67.7	69.3	31.1	19.8	13.2	25.0	14.8
AnnV+/7ADD- Early apoptotic	1.2	5.6	3.3	5.1	4.6	5.8	1.4	5.6	1.9	2.0	1.3	2.3
AnnV+/7ADD+ Late apoptotic	2.0	4.1	2.9	3.9	7.3	11.0	5.4	24.4	24.4	29.9	13.7	52.2

AnnV-/7ADD+ Necrotic/Lysed	2.0	3.7	3.7	3.7	7.0	15.5	23.9	38.7	53.8	54.8	59.8	30.6
PAS 75%												
AnnV-/7ADD- Viable cells	82.2	71.1	77.6	40.1	49.2	20.4	22.6	28.9	26.6	32.8	11.4	15.1
AnnV+/7ADD- Early apoptotic	7.2	6.0	8.6	15.3	1.6	2.0	2.4	5.2	3.9	2.4	0.1	0.7
AnnV+/7ADD+ Late apoptotic	5.5	9.6	6.9	34.2	10.8	12.7	19.6	20.3	17.7	11.6	19.0	15.1
AnnV-/7ADD+ Necrotic/Lysed	5.0	13.2	6.9	10.3	38.2	64.8	55.3	45.6	51.8	53.1	68.7	69.1

Bibliography

Abd-Elghaffar, A. A., Rashed, M. E., Ali, A. E., Amin, M. A. 2020. *In-Vitro* Inactivation of Sabin-Polioviruses for Development of Safe and Effective Polio Vaccine. *Vaccines*, 8(4):601.

Abdel-Sayed, P., Tornay, D., Hirt-Burri, N., de Buys Roessingh, A., Raffoul, W., Applegate, L. A. 2020. Implications of chlorhexidine use in burn units for wound healing. *Burns*, 46(5), 1150-1156.

Aboubakr, H. A., Williams, P., Gangal, U., Youssef, M. M., El-Sohaimy, S. A. A., Bruggeman, P. J., Goyal, S. M. 2015. Virucidal Effect of Cold Atmospheric Gaseous Plasma on Feline Calicivirus, a Surrogate for Human Norovirus. *Applied and Environmental Microbiology*, 81(11), 3612.

Adachi, T., Tanaka, H., Nonomura, S., Hara, H., Kondo, S., Hori, M. 2015. Plasma-activated medium induces A549 cell injury via a spiral apoptotic cascade involving the mitochondrial-nuclear network. *Free Radical Biology and Medicine*, 79, 28-44.

Adhikari, M., Adhikari, B., Kaushik, N., Lee, S.-J., Kaushik, N. K., Choi, E. H. 2019. Melanoma Growth Analysis in Blood Serum and Tissue Using Xenograft Model with Response to Cold Atmospheric Plasma Activated Medium. *Applied Sciences*, 9(20), 4227.

Amiran, M. R., Akhavan Sepahi, A., Zabiollahi, R., Ghomi, H., Momen, S. B., Aghasadeghi, M. R. 2016. In vitro Assessment of Antiviral Activity of Cold Atmospheric Pressure Plasma Jet against the Human Immunodeficiency Virus (HIV). *Journal of Medical Microbiology and Infectious Diseases,* 4(3), 62-67.

Arjunan, K. P. and Clyne, A. M. 2011. Non-thermal dielectric barrier discharge plasma induces angiogenesis through reactive oxygen species. *Annual International Conference of the IEEE Engineering in Medicine and Biology Society*, 30 Aug.-3 Sept, 2447-2450.

Arndt, S., Landthaler, M., Zimmermann, J. L., Unger, P., Wacker, E., Shimizu, T., Li, Y.-F., Morfill, G. E., Bosserhoff, A.-K., Karrer, S. 2015. Effects of cold atmospheric plasma (CAP) on ß-defensins, inflammatory cytokines, and apoptosis-related molecules in keratinocytes in vitro and in vivo. *PloS one*, 10(3), e0120041.

Arndt, S., Unger, P., Wacker, E., Shimizu, T., Heinlin, J., Li, Y., Thomas, H., Morfill, G., Zimmermann, J., Bosserhoff, A., Karrer, S. 2013. Cold Atmospheric Plasma (CAP) Changes Gene Expression of Key Molecules of the Wound Healing Machinery and Improves Wound Healing In Vitro and In Vivo. *PloS one*, 8, e79325.

Ayala, A., Munoz, M. F., Arguelles, S. 2014. Lipid peroxidation: production, metabolism, and signaling mechanisms of malondialdehyde and 4-hydroxy-2-nonenal. *Oxidative Medicine and Cellular Longevity*, 2014, 360438.

Azzariti, A., Iacobazzi, R. M., Di Fonte, R., Porcelli, L., Gristina, R., Favia, P., Fracassi, F., Trizio, I., Silvestris, N., Guida, G., Tommasi, S. and Sardella, E. 2019. Plasma-activated medium triggers cell death and the presentation of immune activating danger signals in melanoma and pancreatic cancer cells. *Scientific Reports*, 9(1), 4099.

Babington, P., Rajjoub, K., Canady, J., Siu, A., Keidar, M., Sherman, J. H. 2015. Use of cold atmospheric plasma in the treatment of cancer. *Biointerphases*, 10(2), 029403.

Balan, G. G., Rosca, I., Ursu, E. L., Doroftei, F., Bostanaru, A. C., Hnatiuc, E., Nastasa, V., Sandru, V., Stefanescu, G., Trifan, A., Mares, M. 2018. Plasma-activated water: a new and effective alternative for duodenoscope reprocessing. *Infection and Drug Resistance*, 11, 727-733.

Barrera, G. 2012. Oxidative stress and lipid peroxidation products in cancer progression and therapy. *ISRN Oncology*, 137289.

Barton, A., Wende, K., Bundscherer, L., Hasse, S., Schmidt, A., Bekeschus, S., Weltmann, K.-D., Lindequist, U., Masur, K. 2014. Nonthermal Plasma Increases Expression of Wound Healing Related Genes in a Keratinocyte Cell Line. *Plasma Medicine*, 3, 125-136.

Bekeschus, S., Brüggemeier, J., Hackbarth, C., von Woedtke, T., Partecke, L.-I., van der Linde, J. 2017a. Platelets are key in cold physical plasma-facilitated blood coagulation in mice. *Clinical Plasma Medicine*, 7-8, 58-65.

Bekeschus, S., Freund, E., Wende, K., Gandhirajan, R. K., Schmidt, A. 2018a. Hmox1 Upregulation Is a Mutual Marker in Human Tumour Cells Exposed to Physical Plasma-Derived Oxidants. *Antioxidants*, 7(11), 151.

Bekeschus, S., Kolata, J., Winterbourn, C., Kramer, A., Turner, R., Weltmann, K. D., Broker, B., Masur, K. 2014. Hydrogen peroxide: A central player in physical plasma-induced oxidative stress in human blood cells. *Free Radical Research*, 48(5), 542-9.

Bekeschus, S., Mueller, A., Gaipl, U., Weltmann, K.-D. 2017b. Physical plasma elicits immunogenic cancer cell death and mitochondrial singlet oxygen, IEEE Transactions on Radiation and Plasma Medical Sciences, 2(2), 138-146.

Bekeschus, S., Scherwietes, L., Freund, E., Liedtke, K. R., Hackbarth, C., von Woedtke, T., Partecke, L.-I. 2018b. Plasma-treated medium tunes the inflammatory profile in murine bone marrow-derived macrophages. *Clinical Plasma Medicine*, 11, 1-9.

Bekeschus, S., Schmidt, A., Bethge, L., Masur, K., von Woedtke, T., Hasse, S., Wende, K. 2015. Redox Stimulation of Human THP-1 Monocytes in Response to Cold Physical Plasma. *Oxidative Medicine and Cellular Longevity*, Article ID 607969.

Bekeschus, S., Schmidt, A., Weltmann, K.-D., von Woedtke, T. 2016. The plasma jet kINPen – A powerful tool for wound healing. *Clinical Plasma Medicine*, 4(1), 19-28.

Bigliardi, P., Langer, S., Cruz, J., Kim, S., Nair, H., Srisawasdi, G. 2017. An Asian Perspective on Povidone Iodine in Wound Healing. *Dermatology*, 233(2-3):223-233.

Blackert, S., Haertel, B., Wende, K., von Woedtke, T., Lindequist, U. 2013. Influence of non-thermal atmospheric pressure plasma on cellular structures and processes in human keratinocytes (HaCaT). *Journal of Dermatological Science*, 70(3), 173-81.

Boehm, D., Curtin, J., Cullen, P. J., Bourke, P. 2018. Hydrogen Peroxide and Beyond-the Potential of High-voltage Plasma-activated Liquids Against Cancerous Cells, *Anticancer Agents in Medicinal Chemistry*, 18(6), 815-823.

Boehm, D., Heslin, C., Cullen, P. J., Bourke, P. 2016. Cytotoxic and mutagenic potential of solutions exposed to cold atmospheric plasma. *Scientific Reports*, 6, 21464.

Boxhammer, V., Li, Y. F., Koritzer, J., Shimizu, T., Maisch, T., Thomas, H. M., Schlegel, J., Morfill, G. E., Zimmermann, J. L. 2013. Investigation of the mutagenic potential of cold atmospheric plasma at bactericidal dosages. *Mutation Research*, 753(1), 23-8.

Brannon, J. R., Dunigan, T. L., Beebout, C. J., Ross, T., Wiebe, M. A., Reynolds, W. S., Hadjifrangiskou, M. 2020. Invasion of vaginal epithelial cells by uropathogenic *Escherichia coli*. *Nature Communications*, 11(1), 2803.

Brisset, J.-L. and Pawlat, J. (2015) Chemical Effects of Air Plasma Species on Aqueous Solutes in Direct and Delayed Exposure Modes: Discharge, Post-discharge and Plasma Activated Water. *Plasma Chemistry and Plasma Processing*, 36, 355-381.

Bruggeman, P., J. Kushner, M., Locke, B., Gardeniers, H., Graham, W., B. Graves, D., Hofman-Caris, R., Marić, D., P. Reid, J., Ceriani, E., Rvs, D., E. Foster, J., Garrick, S., Gorbanev, Y., Hamaguchi, S., Iza, F., Jablonowski, H., Klimova, E., Kolb, J., Zvereva, G. 2016. Plasma-liquid interactions: A review and roadmap. *Plasma Sources Science and Technology*, 25, 053002.

Brun, P., Russo, V., Tarricone, E., Corrao, S., Deligianni, V., Leonardi, A., Cavazzana, R., Zuin, M., Martines, E. 2015. Using helium-generated cold plasma to control infection and healing. *Plasma Medicine*, 5(2-4), 237-247.

Brun, P., Vono, M., Venier, P., Tarricone, E., Deligianni, V., Martines, E., Zuin, M., Spagnolo, S., Cavazzana, R., Cardin, R., Castagliuolo, I., La Gloria Valerio, A., Leonardi, A. 2012. Disinfection of Ocular Cells and Tissues by Atmospheric-Pressure Cold Plasma. *PLOS ONE*, 7(3), e33245.

Bunz, O., Mese, K., Zhang, W., Piwowarczyk, A., Ehrhardt, A. 2018. Effect of cold atmospheric plasma (CAP) on human adenoviruses is adenovirus type-dependent. *PLoS One*, 13(10), e0202352.

Burlica, R., Grim, R. G., Shih, K. Y., Balkwill, D., Locke, B. R. 2010. Bacteria Inactivation Using Low Power Pulsed Gliding Arc Discharges with Water Spray. *Plasma Processes and Polymers,* 7(8), 640-649.

Bührer, C., Bahr, S., Siebert, J., Wettstein, R., Geffers, C., Obladen, M. 2002. Use of 2% 2-phenoxyethanol and 0.1% octenidine as antiseptic in premature newborn infants of 23-26 weeks gestation. *Journal of Hospital Infection*, 51(4), 305-7.

Chapman, A. K., Aucott, S. W., Milstone, A. M. 2012. Safety of chlorhexidine gluconate used for skin antisepsis in the preterm infant. *Journal of Perinatology*, 32(1), 4-9.

Chauvin, J., Judee, F., Merbahi, N., Vicendo, P. 2018. Effects of Plasma Activated Medium on Head and Neck FaDu Cancerous Cells: Comparison of 3D and 2D Response. *Anticancer Agents in Medicinal Chemistry*, 18(6), 776-783.

Chauvin, J., Judée, F., Yousfi, M., Vicendo, P., Merbahi, N. 2017. Analysis of reactive oxygen and nitrogen species generated in three liquid media by low temperature helium plasma jet. *Scientific Reports*, 7(1), 4562.

Chen, T.-P., Su, T.-L., Liang, J. 2016. Plasma-Activated Solutions for Bacteria and Biofilm Inactivation. *Current Bioactive Compounds*, 13, 59-65.

Chen, Z., Lin, L., Cheng, X., Gjika, E., Keidar, M. 2016. Effects of cold atmospheric plasma generated in deionized water in cell cancer therapy. *Plasma Processes and Polymers*, 9999: 1–6

Cheng, Y.-C., Wu, C.-H., Liu, C.-T., Lin, C.-Y., Chiang, H.-P., Chen, T.-W., Chen, C.-Y., Wu, J. S. 2017. Tooth bleaching by using a helium-based low-temperature atmospheric pressure plasma jet with saline solution. *Plasma Processes and Polymers*, 14, e201600235.

Chia Shi Zhe, G., Green, A., Fong, Y. T., Lee, H. Y., Ho, S. F. 2016. Rare case of type I hypersensitivity reaction to sodium hypochlorite solution in a healthcare setting. *BMJ Case Reports*, bcr2016217228.

Conrads, H., Schmidt, M. 2000. Plasma generation and plasma sources. *Plasma Sources Science and Technology*, 9, 441.

Cueva, C., Moreno-Arribas, M. V., Martín-Alvarez, P. J., Bills, G., Vicente, M. F., Basilio, A., Rivas, C. L., Requena, T., Rodríguez, J. M., Bartolomé, B. 2010. Antimicrobial activity of phenolic acids against commensal, probiotic and pathogenic bacteria. *Research in Microbiology*, 161(5), 372-82.

Daeschlein, G., Hillmann, A., Gümbel, D., Sicher, C., Podewils, S. v., Stope, M. B., Jünger, M. 2018. Enhanced Anticancer Efficacy by Drug Chemotherapy and Cold Atmospheric Plasma Against Melanoma and Glioblastoma Cell Lines In Vitro. *IEEE Transactions on Radiation and Plasma Medical Sciences,* 2(2), 153-159.

Daeschlein, G., Scholz, S., Ahmed, R., von Woedtke, T., Haase, H., Niggemeier, M., Kindel, E., Brandenburg, R., Weltmann, K. D., Juenger, M. 2012. Skin decontamination by low-temperature atmospheric pressure plasma jet and dielectric barrier discharge plasma. *Journal of Hospital Infection*, 81(3), 177-183.

Dakal, T. C., Kumar, A., Majumdar, R. S., Yadav, V. 2016. Mechanistic Basis of Antimicrobial Actions of Silver Nanoparticles. *Frontiers in microbiology*, 7, 1831-1831.

Dancer, S. J. 2014. Controlling hospital-acquired infection: focus on the role of the environment and new technologies for decontamination. *Clinical Microbiology Reviews*, 27(4), 665-90.

Dasan, B., Onal-Ulusoy, B., Pawlat, J., Diatczyk, J., Sen, Y., Mutlu, M. 2016. A New and Simple Approach for Decontamination of Food Contact Surfaces with Gliding Arc Discharge Atmospheric Non-Thermal Plasma. *Food Bioprocess Technol*ogy 10:650–661.

Dezest, M., Chavatte, L., Bourdens, M., Quinton, D., Camus, M., Garrigues, L., Descargues, P., Arbault, S., Burlet-Schiltz, O., Casteilla, L., Clément, F., Planat, V., Bulteau, A.-L. 2017. Mechanistic insights into the impact of Cold Atmospheric Pressure Plasma on human epithelial cell lines. *Scientific Reports*, 7(1), 41163.

Dobrynin, D., Fridman, A., Starikovskiy, A. Y. 2012. Reactive oxygen and nitrogen species production and delivery into liquid media by microsecond thermal spark-discharge plasma jet. *IEEE Transactions on Plasma Science*, 40(9), 2163-2171.

Dolezalova, E., Lukes, P. 2015. Membrane damage and active but nonculturable state in liquid cultures of *Escherichia coli* treated with an atmospheric pressure plasma jet. *Bioelectrochemistry*, 103, 7-14.

Doughty, D. 1994. A rational approach to the use of topical antiseptics. *Journal of Wound Ostomy & Continence Nursing,* 21(6), 224-31.

Duarte, B., Cabete, J., Formiga, A., Neves, J. 2017. Dakin's solution: is there a place for it in the 21st century?. *International Wound Journal*, 14(6), 918-920.

Dubuc, A., Monsarrat, P., Virard, F., Merbahi, N., Sarrette, J.-P., Laurencin-Dalicieux, S., Cousty, S. 2018. Use of cold-atmospheric plasma in oncology: a concise systematic review. *Therapeutic advances in medical oncology*, 10, 1758835918786475.

Duerden, B. I. 1994. Virulence factors in anaerobes*. Clinical Infectious Diseases*, 18 Suppl 4, S253-9.

Edwards, R. and Harding, K. 2004. Bacteria and wound healing. *Current opinion in infectious diseases*, 17, 91-6.

Ehlbeck, J., Schnabel, U., Polak, M., Winter, J., Von Woedtke, T., Brandenburg, R., Von Dem Hagen, T., Weltmann, K.-D. 2011. Low temperature atmospheric pressure plasma sources for microbial decontamination*. Journal of Physics D: Applied Physics*, 44, 013002.

Ercan, U., S Joshi, S., Yost, A., Gogotsi, N., O'Toole, S., Paff, M., Melchior, E., Joshi, S. 2014. Inhibition of Biofilms by Non-Thermal Plasma Treated Novel Solutions. *Advances in Microbiology*, 4, 1188-1196.

Ermolaeva, S. A., Varfolomeev, A. F., Chernukha, M. Y., Yurov, D. S., Vasiliev, M. M., Kaminskaya, A. A., Moisenovich, M. M., Romanova, J. M., Murashev, A. N., Selezneva, II, Shimizu, T., Sysolyatina, E. V., Shaginyan, I. A., Petrov, O. F., Mayevsky, E. I., Fortov, V. E., Morfill, G. E., Naroditsky, B. S. and Gintsburg, A. L. 2011. Bactericidal effects of non-thermal argon plasma in vitro, in biofilms and in the animal model of infected wounds, *Journal of Medical Microbiology*, 60, 75-83.

Fabrizio, K. A. and Cutter, C. N. 2003. Stability of electrolyzed oxidizing water and its efficacy against cell suspensions of *Salmonella typhimurium and Listeria monocytogenes*. *Journal of Food Protection*, 66(8), 1379-84.

Fang, F. C. 1997. Perspectives series: host/pathogen interactions. Mechanisms of nitric oxide-related antimicrobial activity. *Journal of Clinical Investigation*, 99(12), 2818-2825.

Fazli, M., Bjarnsholt, T., Kirketerp-Møller, K., Jørgensen, B., Andersen, A. S., Krogfelt, K. A., Givskov, M., Tolker-Nielsen, T. 2009. Nonrandom distribution of Pseudomonas aeruginosa and Staphylococcus aureus in chronic wounds. *Journal of Clinical Microbiology*, 47(12), 4084-4089.

Figueira, F., Doria, A., Khouri, S., Maciel, H., Pessoa, R., Antonio, R.-R. 2018. Effect of Storage Temperature on pH and Conductivity of Reverse Osmosis Water Treated with Atmospheric Plasma. *Plasma Medicine*, 8(3):237–244.

Filipić, A., Gutierrez-Aguirre, I., Primc, G., Mozetič, M., Dobnik, D. 2020. Cold Plasma, a New Hope in the Field of Virus Inactivation. *Trends in Biotechnology,* 38(11), 1278-1291.

Finnegan, M., Linley, E., Denyer, S. P., McDonnell, G., Simons, C., Maillard, J.-Y. 2010. Mode of action of hydrogen peroxide and other oxidizing agents: differences between liquid and gas forms. *Journal of Antimicrobial Chemotherapy*, 65(10), 2108-2115.

Franje, C. A., Chang, S.-K., Shyu, C.-L., Davis, J. L., Lee, Y.-W., Lee, R.-J., Chang, C.-C., Chou, C.-C. 2010. Differential heat stability of amphenicols characterized by structural degradation, mass spectrometry and antimicrobial activity. *Journal of Pharmaceutical and Biomedical Analysis*, 53(4), 869-877.

Freund, E., Liedtke, K., Gebbe, R., Heidecke, A., Partecke, L., Bekeschus, S. 2019a. In Vitro Anticancer Efficacy of Six Different Clinically Approved Types of Liquids Exposed to Physical Plasma. *IEEE Transactions on Radiation and Plasma Medical Sciences*, 3(5), 588 – 596.

Freund, E., Liedtke, K. R., van der Linde, J., Metelmann, H.-R., Heidecke, C.-D., Partecke, L.-I. and Bekeschus, S. (2019b). Physical plasma-treated saline promotes an immunogenic phenotype in CT26 colon cancer cells in vitro and in vivo. *Scientific Reports*, 9(1), 634.

Fridman, G., Peddinghaus, M., Balasubramanian, M., Ayan, H., Fridman, A., Gutsol, A., Brooks, A. 2006. Blood Coagulation and Living Tissue Sterilization by Floating-Electrode Dielectric Barrier Discharge in Air. *Plasma Chemistry and Plasma Processing*, 26(4), 425-442.

Fuchs, Y. and Steller, H. 2015. Live to die another way: modes of programmed cell death and the signals emanating from dying cells, *Nature Reviews Molecular Cell Biology*, 16, 329.

Garcia-Alcantara, E., López-Callejas, R., Serment, J., Peña-Eguiluz, R., Muñoz-Castro, A., Rodríguez, B., Mercado-Cabrera, A., Valencia-Alvarado, R., Piedad-Beneitez, A., Contreras-Ortiz, J., Barbabosa-Pliego, A. 2013. Toxicity and Genotoxicity in HeLa and *E. coli* Cells Caused by a Helium Plasma Needle. *Applied Physics Research*, 5(5).

Ghafoor, D., Khan, Z., Khan, A., Ualiyeva, D., Zaman, N. 2021. Excessive use of disinfectants against COVID-19 posing a potential threat to living beings. *Current Research in Toxicology*, 2, 159-168.

Girard, P.-M., Arbabian, A., Fleury, M., Bauville, G., Puech, V., Dutreix, M., Sousa, J. S. 2016. Synergistic Effect of H_2O_2 and NO_2 in Cell Death Induced by Cold Atmospheric He Plasma. *Scientific Reports*, 6, 29098.

Goree, J., Liu, B., Drake, D., Stoffels, E. 2006. Killing of *S. mutans* Bacteria Using a Plasma Needle at Atmospheric Pressure. *IEEE Transactions on Plasma Science*, 34(4), 1317-1324.

Gormley, N. J., Bronstein, A. C., Rasimas, J. J., Pao, M., Wratney, A. T., Sun, J., Austin, H. A., Suffredini, A. F. 2012. The rising incidence of intentional ingestion of ethanol-containing hand sanitizers. *Critical care medicine*, 40(1), 290-294.

Goroncy-Bermes, P., Koburger, T., Meyer, B. 2010. Impact of the amount of hand rub applied in hygienic hand disinfection on the reduction of microbial counts on hands. *Journal of Hospital Infection*, 74(3), 212-8.

Graves, D. (2012). The emerging role of reactive oxygen and nitrogen species in redox biology and some implications for plasma applications to medicine and biology. *Journal of Physics D: Applied Physics,* 45(26) 263001.

Griseti, E., Kolosnjaj-Tabi, J., Gibot, L., Fourquaux, I., Rols, M.-P., Yousfi, M., Merbahi, N., Golzio, M. 2019. Pulsed Electric Field Treatment Enhances the Cytotoxicity of Plasma-Activated Liquids in a Three-Dimensional Human Colorectal Cancer Cell Model. *Scientific Reports*, 9(1), 7583.

Griseti, E., Merbahi, N. and Golzio, M. 2020. Anti-Cancer Potential of Two Plasma-Activated Liquids: Implication of Long-Lived Reactive Oxygen and Nitrogen Species. *Cancers*, 12, 721.

Guerrero-Preston, R., Ogawa, T., Uemura, M., Shumulinsky, G., Valle, B. L., Pirini, F., Ravi, R., Sidransky, D., Keidar, M., Trink, B. 2014. Cold atmospheric plasma treatment selectively targets head and neck squamous cell carcinoma cells. *International Journal of Molecular Medicine* 34(4), 941-6.

Haanen, C. and Vermes, I. 1995. Apoptosis and inflammation. *Mediators of inflammation*, 4(1), 5-15.

Haensch, M., Mann, M., Weltmann, K.-D., von Woedtke, T. 2015. Analysis of antibacterial efficacy of plasma-treated sodium chloride solutions. *Journal of Physics D: Applied Physics*, 48(45) 454001.

Haertel, B., von Woedtke, T., Weltmann, K.-D., Lindequist, U. 2014. Non-thermal atmospheric-pressure plasma possible application in wound healing. *Biomolecules & therapeutics*, 22(6), 477-490.

Han, L., Patil, S., Boehm, D., Milosavljevic, V., Cullen, P. J., Bourke, P. 2015. Mechanism of Inactivation by High Voltage Atmospheric Cold Plasma Differs between *Escherichia coli* and *Staphylococcus aureus. Applied and Environmental Microbiology,* 82(2).

Hao, Z., Xu, Z., Shen, J., Li, X., Ding, L., Ma, J., Lan, Y., Xia, W., Cheng, C., Qiang, S., Zhang, Z., Chu, P. 2015. Effects and Mechanism of Atmospheric-Pressure Dielectric Barrier Discharge Cold Plasma on Lactate Dehydrogenase (LDH) Enzyme. *Scientific reports*, 5, 10031.

Hasse, S., Duong Tran, T., Hahn, O., Kindler, S., Metelmann, H. R., von Woedtke, T., Masur, K. 2016. Induction of proliferation of basal epidermal keratinocytes by cold atmospheric-pressure plasma. *Clinical and Experimental Dermatology*, 41(2), 202-209.

Hattori, N., Yamada, S., Torii, K., Takeda, S., Nakamura, K., Tanaka, H., Kajiyama, H., Kanda, M., Fujii, T., Nakayama, G., Sugimoto, H., Koike, M., Nomoto, S., Fujiwara, M., Mizuno, M., Hori, M., Kodera, Y. 2015. Effectiveness of plasma treatment on pancreatic cancer cells. *International Journal of Oncology*, 47(5), 1655-1662.

He, Z., Liu, K., Scally, L., Manaloto, E., Gunes, S., Ng, S., Maher, M., Brijesh kumar, T., Byrne, H., Bourke, P., Tian, F., Cullen, P. J., Curtin, J. 2019. Low dose Cold Atmospheric Plasma induces membrane oxidation, stimulates endocytosis and enhances uptake of nanomaterials in Glioblastoma multiforme cells. *Scientific Reports,* 10, 6985.

Heinlin, J., Zimmermann, J. L., Zeman, F., Bunk, W., Isbary, G., Landthaler, M., Maisch, T., Monetti, R., Morfill, G., Shimizu, T., Steinbauer, J., Stolz, W., Karrer, S. 2013. Randomized placebo-controlled human pilot study of cold atmospheric argon plasma on skin graft donor sites. *Wound Repair Regen*, 21(6), 800-7.

Herrera, A. G. 2004. Testing disinfectants in the food factory: phenol coefficient method. *Methods Molecular Biology*, 268, 281-8.

Heslin, C., Boehm, D., Gilmore, B., Megaw, J., Freeman, T., Hickok, N., Cullen, P. J., Bourke, P. 2021. Biomolecules as Model Indicators of In Vitro and In Vivo Cold Plasma Safety. *Frontiers in Physics*, 8, 589.

Heslin, C., Boehm, D., Milosavljevic, V., Laycock, M., Cullen, P. J., Bourke, P. 2015. Quantitative Assessment of Blood Coagulation by Cold Atmospheric Plasma. *Plasma Medicine*, 4(1-4), 153-163.

Hewitt, N. J., Edwards, R. J., Fritsche, E., Goebel, C., Aeby, P., Scheel, J., Reisinger, K., Ouédraogo, G., Duche, D., Eilstein, J., Latil, A., Kenny, J., Moore, C., Kuehnl, J., Barroso, J., Fautz, R., Pfuhler, S. 2013. Use of Human In Vitro Skin Models for Accurate and Ethical Risk Assessment: Metabolic Considerations. *Toxicological Sciences*, 133(2), 209-217.

Hirst, A. M., Frame, F. M., Arya, M., Maitland, N. J., O'Connell, D. 2016. Low temperature plasmas as emerging cancer therapeutics: the state of play and thoughts for the future. *Tumour Biology*, 37(6), 7021-31.

Hoeben, W. F. L. M., van Ooij, P. P., Schram, D. C., Huiskamp, T., Pemen, A. J. M., Lukeš, P. 2019. On the Possibilities of Straightforward Characterization of Plasma Activated Water. *Plasma Chemistry and Plasma Processing*, 39(3), 597-626.

Hozak, P., Scholtz, V., Khun, J., Mertová, D., Vaňková, E., Julák, J. 2018. Further Contribution to the Chemistry of Plasma-Activated Water: Influence on Bacteria in Planktonic and Biofilm Forms. *Plasma Physics Reports*, 44, 799–804.

Huang, C., Chen, Y., Sun, G., Yan, K. 2019. Disinfectant Performance of a Chlorine Regenerable Antibacterial Microfiber Fabric as a Reusable Wiper. *Materials* (Basel), 12(1).

Huie, R. E. and Padmaja, S. 1993. The reaction of no with superoxide. *Free Radical Research Communications*, 18(4), 195-9.

Höntsch, M., von Woedtke, T., Weltmann, K.-D., Nebe, B. 2012. Time-dependent effects of low-temperature atmospheric-pressure argon plasma on epithelial cell attachment, viability and tight junction formation in vitro. *Journal of Physics D: Applied Physics*, 45(2), 025206-9.

Ikawa, S., Kitano, K., Hamaguchi, S. 2010. Effects of pH on Bacterial Inactivation in Aqueous Solutions due to Low-Temperature Atmospheric Pressure Plasma Application. *Plasma Processes and Polymers*, 7(1), 33-42.

Ikawa, S., Tani, A., Nakashima, Y. and Kitano, K. 2016. Physicochemical properties of bactericidal plasma-treated water, *Journal of Physics D: Applied Physics*, 49(42), 425401.

Ikehara, S., Sakakita, H., Ishikawa, K., Akimoto, Y., Yamaguchi, T., Yamagishi, M., Kim, J., Ueda, M., Ikeda, J.-i., Nakanishi, H., Shimizu, N., Hori, M., Ikehara, Y. 2015. Plasma Blood Coagulation Without Involving the Activation of Platelets and Coagulation Factors. *Plasma Processes and Polymers*, 12(12), 1348-1353.

Imanishi, J. 2000. Expression of cytokines in bacterial and viral infections and their biochemical aspects. *Journal of Biochemistery*, 127(4), 525-30.

Isbary, G., Heinlin, J., Shimizu, T., Zimmermann, J. L., Morfill, G., Schmidt, H. U., Monetti, R., Steffes, B., Bunk, W., Li, Y., Klaempfl, T., Karrer, S., Landthaler, M., Stolz, W. 2012. Successful and safe use of 2 min cold atmospheric argon plasma in chronic wounds: results of a randomized controlled trial. *British Journal of Dermatology*, 167(2), 404-10.

Isbary, G., Morfill, G., Zimmermann, J., Shimizu, T., Stolz, W. 2011. Cold atmospheric plasma: a successful treatment of lesions in Hailey-Hailey disease. *Archives of Dermatology*, 147(4), 388-90.

J Traylor, M., Pavlovich, M., Karim, S., Hait, P., Sakiyama, Y., S Clark, D., Graves, D. 2011. Long-term antibacterial efficacy of air plasma-activated water. *Journal of Physics D: Applied Physics*, 44, 472001.

Jablonowski, H., Bussiahn, R., Hammer, M. U., Weltmann, K. D., von Woedtke, T., Reuter, S. 2015. Impact of plasma jet vacuum ultraviolet radiation on reactive oxygen species generation in bio-relevant liquids. *Physics of Plasmas*, 22(12), 122008.

Jablonowski, H., Hammer, M., Weltmann, K.-D., Reuter, S. 2013a. Effects of Atmosphere Composition and Liquid Type on Plasma-Generated Reactive Species in Biologically Relevant Solutions. *Plasma Medicine*, 3, 45-55.

Jablonowski, H., Hammer, M., Winter, J., Weltmann, K.-D., Reuter, S. 2013b. Quantitative detection of plasma-generated radicals in liquids by electron paramagnetic resonance spectroscopy. *Journal of Physics D Applied Physics*. 46, 5401.

Jablonowski, H. and von Woedtke, T. 2015. Research on plasma medicine-relevant plasma-liquid interaction: What happened in the past five years?. *Clinical Plasma Medicine*, 3(2), 42-52.

Ji, S. H., Ki, S. H., Ahn, J. H., Shin, J. H., Hong, E. J., Kim, Y. J., Choi, E. H. 2018. 'Inactivation of *Escherichia coli* and *Staphylococcus aureus* on contaminated perilla leaves by Dielectric Barrier Discharge (DBD) plasma treatment. *Archives of Biochemistry and Biophysics*, 643, 32-41.

Jia, X., Chen, Q., Yang, Y., Tang, Y., Wang, R., Xu, Y., Zhu, W., Qian, X. 2016. FRET-Based Mito-Specific Fluorescent Probe for Ratiometric Detection and Imaging of Endogenous Peroxynitrite: Dyad of Cy3 and Cy5. *Journal of the American Chemical Society*, 138(34), 10778-81.

Joshi, S. G., Cooper, M., Yost, A., Paff, M., Ercan, U. K., Fridman, G., Friedman, G., Fridman, A., Brooks, A. D. 2011. Nonthermal dielectric-barrier discharge plasma-induced inactivation involves oxidative DNA damage and membrane lipid peroxidation in *Escherichia coli*. *Antimicrobial Agents Chemotherapy*, 55(3), 1053-62.

Judée, F., Fongia, C., Ducommun, B., Yousfi, M., Lobjois, V., Merbahi, N. 2016. Short and long time effects of low temperature Plasma Activated Media on 3D multicellular tumour spheroids. *Scientific Reports*, 6, 21421.

Kamgang Youbi, G., Herry, J.-M., Meylheuc, T., Laminsi, S., Naïtali, M. 2018. Microbial decontamination of stainless steel and polyethylene surfaces using GlidArc plasma activated water without chemical additives. *Chemical Technology and Biotechnology*, 93(9), 2544-2551.

Kampf, G. 2016. Acquired resistance to chlorhexidine – is it time to establish an “antiseptic stewardship” initiative?. *Journal of Hospital Infection*, 94, 213-227.

Kampf, G. 2018. Efficacy of ethanol against viruses in hand disinfection. *Journal of Hospital Infection*, 98(4), 331-338.

Kampf, G., Fliss, P. M., Martiny, H. 2014. Is peracetic acid suitable for the cleaning step of reprocessing flexible endoscopes?. *World journal of gastrointestinal endoscopy*, 6(9), 390-406.

Kampf, G., Marschall, S., Eggerstedt, S., Ostermeyer, C. 2010. Efficacy of ethanol-based hand foams using clinically relevant amounts: a cross-over controlled study among healthy volunteers. *BMC Infectious Diseases*, 10(1),78.

Kampf, G., Todt, D., Pfaender, S., Steinmann, E. 2020. Persistence of coronaviruses on inanimate surfaces and their inactivation with biocidal agents. *Journal of Hospital Infection*, 104(3), 246-251.

Kaushik, N., Ghimire, B., Li, Y., Adhikari, M., Veerana, M., Kaushik, N., Jha, N., Adhikari, B., Lee, S.-J., Masur, K., von Woedtke, T., Weltmann, K.-D., Choi, E. 2018. Biological and medical application of plasma-activated media, water and solutions. *Biological Chemistry*, 400(1), 39-62.

Kaushik, N., Uhm, H., Choi, E. 2012. Micronucleus formation induced by dielectric barrier discharge plasma exposure in brain cancer cells. *Applied Physics Letters*, 100(8), 084102.

Keidar, M., Walk, R., Shashurin, A., Srinivasan, P., Sandler, A., Dasgupta, S., Ravi, R., Guerrero-Preston, R., Trink, B. 2011. Cold plasma selectivity and the possibility of a paradigm shift in cancer therapy. *British Journal Of Cancer*, 105, 1295.

Khansa, I., Schoenbrunner, A. R., Kraft, C. T., Janis, J. E. 2019. Silver in Wound Care-Friend or Foe?: A Comprehensive Review. *Plastic and Reconstructive Surgery*, 7(8), e2390.

Kilmer, S., Semchyshyn, N., Shah, G., Fitzpatrick, R. 2007. A pilot study on the use of a plasma skin regeneration device (Portrait PSR3) in full facial rejuvenation procedures. *Lasers in Medical Science*, 22(2), 101-9.

Kim, S. J. and Chung, T. H. 2016. Cold atmospheric plasma jet-generated RONS and their selective effects on normal and carcinoma cells. *Scientific Reports*, 6, 20332.

Klebes, M., Lademann, J., Philipp, S., Ulrich, C., Patzelt, A., Ulmer, M., Kluschke, F., Kramer, A., Weltmann, K. D., Sterry, W., Lange-Asschenfeldt, B. 2014. Effects of tissue-tolerable plasma on psoriasis vulgaris treatment compared to conventional local treatment: A pilot study. *Clinical Plasma Medicine*, 2(1), 22-27.

Klinkhammer, C., Verlackt, C., śmiłowicz, D., Kogelheide, F., Bogaerts, A., Metzler-Nolte, N., Stapelmann, K., Havenith, M., Lackmann, J.-W. 2017. Elucidation of Plasma-induced Chemical Modifications on Glutathione and Glutathione Disulphide. *Scientific Reports*, 7(1), 13828.

Koban, I., Holtfreter, B., Hübner, N.-O., Matthes, R., Sietmann, R., Kindel, E., Weltmann, K.-D., Welk, A., Kramer, A., Kocher, T. 2011. Antimicrobial efficacy of non-thermal plasma in comparison to chlorhexidine against dental biofilms on titanium discs in vitro – proof of principle experiment. *Journal of Clinical Periodontology*, 38(10), 956-965.

Kogelschatz, U. 2002. Filamentary, Patterned, and Diffuse Barrier Discharges. *IEEE Transactions on Plasma Science,* 30(4), 1400 – 1408.

Kogelschatz, U. 2003. Dielectric-Barrier Discharges: Their History, Discharge Physics, and Industrial Applications. *Plasma Chemistry and Plasma Processing*, 23, 1–46.

Kramer, A., Dissemond, J., Kim, S., Willy, C., Mayer, D., Papke, R., Tuchmann, F., Assadian, O. 2018. Consensus on Wound Antisepsis: Update 2018. *Skin Pharmacology and Physiology*, 31(1), 28-58.

Krasowski, G., Jawień, A., Tukiendorf, A., Rybak, Z., Junka, A., Olejniczak-Nowakowska, M., Bartoszewicz, M., Smutnicka, D. 2015. A comparison of an antibacterial sandwich dressing vs dressing containing silver. *Wound Repair Regen*, 23(4), 525-30.

Kumar, N., Hoon Park, J., Nam Jeon, S., Sang Park, B., Choi, E., Attri, P. 2016. The action of microsecond-pulsed plasma-activated media on the inactivation of human lung cancer cells. *Journal of Physics D: Applied Physics*, 49, 115401.

Kunigk, L., Gomes, D. R., Forte, F., Vidal, K. P., Gomes, L. F., Sousa, P. F. 2001. The influence of temperature on the decomposition kinetics of peracetic acid in solutions. *Brazilian Journal of Chemical Engineering*, 18(2).

La Fauci, V., Costa, G. B., Genovese, C., Palamara, M. A. R., Alessi, V., Squeri, R. 2019 Drug-resistant bacteria on hands of healthcare workers and in the patient area: an environmental survey in Southern Italy's hospital, *Revista espanola de quimioterapia*, 32(4), 303-310.

Lachapelle, J. M. 2014. A comparison of the irritant and allergenic properties of antiseptics. *European Journal of Dermatology*, 24(1), 3-9.

Laroussi, M. 1996. Sterilization of contaminated matter with an atmospheric pressure plasma. *IEEE Transactions on Plasma Science*, 24(3), 1188-1191.

Laroussi, M. 2018. Plasma Medicine: A Brief Introduction. *Plasma,* 1(1), 47-60.

Laroussi, M. and Leipold, F. 2004. Evaluation of the roles of reactive species, heat, and UV radiation in the inactivation of bacterial cells by air plasmas at atmospheric pressure. *International Journal of Mass Spectrometry*, 233(1), 81-86.

Laroussi, M., Lu, X., Keidar, M. 2017. Perspective: The physics, diagnostics, and applications of atmospheric pressure low temperature plasma sources used in plasma medicine. *Journal of Applied Physics*, 122, 020901.

Laroussi, M., Mendis, D. A., Rosenberg, M. 2003. Plasma interaction with microbes. *New Journal of Physics*, 5, 41-41.

Laurita, R., Barbieri, D., Gherardi, M., Colombo, V., Lukes, P. 2015. Chemical analysis of reactive species and antimicrobial activity of water treated by nanosecond pulsed DBD air plasma. *Clinical Plasma Medicine*, 3(2), 53-61.

Leduc, M., Guay, D., Leask, R., Coulombe, S. 2009. Cell permeabilization using a non-thermal plasma. *New Journal of Physics*, 11, 115021.

Lee, K., Paek, K.-h., Ju, W. T., Lee, Y. 2006. Sterilization of bacteria, yeast, and bacterial endospores by atmospheric-pressure cold plasma using helium and oxygen. *Journal of Microbiology,* 44(3):269-75.

Lee, S. H. I., Fröhling, A., Schlüter, O., Corassin, C. H., De Martinis, E. C. P., Alves, V. F., Pimentel, T. C., Oliveira, C. A. F. 2021. Cold atmospheric pressure plasma inactivation of

dairy associated planktonic cells of *Listeria monocytogenes* and *Staphylococcus aureus. Lebensmittel-Wissenschaft & Technologie*, 146, 111452.

Lengheden, A. and Jansson, L. 1995. pH effects on experimental wound healing of human fibroblasts in vitro. *European journal of oral sciences*, 103(3), 148-155.

Lerones, C., Mariscal, A., Carnero, M., García-Rodríguez, A., Fernández-Crehuet, J. 2004. Assessing the residual antibacterial activity of clinical materials disinfected with glutaraldehyde, o-phthalaldehyde, hydrogen peroxide or 2-bromo-2-nitro-1,3-propanediol by means of a bacterial toxicity assay. *Clinical Microbiology and Infection*, 10(11), 984-989.

Levine, J. M. 2013. Dakin's solution: past, present, and future. *Advanced Skin Wound Care*, 26(9), 410-4.

Li, B., Shan, C. L., Zhou, Q., Fang, Y., Wang, Y. L., Xu, F., Han, L. R., Ibrahim, M., Guo, L. B., Xie, G. L., Sun, G. C. 2013. Synthesis, characterization, and antibacterial activity of cross-linked chitosan-glutaraldehyde', *Marine Drugs*, 11(5), 1534-52.

Li, Y., Pan, J., Wu, D., Tian, Y., Zhang, J., Fang, J. 2019. Regulation of *Enterococcus faecalis* Biofilm Formation and Quorum Sensing Related Virulence Factors with Ultra-low Dose Reactive Species Produced by Plasma Activated Water. *Plasma Chemistry and Plasma Processing*, 39(1), 35-49.

Li, Y., Pan, J., Ye, G., Zhang, Q., Wang, J., Zhang, J. and Fang, J. 2017. In vitro studies of the antimicrobial effect of non-thermal plasma-activated water as a novel mouthwash. *European Journal of Oral Science*, 125(6), 463-470.

Liakos, I., Rizzello, L., Hajiali, H., Brunetti, V., Carzino, R., Pompa, P. P., Athanassiou, A., Mele, E. 2015. Fibrous wound dressings encapsulating essential oils as natural antimicrobial agents. *Journal of Materials Chemistry B*, 3(8), 1583-1589.

Liao, X., Su, Y., Liu, D., Chen, S., Hu, Y., Ye, X., Wang, J., Ding, T. 2018. Application of atmospheric cold plasma-activated water (PAW) ice for preservation of shrimps (Metapenaeus ensis). *Food Control*, 94, 307-314.

Liedtke, K. R., Freund, E., Hackbarth, C., Heidecke, C.-D., Partecke, L.-I., Bekeschus, S. 2018a. A myeloid and lymphoid infiltrate in murine pancreatic tumours exposed to plasma-treated medium. *Clinical Plasma Medicine*, 11, 10-17.

Liedtke, K. R., Hackbarth, C., Partecke, L. I., Bekeschus, S. 2018b. Reduction of Metastasis With Plasma-Treated Liquid In Mice: The Role Of Myleoid Cells In The Tumour Microenvironment. *Clinical Plasma Medicine*, 9, 45-46.

Lin, A. G., Xiang, B., Merlino, D. J., Baybutt, T. R., Sahu, J., Fridman, A., Snook, A. E., Miller, V. 2018. Non-thermal plasma induces immunogenic cell death in vivo in murine CT26 colorectal tumours. *Oncoimmunology*, 7(9), e1484978.

Linley, E., Denyer, S. P., McDonnell, G., Simons, C., Maillard, J.-Y. 2012. Use of hydrogen peroxide as a biocide: new consideration of its mechanisms of biocidal action. *Journal of Antimicrobial Chemotherapy*, 67(7), 1589-1596.

Liu, F., He, D., Yu, Y., Cheng, L., Zhang, S. 2019. Quaternary Ammonium Salt-Based Cross-Linked Micelles to Combat Biofilm. *Bioconjugate Chemistry*, 30(3), 541-546.

Lou, B., Hsieh, J.H., Chen, C.M., Hou, C.W., Wu, H.Y., Chou, P.Y., Lai, C.H., Lee, J.W. 2020. Helium/Argon-Generated Cold Atmospheric Plasma Facilitates Cutaneous Wound Healing. *Frontiers in Bioengineering and Biotechnology*, 8, 683.

Lu, P., Boehm, D., Bourke, P.J. Cullen, P. 2017a. Achieving Reactive Species Specificity within Plasma Activated Water through Selective Generation using Air Spark and Glow Discharges. *Plasma Processes and Polymers*, 14(8), 1600207.

Lu, P., Boehm, D., Cullen, P., Bourke, P. 2017b. Controlled cytotoxicity of plasma treated water formulated by open-air hybrid mode discharge. *Applied Physics Letters*, 110, 264102.

Lukes, P., Dolezalova, E., Sisrova, I., Clupek, M. 2014. Aqueous-phase chemistry and bactericidal effects from an air discharge plasma in contact with water: Evidence for the formation of peroxynitrite through a pseudo-second-order post-discharge reaction of H_2O_2 and HNO_2. *Plasma Sources Science and Technology*, 23, 015019.

Lukes, P., Locke, B., Brisset, J.-L. 2012. Aqueous-Phase Chemistry of Electrical Discharge Plasma in Water and in Gas-Liquid Environments, *Plasma Chemistry and Catalysis in Gases and Liquids*,7, 243-308.

López-Callejas, R., Peña-Eguiluz, R., Valencia-Alvarado, R., Mercado-Cabrera, A., Rodríguez-Méndez, B. G., Serment-Guerrero, J. H., Cabral-Prieto, A., González-Garduño, A. C., Domínguez-Cadena, N. A., Muñoz-Infante, J., Betancourt-Ángeles, M. 2018. Alternative method for healing the diabetic foot by means of a plasma needle. *Clinical Plasma Medicine*, 9, 19-23.

Ma, R., Wang, G., Tian, Y., Wang, K., Zhang, J., Fang, J. 2015. Non-thermal plasma-activated water inactivation of food-borne pathogen on fresh produce. *Journal of Hazardous Materials*, 300, 643-651,

Ma, Y., Ha, C. S., Hwang, S. W., Lee, H. J., Kim, G. C., Lee, K. W., Song, K. 2014. Non-thermal atmospheric pressure plasma preferentially induces apoptosis in p53-mutated cancer cells by activating ROS stress-response pathways. *PLoS One*, 9(4), e91947.

Machala, Z., Tarabová, B., Hensel, K., Dolezalova, E., Sikurova, L., Lukes, P. 2013. Formation of ROS and RNS in Water Electro-Sprayed through Transient Spark Discharge in Air and their Bactericidal Effects. *Plasma processes and Polymers*, 10(7), 649-659.

Mai-Prochnow, A., Clauson, M., Hong, J., Murphy, A. B. 2016. Gram positive and Gram negative bacteria differ in their sensitivity to cold plasma. *Scientific Reports*, 6, 38610.

Maisch, T., Bosserhoff, A. K., Unger, P., Heider, J., Shimizu, T., Zimmermann, J. L., Morfill, G. E., Landthaler, M., Karrer, S. 2017. Investigation of toxicity and mutagenicity of cold atmospheric argon plasma. *Environmental and Molecular Mutagenesis,* 58(3), 172-177.

Maisch, T., Shimizu, T., Isbary, G., Heinlin, J., Karrer, S., Klampfl, T. G., Li, Y. F., Morfill, G., Zimmermann, J. L. 2012. Contact-free inactivation of *Candida albicans* biofilms by cold atmospheric air plasma. *Applied Environmental Microbiology*, 78(12), 4242-7.

Makvandi, P., Jamaledin, R., Jabbari, M., Nikfarjam, N., Borzacchiello, A. 2018. Antibacterial quaternary ammonium compounds in dental materials: A systematic review. *Dental Materilas*, 34(6), 851-867.

Manner, H. 2008. Argon plasma coagulation therapy. *Current Opinion in Gastroenterology*, 24(5), 612-6.

Martins, E. A. and Meneghini, R. 1994. Cellular DNA damage by hydrogen peroxide is attenuated by hypotonicity. *The Biochemical journal*, 299, 137-140.

Mateu Sanz, M., Tornín Cavielles, J., Brulin, B., Khlyustova, A., Ginebra, M.-P., Layrolle, P., Canal, C. 2020. Cold Plasma-Treated Ringer's Saline: A Weapon to Target Osteosarcoma. *Cancers*, 12, 227.

Mateu Sanz, M., Tornín Cavielles, J., Ginebra, M.-P., Canal, C. 2021. Cold Atmospheric Plasma: A New Strategy Based Primarily on Oxidative Stress for Osteosarcoma Therapy. *Journal of Clinical Medicine*, 10, 893.

Mc Carlie, S., Boucher, C. E., Bragg, R. R. 2020. Molecular basis of bacterial disinfectant resistance. *Drug Resistance Updates*, 48, 100672.

McDonnell, G. and Russell, A. D. 1999. Antiseptics and disinfectants: activity, action, and resistance. *Clinical microbiology reviews*, 12(1), 147-179.

McGucken, P. V. and Woodside, W. 1973. Studies on the mode of action of glutaraldehyde on *Escherichia coli*. *Journal of Applied Bacteriology*, 36(3), 419-26.

Menezes de Pádua, C. A., Schnuch, A., Lessmann, H., Geier, J., Pfahlberg, A., Uter, W. 2005. Contact allergy to neomycin sulfate: results of a multifactorial analysis. *Pharmacoepidemiology and Drug Safety*, 14(10),725-33.

Mercier, R.-C., Stumpo, C., Rybak, M. J. 2002. Effect of growth phase and pH on the in vitro activity of a new glycopeptide, oritavancin (LY333328), against *Staphylococcus aureus* and *Enterococcus faecium. Journal of Antimicrobial Chemotherapy*, 50(1), 19-24.

Merkl, R., Hradkova, I., Filip, V., Šmidrkal, J. 2010. Antimicrobial and Antioxidant Properties of Phenolic Acids Alkyl Esters. *Czech Journal of Food Sciences*, 28, 275-279.

Merritt, K., Hitchins, V. M., Brown, S. A. 2000. Safety and cleaning of medical materials and devices. *Journal of Biomedical Materials Research*, 53(2), 131-6.

Metelmann, H.-R., Podmelle, F., Waite, P. D., Müller-Debus, C. F., Hammes, S., Funk, W. 2013a. Conditioning in laser skin resurfacing – Betulin emulsion and skin recovery. *Journal of Cranio-Maxillofacial Surgery*, 41(3), 249-253.

Metelmann, H.-R., Vu, T. T., Do, H. T., Le, T. N. B., Hoang, T. H. A., Phi, T. T. T., Luong, T. M. L., Doan, V. T., Nguyen, T. T. H., Nguyen, T. H. M., Nguyen, T. L., Le, D. Q., Le, T. K. X., von Woedtke, T., Bussiahn, R., Weltmann, K.-D., Khalili, R., Podmelle, F. 2013b Scar formation of laser skin lesions after cold atmospheric pressure plasma (CAP) treatment: A clinical long term observation. *Clinical Plasma Medicine*, 1(1), 30-35.

Miller, V., Lin, A., Fridman, A. 2016. Why Target Immune Cells for Plasma Treatment of Cancer. *Plasma Chemistry and Plasma Processing*, 36(1), 259-268.

Mohades, S., Laroussi, M., Sears, J., Barekzi, N., Razavi, H. 2015. Evaluation of the effects of a plasma activated medium on cancer cells. *Physics of Plasmas*, 22(12), 122001.

Moiseev, T., Misra, N. N., Patil, S., Cullen, P. J., Bourke, P., Keener, K., Mosnier, J. P. 2014. Post-discharge gas composition of a large-gap DBD in humid air by UV-Vis absorption spectroscopy. *Plasma Sources Science and Technology*, 23(6):065033.

Mokhtar Hefny, M., Pattyn, C., Lukes, P., Benedikt, J. 2016. Atmospheric plasma generates oxygen atoms as oxidizing species in aqueous solutions. *Journal of Physics D: Applied Physics*, 49, 404002.

Molloy-Simard, V., Lemyre, J.-L., Martel, K., Catalone, B. J. 2019. Elevating the standard of endoscope processing: Terminal sterilization of duodenoscopes using a hydrogen peroxide–ozone sterilizer. *American Journal of Infection Control*, 47(3), 243-250.

Morales-Ramirez, P., Cruz-Vallejo, V., Pena-Eguiluz, R., Lopez-Callejas, R., Rodriguez-Mendez, B. G., Valencia-Alvarado, R., Mercado-Cabrera, A., Munoz-Castro, A. E. 2013. Assessing cellular DNA damage from a helium plasma needle. *Radiation Research*, 179(6), 669-73.

Münzenmayer, L., Geiger, T., Daiber, E., Schulte, B., Autenrieth, S. E., Fraunholz, M., Wolz, C. 2016. Influence of Sae-regulated and Agr-regulated factors on the escape of *Staphylococcus aureus* from human macrophages. *Cellular Microbiology*, 18(8), 1172-1183.

Nam, S. H., Lee, H. W., Cho, S. H., Lee, J. K., Jeon, Y. C., Kim, G. C. 2013. High-efficiency tooth bleaching using non-thermal atmospheric pressure plasma with low concentration of hydrogen peroxide. *Journal of Applied Oral Science,* 21(3), 265-270.

Napp, M., Daeschlein, G., von Podewils, S., Hinz, P., Emmert, S., Haase, H., Spitzmueller, R., Gumbel, D., Kasch, R., Junger, M. 2016. In vitro susceptibility of methicillin-resistant and methicillin-susceptible strains of *Staphylococcus aureus* to two different cold atmospheric plasma sources. *Infection*, 44(4), 531-7.

Nastuta, A., Topala, I., Grigoras, C., Pohoata, V., Popa, G. 2011. Stimulation of wound healing by helium atmospheric pressure plasma treatment. *Journal of Physics D: Applied Physics,* 44, 105204.

Naïtali, M., Kamgang-Youbi, G., Herry, J. M., Bellon-Fontaine, M. N. and Brisset, J. L. 2010. Combined Effects of Long-Living Chemical Species during Microbial Inactivation Using Atmospheric Plasma-Treated Water. *Applied Environmental Microbiology*, 22, 7662-4.

Ng, S. W., Lu, P., Rulikowska, A., Boehm, D., O'Neill, G., Bourke, P. 2020a. The effect of atmospheric cold plasma treatment on the antigenic properties of bovine milk casein and whey proteins. *Food Chemistry*. 128283.

Ng, S. W., Tsoukou, E., Chaple, S., Boehm, D., Bourke, P. 2020b. Plasma Treatment of Liquids. *Innovative Food Processing Technologies*. 610-634.

Niemira, B. A. 2012. Cold plasma decontamination of foods. *Annual Review of Food Science and Technology*, 3, 125-42.

Nikolic, P., Mudgil, P., Whitehall, J. 2019. Formaldehyde as an alternative to antibiotics for treatment of refractory impetigo and other infectious skin diseases*. Expert Review of Anti-infective Therapy*, 17(9), 681-687.

Niquet, R., Boehm, D., Schnabel, U., Cullen, P., Bourke, P., Ehlbeck, J. 2017. Characterising the impact of post-treatment storage on chemistry and antimicrobial properties of plasma

treated water derived from microwave and DBD sources. *Plasma Processes and Polymers,* 15(3):e1700127.

Norberg, Seth A., Tian, W., Johnsen, E., Kushner, Mark J. 2014. Atmospheric pressure plasma jets interacting with liquid covered tissue: Touching and not-touching the liquid. *Journal of Physics D: Applied Physics*, 47, 475203.

Oehmigen, K., Winter, J., Hähnel, M., Wilke, C., Brandenburg, R., Weltmann, K.-D. and von Woedtke, T. 2011. Estimation of Possible Mechanisms of *Escherichia coli* Inactivation by Plasma Treated Sodium Chloride Solution. *Plasma Processes and Polymers*, 8, 904-913.

P. Papapanagiotou, E., J. Fletouris, D., Psomas, A. 2005. Effect of various heat treatments and cold storage on sulphamethazine residues stability in incurred piglet muscle and cow milk samples, *Analytica Chimica Acta*, 529, 305-309.

Padnya, P. L., Terenteva, O. S., Akhmedov, A. A., Iksanova, A. G., Shtyrlin, N. V., Nikitina, E. V., Krylova, E. S., Shtyrlin, Y. G., Stoikov, II 2021. Thiacalixarene based quaternary ammonium salts as promising antibacterial agents. *Bioorganic & Medicinal Chemistry*, 29, 115905.

Pan, J., Sun, K., Liang, Y., Sun, P., Yang, X., Wang, J., Zhang, J., Zhu, W., Fang, J., Becker, K. H. 2013. Cold Plasma Therapy of a Tooth Root Canal Infected with *Enterococcus faecalis* Biofilms In Vitro*, Journal of Endodontics*, 39(1), 105-110.

Pandey, C. K., Agarwal, A., Baronia, A., Singh, N. 2000. Toxicity of ingested formalin and its management, *Human & Experimental Toxicology*, 19(6), 360-6.

Park, J., Suh, D., Tang, T., Lee, H. J., Roe, J.-S., Kim, G. C., Han, S., Song, K. 2020. Non-thermal atmospheric pressure plasma induces epigenetic modifications that activate the expression of various cytokines and growth factors in human mesoderm-derived stem cells. *Free Radical Biology and Medicine*, 148, 108-122.

Park, J. H., Kim, M., Shiratani, M., Cho, A. E., Choi, E. H., Attri, P. 2016. Variation in structure of proteins by adjusting reactive oxygen and nitrogen species generated from dielectric barrier discharge jet. *Scientific Reports*, 6(1), 35883.

Park, J. K., Nam, S. H., Kwon, H. C., Mohamed, A. A., Lee, J. K., Kim, G. C. 2011. Feasibility of nonthermal atmospheric pressure plasma for intracoronal bleaching. *International Endodontic Journal*, 44(2), 170-5.

Patange, A., Boehm, D., Giltrap, M., Lu, P., Cullen, P. J., Bourke, P. 2018. Assessment of the disinfection capacity and eco-toxicological impact of atmospheric cold plasma for treatment of food industry effluents. *Science of The Total Environment*, 631-632, 298-307.

Patange, A., Boehm, D., Ziuzina, D., Cullen, P. J., Gilmore, B., Bourke, P. 2019. High voltage atmospheric cold air plasma control of bacterial biofilms on fresh produce*. International Journal of Food Microbiology,* 16;293:137-145.

Pavlovich, M. J., Ono, T., Galleher, C., Curtis, B., Clark, D. S., Machala, Z., Graves, D. B. 2014. Air spark-like plasma source for antimicrobial NOx generation, *Journal of Physics D: Applied Physics*, 47(50), 505202.

Pawłat, J., Terebun, P., Kwiatkowski, M., Tarabová, B., Kovaľová, Z., Kučerová, K., Machala, Z., Janda, M., Hensel, K. 2019. Evaluation of Oxidative Species in Gaseous and Liquid Phase

Generated by Mini-Gliding Arc Discharge. *Plasma Chemistry and Plasma Processing*, 39(3), 627-642.

Pelicano, H., Carney, D., Huang, P. 2004. ROS stress in cancer cells and therapeutic implications. *Drug Resistance Updates*, 7(2), 97-110.

Plattfaut, I., Besser, M., Severing, A.-L., Stürmer, E. K., Opländer, C. 2021. Plasma medicine and wound management: Evaluation of the antibacterial efficacy of a medically certified cold atmospheric argon plasma jet. *International Journal of Antimicrobial Agents*, 57(5), 106319.

Poss, K. D. and Tonegawa, S. 1997. Reduced stress defense in heme oxygenase 1-deficient cells. *Proceedings of the National Academy of Sciences of the United States of America,* 94(20), 10925-30.

Pucci, C., Martinelli, C., Ciofani, G. 2019. Innovative approaches for cancer treatment: current perspectives and new challenges. *Ecancermedicalscience*, 13, 961.

Raffellini, S., Schenk, M., Guerrero, S., Alzamora, S. M. 2011. Kinetics of *Escherichia coli* inactivation employing hydrogen peroxide at varying temperatures, pH and concentrations. *Food Control*, 22(6), 920-932.

Rahman, I., Biswas, S. K., Jimenez, L. A., Torres, M., Forman, H. J. 2005. Glutathione, stress responses, and redox signaling in lung inflammation. *Antioxidants & Redox Signaling,* 7(1-2), 42-59.

Reuter, S., von Woedtke, T., Weltmann, K.-D. 2018. The kINPen - A review on physics and chemistry of the atmospheric pressure plasma jet and its applications*. Journal of Physics D: Applied Physics,* 51 23300.

Rezvani Ghomi, E., Khalili, S., Nouri Khorasani, S., Esmaeely Neisiany, R., Ramakrishna, S. 2019. Wound dressings: Current advances and future directions, *Journal of Applied Polymer Science,* 136(27), 47738.

Rohr, U., Mueller, C., Wilhelm, M., Muhr, G., Gatermann, S. 2003. Methicillin-resistant Staphylococcus aureus whole-body decolonization among hospitalized patients with variable site colonization by using mupirocin in combination with octenidine dihydrochloride. *Journal of Hospital Infection*, 54(4), 305-9.

Ruddy, M. and Kibbler, C. C. 2002. Endoscopic decontamination: an audit and practical review*. Journal of Hospital Infection*, 50(4), 261-8.

Rutala, W. A. and Weber, D. J. 2004. Disinfection and sterilization in health care facilities: what clinicians need to know. *Clinical Infectious Diseases*, 39(5), 702-9.

Rutala, W. A. and Weber, D. J. 2015. Disinfection, Sterilization, and Control of Hospital Waste. Mandell, Douglas, and Bennett's Principles and Practice of Infectious Diseases, 3294-3309.e4.

Sah, P., Al-Tamimi, B., Al-Nassri, N., Al-Mamari, R. 2012. Effect of Temperature on Antibiotic Properties of Garlic (*Allium sativum L*.) and Ginger (*Zingiber officinale Rosc*.) *AFRICAN JOURNAL OF BIOTECHNOLOGY*, 11, 16192-16195.

Sakai, Y., Khajoee, V., Ogawa, Y., Kusuhara, K., Katayama, Y., Hara, T. 2006. A novel transfection method for mammalian cells using gas plasma. *Journal of Biotechnology*, 121(3), 299-308.

Salzmann, C. 2018. Advances in the experimental exploration of water's phase diagram. *The Journal of Chemical Physics,* 150, 060901.

Santos, G. M. P., Oliveira, S., Monteiro, J. C. S., Fagnani, S. R., Sampaio, F. P., Correia, N. A., Crugeira, P. J. L., Pinheiro, A. L. B. 2018. ROS-induced autophagy reduces B16F10 melanoma cell proliferative activity. *Lasers in Medical Science,* 33(6), 1335-1340.

Sato, Y., Yamada, S., Takeda, S., Hattori, N., Nakamura, K., Tanaka, H., Mizuno, M., Hori, M., Kodera, Y. 2018. Effect of Plasma-Activated Lactated Ringer's Solution on Pancreatic Cancer Cells In Vitro and In Vivo. *Annals of Surgical Oncology*, 25(1), 299-307.

Sauerbrei, A. 2020. Bactericidal and virucidal activity of ethanol and povidone-iodine. *MicrobiologyOpen*, 9(9), e1097.

Sauerbrei, A. and Wutzler, P. 2010. Virucidal efficacy of povidone-iodine-containing disinfectants. *Letters in Applied Microbiology*, 51(2), 158-63.

Schick, J. B. and Milstein, J. M. 1981. Burn hazard of isopropyl alcohol in the neonate. *Pediatrics*, 68(4), 587-8.

Schmidt, A., Bekeschus, S., Jarick, K., Hasse, S., von Woedtke, T., Wende, K. 2019a. Cold Physical Plasma Modulates p53 and Mitogen-Activated Protein Kinase Signaling in Keratinocytes. *Oxidative Medicine and Cellular Longevity*, 16.

Schmidt, A., Bekeschus, S., Wende, K., Vollmar, B., von Woedtke, T. 2017. A cold plasma jet accelerates wound healing in a murine model of full-thickness skin wounds, *Experimental Dermatology*, 26(2), 156-162.

Schmidt, A., von Woedtke, T., Vollmar, B., Hasse, S., Bekeschus, S. 2019b. Nrf2 signaling and inflammation are key events in physical plasma-spurred wound healing, *Theranostics*, 9(4), 1066-1084.

Schmidt, K., Estes, C., McLaren, A., Spangehl, M. J. 2018. Chlorhexidine Antiseptic Irrigation Eradicates *Staphylococcus epidermidis* From Biofilm: An *In Vitro* Study. *Clinical orthopaedics and related research*, 476(3), 648-653.

Schnabel, U., Balazinski, M., Wagner, R., Stachowiak, J., Boehm, D., Andrasch, M., Bourke, P., Ehlbeck, J. 2021. Optimizing the application of plasma functionalised water (PFW) for microbial safety in fresh-cut endive processing, *Innovative Food Science & Emerging Technologies*, 102745.

Schnabel, U., Niquet, R., Schmidt, C., Stachowiak, J., Schlüter, O., Andrasch, M., Ehlbeck, J. 2016. Antimicrobial efficiency of non-thermal atmospheric pressure plasma processed water (PPW) against agricultural relevant bacteria suspensions. *International Journal of Environmental & Agriculture Research*, 2(5), 212-224.

Schnabel, U., Sydow, D., Schlüter, O., Andrasch, M., Ehlbeck, J. 2015. Decontamination of Fresh-Cut Iceberg Lettuce and Fresh Mung Bean Sprouts by Non-Thermal Atmospheric Pressure Plasma Processed Water (PPW). *Modern Agricultural Science and Technology*, 1(1),23-39.

Schneider, C., Arndt, S., Zimmermann, J., Li, Y., Karrer, S., Bosserhoff, A. 2018. Cold atmospheric plasma treatment inhibits growth in colorectal cancer cells. *Biological Chemistry*, 400(1):111-122.

Schneider, L. A., Korber, A., Grabbe, S., Dissemond, J. 2007. Influence of pH on wound-healing: a new perspective for wound-therapy?. *Archieves of Dermatological Research*, 298(9), 413-20.

Scholtz, V., Pazlarova, J., Souskova, H., Khun, J., Julak, J. 2015. Nonthermal plasma-A tool for decontamination and disinfection. *Biotechnol Advances*, 33(6 Pt 2), 1108-19.

Sersenová, D., Machala, Z., Repiská, V., Gbelcová, H. 2021. The Effect of Plasma Activated Medium and PBS on Human Melanoma Cells Compared With Other Cancer and Normal Cells. *Preprints*, 2021010068.

Shah, J. M. Y., Omar, E., Pai, D. R., Sood, S. 2012. Cellular events and biomarkers of wound healing. *Indian journal of plastic surgery*, 45(2), 220-228.

Shaw, P., Kumar, N., Kwak, H. S., Park, J. H., Uhm, H. S., Bogaerts, A., Choi, E. H., Attri, P. 2018. Bacterial inactivation by plasma treated water enhanced by reactive nitrogen species. *Scientific Reports*, 8(1), 11268.

Shen, J., Tian, Y., Li, Y., Ma, R., Zhang, Q., Zhang, J., Fang, J. 2016. Bactericidal Effects against *S. aureus* and Physicochemical Properties of Plasma Activated Water stored at different temperatures. *Scientific reports*, 6, 28505-28505.

Sidhwa, F. and Itani, K. M. 2015. Skin preparation before surgery: options and evidence. *Surg Infect (Larchmt)*, 16(1),14-23.

Sivathasan, N., Ramamurthy, N. K., Pabla, R. S. 2010. Chemical burns associated with chlorhexidine-alcohol solution: an avoidable complication?. *Journal of Burn Care & Research*, 31(5), 833.

Sladek, R. E. J., Stoffels, E., Walraven, R., Tielbeek, P. J. A., Koolhoven, R. A. 2004. Plasma treatment of dental cavities: a feasibility study. *IEEE Transactions on Plasma Science*, 32(4), 1540-1543.

Slaughter, R. J., Watts, M., Vale, J. A., Grieve, J. R., Schep, L. J. 2019. The clinical toxicology of sodium hypochlorite. *Clinical Toxicology (Philadelphia)*. 57(5), 303-311.

Smet, C., Govaert, M., Kyrylenko, A., Easdani, M., Walsh, J., Van Impe, J. 2019. Inactivation of Single Strains of *Listeria monocytogenes* and *Salmonella Typhimurium* Planktonic Cells Biofilms With Plasma Activated Liquids. *Frontiers in Microbiology*,10:1539.

Smet, C., Noriega, E., Rosier, F., Walsh, J. L., Valdramidis, V. P., Van Impe, J. F. 2017. Impact of food model (micro)structure on the microbial inactivation efficacy of cold atmospheric plasma. *International Journal of Food Microbiology*, 240, 47-56.

Solé-Martí, X., Espona Noguera, A., Ginebra, M.-P., Canal, C. 2021. Plasma-Conditioned Liquids as Anticancer Therapies *In Vivo*: Current State and Future Directions. *Cancers*, 13, 452.

Spear, M. 2011. Wound cleansing: solutions and techniques. *Plastic Surgical Nursing,* 31(1), 29-31.

Starodubtseva, M., Cherenkevich, S., Semenkova, G. 1999. Investigation of the interaction of sodium nitrite with hydrogen peroxide in aqueous solution by chemiluminescence method. *Journal of Applied Spectroscopy*, 66, 473-476.

Stará, Z. and Krcma, F. 2004. The study of H_2O_2 generation by DC diaphragm discharge in liquids. *Czechoslovak Journal of Physics*, 54, C1050-C1055.

Stoffels, E., Flikweert, A. J., W Stoffels, W., Kroesen, G. M. W. 2002. Plasma needle: a non-destructive atmospheric plasma source for fine surface treatment of (bio)materials. *Plasma Sources Science and Technology* 11(4): 383.

Stone, H. H. 1966. Review of pseudomonas sepsis in thermal burns: verdoglobin determination and gentamicin therapy. *Annals of Surgery*, 163(2), 297-305.

Su, X., Tian, Y., Zhou, H., Li, Y., Zhang, Z., Jiang, B., Yang, B., Zhang, J., Fang, J. 2018. Inactivation Efficacy of Nonthermal Plasma-Activated Solutions against Newcastle Disease Virus. *Applied Environmental Microbiol*ogy, 84(9):e02836-17.

Sun, P. P., Wu, H., Bai, N., Zhou, H., Wang, R., Feng, H., Zhu, W., Zhang, J., Fang, J. 2012. Inactivation of *Bacillus subtilis* Spores in Water by a Direct-Current, Cold Atmospheric-Pressure Air Plasma Microjet. *Plasma Processes and Polymers*, 9, 157.

Sung, S. J., Huh, J. B., Yun, M. J., Chang, B. M., Jeong, C. M., Jeon, Y. C. 2013. Sterilization effect of atmospheric pressure non-thermal air plasma on dental instruments. *The Journal of Advanced Prosthodontics*, 5(1), 2-8.

Szabo, C., Ischiropoulos, H., Radi, R. 2007. Peroxynitrite: biochemistry, pathophysiology and development of therapeutics. *Nature Reviews Drug Discovery*, 6(8), 662-80.

Takai, E., Kitamura, T., Kuwabara, J., Ikawa, S., Yoshizawa, S., Shiraki, K., Kawasaki, H., Ryuichi, A., Kitano, K. 2014. Chemical modification of amino acids by atmospheric-pressure cold plasma in aqueous solution. *Journal of Physics D: Applied Physics*, 47, 285403.

Takeda, S., Yamada, S., Hattori, N., Nakamura, K., Tanaka, H., Kajiyama, H., Kanda, M., Kobayashi, D., Tanaka, C., Fujii, T., Fujiwara, M., Mizuno, M., Hori, M., Kodera, Y. 2017. Intraperitoneal Administration of Plasma-Activated Medium: Proposal of a Novel Treatment Option for Peritoneal Metastasis From Gastric Cancer. *Annals of Surgical Oncology*, 24(5), 1188-1194.

Takigawa, T. and Endo, Y. 2006. Effects of glutaraldehyde exposure on human health. *Journal of Occupational Health*, 48(2), 75-87.

Tampieri, F., Ginebra, M.-P., Canal, C. 2021. Quantification of Plasma-Produced Hydroxyl Radicals in Solution and Their Dependence on the pH. *Analytical Chemistry*, 93, 3666–3670.

Tanaka, H., Mizuno, M., Ishikawa, K., Kondo, H., Takeda, K., Hashizume, H., Nakamura, K., Utsumi, F., Kajiyama, H., Kano, H., Okazaki, Y., Toyokuni, S., Akiyama, S. i., Maruyama, S., Yamada, S., Kodera, Y., Kaneko, H., Terasaki, H., Hara, H., Hori, M. 2015. Plasma with High electron density and Plasma-Activated Medium for Cancer Treatment. *Clinical Plasma Medicine*, 3(2), 72-76.

Tanaka, H., Mizuno, M., Ishikawa, K., Nakamura, K., Kajiyama, H., Kano, H., Kikkawa, F., Hori, M. 2011. Plasma-Activated Medium Selectively Kills Glioblastoma Brain Tumour Cells

by Down-Regulating a Survival Signaling Molecule, AKT Kinase. *Plasma Medicine*, 1, 265-277.

Tanaka, H., Mizuno, M., Ishikawa, K., Nakamura, K., Utsumi, F., Kajiyama, H., Kano, H., Maruyama, S., Kikkawa, F., Hori, M. 2012. Cell survival and proliferation signaling pathways are downregulated by plasma-activated medium in glioblastoma brain tumour cells. *Plasma Medicine*, 2, 207-220.

Tanaka, H., Nakamura, K., Mizuno, M., Ishikawa, K., Takeda, K., Kajiyama, H., Utsumi, F., Kikkawa, F., Hori, M. 2016. Non-thermal atmospheric pressure plasma activates lactate in Ringer's solution for anti-tumour effects, *Scientific reports*, 6, 36282-36282.

Tarabová, B., Lukes, P., Hammer, M., Jablonowski, H., von Woedtke, T., Reuter, S., Machala, Z. 2019. Fluorescent measurements of peroxynitrite/peroxynitrous acid in cold air plasma treated aqueous solutions. *Physical Chemistry Chemical Physics*, 21, 8883-8896.

Tendero, C., Tixier, C., Tristant, P., Anaesmaison, J., Leprince, P. 2006. Atmospheric pressure plasmas: A review. *Spectrochimica Acta Part B: Atomic Spectroscopy*, 61(1), 2-30.

Thomas, G. W., Rael, L. T., Bar-Or, R., Shimonkevitz, R., Mains, C. W., Slone, D. S., Craun, M. L., Bar-Or, D. 2009. Mechanisms of Delayed Wound Healing by Commonly Used Antiseptics. *Journal of Trauma and Acute Care Surgery*, 66(1).

Tian, Y., Ma, R., Zhang, Q., Feng, H., Liang, Y., Zhang, J., Fang, J. 2015. Assessment of the Physicochemical Properties and Biological Effects of Water Activated by Non-thermal Plasma Above and Beneath the Water Surface, *Plasma Processes and Polymers*, 12(5), 439-449.

Traub, W. H., Leonhard, B. 1995. Heat stability of the antimicrobial activity of sixty-two antibacterial agents. *Journal of Antimicrobial Chemotherapy*, 35(1), 149-54.

Tsoukou, E., Delit, M., Treint, L., Bourke, P., Boehm, D. 2021. Distinct Chemistries Define the Diverse Biological Effects of Plasma Activated Water Generated with Spark and Glow Plasma Discharges. *Applied Sciences*, 11(3).

Tsoukou, E., Bourke, P., Boehm, D. 2020. Temperature stability and effectiveness of plasma activated-liquids over an 18 months period. *Water,* 12(11), 3021.

Ulrich, C., Kluschke, F., Patzelt, A., Vandersee, S., Czaika, V. A., Richter, H., Bob, A., Hutten, J. v., Painsi, C., Hüge, R., Kramer, A., Assadian, O., Lademann, J., Lange-Asschenfeldt, B. 2015. Clinical use of cold atmospheric pressure argon plasma in chronic leg ulcers: A pilot study. *Journal of Wound Care*, 24(5), 196-203.

Utsumi, F., Kajiyama, H., Nakamura, K., Tanaka, H., Hori, M., Kikkawa, F. 2014. Selective cytotoxicity of indirect nonequilibrium atmospheric pressure plasma against ovarian clear-cell carcinoma. *SpringerPlus*, 3, 398-398.

Utsumi, F., Kajiyama, H., Nakamura, K., Tanaka, H., Mizuno, M., Ishikawa, K., Kondo, H., Kano, H., Hori, M., Kikkawa, F. 2013. Effect of indirect nonequilibrium atmospheric pressure plasma on anti-proliferative activity against chronic chemo-resistant ovarian cancer cells in vitro and in vivo, *PLoS One*, 8(12), e81576.

Van Boxem, W., Van der Paal, J., Gorbanev, Y., Vanuytsel, S., Smits, E., Dewilde, S., Bogaerts, A. 2017. Anti-cancer capacity of plasma-treated PBS: effect of chemical composition on cancer cell cytotoxicity, *Scientific Reports*, 7(1), 16478.

Van Loenhout, J., Deben, C., Jacobs, J., De Waele, J., Van Audenaerde, J., Marcq, E., Dewilde, S., Bogaerts, A., Smits, E. 2018. Immunogenic Potential Of Cold Atmospheric Plasma For The Treatment Of Pancreatic Cancer. *Clinical Plasma Medicine*, 9, 26.

Vandamme, M., Robert, E., Lerondel, S., Sarron, V., Ries, D., Dozias, S., Sobilo, J., Gosset, D., Kieda, C., Legrain, B., Pouvesle, J. M. Pape, A. L. 2012. ROS implication in a new antitumour strategy based on non-thermal plasma. *International Journal of Cancer*, 130(9), 2185-94.

Vatansever, F., de Melo, W. C., Avci, P., Vecchio, D., Sadasivam, M., Gupta, A., Chandran, R., Karimi, M., Parizotto, N. A., Yin, R., Tegos, G. P., Hamblin, M. R. 2013. Antimicrobial strategies centered around reactive oxygen species--bactericidal antibiotics, photodynamic therapy, and beyond. *FEMS Microbiological Reviews*, 37(6), 955-89.

Vlad, I.-E. and Anghel, S. D. 2017. Time stability of water activated by different on-liquid atmospheric pressure plasmas. *Journal of Electrostatics*, 87, 284-292.

Von Woedtke, T., Oehmigen, K., Brandenburg, R., Hoder, T., Wilke, C., Hähnel, M. and Weltmann, K. D. 2012. Plasma-liquid interactions: Chemistry and antimicrobial effects. NATO Science for Peace and Security Series A: Chemistry and Biology: *Plasma for Bio-Decontamination, Medicine and Food Security*. 67-78.

Walsh, S. E., Maillard, J. Y., Russell, A. D. Ortho-phthalaldehyde: a possible alternative to glutaraldehyde for high level disinfection. *Journal of Applied Microbiology*, 86(6), 1039-46.

Wang, S., Xu, D., Qi, M., Li, B., Peng, S., Li, Q., Zhang, H., Liu, D. 2021a. Plasma-Activated Water Promotes Wound Healing by Regulating Inflammatory Responses. *Biophysica*, 1(3).

Wang, Y., Wu, Q., Muskhelishvili, L., Davis, K., Wynne, R., Tripathi, P., Bryant, M. S., Rua, D., Cao, X. 2021b. Toxicity of Ortho-phthalaldehyde Aerosols in a Human In Vitro Airway Tissue Model. *Chemical Research in Toxicology*, 34(3), 754-766.

Was, H., Dulak, J., Jozkowicz, A. 2010.Heme oxygenase-1 in tumour biology and therapy. *Current Drug Targets*, 11(12), 1551-70.

Wei Chen, C., Lee, H., Chang, M. 2008. Inactivation of Aquatic Microorganisms by Low-Frequency AC Discharges. *Plasma Science, IEEE Transactions*, 36, 215-219.

Wei, H., Brandt, M., Wolf, G., Peter Hammes, W. 2005. Optimization of acidified warm water treatment to improve the microbiological status and sensory quality of iceberg lettuce. *European Food Research and Technology*, 220, 168-175.

Weiss, M., Daeschlein, G., Kramer, A., Burchardt, M., Brucker, S., Wallwiener, D., Stope, M. B. 2017. Virucide properties of cold atmospheric plasma for future clinical applications. *Journal of Medical Virology*, 89(6), 952-959.

Wende, K., Williams, P., Dalluge, J., Gaens, V., Aboubakr, H., Bischof, J., von Woedtke, T., Goyal, S., Weltmann, K.-D., Bogaerts, A., Masur, K., Bruggeman, P. 2015. Identification of the biologically active liquid chemistry induced by a nonthermal atmospheric pressure plasma jet. *Biointerphases*, 10, 29518-103307.

Whittaker, A. G., Graham, E. M., Baxter, R. L., Jones, A. C., Richardson, P. R., Meek, G., Campbell, G. A., Aitken, A., Baxter, H. C. 2004. Plasma cleaning of dental instruments. *Journal of Hospital Infection*, 56(1), 37-41.

Winter, J., Brandenburg, R., Weltmann, K. D. 2015. Atmospheric pressure plasma jets: An overview of devices and new directions. *Plasma Sources Science and Technology*, 24(6), 064001.

Winter, J., Jablonowski, H., Hammer, M., Iséni, S., Kupsch, S., Schmidt-Bleker, A., Wende, K., Duennbier, M., Masur, K., Weltmann, K. D., Reuter, S. 2014. Tracking plasma generated H_2O_2 from gas into liquid phase and revealing its dominant impact on human skin cells. Journal of Physics D: *Applied Physics*, 47, 285401.

Wysowski, D. K., Flynt, J. W., Jr., Goldfield, M., Altman, R., Davis, A. T. 1978. Epidemic neonatal hyperbilirubinemia and use of a phenolic disinfectant detergent. *Pediatrics,* 61(2), 165-70.

Xiang, Q., Kang, C., Zhao, D., Niu, L., Liu, X., Bai, Y. 2019. Influence of organic matters on the inactivation efficacy of plasma-activated water against *E. coli* O157:H7 and *S. aureus*, *Food Control*, 99, 28-33.

Xiao, Y., Cui, J., Shi, Y. H., Sun, J., Wang, Z. P., Le, G. W. 2010. Effects of duodenal redox status on calcium absorption and related genes expression in high-fat diet-fed mice, *Nutrition*, 26 (11-12), 1188-94.

Xu, D., Wang, S., Li, B., Qi, M., Feng, R., Li, Q., Zhang, H., Chen, H. Kong, M. G. 2020. Effects of Plasma-Activated Water on Skin Wound Healing in Mice. *Microorganisms*, 8(7), 1091.

Xu, Y., Tian, Y., Ma, R., Liu, Q., Zhang, J. 2016. Effect of plasma activated water on the postharvest quality of button mushrooms, *Agaricus bisporus*. *Food Chemistry*, 197, 436-444.

Yan, D., Sherman, J.H., Cheng, X., Ratovitski, E., Canady, J., Keidar, M. 2014. Controlling plasma stimulated media in cancer treatment application. *Applied Physics Letters*, 105, 224101.

Yan, D., Cui, H., Zhu, W., Nourmohammadi, N., Milberg, J., Zhang, L. G., Sherman, J. H., Keidar, M. 2017. The Specific Vulnerabilities of Cancer Cells to the Cold Atmospheric Plasma-Stimulated Solutions. *Scientific Reports*, 7(1), 4479.

Yan, D., Nourmohammadi, N., Bian, K., Murad, F., Sherman, J. H., Keidar, M. 2016 Stabilizing the cold plasma-stimulated medium by regulating medium's composition, *Scientific Reports*, 6, 26016.

Yan, D., Sherman, J. H., Keidar, M. 2017. Cold atmospheric plasma, a novel promising anti-cancer treatment modality. *Oncotarget*, 8(9), 15977-15995.

Yan, D., Talbot, A., Nourmohammadi, N., Cheng, X., Canady, J., Sherman, J., Keidar, M. 2015a. Principles of using Cold Atmospheric Plasma Stimulated Media for Cancer Treatment. *Scientific Reports*, 5, 18339.

Yan, D., Talbot, A., Nourmohammadi, N., Sherman, J. H., Cheng, X., Keidar, M. 2015b. Toward understanding the selective anticancer capacity of cold atmospheric plasma--a model based on aquaporins (Review), *Biointerphases*, 10(4), 040801.

Yan, K., Jin, Q., Zheng, C., Deng, G., Yin, S., Liu, Z. 2018. Pulsed cold plasma-induced blood coagulation and its pilot application in stanching bleeding during rat hepatectomy. *Plasma Science and Technology*, 20(4), 044005.

Yazici, E. and Deveci, H. 2010. Factors Affecting Decomposition of Hydrogen Peroxide. Conference: Proceedings of the XIIth. International Mineral Processing Symposium, Gülsoy Ö.Y., Ergün L.Ş., Can N.M. and Çelik İ.B.

Yost, A. D. and Joshi, S. G. (2015). Atmospheric Nonthermal Plasma-Treated PBS Inactivates *Escherichia coli* by Oxidative DNA Damage. *PLOS ONE*, 10(10), e0139903.

Yusupov, M., Bogaerts, A., Huygh, S., Snoeckx, R., van Duin, A. C. T., Neyts, E. C. 2013. Plasma-Induced Destruction of Bacterial Cell Wall Components: A Reactive Molecular Dynamics Simulation, *The Journal of Physical Chemistry C*, 117(11), 5993-5998.

Zhang, J., Qu, K., Zhang, X., Wang, B., Wang, W., Bi, J., Zhang, S., Li, Z., Kong, M. G., Liu, D., Liu, C. 2019. Discharge Plasma-Activated Saline Protects Against Abdominal Sepsis by Promoting Bacterial Clearance. *Shock*, 52(1), 92-101.

Zhang, J.-M. and An, J. 2007. Cytokines, inflammation, and pain', *International anesthesiology clinics*, 45(2), 27-37.

Zhang, Q., Ma, R., Tian, Y., Su, B., Wang, K., Yu, S., Zhang, J., Fang, J. 2016. Sterilization Efficiency of a Novel Electrochemical Disinfectant against *Staphylococcus aureus*, *Environmental Science & Technology,* 50(6), 3184-92.

Zhou, J., Wang, G., Chen, Y., Wang, H., Hua, Y., Cai, Z. 2019a. Immunogenic cell death in cancer therapy: Present and emerging inducers*, Journal of Cellular and Molecular Medicine*, 23(8), 4854-4865.

Zhou, R., Rusen, Z., Prasad, K., Fang, Z., Speight, R., Bazaka, K., Ostrikov, K. 2018. Cold atmospheric plasma activated water as a prospective disinfectant: The crucial role of peroxynitrite. *Green Chemistry*, 20, 52760-5284.

Ziech, D., Franco, R., Pappa, A., Panayiotidis, M. I. 2011. Reactive oxygen species (ROS)--induced genetic and epigenetic alterations in human carcinogenesis, *Mutation Research*, 711(1-2), pp. 167-73.

Ziuzina, D., Boehm, D., Patil, S., Cullen, P. J., Bourke, P. 2015. Cold Plasma Inactivation of Bacterial Biofilms and Reduction of Quorum Sensing Regulated Virulence Factors, *PLOS ONE*, 10(9), e0138209.

Ziuzina, D., Patil, S., Cullen, P. J., Boehm, D., Bourke, P. 2014. Dielectric Barrier Discharge Atmospheric Cold Plasma for Inactivation of *Pseudomonas aeruginosa* Biofilms. *Plasma Medicine.*4(1-4), 137-152.